Molecular Mechanisms Controlling Immunity, Fertility, and Longevity

by

Nikki Naim

B.S., Binghamton University, 2016

Submitted to the Graduate Faculty of the

School of Medicine in partial fulfillment

of the requirements for the degree of

Doctor of Philosophy

University of Pittsburgh

2022

UNIVERSITY OF PITTSBURGH

SCHOOL OF MEDICINE

This dissertation was presented

by

Nikki Naim

It was defended on

February 16, 2022

and approved by

Dr. Anne Carlson, Associate Professor, Department of Biological Sciences

Dr. Todd Lamitina, Associate Professor, Department of Cell Biology

Dr. Udai Pandey, Associate Professor, Department of Pediatrics and Human Genetics

Dr. Michael Tsang, Professor, Department of Developmental Biology

Dr. Judith Yanowitz, Associate Professor, Department of Obstetrics, Gynecology, & Reproductive Sciences

Dissertation Director: Dr. Arjumand Ghazi, Associate Professor, Depts. Of Cell Biology, Physiology, and Developmental Biology

Molecular Mechanisms Controlling Immunity, Fertility, and Longevity

Nikki Naim, Ph.D.

University of Pittsburgh, 2022

All organisms must balance their cellular resources to invest in life processes such as reproduction, immunity, and longevity to persist as a species. For this reason, animal fertility often wanes during an immune response and *vice versa*. Increased reproductive activity has also been associated with reduced lifespan in many species. Studies suggest that animals possess genetic mechanisms which coordinate such life history traits, yet, the molecular mechanisms underlying these reproduction-immunity-longevity (RIL) relationships remain largely unexplored. The nematode *Caenorhabditis elegans* is a model organism which has long been used to characterize conserved genetic regulators of reproduction, immunity, and longevity. Work from our laboratory, which identified that two *C. elegans* transcription factors, NHR-49 and TCER-1, impact RIL processes therefore opened avenues to investigate RIL coordination in animals. NHR-49, proposed functional homolog of the vertebrate protein, PPARα, is a nuclear hormone receptor noted to promote lifespan and lipid homeostasis. TCER-1, shown to promote lifespan and fertility, is the *C. elegans* homolog of the human transcription and elongation splicing factor, TCERG1. My work exploring RIL coordination by these factors has shown that NHR-49 promotes both immune resistance and longevity but acts in distinct tissues to regulate these traits. Studying TCER-1 revealed that the protein additionally suppresses immunity while promoting fertility, supporting previous hypotheses that TCER-1 enacts RIL tradeoffs. Further characterization based on these findings showed that TCER-1 likely promotes small RNA

production to suppress immunity in fertile animals. The results of these projects therefore describe (a) new functions of well-studied proteins in the RIL dialogue, (b) new mechanisms of context-dependent regulation by these genes, and (c) new effectors of these pathways. These findings support emerging concepts in aging biology that genetic mechanisms which control reproduction, immunity, and longevity are both distinct and interconnected. For humans, these studies may uncover what immune mechanisms are suppressed in fertility and how to target drugs that improve health as well as lifespan.

Table of Contents

List of Tables

List of Files

List of Figures

Preface

At the height of the Transcendentalist movement, John Keats' poem, "Ode to a Grecian Urn" left us with a compelling message:

"Beauty is truth, truth beauty— that is all ye know on earth, and all ye need know."

In this poem he confronts the bucolic scenes painted on a Grecian artifact and finds its depiction of lovers in pursuit, although frozen in time, are of an everlasting beauty.

Graduate studies and publication instill a similar realization. Although we train to become experts in our field of study, the work we leave behind can only remain a snapshot of what we knew. Our discoveries may not immediately be applied in medicine, yet, each finding is one step towards positive change. In many ways, this earnest pursuit is a mindset which society would see no progress without. I am proud to serve as one of the many dedicated scientists who see the importance of uncovering truth to better this world. My studies center on the complex mechanisms of healthy aging and I believe the maturation of these findings will improve our quality of life as individuals and a society.

I would like to give a warm thanks to my circles of support; from my family, friends, and colleagues in Pittsburgh, to the mentors who cheered me on. The pandemic posed many challenges when it came to completing this achievement, yet, it also gave me time to imagine the path ahead. Without fail, these people helped me find inspiration and encouraged me such that I could build my skills as a scientist and a person. Dr. Arjumand Ghazi has been my amazing and motivating advisor, and the experience of working and learning in her lab, with Francis, Julia,

Laura, Margaret, Rachana, Hye Jin, Carter, and Sierra—in the vibrant research community of Pitt—has been incredible. The members of my Thesis Committee: Dr. Yanowitz, Dr. Lamitina, Dr. Tsang, Dr. Carlson, and Dr. Pandey have been a huge support and source of advice. Last, I'd like to give a big thanks to my mom and dad, my "twin" sisters Nyla & Nadia, my partner Kalyan, the scat-cats of the Dance House, The Silver Maples, my Tai Chi family, and all the gorgeous walking paths of Pittsburgh which strengthened my legs to take this next step.

1.0 Introduction

Chapter sections 1.1 and 1.3 include modified excerpts from Naim et al 2020, Bioessays. DOI: 10.1002/bies.202000103. Reuse permission was obtained from the copyright holder, 2020 Wiley Periodicals LLC.

Animals' ability to coordinate key life history traits like reproduction, immunity, and longevity is a product of evolution critical for species' survival (1, 2). Changes in the environment force an animal to regulate when to invest in reproduction or use precious cell resources for other processes like immunity, or, cell-maintenance for longevity. Strategic investment in these traits can be a feature of a species or an adaptive response in individuals, the latter being the focus of this thesis. For instance, an animal can delay reproduction, and even focus resources on cell-maintenance, to avoid bearing young in an unfavorable environment (3). This particularly applies when an animal needs to mount an immune response to infection; the energy invested in this response tends to decrease fertility (4, 5). When conditions are good (i.e. food abundance, lack of infection, temperature) animals are noted to invest in procreation. Yet, once reproductive processes (e.g. fecundity, gestation, mating) begin, animals become vulnerable. For this reason, reproduction and fertility are found to be associated with weakened immune function and a shortened lifespan in many species (6). Uncovering the factors regulating this **reproduction-immunity-longevity (RIL)** dialogue may be the key to controlling them to our benefit in medicine.

The molecular mechanisms controlling the ancient processes of reproduction, immunity, and longevity are the focus of this work. In animals, reproductive processes can include sperm production, oocyte quality maintenance, pregnancy, mating, and post-partum care in many

species. Immunity refers to mounting and sustaining the activity of the innate and adaptive immune systems to fight infection. Lastly, longevity is a trait with many hypothesized drivers, but is often considered the byproduct of anti-aging somatic maintenance (7). Although these three traits differ widely across species, studies suggest the regulatory pathways which control them in animals are conserved, and ubiquitous features can be identified. In this introductory chapter, I will describe the prevalence of RIL tradeoffs in nature, explain *C. elegans* utility as a model to understand these traits, and introduce the conserved proteins and molecular mechanisms of interest in my study of their relationships.

My project used the *C. elegans* nematode to model the RIL dialogue and dissect the genetic pathways which govern its tradeoffs. Through these studies, I discovered that a conserved longevity determinant, NHR-49, promotes both longevity and immunity, but acts in distinct tissues, and through distinct genetic mechanisms, to influence the two processes (8). Our work also showed that another conserved longevity factor, TCER-1, increases lifespan but suppresses innate immunity exclusively during an animals' reproductive period. These discoveries have established the role of TCER-1 as a regulator of immunity-fertility tradeoffs in *C. elegans* (9, 10). Intriguingly, further characterization showed TCER-1 likely promotes siRNA production to suppress immunity. These discoveries demonstrate that reproduction, immunity, and longevity traits can be regulated both distinctly and cohesively by conserved genetic controls. My findings therefore identify novel regulatory mechanisms and effectors of the RIL dialogue, contributing new insights to this relationship in multicellular organisms.

1.1 Coordination of lifespan, fertility, and immunity across species

Historical Perspective: Life history theory (LHT), first proposed by MacArthur and Wilson in 1967, posits that there are "trade-offs" between competing life history traits (e.g., growth, procreation, longevity, immunity) where organisms will invest more in one function at the expense of another. In this framework, reproduction, immunity, and cell-maintenance for longevity—which are highly energy-dependent and plastic functions—are proposed to be mutually antagonistic due to a competing reliance on limited cellular resources. Tradeoff strategies have been found to be remarkably prevalent across phylogenetic groups. Studies of life history traits in invertebrates have provided the earliest documentation of, and insights into, the complexities of the RIL axis. These works have shown RIL tradeoffs can be facultative (occurring only when resources are limiting) or obligate (independent of resource availability) (1, 2). A recent analysis of 121 invertebrate and vertebrate species suggested that tradeoff relationships may shape over 70% of life-history strategies seen (11). Despite its popularity, LHT has limitations as well as exceptions. For instance, poor correlation has been observed between the energetic demands of reproduction and consequent degree of reduction in immunity and lifespan, emphasizing the existence of resource-independent features (7). Similarly, despite the association between high reproductive activity and short lifespan, nature also sees instances where this pattern is defied (12-15). In some species (e.g., Queen Ants, Bumble Bees), mating is in fact beneficial to the mother's immunity (16, 17). Thus, the rather simplistic view of LHT tradeoffs being based off resource allocation has been detailed by the acknowledgement of other variables in these processes (18). The molecular determinants of the RIL tradeoffs described in the upcoming sections (1.1.1-1.1.3) are therefore liable to both match and defy the classical LHT tradeoff paradigm, and likely explain the more nuanced aspects of this relationship.

1.1.1 The associations between longevity and life history traits

Achieving longevity has long been a goal in history and medicine. The fact that members of the same species can exhibit a range of lifespans, and certain organisms display negligible senescence, has suggested that the careful study of longevity could someday extend the human lifespan. Thus, the lifespan of animals across phyla have been observed to study aging. These efforts have contributed both useful findings, and room to improve our understanding, of the process (11). Such studies eventually revealed the patterns between lifespan and the diverse life history traits of organisms. Particularly, many studies noted an inverse relationship between lifespan and fertility, and the positive correlation between lifespan and stress resistance. The exceptions to these relationships found in my work have revealed the nuance of the RIL dialogue and formed the crux of my studies.

The longevity-fertility relationship: The inverse relationship between lifespan and fertility is one of the most influential dogmas in the aging field. It arose from early evolutionary biology theories based on the "live fast, die young" principle which posited that prolific and early-mating organisms possess shorter lifespans (2, 12). This concept also formed the basis of the 'Disposable Soma' Theory of Aging, proposed by Tom Kirkwood, which states that organismal investment in germ line and fertility maintenance leads to reduced resources for the maintenance of somatic tissues and hence, aging. This notion has been supported by observational studies in many species, including humans, and tested using model organisms (11, 19). For instance, some of the best examples of the lifespan-fertility tradeoff have been shown in *Drosophila* where artificial selection for extended lifespan yielded flies with decreased reproductive activity (20). Selection for flies that are fertile at older ages also increased the

lifespan of strains while reducing early fertility (21, 22). Additional findings in worms and human studies have produced similar results (23, 24). However, numerous examples from nature and in lab, and increasingly from clinical data, also disprove a fertility-longevity trade off. For example, Cynthia Kenyon's lab found that, rather than sterility *per se*, the genetic or laser removal of a specific population of germline stem cells induced lifespan extension in *C. elegans* (25, 26). Studies in mouse and invertebrate models also show that mutations and dietary interventions which extend lifespan do not always reduce fecundity (27). An atypical positive correlation between fertility and lifespan is even noted in many species, such as ants and African mole rats (28, 29). Similarly, the transplantation of ovaries from young mice into older females increases the recipients' lifespan and cardio-protective advantage (30). Human clinical data also indicate that reproductive defects can be a harbinger of long-term deficits in length and quality of life for both sexes. For instance, premature ovarian failure is associated with increased late-life morbidity and mortality (31, 32). Such studies have illustrated that fertility and lifespan may be controlled by interconnected, yet distinct, pathways and form the basis of this work (15, 33).

The Longevity-Stress Resistance Relationship: The reduced ability to combat stressful stimuli is a conserved age-related deterioration. Continued study of longevity models have also revealed a strong positive correlation between lifespan and stress resistance (e.g., resistance to heat, desiccation, and infection). This pattern was particularly noted in genetic screens using *C. elegans*: mutations which improved lifespan were also more likely to improve various, if not all, tested stress resistance traits (34, 35). Studies in other models supported this relationship as well (reviewed in (36-38)). This pattern was so strong that genetic screens often used stress resistance as a proxy to identify lifespan regulators (39). Similarly, increases in immune function—the

aspect of stress resistance of interest to this thesis—were often found to accompany longevity phenotypes (40, 41). In this, the DAF-2/Insulin/IGF-1-like signaling (IIS) pathway became recognized as an arbiter of longevity and stress resistance, first in *C. elegans*, then other models (described further in section 1.2.1). However, an increasing body of evidence has indicated that linkages between stress resistance, including immune resistance, and longevity, can be genetically uncoupled (10, 42, 43). For instance, our lab found that the longevity-promoting protein, TCER-1, additionally represses innate immunity and other stress responses in *C. elegans* (10). Many studies also report genes that exclusively impact lifespan or stress resistance, or, have opposite impacts on the two processes (17, 42, 44-47). This implies that genetic regulators exert distinct, context-specific, control over lifespan and survival traits, making way for research on the mechanisms underlying observed tradeoffs.

Importantly, such discoveries have allowed the aging field to shift from using lifespan as a measure of aging to examining individual features of health and stress resistance (i.e., healthspan studies). Healthspan is a more nuanced way to assess aging as it considers several age-sensitive metrics of health like fertility, immunity, mobility, and cognition instead of just lifespan (48). Although the two transcription factors I study were first identified for their pro-longevity effects, our work has revealed them to have distinct impacts on each 'RIL' trait. Thus, while this section discussed the associations between longevity and other survival traits, the next sections (1.1.2-1.1.3) will describe the relationship between fertility and immunity, particularly from a tradeoffs perspective, in humans and model organisms.

1.1.2 The mutual impacts of pregnancy and immune activation in humans

The pattern where fertility is accompanied by immunosuppression, while infection and immune-activation lowers reproduction is a noted phenomenon in humans. For instance, the female immune system undergoes extensive remodeling upon pregnancy. An interesting indication of these changes is that the severity of many diseases are exacerbated while some are reduced (49). For instance, influenza carries a 5-fold higher risk of death in pregnant women, who famously have reduced inflammatory response (50). The expansion of the anti-inflammatory Treg cell population in pregnancy also decreases maternal resistance to malaria (51, 52). By the same token, pregnancy ameliorates diseases of chronic inflammation such as multiple sclerosis or rheumatoid arthritis, which are characterized by Th17 numbers which attack self-tissue (53). Indeed, additional studies find an array of immununologic effects can plague a mother and fetus. This often depends on the way a disease is typically combated, and if it alters immune cell ratios further (54, 55). Thus, pathogen-specific strategies and the immune-profile of mothers influence the impact of infections during pregnancy. The molecular mechanisms underlying these variable susceptibilities are poorly understood. Progesterone is one example driver of immune-remodeling as its high levels during pregnancy leads to repression of Th1 responses and pro-inflammatory prostaglandins while increasing Th2-secreted cytokines (56). Yet, many additional factors are suspected to guide fertility-immunity tradeoffs in mothers and humans overall.

Immune activation is also noted to harm human reproductive fitness. Extensive evidence shows that infections and/or immune dysfunction can negatively impact every aspect of human reproduction from gamete production, establishment and maintenance of pregnancy, to fetal and neonatal health (4, 57). Preexisting immune disorders are linked to premature ovarian failure,

recurrent miscarriages, and poor pregnancy outcomes (57, 58). Infectious diseases such as malaria or pneumonia are also associated with increased incidence of fetal growth restriction, premature births. and adverse pregnancy outcomes (49). Similarly, aberrant maternal immune activation has been implicated in a range of child neurocognitive and respiratory defects (59). Complications from maternal immune response itself are even noticeable during infections with TORCH (**T**oxoplasmosis, **O**ther (syphilis, varicella-zoster, parvovirus B19), **R**ubella, **C**ytomegalovirus (CMV), and **H**erpes infections) pathogens, known for their ability to cross the placenta and directly infect the fetus (60). In many cases, the detrimental effects of maternal infection have been ascribed to the production of inflammatory factors such as IL-6, which cause conversion of Treg cells into Th17 cells thus disrupting the Treg:Th17 ratio critical for healthy pregnancy (61). Yet, the molecular mechanisms which control these shifts, and the additional regulatory factors at-play, remain largely unknown.

1.1.3 The fertility-immunity relationship in model organisms

Studies in more simplistic model organisms have the potential to shed light on conserved determinants of RIL tradeoffs. Indeed, the antagonistic relationship between fertility and immunity is mirrored in diverse model organisms. Immune activity in females of a wide variety of insect species has been reported to be associated with reduced fertility (62). In flies, mosquitoes, crickets, and beetles, exposure to pathogen or even bacterial cell-wall components, cause reductions in ovarian protein content, egg number, and overall fecundity (reviewed in (62)). Using *C. elegans*, our laboratory even found that 4 hours of exposure to the opportunistic human pathogen, *Pseudomonas aeruginosa* (strain PA14), caused a reduction in the number of eggs laid far before the animal showed overt signs of infection (10). Similarly, fertility is reduced

in the presence of Shiga toxin producing *Escherichia coli* (SHEC) strains, and worms exposed to yeast *Cryptococcus neoformans* fail to reproduce almost completely (63, 64). In fact, the dramatic fertility suppression induced by *C. neoformans* has been used as a screening measure to identify conserved, virulence genes (65). *Drosophila* strains selected for high bacterial resistance show reduced fecundity even when uninfected, suggesting that constitutive immune induction is detrimental to reproduction. This is reminiscent of the poor reproductive outcomes associated with chronic inflammatory diseases in women (49, 66, 67).

Conversely, increased reproductive activity is associated with reduced immune fitness in many species (62, 68). The most explicit proofs of this effect have been made in *Drosophila*, where mating was shown to reduce female survival of infection. Mated females exhibit higher pathogen loads and reduced anti-bacterial peptide levels (69). The molecular basis of this effect can be traced to specific proteins in the seminal fluid transferred by the male during copulation. In fact, transferring just the seminal fluid without sperm, or just the sperm proteins alone is sufficient to make un-mated female flies immune-susceptible (70). Interestingly, the act of mating also shortens female longevity in worm and flies, even in the absence of infection (71, 72). Also, while mating's impact on immunity has not been directly tested in *C. elegans*, many sterile mutants have increased immunity (43). Thus, the pervasive antagonistic relationship seen between fertility and immunity across species also offers an opportunity to study these complex relationships in simpler systems.

1.2 *C. elegans* as a model for lifespan, fertility, and immunity

The *C. elegans* nematode is a soil-dwelling organism which was first cultivated by Sydney Brenner as a model to understand the complex genetic regulation of animal behavior and morphology. This roundworm, more complex than other well-understood organisms like bacteria—yet still simple enough to study closely—was a perfect candidate for unbiased genetic screens and laboratory manipulation. Its status as a self-fertilizing hermaphrodite with a transparent body has made screens (e.g., using mutagen ethyl methanesulfonate (EMS)) easier because mutant alleles could be maintained through self-propagation without mating. Ever since Brenner introduced *C. elegans* to the scientific community, this model organism has proven instrumental to the identification and characterization of conserved and diverse genetic pathways. This chapter section will therefore introduce and describe the features of the *C. elegans* nematode, which has made it a powerful model for studies in lifespan (Section 1.2.1), fertility (1.2.2), and innate immunity (1.2.3). It will also present the pro-longevity transcription factors, NHR-49 and TCER-1, which are of prime interest to this thesis.

C. elegans is well suited to dissect conserved genetic pathways, particularly those related to lifespan, fertility, and immunity. The first advantage of *C. elegans*, which increases its utility in lifespan research, is its rapid lifecycle. When maintained at 20°C, *C. elegans* progress through four larval stages (L1-L4) before reaching adulthood in ~3 days. From this point, mature animals live for another ~2 weeks, but only lay viable eggs for another ~5 days. From a simplistic perspective, this short overall lifespan makes it easy to monitor the lifespan of *C. elegans* strains in repeated trials. However, these timescales also set up a pattern where worms are alive, yet reproductively inactive for roughly one-third of their lives. Considering the average age of menopause in human females, this similar proportion of life spent in the post-reproductive phase

makes *C. elegans* a compelling aging model. During this time, the worm outer cuticle also becomes visibly wrinkled and all components of health (i.e. motility, immunity, and neurological function) decline. While many studies monitor lifespan alone, this additional number of analogous, measurable, aging phenotypes enhance *C. elegans* value for understanding the elusive aging process.

As detailed in section 1.2.2, hermaphroditic *C. elegans* is also a useful model for understanding fertility. The fact their brood size is so easy to monitor—and is more of a reflection of the mother's fertility rather than external variables—has been of particular value for my work. Without needing to wait for a mate, *C. elegans* hermaphrodites continuously fertilize their own oocytes with self-sperm in the spermatheca during their reproductive period. This therefore results in the production of ~300, genetically identical offspring, where reduced brood sizes generally indicate a reproductive dysfunction of the mother since their reproductive process is so self-sufficient. For these, and additional reasons, reproduction has been extensively studied in *C. elegans* (reviewed in (73, 74)), including the genetic pathways involved in oocyte quality maintenance and the transport of lipids from adult tissues to oocytes (75, 76).

As detailed in section 1.2.3, *C. elegans* is also a powerful model for immunity, particularly for understanding RIL tradeoffs. Because *C. elegans* evolutionarily predates many organisms with more complex forms of immunity, its immune system does not include dedicated immune cells. Although this reduces direct homology with human mechanisms this lack of interference from the adaptive immune system allows for the isolated study of innate immunity. This trait is very important in my studies of the RIL dialogue as the regulation of such a pervasive pattern across species is also likely regulated by ubiquitous mechanisms. Alongside their simplistic immune system, *C. elegans'* multicellularity and status as an *in vivo* model is

additionally useful for immunity studies. Adult animals possess many cell types, including neurons, intestine, muscle, and hypodermis, analogous to tissue types in mammals (77). This has allowed me, and others, to study the tissue-specific effects of gene expression on lifespan and immunity (Chapter 2.0). Unlike single-cell models like yeast or cell culture, *C. elegans* also provides a platform to observe physiologic effects across tissues *in vivo*. The fact that *C. elegans* is transparent, and the interior of the worm can be observed microscopically without disrupting its tissues enhances this advantage. For this reason, studies have been able to characterize the effects of infection on specific tissues as well as neuron and damage-triggered detection of infection (78-80). In reference to my studies on immune response to *Pseudomonas*, the worm model has additionally allowed us to observe the effects of infections which begin in the gut on a whole-organism level.

Furthermore, the conservation of genes from *C. elegans* to humans together with the ability to modify its genome make it a great model for dissecting genetic pathways. Studies have shown that 83% of the *C. elegans* proteome has homologous human proteins while only 11% is nematode-specific (81). As mentioned, unbiased screens have leveraged the conservation of *C. elegans* genes to understand animal physiologic pathways (e.g. development, neuronal signaling, aging, reproduction). This is because studies with *C. elegans* can reveal novel signaling mechanisms more quickly than studies using traditional mammalian models or cell-biological methods. Considering how ancient reproduction, immunity, and longevity traits are to animals—and that *C. elegans* sees similar RIL tradeoffs as humans—this further makes it an attractive system to study complex RIL relationships. Already, a handful of conserved regulators of RIL tradeoffs have been identified by our lab and others using *C. elegans* (e.g., (10, 82); discussed further in Section 1.3.2). Thus, my studies take advantage of *C. elegans'* unique traits to better

understand the RIL axis. In the next sections (1.2.1-1.2.5) I will provide an overview of the biology of lifespan, fertility, and immunity in *C. elegans*.

1.2.1 Lifespan studies in *C. elegans*

In the context of aging research, scientists wanted a model with a relatively short lifespan which could be easily monitored in bulk (83). In alignment with this, the *C. elegans* nematode lives approximately 17 days at 20°C and produces roughly 300 offspring on standard agar feeding plates with an *E. coli* lawn. The ease of maintaining many worms in one assay, and the fact that their clonal populations are largely genetically invariant, allow researchers to easily conduct lifespan assays with high statistical power and identify individual lifespan-altering genes, even if they cause a modest (10-15%) effect. Further advancements have also allowed for the automation of these assays in multiple platforms (84, 85). Thus, the simplicity of performing lifespan assays in the *C. elegans* model has made it a powerful tool to study aging and forwarded the field.

In 1977, Michael Klass had established the first method to consistently measure *C. elegans* lifespan which led to the discovery of the first *C. elegans*-identified lifespan gene, *age-1*. In 1983, Klass developed an EMS screening procedure using a temperature-sensitive sterile strain which could detect lifespan increases as small as 20%. This experiment yielded five mutants, which were all found to map to a single *age-1* locus (86, 87). This finding showed that *C. elegans* could be used to screen the genome for individual genetic lifespan modulators. Together, such techniques have allowed for the identification of >200 *C. elegans* genes which modulate lifespan, revealing conserved longevity pathways (88).

Years after *age-1* was identified, Cynthia Kenyon discovered the powerful *daf-2* mutation that caused *C. elegans* to live two-times longer than wild type, invigorating the aging field (89, 90). DAF-2 was found to encode the *C. elegans* insulin-like growth factor 1 (IGF-1) receptor of the insulin/IGF-1 signaling (IIS) pathway. AGE-1 was later found to encode the *C. elegans* ortholog to the phosphoinositide 3-kinase (PI3K) catalytic subunit of the same pathway. The IIS pathway is a fundamental system which connects nutrient levels to metabolism, development, and longevity by the sensing of insulin-like peptides binding to the IGF-1/DAF-2 receptor. Mutations in *daf-2* have been shown to control many genes which extend life and alter the expression of both metabolic and stress responsive genes (91, 92). Accordingly, the main transcription factors activated in reduced-IIS are heat-shock transcription factor-1 (HSF-1), oxidative stress-responsive Nrf transcription factor (SKN-1), and most notably DAF-16, homolog of human Forkhead box O (FOXO) protein, FOXO3A. Alterations in IIS pathway genes were eventually found to increase longevity across species (93, 94). Polymorphisms in FOXO3A and IGF-1-pathway genes were also found to be associated with extreme longevity in humans (95, 96). There exist arguments that *daf-2 C. elegans* strains are an unsuitable aging model because they are healthy and youthful for a shorter proportion of their lifespan compared to wild type (42). However, *C. elegans* studies also revealed that transcriptional activation from reduced DAF-2 signaling undeniably targets genes of molecular longevity programs, including antioxidants, antimicrobials, and chaperones for proteostasis, supporting its relevance to mammalian aging (91, 97). The *C. elegans* model has therefore enabled scientists to study complex regulation of aging, with the DAF-2/IIS pathway as its premier discovery.

The reproductive control of longevity: Shortly after discovering *daf-2*, Cynthia Kenyon's laboratory made another landmark finding that signals from the reproductive system regulate lifespan. In this study, they found laser removal of the two germ cell precursors of the entire adult germ line, induced a 60% lifespan extension in *C. elegans* strains (25). However, this lifespan extension was not a trivial consequence of sterility, as ablation of the entire gonad (including the germ line and the somatic gonad), caused sterility but did not induce longevity. Using temperature-sensitive mutants in *glp-1*, a gene that is essential for germ line proliferation, they showed the absence of a population of totipotent germline stem cells exclusively extended lifespan (98). Germline-less mutants required the presence of other reproductive somatic structures (i.e. uterus and spermatheca), and transcription factors like *daf-16*, to increase lifespan (26). This created a direct molecular-genetic link between germ line status and longevity which has been supported across models (23, 24). This ultimately led to widespread acknowledgement of the reproductive control of aging. Since then, studies have identified a network of transcription factors which promote longevity in response to germ line loss (**Fig. 1.1**) (99). These proteins have been shown to modulate critical somatic maintenance processes such as lipid metabolism, autophagy, and proteasomal function to confer longevity. Indeed, the two proteins which are the focus of my thesis, TCER-1 and NHR-49, were first selected for study because they are essential for germline-less longevity. Their additional roles in reproduction and immunity have positioned them as ideal targets in our study of the RIL dialogue.

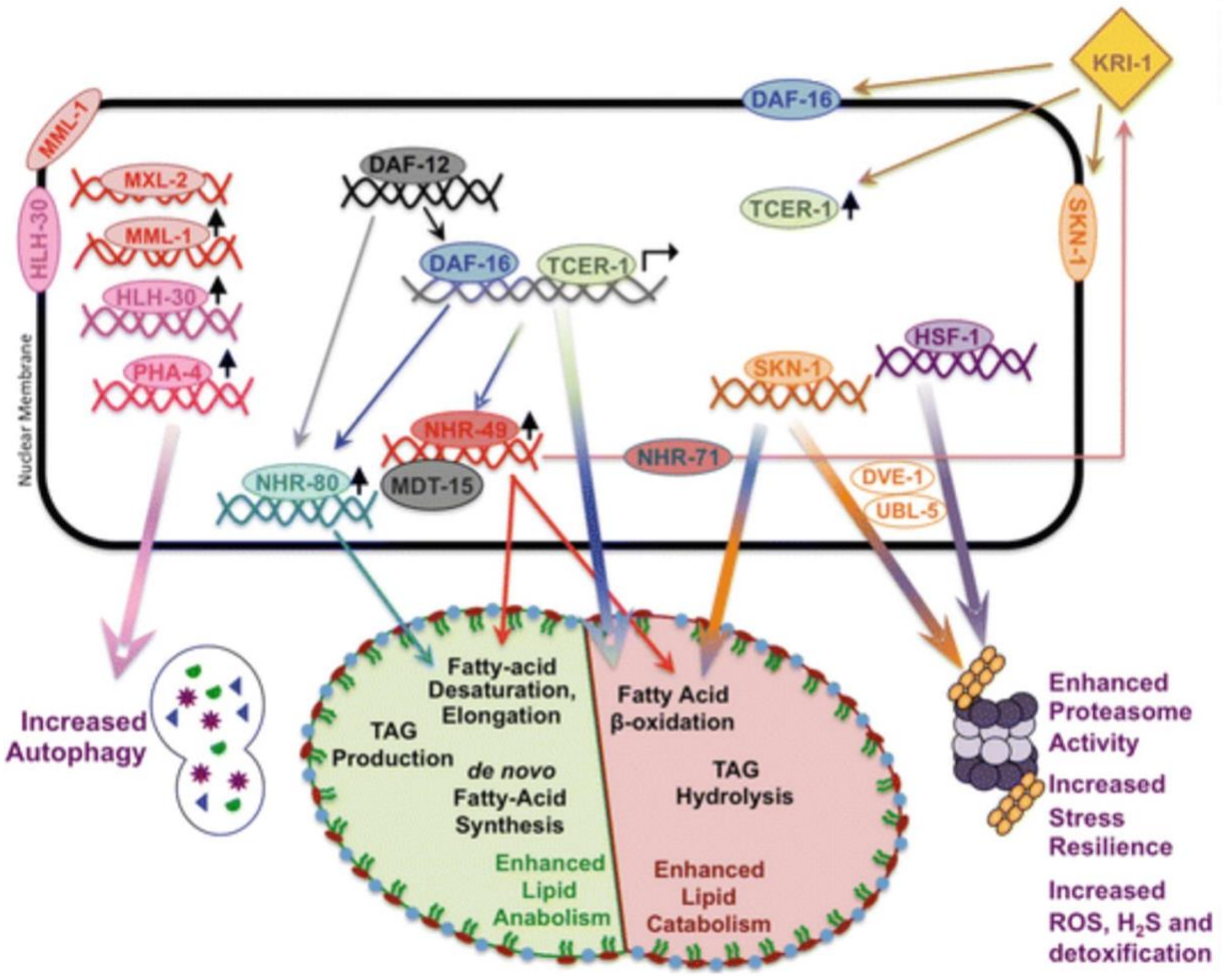

Figure 1.1 Key transcription factors activated by germline stem cell removal in *C. elegans*. Following the removal of germline stem cells, transcription factors localize to the nucleus and induce the expression of a concert of overlapping and specific genes that promote longevity. Proteins undergoing nuclear relocation (DAF-16/FOXO3A, SKN-1/ NRF2, HLH-30/TFEB and MML-1) are shown on membrane of, and within, the nucleus. Upward arrow next to proteins indicates transcriptional upregulation upon GSC loss (TCER-1/TCERG1, PHA-4/FOXA, NHR-80/HNF4 and NHR-49/PPARα). DAF-16/FOXO3A nuclear localization is governed by multiple inputs, including the dafachronic-acid cascade. KRI-1 also enhances TCER-1/TCERG1 transcription and SKN-1/NRF2 nuclear entry. NHR-80/HNF4 upregulation is controlled by

DAF-12/VDR and, in part, by DAF-16/FOXO3A. NHR-49/PPARα upregulation is partially triggered by DAF-16/FOXO3A and TCER-1/TCERG1. NHR-49/PPARα participates in a positive feed-back loop, possibly in collaboration with NHR-71/HNF4, to potentiate DAF-16/ TCER-1 activity by altering the subcellular localization of KRI-1/KRIT1. The main cellular processes modulated by these factors include lipid metabolism, autophagy and protein homeostasis. DAF-16/FOXO3A acts with TCER-1/TCERG1 to elevate both lipid-synthetic and lipid-degradative pathways. SKN-1/NRF2 shares the regulation of some of these processes. NHR-49/PPARα (in cooperation with MDT-15) stimulates β-oxidation and fatty-acid desaturation, whereas NHR- 80/HNF4 promotes fatty-acid desaturation alone. SKN-1/NRF2 and DAF-16/FOXO3A enhance proteasomal activity, while autophagy is augmented by PHA-4/FOXA, HLH-30/TFEB and the MML-1/MXL-2 complex. Improved heat- and oxidative stress resistance is mediated by HSF-1/HSF, SKN-1/NRF2 and, partly, DAF-16/FOXO3A. Figure adapted from (99).

1.2.2 NHR-49 and TCER-1

NHR-49 and TCER-1 are conserved pro-longevity transcription factors which are part of the network of regulators that enable *glp-1* germline-less longevity. My work centers on these two genes due to their functions in fertility, lifespan, and immunity. The first characterizations of these genes provided a critical foundation for my studies.

NHR-49 is a Nuclear Hormone Receptor (NHR), which is an ancient superfamily of ligand-activated transcription factors in metazoans which regulate gene expression in response to environmental, developmental, and nutritional cues. These transcription factors are known for their ability to fine-tune the expression of diverse and specific gene networks in a context-

dependent manner (100). Due to the ~6X expansion of the NHR family in worms compared to humans, *C. elegans* NHRs are attractive to study as they perform more specialized functions than their mammalian counterparts (100). Among the 48 NHRs in humans, PPARα is the central regulator of fatty acid metabolism (101). In accordance with this gene's role to reduce free fatty acids levels in the body, PPARα ligands are effective lipid-lowering drugs for diabetics (102). NHR-49 is the one identified *C. elegans* NHR which functionally resembles the critical PPARα. Similar to PPARα effects in mice and humans, NHR-49 is necessary for induction of fatty acid β-oxidation and desaturation genes. Thus, *C. elegans nhr-49* mutants were reported to have elevated fat content, with a higher proportion of saturated fats (103).

NHR-49 was initially of interest because it enables longevity in the *glp-1* germline-less model and was shown to be a pro-longevity factor in normal worms. Studies from our laboratory and others have since characterized the broad effects of NHR-49 activity on lifespan and stress resistance, leading to this thesis. For instance, our laboratory found that NHR-49 enhancement of fatty acid β-oxidation and lipid desaturation was the mechanism by which NHR-49 promotes longevity in germline-less and wild-type worms (104). Other studies also found that NHR-49 lipid metabolic regulation and transcriptional control is necessary for resistance to oxidative stress (105). Notably, this effect in stress resistance led us to find that NHR-49 promotes immunity to *P. aeruginosa*. Considering this gene's identity as an NHR, and other trends with pro-longevity genes, this led to our interrogation of the tissue-specific effects of NHR-49 on immunity and lifespan in Chapter 2.0.

TCER-1, another pro-longevity transcription factor of interest, is the worm homologue of human Transcription Elongation Regulator 1 (TCERG1). TCER-1/TCERG1 is a nuclear protein known to regulate transcriptional elongation and pre-mRNA splicing, as well as the expression

of a concert of genes (106, 107). TCER-1 was initially used to better understand neurodegenerative disease, as it was found to interact with the Huntingtin protein (108). TCER-1 was then identified by my advisor, Dr. Arjumand Ghazi, as a factor necessary for the long life of germline-less *glp-1* models (109). Further studies by our laboratory then cemented TCER-1's status as a conserved pro-longevity gene. My advisor found TCER-1 overexpression increases lifespan in normal, fertile worms (109). Our group then showed that TCER-1 promotes longevity in cooperation with DAF-16/FOXO3A by establishing lipid homeostasis following germ line loss (110). During these studies TCER-1 was found to be required for the optimal fertility of wild-type animals and a suppressor of reproduction-related genes in sterile *glp-1* animals (110). In support of its conservation in fertility, TCERG1 is highly enriched in vertebrate oocytes, including mice, monkeys and humans (111, 112). Also, TCERG1 levels diminish significantly with age in both women and mouse oocytes in a manner similar to our observations that TCER-1 declines with age in the worm germ line (10, 113, 114). This work led to discussion that TCER-1 serves to balance fertility and longevity investments in animals throughout its lifetime; leading to our key discovery that TCER-1 also suppresses immunity (Chapter 3.0). Thus, TCER-1—which impacts reproduction, immunity, and lifespan—is an ideal target for the study of RIL tradeoffs. The next sections will describe the fertility and immunity traits of *C. elegans* which further make it a suitable model to assess the molecular mechanisms exerted by the 'RIL regulators,' NHR-49 and TCER-1.

1.2.3 Fertility studies in *C. elegans*

C. elegans is a self-fertilizing hermaphrodite whose reproductive system gives rise to both sperm and eggs. Nicknamed "a transparent window into biology" in Corsi *et al.*, they have

two gonad arms which hold germ cells in a gradient of meiotic progression (115). In these hermaphrodites sperm is produced during larval development before the organism "switches" to oogenesis with adulthood. As oocytes undergo meiotic maturation, they may become fertilized with self-sperm in the spermatheca. The eggs then enter a shared uterus and are laid through vulva. Thus, without mating, *C. elegans* can lay approximately 300 fertilized embryos over ~5 days after reaching adulthood. Hermaphrodite fertility is at its peak in Day 2 of adulthood, and the number of eggs laid daily wane until worms are post-reproductive for the final half of their lifespan. While males in the species exist, I only utilize males for genetic crossing and have not examined any potential sex differences in the RIL axis.

The *C. elegans* model possesses many strengths for studying reproduction. As noted, single hermaphrodites self-fertilize without needing to wait for a mate and produce a large brood which is easy to monitor for perturbations in fertility. Early on, *C. elegans* reproductive research mostly involved the identification of sterile mutants, which helped detail mechanisms underlying spermatogenesis, embryogenesis (116, 117) and gonadogenesis (118, 119). *C. elegans'* utility in meiosis studies have also helped dissect intricate problems, such as how chromosomes identify their homologous partners and how they are structurally remodeled in pairing and synapsis (120). *C. elegans* work has also described meiotic processes that promote accurate chromosome segregation, as its simple to monitor for a 'high incidence of male progeny' caused by X chromosome missegregation (121). Researchers were also able to study sperm- and oocyte-specific effects using feminized *C. elegans* mutants which do not produce sperm and test the effect of mating to males separately (122, 123). Reproductive studies have since looked at reproductive span (124, 125), oocyte quality (75, 123, 126), and sperm-oocyte communication

(127). In sum, these works have led to the naming of reproductive-aging pathways, from the aging of oocytes to the coordinate effects of germline signaling to the soma (128).

C. elegans is a particularly useful reproductive model in the context of this thesis, which seeks to understand the relationship between reproduction, lifespan, and immunity. Indeed, *C. elegans* exhibit strong fertility-lifespan tradeoffs, particularly in challenging environments (129, 130). For instance, it is known that starved *C. elegans* produce fewer self-progeny than well-fed animals (131). Similarly, our laboratory has recorded a diminished brood size in worms infected with pathogen (10). This supports the premise that fertility and immunity have energetic costs, and their tradeoffs hinge on limited cellular resources going to one process or the other. One of these "cellular resources" is likely to be fats, as adipose tissues serve as both an energetic reserve and active signaling component in fertility and immunity (132, 133) . In fertile *C. elegans*, fat allocation from the soma to the germ line occurs in a highly visible manner (134). This trafficking is mediated by yolk proteins known as vitellogenins, common to most all egg-laying animals, to promote progeny health (135). In support of fat resources mediating tradeoffs, studies have found vitellogenins support fertility and suppress immunity (76, 136, 137). While the study of fat allocation in tradeoffs is not a focus in this thesis, it is pertinent to this work because (a) both NHR-49 and TCER-1 have been shown to impact lipid metabolism, and (b) other studies in our laboratory have suggested that TCER-1 controls lipid-hydrolysis genes to govern the deposition of fats into embryos (Bahr, Amrit, and Ghazi, unpublished).

1.2.4 Innate immunity studies in organisms and *C. elegans*

C. elegans possesses an ancestral innate immune system to survive pathogens in their environment. As soil and water-dwelling organisms, they naturally encounter an array of

pathogens while feeding, and have developed mechanisms to endure them. Infection in *C. elegans* often occurs from contact with the epidermis, or after intestinal colonization following ingestion. Like most animals, their tissue linings provide a measure of protection as physical barriers. Yet, studies make it clear that *C. elegans* upregulate a concert of specific and shared effectors to fight varied infections (138, 139). This ability to resist infection in such coordinated and specific ways, while their immune system is relatively simple overall, has long made *C. elegans* an attractive model in innate immunity studies (reviewed in (79, 140)). Work with this model has yielded a better understanding of immune regulation and its connection with the often-correlated traits of stress resistance and longevity (141). At many points in this work, this system has helped me test for immune phenotypes and identify novel immune effectors that may underlie RIL tradeoffs.

C. elegans immunity evolutionarily predates more complex mechanisms of immunity seen in higher organisms and mammals. For this reason, *C. elegans* have no dedicated immune cells like the hemocytes in most invertebrates, and they do not synthesize antibodies for immune memory like mammals. Yet, they possess components of the innate immune response that are shared across species (**Fig. 1.2**). Beyond the barrier defenses mentioned, their secretion of antimicrobial proteins (AMPs) is a highly conserved innate immune mechanism shared across species. *C. elegans* AMPs include caenopores/saposin-like proteins, defensin-like peptides, caenacins/neuropeptide-like proteins, and lysozymes, which are mostly thought to attack bacteria by permeabilizing their cell wall (142). Like other animals, *C. elegans* also has **cell surveillance mechanisms (CSMs)** which trigger the transcription of immune effectors. CSMs are a collection of signaling pathways activated by cell damage, which can often be caused by infection. CSMs include the cytoprotective signaling of the **heat-shock response (HSR), oxidative stress**

response (OSR), the unfolded protein response of the ER (UPRer) and mitochondria (UPRmt), and others (reviewed in (143, 144)). Immune regulation using small RNAs (smRNAs), often associated with antiviral defense, is another conserved immune mechanism which will be discussed in depth in the next section.

Regardless of the mechanism for sensing pathogen infection, the ubiquitous upregulation of critical immune effectors across species is largely attributed to the activity of signal transduction pathways, such as the mitogen-activated protein kinase (MAPK) cascade (**Fig. 1.3**). The main immune regulatory signaling pathways of *C. elegans* include the PMK-1/p38 MAPK, Sma/TGFβ, and Insulin/IGF-1 (IIS) axes. MAPKs are sequentially-activating protein kinases which can convert extracellular stimuli into the coordinate upregulation of genes essential for proliferation, stress response, and immune defense (145). Conversely, the conserved PMK-1/p38 MAPK pathway is the main *C. elegans* MAPK module controlling immunity (reviewed in (79, 146)). A significant proportion of transcriptional upregulation of immunity is dependent on PMK-1, the *C. elegans* p38 MAPK homologue (147, 148). Research of the p38 MAPK pathway using *C. elegans* has been instrumental in dissecting MAPK crosstalk and identifying immune effectors (148, 149). Studies also show the conserved Sma/TGFβ pathway to be a central immune regulator. For instance, DBL-1, encoding one of four TGF-β-like ligands in *C. elegans*, is associated with the induction of important lectins, lysozymes, and lipases for immune defense (150). In fact, loss of Sma/TGFβ pathway genes lowers *C. elegans* resistance to a number of clinically-relevant pathogens, including *Escherichia coli*, *Enterococcus faecalis*, *Pseudomonas aeruginosa*, and *Serratia marcescen* which infect a broad range of hosts (151). Yet, here it is worth noting *C. elegans* in the wild have different natural pathogens than what is typically tested in *C. elegans* immunity studies. For instance, *C. elegans* experience natural infections from

oomycete *Myzocytiopsis humicola*, microsporidia *Nematocida parisii,* fungus *Drechmeria coniospora,* and the Nodavirus-like Orsay virus (152, 153). Nonetheless, as stated previously, work assessing infections from non-natural pathogens has identified conserved Insulin/IGF-1 pathway as another pillar of innate immune regulation which controls numerous aging- and stress- associated processes (154, 155). In fact, transcriptional profiling of DAF-16 regulation concludes that many stress response and immunity genes overlap in support of pathogen survival. DAF-16 activation upregulates a unique signature of antimicrobial genes for immunity (138). Yet, since the immune resistance of *daf-2* mutants is partially dependent on PMK-1 activity, the IIS and p38 MAPK axes are recognized as pathways with overlapping, yet distinct, immune targets (148). Taken together, these three central immunity pathways provide a framework to better characterize immune alterations in animals and help us identify unexplored mechanisms of RIL tradeoffs.

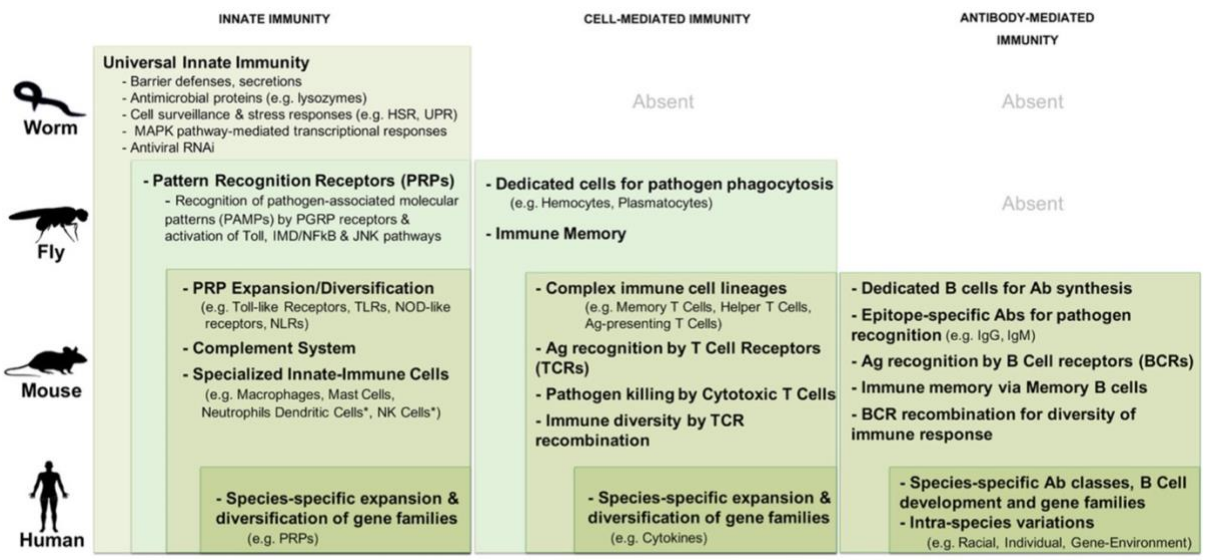

Figure 1.2 Comparison of immune systems across invertebrate and vertebrate species.

The main constituents of the immune systems of the invertebrate (worms, flies) and vertebrate (mice, humans) species are depicted. A universal innate immune response (left column) is conserved from worms to flies, whereas vertebrate lack several major elements of adaptive immunity (middle and right columns) in mammals. The major features of each arm of the immune system are recapitulated along with layers of complexity added at each evolutionary level (shown by nested rectangles). Ab, antibody; Ag, antigen; HSR, heat shock response; PGRP, peptidoglycan pattern recognition receptor; UPR, unfolded protein response. Figure from (9).

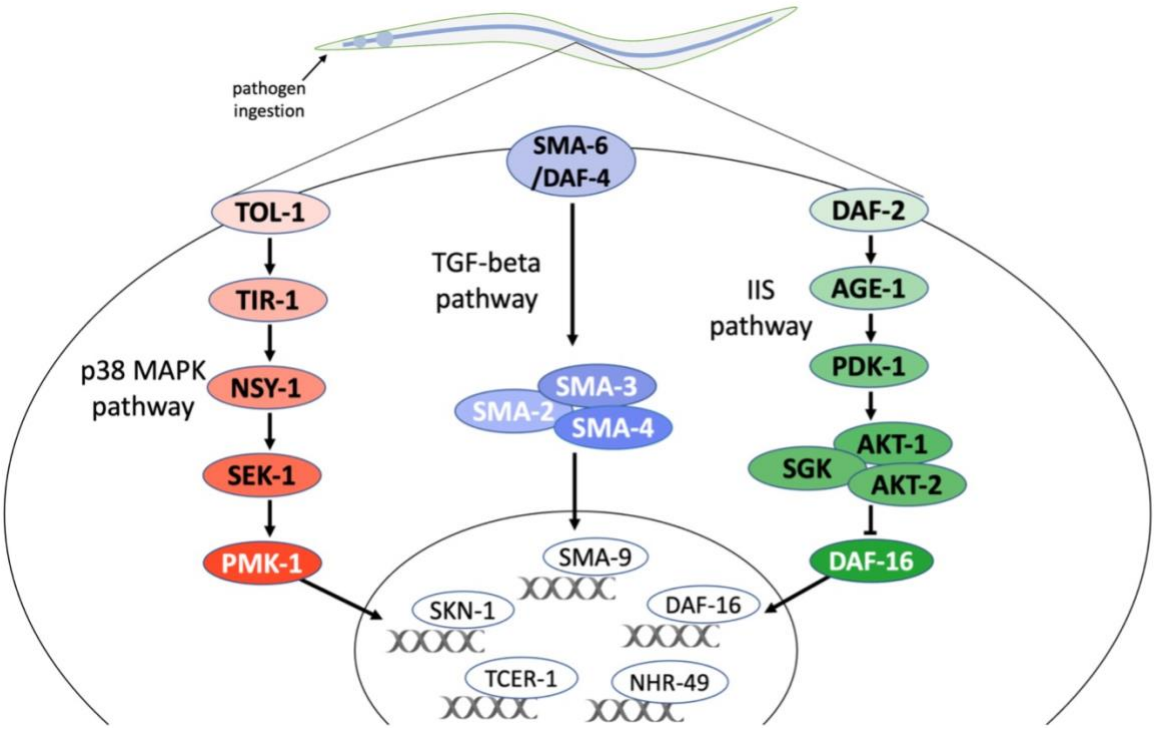

Figure 1.3 Key *C. elegans* immunity pathways.

Schematic of the most influential innate immunity signaling pathways in *C. elegans*. These pathways include the conserved p38 MAPK, TGF-beta, and Insulin/IGF-1 Signaling (IIS) pathways. Represented genes with receptor activity (on cell membrane) include the TOL-1/TLR, SMA-6/DAF-4/TGFβR, and DAF-2/IGF1R. Activated transcription factors within the nucleus include SKN-1, SMA-9, and DAF-16. Additional immunity transcription factors discussed in this thesis are NHR-49 (exerts tissue-specific control over immunity) and TCER-1 (suppresses immunity). Figure adapted from (156) and (157).

1.2.5 Small RNAs in immunity

Post-transcriptional gene silencing mediated by small RNAs (smRNAs) modulates a panoply of biologic processes across species (158). Their ability to regulate gene expression on such a fundamental level, with ranging specificity, is what allows them to make profound

functional changes in animals. Thus, smRNAs play critical roles in diverse processes including development, fertility, and genomic stability (159). The conservation of this mechanism in animals has allowed *C. elegans* work to drive smRNA studies, with the discovery of the first micro-RNA, *lin-4*, and other seminal findings attributed to the model (reviewed in (159, 160)). Subsequent advancements in technology, particularly deep sequencing and smRNA-specific sequencing techniques, has steadily revealed the wide diversity of smRNA species in animals and their functions (161, 162)).

The three main smRNA types are **microRNAs (miRNAs), small-interfering RNAs (siRNAs), and Piwi-interacting RNAs (piRNAs)** whose biosynthesis pathways generate short (~18-30nt) RNA molecules mostly known for their ability to silence complementary mRNA (**Fig. 1.4**). These pathways have both shared and distinct biosynthesis proteins, origin loci, and targets that define each. For instance, DCR-1 is used in both miRNA and siRNA pathways to cleave precursor dsRNA in biogenesis. Yet, several argonaute genes, such as ALG-1/2, ALG-3/4, and PRG-1, are specific to the mi, si, and piRNA pathways, respectively, and are largely responsible for their unique functionality. miRNAs, which can silence imperfectly-matching mRNAs outside of their heptameric "seed" sequence, regulate a diverse set of mRNA targets most notably essential to development. In fact, miRNA-defective *alg-1;alg-2* double mutants show lethality from a range of developmental effects (163). piRNAs and siRNA are known for their conserved role in maintaining genome stability in animals, as they silence transposon activity in the germ line (164). Yet while piRNA activity is restricted to the germ line, additional roles of the siRNA pathway in the soma are still being explored (165). The siRNA pathway is of particular interest to my work because, not only do they require perfect complementarity to silence mRNA, TCER-1 loss disproportionately affects siRNA production compared to other

smRNA types (Chapter 4.0). Although exogenous smRNAs can influence gene expression as well, this work focuses on endogenously-produced smRNAs to understand inbuilt regulators of RIL tradeoffs.

The siRNA branch can be further divided into two '22G' (22nt 5' guanosine) small RNA classes after synthesis of its larger '26G' precursors. These two 'WAGO' and 'CSR' 22G siRNA classes are named after the argonautes which they bind. WAGOs are worm-specific argonautes which bind 22G RNAs to silence transposable elements, pseudogenes, and other somatic genes. CSRs control germline-expressed transcripts, mainly to promote proper chromatin organization in mitosis (161). Importantly, WAGO accumulation depends on Mutator foci activity, which is why WAGO siRNAs are sometimes referred to as 'MUTs.' Mutator foci are complexes which surveil mRNAs exiting the nucleus near the protein- and RNA-rich nuclear pore-associated P granules in the germ line. Although Mutator proteins are primarily localized to the germ line, many studies propose that WAGOs also regulate somatic gene silencing (164, 166, 167). Our study of immune-suppressing TCER-1, which shows TCER-1 promotes WAGO siRNA production, and that many Mutator mutants have increased immune resistance (Chapter 4.0), supports this notion that WAGOs can affect non-germline processes as well.

Other than its functions in development, smRNA mechanisms are typically associated with their role in viral resistance (168). Yet, over the years studies of smRNA regulation have increasingly acknowledged their impact on bacterial immunity. For instance, studies in both *C. elegans* and mammals have found miRNAs reshape immune response (169, 170). Mammalian studies attribute these effects to smRNAs regulating gene expression in cells of the innate and adaptive immune system (171). Yet further work in *C. elegans*—which do not possess dedicated immune cells—has shown that smRNAs impact ubiquitous components of innate immunity.

These components include the IIS pathway, p38 MAPK axis, and the UPR (172, 173), often identified in studies using *P. aeruginosa* exposure (174, 175). Early indications from other studies that TCER-1 modulates smRNA pathways therefore led us to study the potential role of TCER-1-dependent smRNAs in its immune suppression (Chapter 4.0). That is, a previous unbiased, whole-genome screen identified TCER-1 as a gene essential for *C. elegans* RNAi fidelity, which is a process that depends on functioning smRNA biosynthesis (176). Another study reported that *tcer-1* mutants also have reduced endogenous siRNA activity (177). Thus, my findings in Chapter 4.0, which shows TCER-1 suppresses immunity by controlling the biogenesis of specific smRNAs, further supported the role of this mechanism in antibacterial immunity.

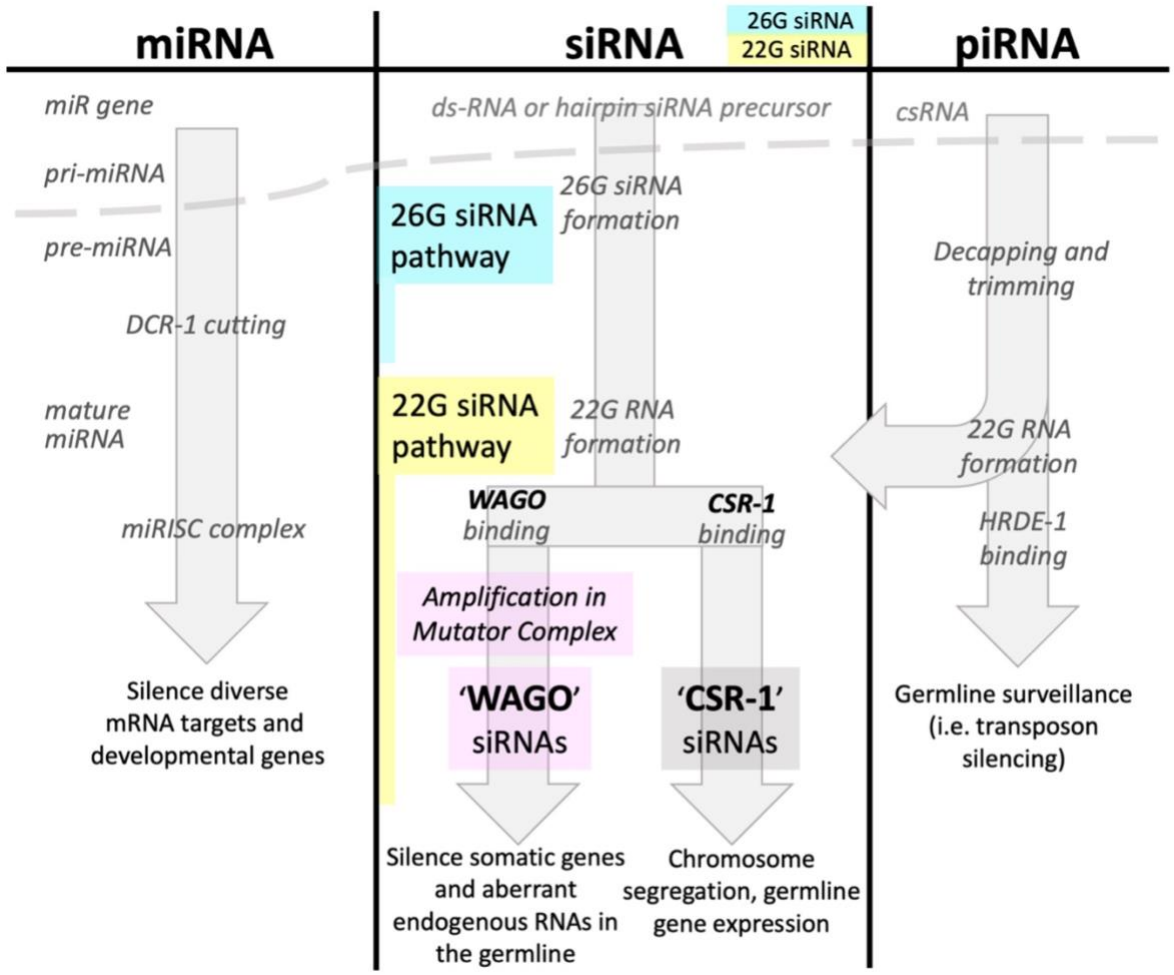

Figure 1.4 Key endogenous small RNA pathways in *C. elegans*.

Schematic of the endogenous micoRNA, siRNA, and piRNA pathways in *C. elegans*, including the additional 26G and 22G siRNA classes that bind WAGO or CSR-1 argonautes. Pink box highlights influence of the Mutator Complex, involved in WAGO siRNA amplification. Functional impacts of each smRNA class include, but are not limited to, the processes listed. Participating proteins necessary for the biogenesis, amplification, and argonaute loading for target effects, include, but are not limited to, the proteins listed. Schematic adapted from Hoogstrate et al 2014 (161).

1.3 Molecular mechanisms governing the lifespan-fertility-immunity axis

Understanding the molecular mechanisms governing animals' investments in lifespan, fertility, and immunity traits has proven to be a challenge in research. For instance, much of our knowledge the immune adaptations of pregnancy, and the links between inflammation and poor pregnancy outcomes (described in Section 1.1.2), are derived from investigations in rodent models (54, 178). In particular, studies in knock-out mice have allowed for comparisons of lifespan, pregnancy rates, and tissue effects, linking these to changes in specific immune populations (179, 180). However, studies with rodent models, while mirroring human biology closely, are hampered by their long lives and low progeny number compared to other models (mice live ~2 years, worms live for ~3 weeks). The inherent complexities of the adaptive immune system in vertebrates also pose challenges to performing mechanistic studies. Assessment of lifespan-fertility-immunity crosstalk in invertebrates which are often short-lived, yield large broods, and rely on innate immunity alone, is therefore critical to understanding their relationships (181, 182). Thus, an extensive body of invertebrate literature—originating from life history research—has documented the relationships between lifespan, reproductive activity, and immune resistance (reviewed in Section 1.1.3 and (1, 62)). *Drosophila* studies were some of the first to detail the relationship between mating, immune resistance, and longevity (62, 70). Further studies in *C. elegans* have been instrumental In revealing the genes and pathways involved in the RIL dialogue (9). Thus, following sections will discuss the central signaling pathways and proposed transcriptional regulators of the RIL axis. Beyond its unique establishment as a model in lifespan, fertility, and immunity, the fact *C. elegans* studies are responsible for many of these discoveries assert its value as a system to study the RIL dialogue.

1.3.1 Signaling pathways involved in the lifespan-fertility-immunity axis

Assessment of the lifespan-fertility-immunity crosstalk in invertebrates has proposed control from several signaling pathways. In *Drosophila*, two aging-associated signaling pathways have been implicated in directly linking the immune and reproductive systems. These are the juvenile hormone (JH) and 20-hydroxyecdysone (20E) pathway, and the insulin/IGF1 (IIS) signaling pathway (62) (**Fig. 1.5**). In insects, JH and 20E are major endocrine regulators whose balance mediates proper progression through development and metamorphosis, and whose activity both antagonize longevity (183-185). For many insect species, the elevation of JH levels and depression of 20E levels during mating is thought to mediate RIL tradeoffs. This is because JH is anti-immunity and 20E is pro-immunity, suggesting that immune suppression during mating benefits fertility. This is supported by additional evidence that JH impacts resource allocation and longevity in some insects, whereas, it drives the tradeoff between reproduction and flight capacity in others (186-189).

The insulin/IGF1 signaling (IIS) pathway is another prominent candidate mediator of the RIL dialogue. The IIS pathway, which links nutritional status to growth and proliferation, is shown to have many conserved effects across species. Studies in *Drosophila* have particularly given insight into this pathway's role in the RIL dialogue. For instance, fly research has shown that IIS drives oogenesis in the female and, conversely, reduced-IIS decreases egg production (190). IIS also represses immune resistance and longevity such that reduced-IIS increases immunity in many species (62, 191). Although JH is restricted to insects, it is interesting to note that IIS similarly promotes *C. elegans* reproduction as it acts in meiotic progression and sperm guidance (192, 193). Indeed, suppressing IIS results in the elevated expression of a spectrum of longevity and immune-associated genes in the *C. elegans* model (79). Yet, the downstream

molecular mechanisms of IIS effects, which might explain why suppression of immunity is associated with increased fertility—and other RIL relationships—have not been fully characterized. Thus, the IIS pathway is a proposed regulator of reproduction, immunity, and lifespan tradeoff relationships which, despite its extensive study, is still being explored.

Other signaling cascades also have plausible roles in regulating the RIL axis. The immune-responsive Jun-N Kinase (JNK) cascade is reported to repress IIS signaling for longevity in *Drosophila* (194). The TGFβ pathway plays a protective role during pathogenesis in *C. elegans*, and additionally regulates reproductive aging (79, 123). The conserved p38 MAPK cascade—a cornerstone of worm immunity and lifespan—similarly controls germline apoptotic maintenance during infection (79, 195, 196). *Drosophila* studies also see that both the p38-mediated MAPK and TGFβ pathways promote immunity and influence reproductive fitness (197-200). Hence, it is conceivable that these pathways' interactions shape RIL traits in a functionally conserved manner. Nonetheless, the characterization of regulators which control the RIL dialogue more directly is a driving motivation of this thesis.

1.3.2 Transcriptional regulators involved in the lifespan-fertility-immunity axis

Signal transduction cascades transmit physiological and environmental information to downstream transcription factors to enact gene expression changes. Thus, transcription factors themselves also impact the RIL dialogue. Indeed, reduced IIS signaling enables the activity of several transcription factors—including the conserved FOXO members, DAF-16 in worms and dFOXO in flies—to trigger the transcription of a cytoprotective gene network complementary to RIL processes (201). Considering this, recent studies have proposed that certain transcription factors could be 'master regulators' of RIL tradeoffs. We have discovered such a role for TCER-

1, the *C. elegans* homolog of the human transcription elongation and splicing factor, TCERG1 (106, 107). As described in section (1.2.1), we first identified TCER-1 as a factor that conferred enhanced lifespan in *C. elegans* adults lacking a germ line (109). In investigating its functions in normal, fertile animals, we discovered that TCER-1 was essential for fertility and reproductive health. *tcer-1* mutants laid fewer, and less healthy, eggs and showed signs of premature reproductive senescence (110). Interestingly, our ensuing work showed that *tcer-1* mutants have exceptional resistance against *P. aeruginosa* and other Gram-positive and Gram-negative pathogens. Conversely, TCER-1 overexpression decreased resistance upon infection and even blunted fertility loss in this condition (10). Given that pro-longevity genes often enhance stress resistance, this unexpected discovery led to our classification (Chapter 3.0) of TCER-1 as a novel pro-longevity factor which promotes fertility and widely suppresses immunity, ultimately regulating RIL tradeoffs.

Our discovery that TCER-1 is one of the first identified arbiters of the RIL crosstalk is particularly interesting because it opens avenues to explore the complex molecular basis of resource allocation. In both invertebrates and vertebrates, the primary cellular resource suspected to meet the high energetic demands of reproduction (i.e., massive production and deposition of fat, proteins, and organelles in eggs) is stored fat. Fat also fulfills the high-energy required to mount immune response during infections across phyla (202, 203). Lipids therefore serve as key signaling molecules for orchestrating immune/stress tolerance gene expression and progression of many, if not all, steps of reproduction (202). Indeed, several strong lines of evidence in both flies and worms that suggest that cellular lipids form a vital link between fertility and immunity in aging. For instance, TCER-1 promotes longevity by mediating widespread changes in lipid anabolic and catabolic pathways and maintaining lipid homeostasis in germline-less worms,

suggesting its regulation of lipid metabolism supports fertility and inhibits immunity (110). Interestingly, another conserved pro-longevity factor, SKN-1, worm homolog of the human protein NRF2, has been shown to direct lipid deposition in tradeoff situations (204). Indeed, the Curran lab found that exposure to pathogenic *P. aeruginosa* caused a rapid depletion of somatic lipids similar to the SKN-1-dependent transfer of somatic fats to the eggs. On this note, SKN-1 gain-of-function mutants are also susceptible to pathogen-induced death while restoring their low somatic fat levels also restores their immunity (204).

Evidence that lipid allocation underlies immunity and fertility investments also comes from the study of CEH-60 and UNC-62, which are *C. elegans* orthologs of the TALE class of homeodomain transcription factors PBX and MEIS, respectively. In a recent study, Robert Dowen demonstrated that CEH-60 and UNC-62 act in a complex to directly activate the expression of vitellogenin proteins that transport fat into eggs and repress stress- and immune-responsive genes (**Fig. 1.5**) (82). Consequently, *ceh-60* mutants have both reduced fat deposition in their eggs and increased immunity against *P. aeruginosa* (82). The RIL-influencing signaling cascades discussed in the previous section also link fats to immune response. *Drosophila* JH, linked to conserved IIS function, is critical for the incorporation of vitellogenins and associated lipids into maturing oocytes. Conversely, pathogen exposure (or genetic immune activation), which suppresses IIS, leads to decreased triglyceride levels in the fly fat body (205, 206). Whether lipids are the only resource whose allocation directs the immunity-fertility balance, and the changes lipids undergo to cause such effects, remains unknown. Although the study of fat allocation in tradeoffs is not a focus in this thesis, these findings suggest the potential molecular mechanisms employed by RIL axis 'master regulators,' supporting the importance of studying them.

Many questions remain about the role of identified transcription factors in the RIL dialogue. Indeed, the CEH-60 complex is a compelling regulator of immunity and fertility, but we were also interested in ways longevity might be regulated. When I began the work of this thesis, studying longevity-promoting factors was a particularly attractive option to understand reproduction, immunity, and longevity regulation alike. NHR-49 and TCER-1 were therefore prime candidates to study the RIL axis due to their effects in reproduction, immunity, and lifespan.

As noted, NHR-49 is a pro-longevity transcription factor with clear roles in other RIL traits. Our laboratory has shown that this gene, and proposed functional homologue to vertebrate protein PPARα, upholds a 'healthy' lipid profile by promoting fatty acid β-oxidation and lipid desaturation. Further work then showed that these lipid metabolic effects are the mechanism by which NHR-49 promotes longevity (104). Later findings that NHR-49 was also important to resistance against oxidative stress then prompted my study of this gene in immune resistance (105, 207). My preliminary experiments revealed that NHR-49 increased immunity to *P. aeruginosa* (PA14) in both wild-type and *glp-1* germline-less animals (8). Due to our awareness of (a) potentially distinct control of lifespan and immunity traits by genetic factors in animals and (b) the frequently context-dependent gene regulation exerted by NHR's, this made NHR-49 an excellent candidate to test for tissue- and sterility-dependent control of these traits. As described in Chapter 2.0, this work showed that although NHR-49 generally promotes innate immunity and lifespan, it regulates these processes distinctly depending on context. Findings like these demonstrate the importance of performing site-of-action studies on alleged health-promoting genes and supports the body of work showing that improving healthspan is an intricately different matter than simply extending lifespan (43, 208).

Much like NHR-49, TCER-1 was a prime candidate to understand the RIL dialogue for its established effects in longevity and fertility. When I began my study of this gene, lab member Dr. Francis RG Amrit soon found that TCER-1 suppresses resistance to a range of stresses. Specifically, *tcer-1* loss-of-function mutants were more resistant to heat, oxidative stress, and DNA damage than wild-type animals. Further work along these lines then revealed that TCER-1 suppresses immunity to the Gram-positive human opportunistic pathogen *Staphylococcus aureus*, and particularly the Gram-negative pathogen *P. aeruginosa.* Interestingly, this phenotype meant that, despite the widely-observed correlation that lifespan-extending mutations also improve stress resistance, TCER-1 simultaneously promotes longevity while suppressing immunity and stress resistance (34, 37). This set TCER-1 apart as a novel pro-longevity gene that widely suppresses immunity and stress resistance and served as the foundation for our publication discussed in Chapter 3.0. These early findings led to our hypothesis that TCER-1 was a regulator of the RIL dialogue. My studies supported this concept as I conducted an experiment that found TCER-1 no longer inhibits innate immunity in post-reproductive worms (10). I also identified downstream functional immune targets of TCER-1 that were independent, and dependent on, the canonical p38 MAPK pathway in *C. elegans* immunity. My later molecular characterizations then showed TCER-1 promotes the production of certain smRNA species to suppress immunity in fertile animals (Chapter 4.0). Since TCER-1 so uniquely recapitulates RIL tradeoffs—and the fact longevity, innate immunity, and reproduction are such conserved processes—my studies therefore contribute vital description of molecular mechanisms impacting the RIL axis.

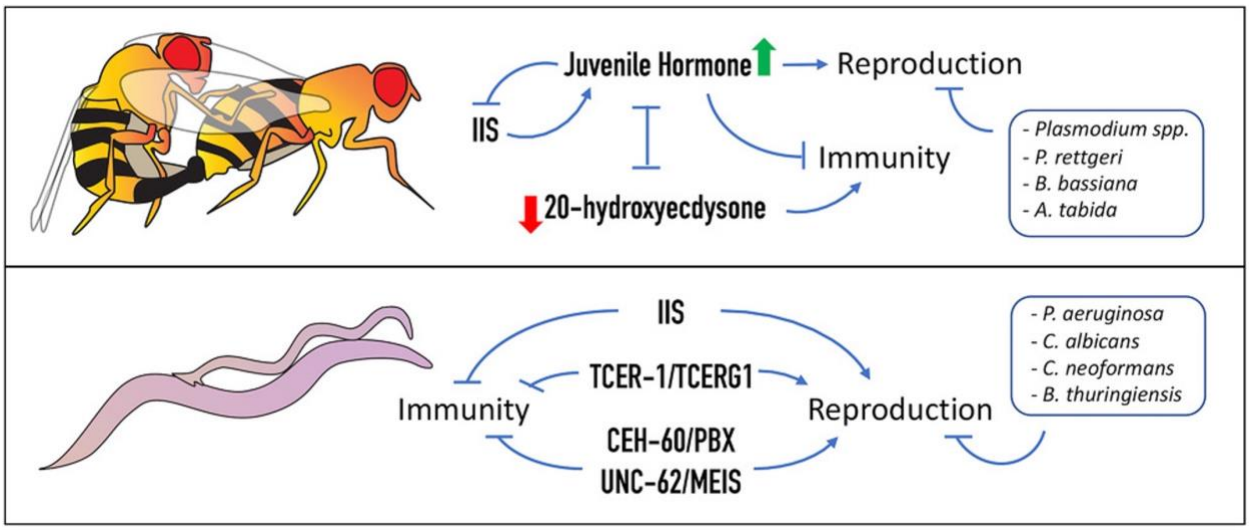

Figure 1.5 Molecular Determinants Governing the Fertility-Immunity Axis in Invertebrates.

There is extensive literature documenting the mutual impacts of reproductive activity and immunity in invertebrates. Studies in the fruit fly, *D. melanogaster* (top), and the nematode, *C. elegans* (bottom), have begun to reveal the underlying molecular pathways. In *D. melanogaster* (top panel), major endocrine signaling cascades, the juvenile hormone (JH) pathway and the 20 hydroxy ecdysterone (20E) pathway, that control growth and maturation, have antagonistic impacts on fertility and immunity. JH promotes reproduction and inhibits immunity, along with the conserved growth regulator, the insulin/IGF1 signaling (IIS) pathway, whereas, 20E acts as an immune activator. The IIS pathway also inhibits immune activity and supports reproductive health in *C. elegans* (bottom panel). Recent studies in worms have also identified transcription factors with roles in this relationship. TCER-1, worm homolog of human transcription elongation and splicing factor, TCERG1, promotes reproductive fitness and represses innate immunity. CEH-60 and UNC-62, worm orthologs of the TALE class of homeodomain proteins, PBX and MEIS, act in a complex to mediate fat transport into oocytes,

and to repress innate-immune genes' expression, facilitating allocation of lipids towards fertility. Figure from (9).

2.0 Cell nonautonomous roles of NHR-49 in promoting longevity and innate immunity

This chapter (2.1-2.4) is a slightly modified version of Naim et al 2020, Aging Cell. DOI: 10.1111/acel.13413.

Aging and immunity are inextricably linked and many genes that extend life span also enhance immunoresistance. However, it remains unclear whether longevity- enhancing factors modulate immunity and longevity by discrete or shared mechanisms. This chapter describes our finding that the *Caenorhabditis elegans* pro-longevity factor, NHR-49, also promotes resistance against the pathogen *Pseudomonas aeruginosa* but modulates immunity and longevity distinctly. NHR-49 expression increased upon germ line ablation, an intervention that extends life span, but was lowered by *Pseudomonas* infection. The immunosusceptibility induced by *nhr-49* loss of function was rescued by expression of NHR-49 in neurons alone, whereas the longevity reduction was rescued by expression in multiple somatic tissues. The well-established NHR-49 target genes, *acs-2* and *fmo-2*, were also differentially regulated following germ line elimination or *Pseudomonas* exposure. Interestingly, neither gene conferred immunity toward Gram-negative *Pseudomonas*, unlike their known functions against gram-positive pathogens. Instead, genes encoding antimicrobial factors and xenobiotic-response proteins upregulated by NHR-49 contributed to resistance against *Pseudomonas*. Thus, NHR-49 is differentially regulated by interventions that bring about long-term changes (life span extension) versus short-term stress (pathogen exposure) and in response it orchestrates discrete outputs, including pathogen-specific transcriptional programs. The findings discussed in this chapter therefore uphold many themes discussed about RIL regulation in Chapter 1.0, and describes novel functions of the well-studied pro-longevity protein, NHR-49.

2.1 Introduction

Recent advances in aging research have led to a shift in focus from increasing lifespan to improving healthspan, a concept that encompasses measures of physiological health, including stress resistance (48, 209-211). As discussed in Chapter 1.1, a strong positive correlation exists between longevity and stress resistance in model organisms and in nature, and many genes that increase lifespan have been reported to enhance stress resilience (34, 36, 37, 212). However, descriptions of long-lived mutants that do not exhibit elevated stress resistance, and *vice versa*, are observed in literature along with instances of pro-longevity genes that do not alter stress resistance (213-215). Our lab, and others, have identified genes that promote longevity but repress stress resilience demonstrating that these attributes are physiologically distinct (10, 216). Nonetheless, a large fraction of known pro-longevity genes promote stress resistance (34). This chapter therefore explores whether a pro-longevity gene, which also promote stress resistance, also governs lifespan and immunity by shared or distinct mechanisms.

Immunity (reviewed in Chapter section 1.2) is central to an organism's stress response and thus an integral measure of healthspan (48, 209). Age-related increase in disease susceptibility occurs across species, including in humans (217), as demonstrated by the COVID-19 pandemic's disproportionate impact on the elderly (218). While both the adaptive and innate immune systems undergo age-associated changes, the latter is a major focus of contemporary aging biology as inflammaging, a derailment of innate immunity causing chronic inflammation, has been postulated to underlie age-related pathologies (219-221). Moreover, longevity-promoting genes and drugs such as FOXO3A and Metformin, respectively, have been shown to ameliorate the inflammaging profile of older immune cells towards that of a younger cohort (222-224). To what extent such genes and drugs modulate immune status directly is unclear, and

has topical relevance to human aging biology. Their associated impacts on the other traits of RIL dialogue, the focus of this thesis, is also of key importance to understanding whole-organism effects.

As discussed in Chapter section 1.1, studies in the nematode, *Caenorhabditis elegans*, have been instrumental in identifying fundamental aging mechanisms, including the discovery that signals from the reproductive system influence lifespan and stress resistance (99). In worms, removal of a population of totipotent germline-stem cells (GSCs) increases lifespan dramatically (25). GSC-less animals also display extraordinary metabolic adaptability and resilience against stressors such as heat, DNA damage or infections by Gram-positive and Gram-negative pathogens (43, 99). The increased longevity of GSC-less worms is attributable to a network of transcription factors activated in somatic cells, including DAF-16, worm homolog of FOXO3A (99, 225). Similar phenomena observed in other species such as flies and mice (15, 23, 30, 226), and human population studies (24, 227) suggest that the reproductive control of aging may be widespread in nature and involve conserved genetic mechanisms (228-230). Previously, our laboratory identified a group of nuclear hormone receptors (NHRs) critical for GSC-less longevity, including NHR-49 (104), the worm functional homolog of the vertebrate energy metabolism regulator, peroxisome proliferator-activated receptor alpha (PPARα) detailed in Section 1.2.1. Our laboratory showed that NHR-49 coordinately upregulates the expression of genes involved in fatty acid β-oxidation as well as lipid desaturation and elongation to preserve lipid homeostasis and promote longevity (104). NHR-49 also orchestrates the transcriptional responses to acute starvation and oxidative stress (105, 207). Yet, whether NHR-49 promotes the immunoresistance of GSC-less worms remained unknown.

In worms and other organisms many cell nonautonomous regulators of longevity and stress resistance, including immunoresistance, have been identified (231-234). For instance, DAF-16, the key regulator introduced in Chapter section 1.2, is sufficient in intestinal cells to confer longevity on GSC-less worms (235) and *Drosophila* dFOXO in the fat body increases lifespan (236). But, intestinal DAF-16 cannot rescue the heat resistance of GSC-less animals and provides little lifespan benefit to the insulin/IGF1 receptor, *daf-2*, mutants whose longevity is also completely reliant upon it (89, 235). Thus, site-of-action and physiological context are both critical in determining gene function (237-239). Neuronal NHR-49 promotes longevity mediated by AMP-activated protein kinase, AMPK (240). But, where the protein acts to modulate lifespan in GSC-less animals, or the stress-response pathways it controls, was unstudied.

This chapter describes a role for NHR-49 in the innate-immune response against the Gram-negative pathogen *Pseudomonas aeruginosa* in long-lived, GSC-less animals as well as normal, fertile adults. Our work ultimately demonstrates that NHR-49 is differentially influenced by GSC loss vs. pathogen exposure. While NHR-49 expression in any somatic tissue rescued longevity, only neuron-derived protein could promote pathogen resistance in multiple genetic backgrounds. These distinct regulatory effects also extended to the expression of well-established NHR-49 target genes, *acs-2* and *fmo-2*, neither of which were required to defend against *P. aeruginosa*, unlike their known roles against other pathogens (241, 242). Instead, NHR-49 targets encoding anti-microbial factors and xenobiotic-response proteins contributed towards *Pseudomonas* resistance. Overall, this Chapter describes our use of the *C. elegans* model to interrogate the tissue- and context-specific activities of key regulatory proteins on life history traits. As such, our data suggest that NHR-49 directs distinct responses to short-term stimuli such

as pathogen attack vs. long-term lifespan changes and orchestrates pathogen-specific transcriptional programs.

2.2 Methods

***C. elegans* strains and lifespan assays:** All strains were maintained by standard techniques at 20°C or 15°C on nematode growth medium (NGM) plates seeded with an *E. coli* strain OP50. For experiments involving RNAi, NGM plates were supplemented with 1 mL 100 mg/mL Ampicillin and 1 mL 1M IPTG (Isopropyl β-D-1-thiogalactopyranoside) per liter of NGM. The main strains used in this study include N2 (wild type), CF1903 *[glp-1(e2144) III]*, AGP12a *[nhr-49(nr2041)I]*, AGP22 [*nhr-49(nr2041)I;glp-1(e2141)III],* AGP110 *[nhr-49(et7)I]*. All strains listed in Supp. Table 2.10. Lifespan experiments were performed as previously described (243). For lifespan in the *glp-1* background, eggs were kept at 20°C for 2-6 h, grown to the L4 stage at 25°C, then shifted back to 20°C for remaining lifespan. In lifespan assays, the L4 stage was counted as Day 0 of adulthood. Fertile strains were transferred to fresh plates every other day to separate parents from progeny. Animals that exploded, bagged, crawled off the plate, or became contaminated were marked as censored upon observation. The program Online Application of Survival Analysis 2 (OASIS 2) (244) was used for statistical analysis of both lifespan and pathogen stress assays. P-values were calculated using the log-rank (Mantel–Cox) test (244). Results were graphed using GraphPad Prism (Version 8).

Pathogen survival assays: Survival in the presence of the Gram-negative pathogen *Pseudomonas aeruginosa* strain PA14 was used in this study to assess the immunoresistance of

C. elegans strains. Luria Bertani (LB) agar plates were streaked with bacteria from -80°C glycerol stocks, incubated at 37°C overnight and stored at 4°C for ≤ 1 week. Single PA14 colonies from streaked plates were then inoculated into 3mL King's Broth (Sigma) overnight (16-18h) in a 37°C shaking incubator. 20 µL of this culture was seeded onto slow-killing (NGM with 0.35% peptone) plates and incubated at 37 °C for 24h (48, 245). Seeded PA14 plates were kept at room temperature for 24h before use.

PA14 survival assays were performed as previously described (48). Age-matched *C. elegans* strains were grown under the same conditions and selected at the L4 stage as for the lifespan experiments. 25-30 L4 worms each were transferred to five PA14 plates per strain and maintained at 25°C till the end of their lives. Strains were monitored at 6-12h intervals to count living, dead, and censored animals as described above. Living animals were transferred to fresh PA14 plates each day for 3-4 days. Statistical analysis of survival data was performed on OASIS 2 and representative trials were graphed with GraphPad Prism (Version 8).

RNA-Sequencing and data analysis: RNA was isolated from 3 biological replicates of Day 2 adults of CF1903 (*glp-1)* and AGP22 (*nhr-49;glp-1)* strains, grown as described above. Following 7 freeze thaw cycles, approximately 3000 worms were harvested for RNA using the Trizol method. RNA was checked for quality and quantity using the Agilent Tapestation and Qubit Fluorometry. Sequencing libraries were prepared using the TruSeq stranded mRNA (PolyA+) kit and the samples were then subjected to 75 base pair paired-end sequencing on an Illumina NextSeq 500 sequencer at the Univ. of Pittsburgh Genomics Research Core. Sequencing data was analyzed using the CLC Genomics Workbench (Version 20.0.3) employing the RNA Seq pipeline. Reads were then filtered for differentially regulated genes with significant

changes based on the criteria of >2 fold change in expression, P Value of <0.05 and a false discovery rate (FDR) of <0.05.

Gene Ontology analyses: Genes that were differentially regulated in a statistically significant manner were classified into two groups as either up-regulated (UP) or down-regulated (DOWN) NHR-49 targets. These groups were analyzed for enrichment of gene classes based on Gene Ontology (GO) Terms using *C. elegans* centered publicly available online resources, Wormbase Gene Set Enrichment Analysis tool and WormCat (wormbase.org/tools/enrichment/tea/tea.cgi), (wormcat.com) (246). Representation Factor was calculated at nemates.org/MA/progs/overlap_stats.html.

Q-PCRs: RNA was isolated as mentioned above by Dr. Amrit and quantified using a Nanodrop and DNAse treated (DNAse kit, Sigma AMPD1). The RNA was then reverse transcribed into cDNA using the High-Capacity cDNA Reverse Transcription kit (Applied Biosystems, 4368814) following the manufacturer's recommendations. RNA samples were collected from three independently isolated 'biological replicates', and three 'technical replicates' of each strain/condition were tested for a given biological replicate. Quantitative PCRs were conducted using the PowerUp SYBR Green Master Mix kit (Applied Biosystems A25741) on the CFX Connect Machine (BioRad). Gene expression data was analyzed using the ΔΔCt method and normalized to the housekeeping gene, *rpl-32*. Melt curves for all reactions were run confirming the integrity of the reaction. Primer sequences used for the experiment were *nhr-49_Fwd* (TTGGCAGAGGTGGATTCTC), *nhr-49_Rev* (CTGTAAAGAGACCGGAGCC), *rpl-32_Fwd* (GATTCCCTTGCGGCTCTT), and *rpl-32_Rev* (GATTCCCTTGCGGCTCTT).

Transgenic strain generation: Tissue-specific NHR-49 expressing strains were generated by plasmid microinjection. A control P*nhr-49::nhr-49::gfp* (pAG4) construct, which drives NHR-49 expression via its endogenous promoter, was created as previously described (104). To drive NHR-49 expression in other tissues, 4.4kb coding region of *nhr-49* was first amplified with modified primers to introduce SbfI and SalI restriction sites at the 5' end and SmaI at the 3' end of the coding region. This product was cloned into the GFP expression vector pPD95.77 (Addgene plasmid 1495) upstream of, and in frame with, GFP. Individual tissue-specific promoters were then amplified and ligated independently into this plasmid using primers modified with the forward primer including SbfI and the reverse including SalI to create plasmids for expressing NHR-49 in the muscle (P*myo-3*::NHR-49::GFP), intestine (P*gly-19*::NHR-49::GFP), hypodermis (P*col-12*::NHR-49::GFP) and neurons (P*unc-119*::NHR-49::GFP). Each of the five constructs were then injected at a concentration of 100 ng/mL with 15 ng/mL of P*myo-2::mCherry* co-injection marker into *nhr-49*, *nhr-49;glp-1*, *glp-1* and WT animals to create transgenic strains carrying the individual extragenic arrays. The *et7* mutation (C > T) was introduced into *Punc-119::nhr-49::GFP* and *Pcol-12::nhr-49::GFP* plasmids using the Q5 Site-Directed Mutagenesis Kit from (New England Biolabs, E0554S). Plasmids were sequenced to confirm the presence of the *et7* mutation and then injected into WT, *nhr-49* and *nhr-49;glp-1* animals as described above. No viable transgenics were obtained for *nhr-49* mutants expressing *Pcol-12::nhr-49::GFP* and *nhr-49;glp-1 mutants* expressing either *Punc-119::nhr-49::GFP* or *Pcol-12::nhr-49::GFP*. For each of the 23 transgenic strains generated in this study, 2-4 independent transgenic lines were generated. Transgene-carrying strains were maintained and selected for lifespan and pathogen stress assays using a Leica M165C

microscope with a fluorescence attachment. A complete listing of all strains used in this study is provided in Supp. Table 2.10.

Fenofibrate supplementation assay: 100 μL of 10 μM Fenofibrate (Sigma F6020) in 0.1% DMSO were placed onto both NGM and slow-killing plates before seeding with OP50 or PA14, respectively, as described above (247, 248). Upon the drying and growth of the bacterial lawn, eggs were grown to L4 on either the Fenofibrate or 0.1% DMSO control plates, then transferred to PA14 plates (similarly supplemented with Fibrate or DMSO) at L4 larval stage and survival monitored. Worms were transferred to fresh plates as described above.

GFP fluorescence imaging and quantitation: GFP expression in transgenic strains was quantified using the COPAS Biosorter (Union Biometrica; Holliston) as described in (249). For setup, progeny of transgenic mothers were grown to the Day 1 of adulthood (when fluorescent signal became clear) under normal conditions on *E. coli* OP50 or HT115 RNAi control strains at 20°C. For strains with the *glp-1* mutation, eggs were kept at 20°C for 2-6 h then grown to Day 1 at 25°C. Day 1 adults were transferred to PA14 plates or OP50 control plates and maintained 25°C for 24hrs before imaging and quantification. Each strain was washed into the COPAS sample cup with ~5 mL deionized water for measurement of individual worms. Intensity of green fluorescence of each animal was normalized to the axial length measured (i.e. GFP fluorescence divided by time-of-flight). Statistical significance was determined using a one-way non-parametric ANOVA with Dunn's post hoc test (Graphpad Prism). Representative whole-body images of transgenic worms were taken using 10 mM sodium azide for immobilization and

imaged at 20x magnification using a Leica DM5500B compound scope with LAS X software (Leica).

NHR-49:GFP nuclear localization: Worms were grown to the L4 on OP50 and transferred to control *E. coli* OP50 or PA14 plates as described above. Following 16h of exposure, animals were immobilized and mounted on agar pads with 20mM Levamisole and imaged using a Leica DM5500B compound scope. Image acquisition and analysis was performed using LAS X software (Leica). For each of the two trials, an average of two to four of the first six anterior intestinal cells were assessed for GFP localization from ≥10 worms. For each intestinal cell, the size normalized nucleus-to-cytoplasm GFP intensity ratio was calculated using the Fiji (ImageJ) software by selecting the nuclear or cytoplasmic area and measuring corrected total cell fluorescence (CTCF) to obtain the nuclear CTCF/cytoplasmic CTCF ratio per cell. An unpaired t test with Welch's correction was used to determine statistical significance.

Data Availability: Original text and full datasets from this study can be found in the publication, Naim, et. al 2021, Aging Cell. DOI: 10.1111/acel.13413.

2.3 Results

2.3.1 NHR-49 co-regulates with DAF-16 and TCER-1 the expression of genes essential for germline-less longevity

Previously, our lab discovered that *nhr-49* inactivation abrogates the enhanced lifespan of temperature sensitive, sterile *glp-1* mutants (250), a well-established model for GSC-less longevity (99). To identify the transcriptional changes orchestrated by NHR-49 upon GSC removal, our lab compared the transcriptomes of *glp-1* vs. *nhr-49;glp-1* mutants using RNA-Seq. This showed that NHR-49 controlled the transcriptional upregulation of 1120 genes (UP class) and downregulation of 1140 genes (DOWN class) in *glp-1* mutants (Supp. Fig. 2.1a, Supp. Table 2.1a-b). Since our previous studies had shown that *nhr-49* is transcriptionally upregulated upon GSC loss by the joint action of two transcription factors, DAF-16 and TCER-1 (104), the overlap between NHR-49 UP and DOWN targets with genes whose expression is altered by DAF-16 and/or TCER-1 in *glp-1* mutants was examined (110). Strikingly, 53% of genes upregulated in *glp-1* mutants *jointly* by DAF-16 and TCER-1 (JOINT UP) (110) were also identified within the NHR-49 UP class (65/123, R factor 8.3, P <4.853e-45) (**Fig. 2.1a**). The overlap with genes specifically upregulated by either of these proteins was also significant ranging from ~24% (DAF-16 UP) to ~40% (TCER-1 UP) (Supp. Fig. 2.1b). The NHR-49 DOWN class also showed a much higher overlap with the genes jointly down-regulated by DAF-16 and TCER-1 (JOINT DOWN) (~36%, 26/73, R 5.5, P <2.094e-13) (**Fig. 2.1a**) as compared to genes specifically down-regulated by either factor alone (Supp. Fig. 2.1b). Notably, 35 of these NHR-49 UP genes were identified in our previous studies as being essential for *glp-1* mutants' longevity (Supp. Fig.

2.1c) (104, 110). Hence, our RNA-Seq analysis revealed functionally relevant genes essential for the lifespan extension induced by GSC loss.

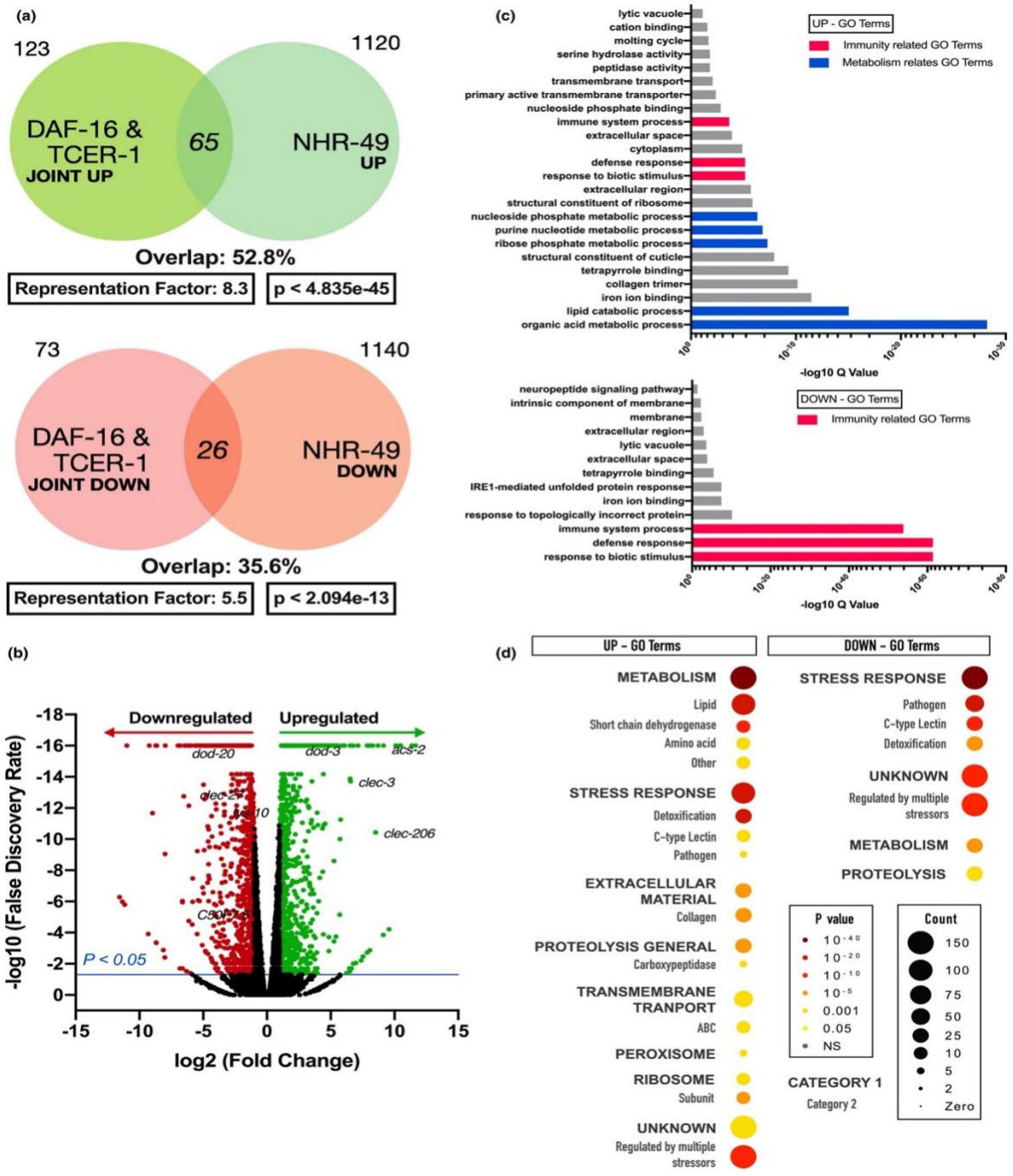

Figure 2.1 NHR-49 dictates a transcriptome upon germline loss that is enriched for innate immunity genes.

(a) Venn diagram comparing the genes upregulated (top, 1,120) and downregulated (bottom, 1,140) by NHR-49 in *glp-1* mutants with genes jointly upregulated (top, 188) and downregulated (bottom, 99) by DAF-16 and TCER-1 following germline loss (110). (b) Volcano plot of gene

expression changes between *glp-1* and *nhr-49*;*glp-1* animals. Differentially expressed genes highlighted as red (NHR-49 DOWN) and green (NHR-49, UP). Absolute log fold change >2, *p* value <0.05 and FDR of <2. Immune-gene classes and factors discussed in this study are labeled. (c) Wormbase Gene Set Enrichment Analysis (GSEA) of NHR-49 targets identified metabolism (blue) and stress response (red) categories as being enriched. (d) Gene ontology (GO) term analysis using WormCat, a *C. elegans* identified pathogen response as one of the most enriched terms in both the UP class and DOWN Class. Figure development and data collection by Francis RG Amrit.

2.3.2 NHR-49 widely modulates the expression of innate-immunity genes

Based on NHR-49's known roles in regulating fat metabolism (105, 251, 252), we anticipated its targets to be enriched for lipid-metabolic functions. Gene Ontology (GO) analysis of the RNA-Seq data by Dr. Amrit revealed that, while metabolic functions were indeed highly represented amongst NHR-49 targets, some of the most enriched GO terms related to stress response, especially immune response (**Fig. 2.1b, c**) (253). Analysis of this data through WormCat, a *C. elegans* bioinformatics platform that allows greater refinement of functional categories within enriched groups (246), substantiated these observations. Within the UP class, stress response, particularly pathogen response, was the second-most enriched category, and within the DOWN class, it was the most enriched one (**Fig. 2.1d**). Notably, 33 of the top 100 genes within the NHR-49 UP class were included in other studies examining gene-expression changes in worms infected by the human opportunistic pathogen *Pseudomonas aeruginosa* (Supp. Fig. 2.2) (147, 148, 241, 254) propelling us to assess NHR-49's role in response to this pathogen.

2.3.3 NHR-49 contributes towards defense against *P. aeruginosa* infection

We tested the impact of *nhr-49* inactivation on survival following infection with *P. aeruginosa* strain PA14 (henceforth PA14) using the Slow Killing (SK) paradigm, wherein PA14 causes *C. elegans* to die over the course of several days (48, 255). As previously reported, *glp-1* mutants survived significantly longer than wild-type (WT) adults (43, 256). However, in *nhr-49;glp-1* mutants this resistance was abrogated. *nhr-49* single mutant's survival was significantly reduced on PA14 compared to WT as well (**Fig. 2.2a**) (241). We then asked if NHR-49 hyperactivation increased immunoresistance and obtained equivocal results. Mutants carrying an NHR-49 gain-of-function *(gof)* allele, *et7* (252, 257), exhibited significantly increased survival ranging from 2% to 15% in three of six trials (**Fig. 2.2b**, Supp. Table 2.2a). Similarly, supplementation of worm food with Fenofibrate, a PPARα agonist and widely prescribed, lipid-lowering drug (102), also increased the survival of worms modestly in an *nhr-49*-dependent manner but in five of eight trials, whereas, in two trials survival was reduced (**Fig. 2.2c**, Supp. Table 2.2b). Taken together, these data suggested that NHR-49 promoted immunoresistance against pathogenic *P. aeruginosa*.

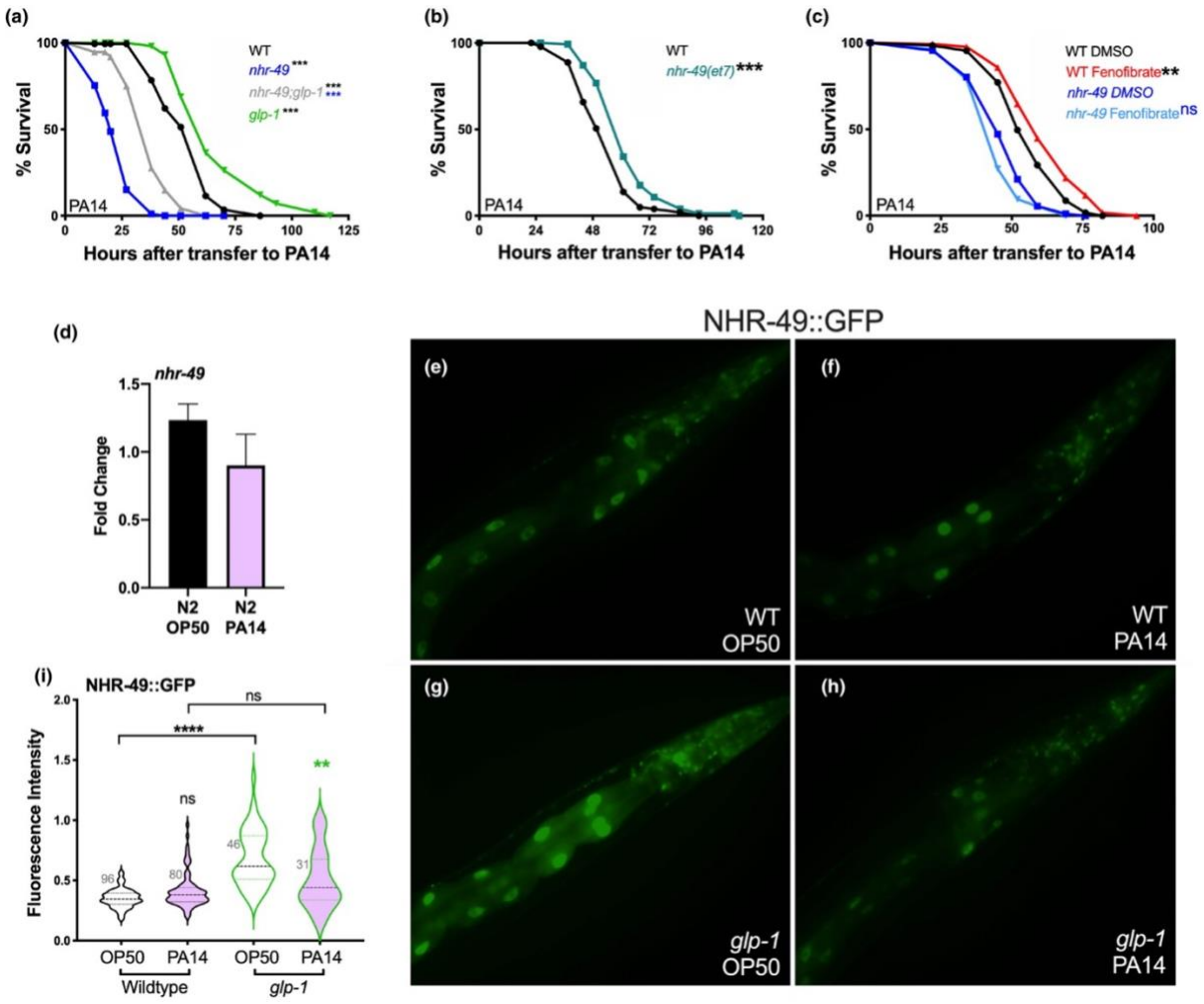

Figure 2.2 NHR-49 contributes toward defense against *P. aeruginosa* pathogen attack.

(a) Survival on PA14 of L4 stage wild-type worms (WT, black, $m = 54.03 \pm 0.99$, $n = 151/198$) as well as *nhr-49* (blue, $m = 23.03 \pm 0.62$, $n = 184/195$), *glp-1* (green, $m = 67.31 \pm 1.86$, $n = 101/113$) and *nhr-49;glp-1* (gray, $m = 37.48 \pm 1.02$, $n = 99/115$) mutants. See Supp. Tables 2.3 and 2.4 for additional trials with these strains. (b) *nhr-49 gof* mutants survives longer on PA14. Survival on PA14 of L4 stage WT worms (black; $m = 54.32 \pm 1.09$, $n = 126/145$) and *nhr-49(et7)* mutants (olive, $m = 62.79 \pm 1.31$, $n = 94/136$). $p < 0.0001$. Data from additional trials in Supp. Table 2.2A. (c) Fenofibrate supplementation increases survival on PA14. Survival on PA14 of

L4 stage DMSO-control grown, WT worms (black; m = 56.81 ± 1.08, n = 103/129) and *nhr-49* mutants (dark blue, m = 47.69 ± 0.98, n = 107/134) compared with Fenofibrate-supplemented WT worms (red, m = 62.1 1.26, n = 93/135) and *nhr-49* mutants (light blue, m = 45.33 ± 0.89, n = 104/134). Data from additional trials in Supp. Table 2.2B. (d–i) PA14 exposure reduces NHR-49 levels. (d) *nhr-49* mRNA levels measured by Q-PCR in Day 1 adults grown on OP50 till L4 stage then transferred to PA14 plates for 8 h (pink) or continued on OP50 (black) p = 0.27. Data combined from three independent biological replicates, each including three technical replicates. *Experiment and figure done by Francis RG Amrit*. (e–h) Representative images of NHR-49::GFP in WT (e, f) and *glp-1* mutants (g, h) grown on OP50 till L4 stage and then transferred to PA14 (f, h) or retained on OP50 (e, g) for 24 h. (i) Violin plot quantification of GFP intensity using a COPAS Biosorter. WT (black outlines), *glp-1* (green outlines) exposed to PA14 (pink) or retained on OP50 (blank). Number of worms assayed shown on each panel. Data from one of three biological replicates with similar results. In (a–c), survival data shown as mean life span in hours (m) ± SEM (see Methods for details). In (d), error bars represent standard error of the mean (SEM). In (i), where all fluorescence measures were normalized to time-of-flight, the center dashed line indicates median intensity and flanking lines the first and third quartiles. Statistical significance was calculated in (a) and (b) using the log-rank method (Mantel Cox, OASIS2), in d by using a two-tailed t test, and in (i) using a one-way nonparametric ANOVA with Dunn's post hoc test. Statistical significance is shown on each panel next to a given strain/condition with the color of the asterisk indicating strain/condition being compared to $p < 0.01$ (**), <0.001 (***), <0.0001 (****), not significant (ns).

2.3.4 Pathogen exposure causes reduction in NHR-49 protein levels

nhr-49 mRNA and protein levels are both elevated in response to germ line ablation (104), so we asked how pathogen exposure impacted it. *nhr-49* mRNA levels were the same between worms fed the normal diet of *Escherichia coli* OP50 (OP50) vs. PA14 in quantitative PCR (Q-PCR) assays performed by Dr. Amrit (**Fig. 2.2d**). Further, *nhr-49* was not identified as a gene whose expression was altered by PA14 exposure in previous reports documenting PA14-induced transcriptomic changes (147, 148, 241, 254). We examined NHR-49 protein levels using a transgenic strain expressing GFP-linked NHR-49 under control of its endogenous promoter (104). Visual examination did not reveal alterations in sub-cellular localization following infection. However, a modest but widespread reduction in GFP levels was noticeable in infected animals as compared to controls. To obviate subjective bias, we performed automated quantification of fluorescence intensity using a COPAS^{TM} BIOSORT platform (258). GFP levels were significantly diminished in *glp-1* mutants exposed to PA14 (**Fig. 2.2e-i**). In fertile animals too, PA14 infection induced a modest reduction that was visually evident but did not attain statistical significance (**Fig. 2.2e-i**). Together, these data suggest that unlike GSC ablation that triggers both transcriptional and translational upregulation of NHR-49, PA14 infection causes a modest reduction in total protein levels in at least *glp-1* mutants.

2.3.5 In *nhr-49;glp-1* mutants, neuronal NHR-49 rescues immunity but longevity is rescued by expression from multiple tissues

NHR-49 is widely expressed in *C. elegans* somatic cells (104). Previously, our lab had found that NHR-49 expression under control of its endogenous/native promoter completely

rescued the short lifespan of *nhr-49;glp-1* mutants to *glp-1* levels when animals were fed the normal OP50 diet. We asked if this transgene also rescued the exceptionally short survival of *nhr-49;glp-1* mutants on a PA14 pathogenic diet. Surprisingly, endogenous promoter-driven NHR-49 not only failed to improve the survival of *nhr-49;glp-1* mutants on PA14, it reduced it even further (**Fig. 2.3a**, Supp. Table 2.3a). Animals carrying the same transgene showed consistent rescue of lifespan on OP50 (**Fig. 2.3b**, Supp. Table 2.3) over-ruling the possibility of transgene toxicity. We checked if PA14 exposure abolished expression from the transgene explaining the lack of rescue. But, though GFP intensity was slightly reduced (as predicted above), it was widely visible in all tissues.

The contradictory observations with the endogenous promoter could be explained if NHR-49's impact on immunoresistance is tissue specific with expression in some sites exerting pro-immunity effects and in others reducing immunity. To test this possibility, we expressed NHR-49 in individual tissues of *nhr-49;glp-1* mutants and examined the effect on their survival upon PA14 infection (**Fig. 2.3c, e, g, i**, Supp. Table 2.3b-e) as well as lifespan on a normal OP50 diet (**Fig. 2.3d, f, h, j**, Supp. Table 2.3b-e). We found that NHR-49 expression selectively in the neurons of *nhr-49;glp-1* mutants (using the *unc-119* promoter) (259) completely and reliably rescued their survival on PA14 to the same level as *glp-1* mutants (**Fig. 2.3c**, Supp. Table 2.3b). Expression in other somatic tissues had marginal and inconsistent impacts. Intestinal NHR-49 (*gly-19* promoter) (260) produced no significant increase in survival in any of three trials (**Fig. 2.3e**, Supp. Table 2.3c), whereas, hypodermal (*col-12* promoter) (249) or muscle (*myo-3* promoter) (261) expression showed sporadic rescues (**Fig. 2.3g, i**, Supp. Table 2.3d, e).

We next asked how NHR-49 expression in individual tissues (using the same promoters as above) impacted *nhr-49;glp-1* mutant's lifespan on OP50. Pan-neuronal expression

completely rescued lifespan to *glp-1* levels in every trial (**Fig. 2.3d**, Supp. Table 2.3b). Interestingly, expression in each of the other three somatic tissues also produced substantial increases in longevity (**Figs. 2.3f, h, j**, Supp. Table 2.3c-e), although rescue to *glp-1* levels was achieved by neuronal NHR-49 alone. We tested if these differential impacts on PA14 survival vs. OP50 lifespan could simply be explained by differences in NHR-49 levels or nuclear localization. The NHR-49 tissue-specific transgenes showed similar expression profiles and sub-cellular localization in the different strains and conditions (Supp. Fig. 2.3). We quantified the nuclear:cytoplasmic ratio of intestinal NHR-49::GFP on OP50 vs. PA14 and found no statistical difference in this either (Supp. Fig. 2.4). Together, these experiments showed that upon GSC loss, NHR-49 expression in individual somatic tissues rescued longevity substantially, whereas, its expression in neurons alone could completely rescue PA14 resistance.

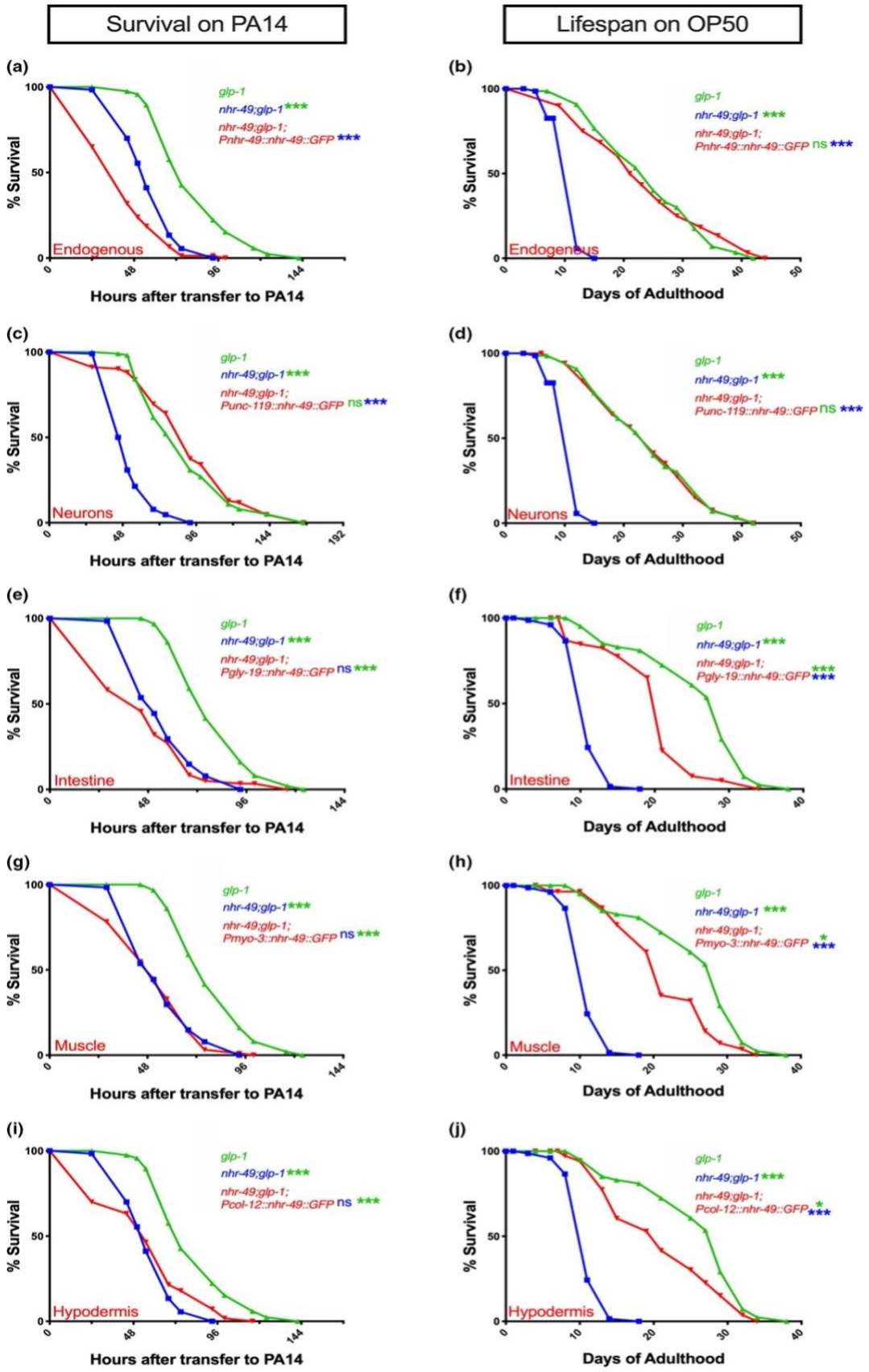
Survival on PA14
Lifespan on OP50
(a)
(b)
(c)
(d)
(e)
(f)
(g)
(h)
(i)
(j)
% Survival
Hours after transfer to PA14
Days of Adulthood
glp-1
nhr-49;glp-1 ***
nhr-49;glp-1;
Pnhr-49::nhr-49::GFP ns ***
Punc-119::nhr-49::GFP ns ***
Pgly-19::nhr-49::GFP ***
Pmyo-3::nhr-49::GFP * ***
Pcol-12::nhr-49::GFP * ***
Endogenous
Neurons
Intestine
Muscle
Hypodermis

Figure 2.3 In germline-less animals, NHR-49 acts cell nonautonomously to promote immunity from neurons but longevity from multiple tissues.

(a, c, e, g, i) NHR-49 expression in neurons alone rescues PA14 resistance of *nhr-49*;*glp-1* mutants. Mean PA14 survival (in hours) of *glp-1* (green), *nhr-49*;*glp-1* (blue), and *nhr-49*;*glp-1* mutants expressing NHR-49 in different tissues (red). (a, i) Survival of *glp-1* (82.88 ± 2.08, *n* = 105/120) and *nhr-49*;*glp-1* (57.92 ± 1.35, *n* = 108/120) mutants compared with transgenic *nhr-49*;*glp-1* mutants expressing NHR-49 via Endogenous promoter (a, 43.33 ± 1.74, *n* = 95/120) or in the Hypodermis (i, 56.06 ± 2.53, *n* = 96/120). (c) Survival of *glp-1* (89.65 ± 2.83, *n* = 104/108), *nhr-49*;*glp-1* (53.32 ± 1.26, *n* = 98/111), and *nhr-49*;*glp-1* mutants expressing NHR-49 in Neurons (c, 92.09 ± 3.49, *n* = 90/102). (e, g) Survival of *glp-1* (80.71 ± 1.62, *n* = 117/124), *nhr-49*;*glp-1* (56.25 ± 1.42, *n* = 111/121), and *nhr-49*;*glp-1* mutants expressing NHR-49 in Intestine (e, 47.82 ± 2.57, *n* = 68/79) and Muscles (g, 52.44 ± 1.67, *n* = 109/115). (b, d, f, h, j) NHR-49 expression in any somatic tissue substantially rescues longevity of *nhr-49*;*glp-1* mutants on OP50. Mean life span on OP50 (in days) of *glp-1* (green), *nhr-49*;*glp-1* (blue), and *nhr-49*;*glp-1* mutants expressing NHR-49 in different tissues (red). (b, d) Life span of *glp-1* (24.43 ± 1.08, *n* = 51/70) and *nhr-49*;*glp-1* (11.28 ± 0.26, *n* = 55/72) mutants compared with transgenic *nhr-49*;*glp-1* mutants expressing NHR-49 via Endogenous promoter (b, 23.72 ± 1.32, *n* = 59/60) or promoters expressed in Neurons (d, 24.41 ± 1.04, *n* = 66/71). (f, h, j) Life span of *glp-1* (25.78 ± 0.98, *n* = 65/77), *nhr-49*;*glp-1* (11.27 ± 0.26, *n* = 72/72), and *nhr-49*;*glp-1* mutants expressing NHR-49 in Intestine (f, 19.79 ± 0.95, *n* = 41/63), Muscles (h, 21.4 ± 1.02, *n* = 34/59) or Hypodermis (j, 21.06 ± 1.36, *n* = 28/42). Survival and life span data shown as mean ± standard error of the mean (SEM). "*n*" refers to number of worms analyzed over total number of worms tested in the

experiment (see Methods for details). Statistical significance calculated using log-rank (Mantel–Cox) method and indicated by asterisks on each panel next to mutant name (color of asterisk indicates strain being compared to). $p < 0.05$ (*), <0.001 (***), not significant (ns). Note: In some panels (a, i; e, g; b, d; f, h, j), assays have the same controls as they were performed in the same biological replicate. Data from additional trials and WT controls presented in Supp. Table 2.3a-e.

2.3.6 In *nhr-49* mutants, hypodermal NHR-49 rescues longevity but diminishes immunity

Since *nhr-49* single mutants also exhibit shortened survival compared to WT, we investigated which tissues NHR-49 acted in to promote their survival on PA14 and OP50. However, unlike in the *nhr-49;glp-1* background, the endogenous-promoter driven NHR-49 transgene rescued the survival of *nhr-49* single mutants reliably on PA14 (98% rescue in 3/4 trials, **Fig. 2.4a**, Supp. Table 2.4) as well as on OP50. In fact, lifespan on OP50 was augmented even further than WT as observed in our previous work (**Fig. 2.4b**, Supp. Table 2.4a) (104). As in *nhr-49;glp-1* mutants, pan-neuronal expression completely rescued both the immunoresistance and lifespan of *nhr-49* mutants (**Fig. 2.4c, d**, Supp. Table 2.4b). Intestinal expression also significantly rescued both longevity and immunity (**Fig. 2.4e, f**, Supp. Table 2.4c), whereas, muscle expression rescued neither (**Fig. 2.4g, h**, Supp. Table 2.4d). Strikingly though, hypodermal NHR-49 completely rescued longevity on OP50, but survival on PA14 was significantly worsened (≥19% reduction in 4/4 trials, **Fig. 2.4i, j**, Supp. Table 2.4e). These results, along with the observations above, demonstrate that NHR-49 acts cell non-autonomously to modulate both longevity and immunity.

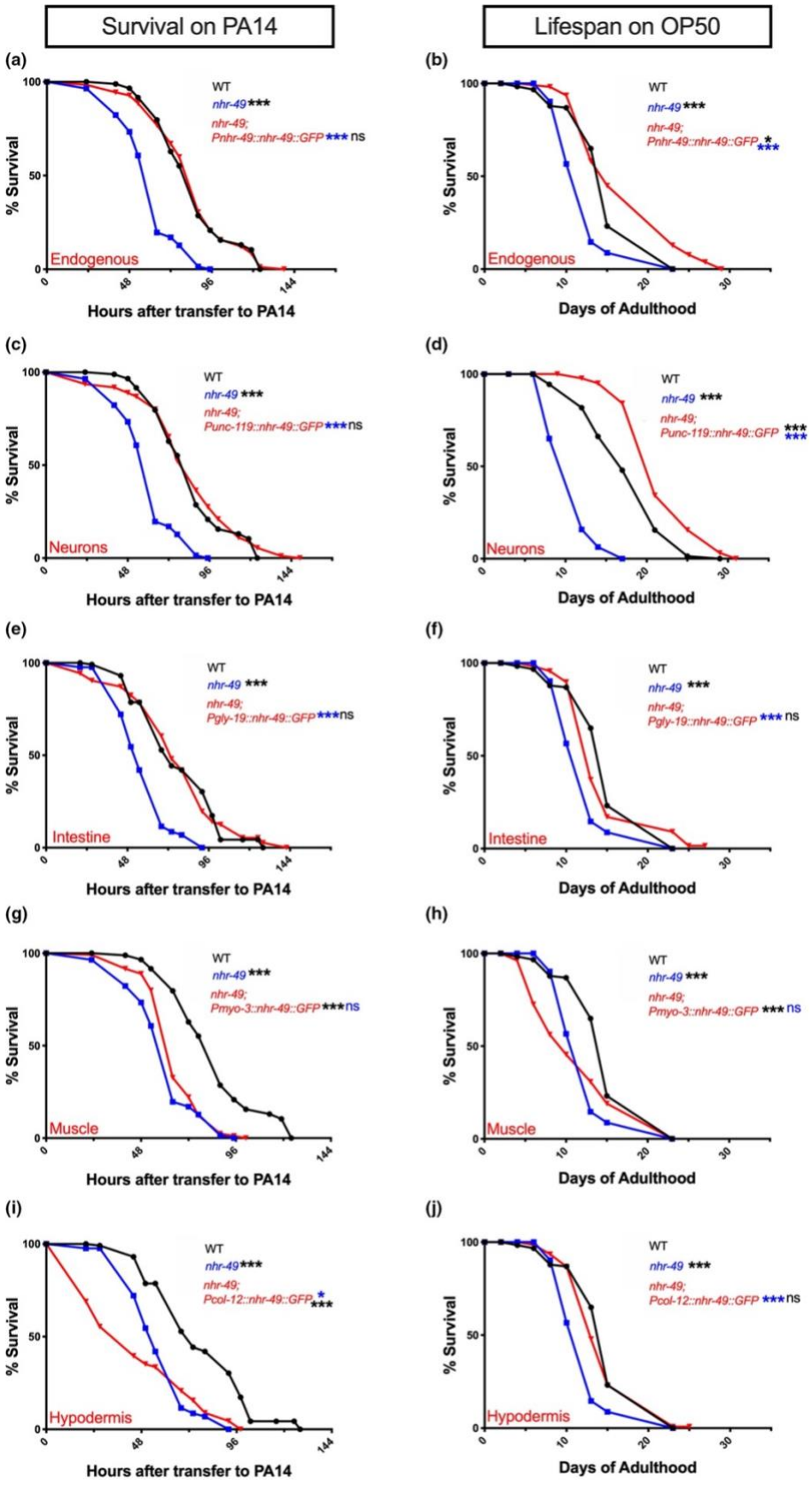
Survival on PA14
Lifespan on OP50
(a)
(b)
(c)
(d)
(e)
(f)
(g)
(h)
(i)
(j)
% Survival
Hours after transfer to PA14
Days of Adulthood
WT
nhr-49 ***
nhr-49; Pnhr-49::nhr-49::GFP *** ns
nhr-49; Pnhr-49::nhr-49::GFP * ***
nhr-49; Punc-119::nhr-49::GFP *** ns
nhr-49; Punc-119::nhr-49::GFP *** ***
nhr-49; Pgly-19::nhr-49::GFP *** ns
nhr-49; Pmyo-3::nhr-49::GFP *** ns
nhr-49; Pcol-12::nhr-49::GFP * ***
nhr-49; Pcol-12::nhr-49::GFP *** ns
Endogenous
Neurons
Intestine
Muscle
Hypodermis

Figure 2.4 In *nhr-49* mutants, neuronal NHR-49 rescues both life span and immunity while hypodermal expression rescues longevity but lowers immunity.

(a, c, e, g, i) NHR-49 expression in neurons and intestine rescues the resistance of *nhr-49* mutants on PA14. Mean PA14 survival (in hours) of WT (black, WT), *nhr-49* (blue), and *nhr-49* mutants expressing NHR-49 in different tissues (red). (a, c, g) Survival of WT (84.82 ± 2.63, *n* = 55/90) and *nhr-49* (60.24 ± 1.52, *n* = 102/113) strains compared to *nhr-49* mutants expressing NHR-49 via Endogenous promoter (a, 84.35 ± 2.17, *n* = 100/125) or promoters expressed in the Neurons (c, 84.44 ± 2.73, *n* = 95/110) or Muscles (g, 65.73 ± 1.27, *n* = 105/119). (e, i) Survival of WT (78.24 ± 2.57, *n* = 63/125), *nhr-49* (58 ± 1.44, *n* = 99/127), and *nhr-49* mutants expressing NHR-49 in Intestine (e, 77.6 ± 2.73, *n* = 87/125) or Hypodermis (i, 46.27 ± 2.72, *n* = 79/100). (b, d, f, h, j) NHR-49 expression in the neurons, intestine or hypodermis substantially improves *nhr-49* mutant's longevity on OP50. Mean life spans on OP50 (in days) of WT (black), *nhr-49* (blue), and *nhr-49* strains expressing NHR-49 in different tissues (red). (b, f, h, j) Life span of WT (15.42 ± 0.49, *n* = 89/122) and *nhr-49* (12.5 ± 0.36, *n* = 110/119) strains compared with *nhr-49* mutants expressing NHR-49 via Endogenous promoter (b, 18 ± 0.97, *n* = 97/112) or promoters expressed Intestine (f, 15.25 ± 0.4, *n* = 97/118), Muscles (h, 12.01 ± 0.71, *n* = 75/80) or Hypodermis (j, 14.86 ± 0.45, *n* = 131/141). (d) Life span of WT (17.99 ± 0.58, *n* = 71/82) and *nhr-49* (11.11 ± 0.33, *n* = 63/65) strains compared with *nhr-49* mutants expressing NHR-49 in Neurons (d, 22.23 ± 0.71, *n* = 33/76). Survival and life span data shown as mean ± standard error of the mean (SEM). "*n*" refers to number of worms analyzed over total number of worms tested in the experiment (see Methods for details). Statistical significance calculated using log-rank (Mantel–Cox) method and indicated by asterisks on each panel next to mutant name (color

of asterisk indicates strain being compared to). $p < 0.05$ (*), <0.001 (***), not significant (ns). Note: assays in some panels (a, c, g; e, i; b, f, h, j) have the same controls as they were performed in the same biological replicate. Data from additional trials and wild-type controls presented in Supp. Table 2.4a-e.

2.3.7 In WT animals, elevating NHR-49 levels in neurons, or intestine, enhances immunoresistance

NHR-49 protein levels are important in determining the animals' lifespan because elevating its levels in normal, fertile adults, either using the endogenous promoter or in neurons alone, induces a modest lifespan extension (104, 240). We asked if endogenous promoter-driven overexpression increased PA14 resistance as well but observed benign effects as survival was increased in only 1/3 trials (**Fig. 2.5a, b**, Supp. Table 2.5a). We next asked if elevating NHR-49 levels in individual tissues could enhance immunoresistance. WT animals' immunity was enhanced by NHR-49 overexpression in the neurons or the intestine (~15-30%) (**Fig. 2.5c, e**, Supp. Table 2.5b, c, respectively), whereas, in the muscles or hypodermis it did not produce consistent impacts (**Fig. 2.5g, i**, Supp. Table 2.5d, e). Interestingly, the benefits obtained by intestinal or neuronal upregulation were restricted to survival during PA14 infection. We did not observe a consistent lifespan extension on OP50 when NHR-49 was overexpressed in any single somatic tissue (**Fig. 2.5d, f, h, j**, Supp. Table 2.5b-e).

Since NHR-49 undergoes lipid ligand-dependent activation one explanation for NHR-49's tissue-specific effects could be a result of different activation levels. Thus, NHR-49 overexpression might only promote immunity and longevity if the protein also experiences activation in that tissue (262). We tested this possibility by expressing the *et7 gof* allele (NHR-

49^{et7}) (252, 257) in the hypodermis (where its expression had no beneficial impact) or in neurons (where its expression had consistently beneficial effects) using transgenic strains created by Dr. Amrit. Surprisingly, we found that either neuronal or hypodermal expression of NHR-49^{et7} drastically shortened survival on both OP50 and PA14 (**Fig. 2.6a-d**, Supp. Table 2.6a). Neuronal NHR-49^{et7} expression produced a small but significant rescue of *nhr-49* mutants' immunity and longevity phenotypes (**Fig. 2.6e, f**; Supp. Table 2.6a). Viable strains that expressed hypodermal NHR-49^{et7} in any *nhr-49* mutant background could not be created suggesting that inappropriate NHR-49 activation may in fact have severe adverse consequences. We also tested if chemical activation of NHR-49 by Fenofibrate supplementation in strains expressing NHR-49 in muscles or hypodermis of *nhr-49* mutants (where no rescue was observed) improved survival on PA14 but observed no rescue in either strain (Supp. Table 2.6b).

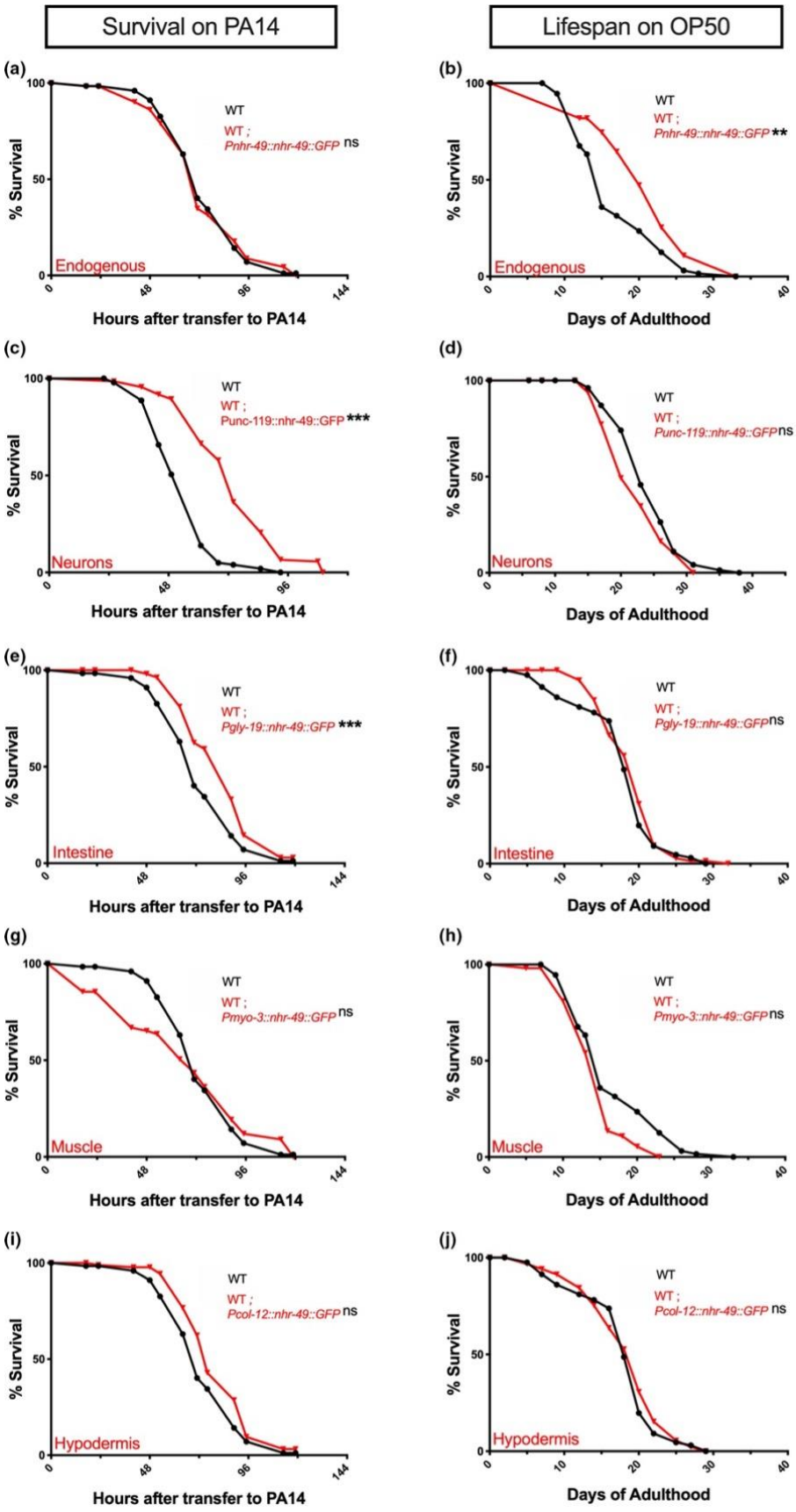
Survival on PA14
Lifespan on OP50
(a)
(b)
(c)
(d)
(e)
(f)
(g)
(h)
(i)
(j)
% Survival
Hours after transfer to PA14
Days of Adulthood
WT
WT ;
Pnhr-49::nhr-49::GFP ns
Pnhr-49::nhr-49::GFP **
Punc-119::nhr-49::GFP ***
Punc-119::nhr-49::GFP ns
Pgly-19::nhr-49::GFP ***
Pgly-19::nhr-49::GFP ns
Pmyo-3::nhr-49::GFP ns
Pcol-12::nhr-49::GFP ns
Endogenous
Neurons
Intestine
Muscle
Hypodermis

Figure 2.5 In wild-type animals, elevating NHR-49 levels in neurons or intestine enhances immunity.

(a, c, e, g, i) NHR-49 overexpression in neurons or intestine increases immunity. Mean survival on PA14 (in hours) of WT worms (black) and strains overexpressing NHR-49 in different tissues (red). (a, e, i, g) Survival of WT (76.98 ± 2.25, *n* = 102/129) and strains overexpressing NHR-49 via Endogenous promoter (a, 76.89 ± 3.06, *n* = 75/121) or promoters expressed in Intestine (e, 91.97 ± 2.65, *n* = 96/124), Muscles (g, 72.11 ± 4.28, *n* = 66/100), or Hypodermis (i, 82.68 ± 2.65, *n* = 63/97). (c) Survival of WT (54.32 ± 1.09, *n* = 125/145) and strain overexpressing NHR-49 in Neurons (c, 73.72 ± 1.61, *n* = 114/136). (b, d, f, h, j) NHR-49 upregulation in individual somatic tissues does not enhance immunity. Mean life span on OP50 (in days) of WT worms (black) and strains overexpressing NHR-49 in different tissues (red). (b, h) Life span of WT (16.67 ± 0.65, *n* = 67/73) and strains overexpressing NHR-49 via Endogenous promoter (b, 20.83 ± 1.01, *n* = 35/44) or promoter expressed in Muscles (h, 14.6 ± 0.55, *n* = 39/52). (d) Life span of WT (24.2 ± 0.55, *n* = 74/91) and strain overexpressing NHR-49 in Neurons (d, 22.35 ± 0.6, *n* = 57/94). (f, j) Life span of WT (17.81 ± 0.56, *n* = 73/121) and strains overexpressing NHR-49 in Intestine (f, 19.06 ± 0.4, *n* = 86/116) or Hypodermis (j, 18.3 ± 0.53, *n* = 95/120). Survival and life span data shown as mean ± standard error of the mean (SEM). "*n*" refers to number of worms analyzed over total number of worms tested in the experiment (see Methods for details). Statistical significance calculated using log-rank (Mantel–Cox) method and indicated by asterisks on each panel next to mutant name (color of asterisk indicates strain being compared to). $p < 0.01$ (**), <0.001 (***), not significant (ns). Note: assays in some panels (a, i, e, g; b, h; f, j) have the same controls as they were performed in the same biological replicate. Data from additional trials are presented in Supp. Table 2.5a-e.

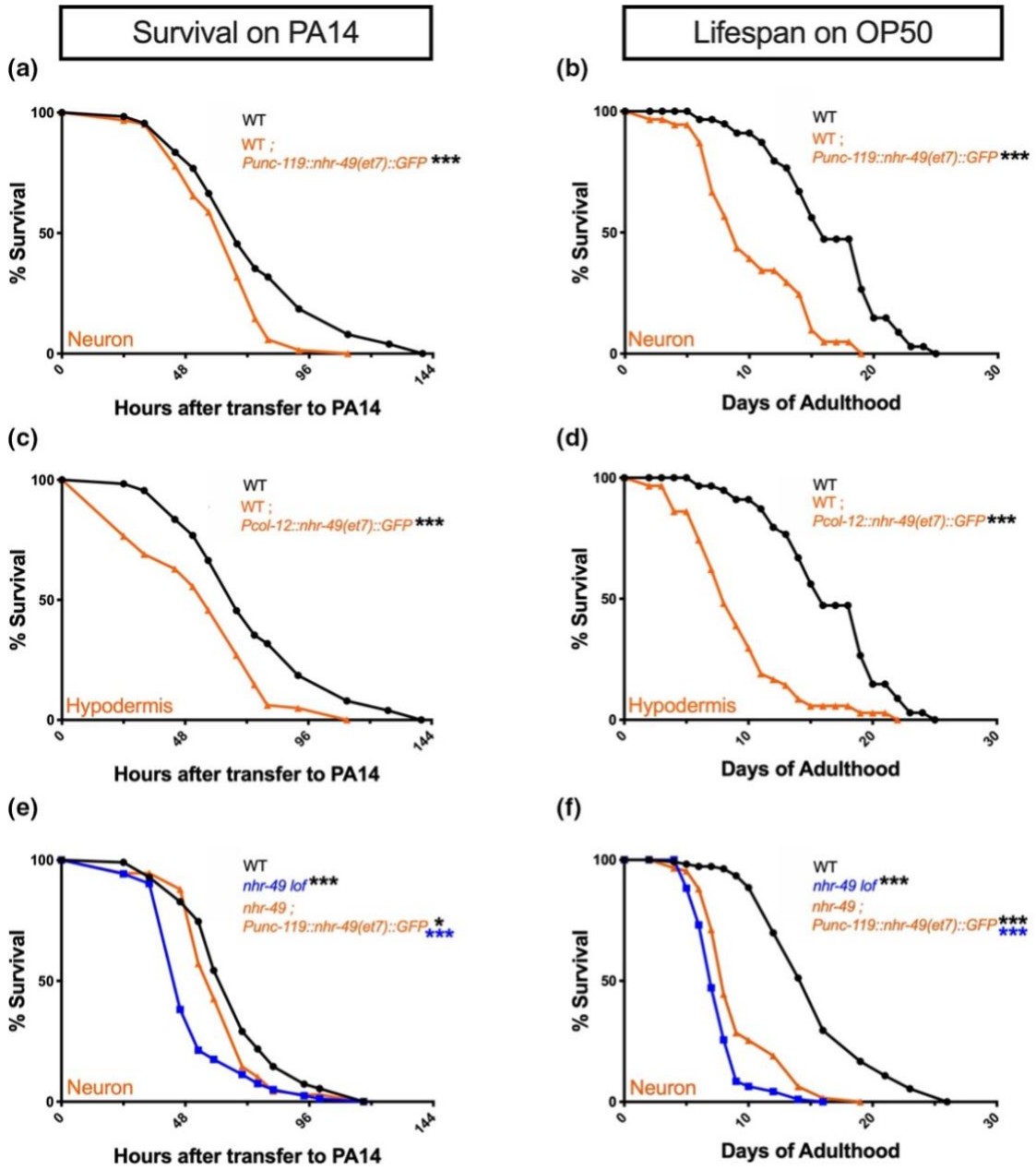

Figure 2.6 Expression of NHR-49^{et7} in neurons or hypodermis reduces immunoresistance and longevity.

(a–d) NHR-49^{et7} in neurons (a, b) or hypodermis (c, d) of wild-type (WT) worms reduces survival upon PA14 exposure (a, c) and life span on OP50 (b, d). Mean survival on PA14 (in hours) of WT (black) and NHR-49^{et7} transgenic strains (orange). (a, c) WT (75.15 ± 2.74, *n* = 94/120), NHR-49^{et7} expressed in Neurons (a, 62.92 ± 1.59, *n* = 98/125) or

Hypodermis (c, 55.46 ± 2.11, *n* = 118/145). (b, d) Mean life span on OP50 (in days) of WT (black) and NHR-49^{et7} transgenic strains (orange). WT (16.49 ± 0.44, *n* = 103/136), NHR-49^{et7} expressed in Neurons (b, 10.23 ± 0.74, *n* = 28/60) or Hypodermis (d, 9.09 ± 0.53, *n* = 60/90). (e, f) Neuronal expression of NHR-49^{et7} partially rescues immunosensitivity of *nhr-49* mutants. (e) Survival on PA14 (in hours) of WT (black, 67.46 ± 2.15, *n* = 78/106), *nhr-49* (blue, 52.23 ± 1.69, *n* = 94/105), and *nhr-49* mutants expressing NHR-49^{et7} in Neurons (orange, 61.77 ± 1.71, *n* = 89/111). (f) Life span on OP50 (in days) of WT (black, 15.61 ± 0.46, *n* = 99/120), *nhr-49* (blue, 7.66 ± 0.2, *n* = 101/119), and *nhr-49* mutants expressing NHR-49^{et7} in Neurons (orange, 9.31 ± 0.38, *n* = 69/89). Survival and life span data shown as mean ± standard error of the mean (SEM). "*n*" refers to number of worms analyzed over total number of worms tested in the experiment (see Methods for details). Statistical significance was calculated using the log-rank (Mantel–Cox) method and is indicated by asterisks on each panel next to mutant name (color of asterisk indicates strain being compared to). $p < 0.05$ (*), <0.001 (***). Note: assays in some panels (a, c; b, d) have the same controls as they were performed in the same biological replicate. Data from additional trials presented in Supp. Table 2.6.

2.3.8 In *glp-1* mutants, elevating NHR-49 levels in somatic tissues does not further enhance immunoresistance

Lastly, we assessed the consequences of raising NHR-49 levels in animals that have elevated protein to begin with, i.e., in *glp-1* mutants wherein NHR-49 is both transcriptionally and translationally upregulated (104). Further overexpression in this genetic background, either using the widespread endogenous promoter or tissue-specific drivers, did not enhance either

longevity or immunity further. In fact, it appeared to diminish survival, especially upon PA14 and in some cases on OP50 as well (Supp. Fig. 2.5a-j, Supp. Table 2.7a-e). Altogether, our site-of-action experiments substantiated the importance of not only the location and levels of NHR-49 but also its tissue-specific activation in determining the impact on lifespan vs. immune status of the animal.

2.3.9 *fmo-2* and *acs-2* are differentially impacted by germ line loss vs. pathogen attack

We asked if the differential impacts of NHR-49 on longevity vs. immunity extended to expression of its downstream targets too. Our NHR-49 UP group included the well-established *nhr-49*-target gene, *acs-2*, that encodes an acyl CoA synthetase involved in mitochondrial β-oxidation (207, 251) and is upregulated in *glp-1* mutants (110), as well as *fmo-2*, that encodes a flavin monooxygenase (Supp. Table 2.1a) (105, 263). Recently, both genes have been reported to be dramatically upregulated upon infection by the Gram-positive pathogens, *Enterococcus faecalis*, and *Staphylococcus aureus* (241, 242). We tested if PA14 exposure altered their expression as well. Instead, *Pfmo-2p::GFP* was significantly downregulated upon PA14 exposure and independent of NHR-49 activity (**Fig. 2.7a-e**). *Pacs-2p::GFP* showed a small NHR-49-dependent increase in expression on PA14 (**Fig. 2.7f-j**). Both genes have been reported to be essential for survival during *E. faecalis* infection, and *fmo-2* mutants are also hyper-susceptible to *S. aureus* infection (241, 242). But, inactivation of neither gene reduced survival upon PA14 exposure (**Fig. 2.7k**).

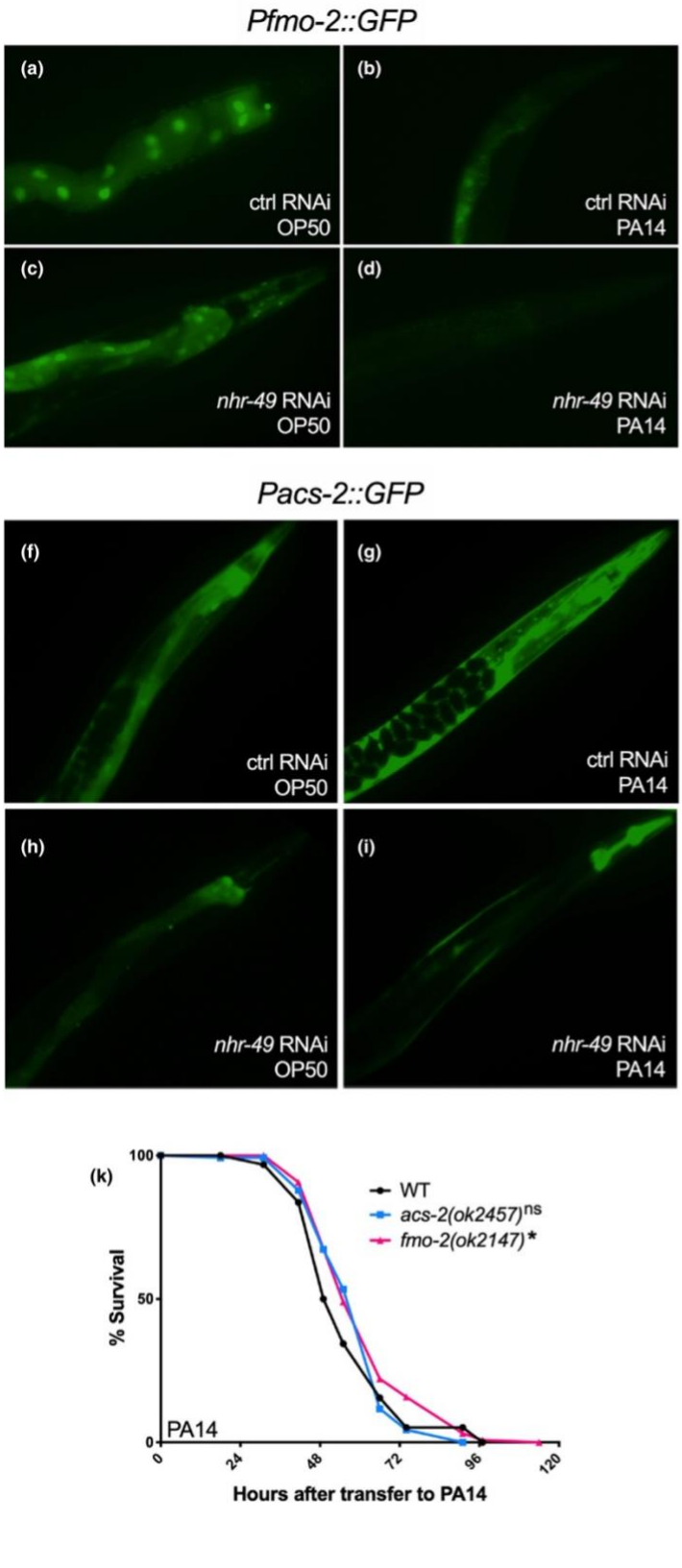
Pfmo-2::GFP
(a)
ctrl RNAi
OP50
(b)
ctrl RNAi
PA14
(c)
nhr-49 RNAi
OP50
(d)
nhr-49 RNAi
PA14
Pacs-2::GFP
(f)
ctrl RNAi
OP50
(g)
ctrl RNAi
PA14
(h)
nhr-49 RNAi
OP50
(i)
nhr-49 RNAi
PA14
(e)
Pfmo-2::GFP
Fluorescence Intensity
ns
ns
****
****
142
78
131
74
OP50
PA14
OP50
PA14
Ctrl RNAi
nhr-49 RNAi
(j)
Pacs-2::GFP
Fluorescence Intensity
***
****
****
32
79
92
28
****
OP50
PA14
OP50
PA14
Ctrl RNAi
nhr-49 RNAi
(k)
% Survival
WT
acs-2(ok2457)ns
fmo-2(ok2147)*
PA14
Hours after transfer to PA14
(l)
Survival on PA14
Mean Survival (hrs)
***
*
**
*
*
*
Ctrl
clec-190
cyp-25A1
dhs-18
spp-12
dhs-2
clec-3
RNAi treatment

Figure 2.7 Known NHR-49 targets, *fmo-2* and *acs-2*, do not contribute toward PA14 resistance.

(a–e) *fmo-2* expression decreases upon PA14 exposure in an *nhr-49*-independent manner. (a–d) Representative GFP images of Day 2 P*fmo-2p*::GFP adults grown till Day 1 on vector control (ctrl, a, b) or *nhr-49* RNAi (c, d) bacteria before transfer to PA14 (b, d) or OP50 (a, c) for 24 h. (e) Violin plot showing quantification of GFP intensity using a COPAS Biosorter. Vector control (Ctrl, black outline) or *nhr-49* RNAi (blue outline). PA14 exposure (pink) or OP50 (blank). Number of worms assayed per condition shown on panel. Data from one of three trials that gave similar results. (f–j) *acs-2* expression increases modestly upon PA14 exposure in an *nhr-49*-dependent manner. (f–i) Representative GFP images of Day 2 P*acs-2p*::GFP adults grown till Day 1 on vector control (ctrl, a, b) or *nhr-49* RNAi (c, d) bacteria before transfer to PA14 (b, d) or OP50 (a, c) for 24 h. (j) Violin plot showing quantification of GFP intensity using a COPAS Biosorter. Vector control (Ctrl, black outline) or *nhr-49* RNAi (blue outline). PA14 exposure (pink) or OP50 (blank). Number of worms assayed per condition shown on panel. (k) Survival of L4 stage wild-type worms (WT, black) and *acs-2* (blue), and *fmo-2* (pink) mutants exposed to PA14. WT (m = 56.66 ± 1.4, n = 97/127), *acs-2* (m = 59.52 ± 1.19, n = 94/137), and *fmo-2* (m = 62.53 ± 1.36, n = 136/153). (l) NHR-49 target genes encoding anti-microbial proteins contribute toward PA14 resistance. Bar graph representation of mean survival (in hours) of wild-type animals exposed till L4 stage to control vector (Ctrl) or RNAi clones targeting NHR-49 target genes (see Methods for details). In (e) and (j), center dashed line indicates median intensity and lines flanking it represent the first and third quartiles; data from one of three trials that gave similar results shown. In (k) and (l), survival data shown as mean life span in hours (m) ± SEM (see Methods for details). Statistical significance was calculated in (e) and (j) using a

one-way nonparametric ANOVA with Dunn's post hoc test (Graphpad Prism). Significance was calculated in (k) and (l) using the log-rank method (Mantel Cox, OASIS2). Statistical significance shown on each panel with the color of the asterisk indicating the strain being compared to. p <0.05 (*), < 0.01 (**), <0.001 (***), <0.0001 (****), not significant (ns).

2.3.10 NHR-49 targets encoding anti-microbial proteins play roles in *Pseudomonas* resistance

In addition to *acs-2*, we had previously identified numerous other genes involved in fatty acid β-oxidation that are upregulated in, and contribute to the longevity of, *glp-1* mutants, dependent upon NHR-49, DAF-16 and TCER-1 (104, 110). Accordingly, our NHR-49 UP group included 24 other genes with roles in β-oxidation and lipid hydrolysis (Supp. Table 2.8). Of these, only 3 were identified as being upregulated upon PA14 exposure, whereas, 7 were in fact downregulated (Supp. Table 2.8) (148, 241, 254). Upon testing the impact of RNAi inactivation of two of these genes, *acox-1.1* (upregulated in both conditions), or *hacd-1* (upregulated in *glp-1*, downregulated on PA14), we observed no consistent change in survival during PA14 exposure (Supp. Table 2.9). The NHR-49 UP class also included multiple members of families encoding anti-microbial proteins (saposins, C-type lectins) and xenobiotic-metabolizing enzymes such as cytochrome P450s and short-chain dehydrogenases (Supp. Table 2.1a) (264). We found that RNAi inactivation of six of eight genes encoding these proteins (*clec-190, clec-3, dhs-18, dhs-2, spp-12*, and *cyp-25A1*) (**Fig. 2.7l**, Supp. Fig. 2.6a, b, Supp. Table 2.9) diminished PA14 resistance of normal worms suggesting that the anti-microbial proteins and xenobiotic enzymes directed by NHR-49 may have functional roles in defense against PA14 infection.

2.4 Discussion

This chapter describes a role for NHR-49 in innate immunity and provides multiple lines of evidence that, although NHR-49 confers both pathogen resistance and long life, it modulates these processes through distinct mechanisms. We show that these mechanistic distinctions (i) arise from differential regulation of NHR-49 by a lifespan-altering intervention such as germline loss vs. the acute stress of pathogen attack, (ii) extend to discrete transcriptional outputs and (iii) culminate in differential functional roles of target genes. Together, these findings underscore the fact the RIL dialogue is controlled by nuanced mechanisms, emphasizing that regulatory effects on lifespan may not reflect immune effects.

In Biology, Context is Critical: In worms and other species, numerous studies have established the cell non-autonomous regulation of longevity and stress-response pathways, and identified tissues where key factors act to modulate these processes (231, 232, 265). Neuron-expressed factors that mediate pathogen recognition and avoidance as well as systemic induction of anti-microbial gene expression have been elucidated as well (233, 234). But, the fact that in addition to site-of-expression, physiological context is crucial in determining whether a protein has beneficial, benign, or detrimental impacts is poorly appreciated. A regulatory factor may act in different tissues to modulate different biological processes (266). Or, within the same tissue, the activity of a protein may have diametrically opposite effects on different aspects of health (10). The cell non-autonomous regulation of longevity vs. stress resistance has been compared for few factors such as DAF-16 (235, 267), XBP-1 (268, 269) and TCER-1 (10). By documenting the impact of NHR-49 expression in each of five different tissues, in each of four genetic backgrounds, on longevity as well as immunity, our study provides substantive evidence

on the importance of physiological context in determining gene function. This has many implications in our effort to understand the RIL tradeoffs, such as the fact that other RIL-regulators may similarly exert tissue-specific effect. For instance, these discoveries drove my attempt to perform a necessity experiment for TCER-1 immunosuppression by restricting its expression to the soma and germ line (Chapter 4.0).

The work described in this chapter displayed that neuronal NHR-49 alone could consistently rescue the immunity deficits of *nhr-49;glp-1* mutants, whereas, their lifespan was substantially restored by expression in any somatic tissue. In *nhr-49* single mutants, immunity was restored by presence in neurons or intestine, but lifespan could be rescued from other tissues as well. This suggests that pathogen response may be more sensitive to NHR-49's location as compared to longevity. Interestingly, NHR-49 expression in muscles provided little or no immunity benefit in any genetic background we tested. In fact, expression in muscles mostly diminished immunity, in contrast to the broad immunity advantages conferred by neuronal NHR-49. Of note, similar observations have been made with the endoplasmic reticulum unfolded protein response (UPR^{er}) regulator, XBP1, whose expression in neurons or intestine increases lifespan and proteostasis but expression in muscles diminishes both (270). Another intriguing observation in our study is the impact of endogenous promoter-driven NHR-49 expression on the PA14 resistance of *nhr-49;glp-1* mutants. Not only was this transgene unable to rescue the mutants' PA14 sensitivity, it further diminished their survival. While it is possible that this is simply a consequence of transgene toxicity, it is unlikely because it is a functional transgene that (a) completely rescued the PA14 resistance of *nhr-49* mutants (b) completely rescued the lifespan on OP50 of both *nhr-49;glp-1* and *nhr-49* mutants (c) did not cause lifespan shortening in WT animals fed OP50 or PA14, and in fact extended lifespan on OP50. These data further

emphasize that pathogen resistance is exquisitely sensitive to NHR-49's site- and level- of expression, and modest changes in either can have major consequences for the animal's immunity. Thus, much like our TCER-1 studies (Chapter 3.0 and 4.0), further investigation of the molecular mechanisms deployed by NHR-49 may provide a deeper understanding of its immune effects, and perhaps its overall role in the RIL dialogue.

Stress and Pathogen-Specific Activities of NHR-49: The experiments of this thesis primarily assess survival of infection against the human opportunistic pathogen, *P. aeruginosa*, to understand immune effects, however, studying resistance to various pathogens can reveal striking nuances in the regulation of immune response itself. NHR-49 has been reported to be involved in defense against pathogens such as *E. faecalis* and *S. auerus* (241, 242). Together with these reports, our data suggest that it orchestrates pathogen specific transcriptional and functional outputs. For instance, expression of *acs-2* and *fmo-2* is upregulated >150 fold and ~1,000 fold, respectively, upon *S. aureus* infection, and on *E. faecalis*, *acs-2* is elevated >20 fold (241, 242, 271). But, we found *fmo-2* to be downregulated by PA14 infection, whereas, *acs-2* showed a small (<2 fold) increase. While these genes are critical for survival upon *E. faecalis* (*acs-2* and *fmo-2*) (241) or *S. aureus* (*fmo-2*) (242) infection, neither one contributed towards PA14 resistance or *glp-1* longevity (Supp. Fig. 2.6c). *fmo-2* shows similarly specific roles in other stress paradigms as mutants are sensitive to starvation but resistant against oxidative stress (105). Interestingly, NHR-49 also appears to differentially regulate β-oxidation and lipid hydrolysis genes between GSC loss (104), other stressors (105, 251, 252) and pathogenic infections (241, 242). Few lipolytic NHR-49 targets elevated in *glp-1* mutants appear to be induced by PA14 infection (Supp. Table 2.8). While inactivation of two such genes did not

reduce PA14 resistance in our study, the broader relevance of NHR-49-driven lipid metabolic changes in PA14 response remains to be investigated. For future studies, this suggests NHR-49 as an attractive candidate for assessment as a RIL regulator, as changes in fat are often associated with fertility deficits (272).

Why does NHR-49 in different tissues impart distinctive effects on immunity and longevity? This chapter does not note differences in levels or cellular localization, and our experiments with NHR-49^{et7} and Fenofibrate overrule the possibility of tissue-specific activation being the sole determinant. This could possibly be attributed to the presence of tissue-specific cofactors that help orchestrate tissue-specific expression profiles. DAF-16 in neurons relies on FKH-9 to drive expression of memory and axon regeneration genes (273), whereas, it's intestinal transcriptome is shared with PQM-1 (274). NHR-49 partners with NHR-80 and NHR-13 to regulate fatty-acid desaturation (262, 275, 276), and with NHR-71 to modulate germline-less longevity, respectively (277). Of these, we found only *nhr-80* RNAi to induce a small reduction in survival on PA14 (Supp. Table 2.9b). Other NHR-49 partners, including 11 NHRs that promote *glp-1* longevity (277) may serve as tissue-specific co-regulators. Like NHR-49, PPARα also has roles in starvation-induced fatty-acid oxidation, oxidative stress, heat-resistance, inflammation and immunotolerance against commensal gut microbiota. Thus, it would be interesting to ask if the immunity-promoting function of NHR-49 also extends to mammalian PPARα. Understanding the corresponding, likely tissue-specific, effects of PPARα on the overall RIL dialogue may then allow for the development of therapeutics which avoid the pitfalls of untargeted gene modulation. In alignment with the goals of this study, the next chapter discusses the unique effects of TCER-1 on reproduction, immunity, and lifespan and proposes it as a regulator of this complex RIL dialogue.

3.0 TCER-1 as a regulator of the Lifespan-Fertility-Immunity Axis

This chapter is a modified version of Amrit, Naim, et al., 2019, Nature Communications, which highlights my contributions. To view the full text, see DOI: 10.1038/s41467-019-10759-z.

Stress resistance and longevity are positively correlated but emerging evidence indicates that they are physiologically distinct. Identifying factors with distinctive roles in these processes is challenging because pro-longevity genes often enhance stress resistance. This chapter demonstrates that TCER-1, the *Caenorhabditis elegans* homolog of human transcription elongation and splicing factor, TCERG1, has opposite effects on lifespan and stress resistance. Our laboratory previously showed that *tcer-1* promotes longevity in germline-less *C. elegans* and reproductive fitness in wild-type animals. We also discovered that *tcer-1* mutants exhibit resistance against multiple stressors, particularly against infection by *Pseudomonas*. Interestingly, my further investigations found TCER-1 only inhibits immunity during fertile stages of life, suggesting that TCER-1 represses immunity to augment fecundity. Subsequent work by first author Dr. Francis RG Amrit showed that elevating TCER-1 levels ameliorates the fertility loss caused by infection. After assessment of TCER-1-targeted genes of the canonical PMK-1/p38 MAPK immunity axis, my studies then contributed to the finding that TCER-1 acts through suppressing both PMK-1-dependent and -independent genes in innate immunity. Taken together, our data establish key roles for TCER-1 in coordinating immunity, longevity, and fertility, revealing mechanisms that distinguish length of life from functional aspects of aging. TCER-1's strong role in these three functions, as the focus of this thesis, therefore sets up this protein's utility to understand the molecular mechanisms governing the RIL dialogue in animals.

3.1 Introduction

In many organisms, a positive correlation has been noted between increased longevity and enhanced tolerance against environmental stressors such as high temperature, oxidative damage and pathogen attack (reviewed in Chapter section 1.1 and (34, 36, 37)). Indeed, stress resistance has been used as a surrogate for lifespan extension in model organisms to identify several longevity genes (38, 278, 279). However, mutants that exhibit increased lifespan without enhanced stress resilience, and vice versa, have been reported intermittently in literature. In fact, in yeast, nematodes, flies and plants, only a fraction of mutants selected for increased stress resistance also exhibit enhanced longevity (38, 278-280). This incomplete correlation implies that stress resistance alone is not sufficient to extend lifespan; other unknown processes may be induced coordinately with stress resistance in long-lived mutants which may underlie their longevity. Importantly, these observations, and other emerging evidence, suggest that stress resilience is physiologically distinct from lifespan (213-215, 281). This is an important distinction because stress resilience is also a major determinant of "healthspan", the multiparametric measure of overall health in aging animals (48, 208, 210). With increasing emphasis on healthspan in the aging field, it is especially exigent to identify genetic and molecular pathways that uncouple stress resistance from lifespan. However, as exemplified in the previous chapter regarding NHR-49, most known longevity-promoting genes also increase stress resistance (reviewed in ref. (34)). Genes that promote longevity but widely inhibit stress resistance or other aspects of healthspan have not been identified. The validation, and experimental modulation of such a gene, could be the key to identifying molecular mechanisms that govern the RIL dialogue.

As discussed in Chapter section 1.1, there is widespread evidence from many species that increased reproduction is accompanied by reduced stress resistance, especially immune resistance, and reciprocally, pathogen infection impairs fertility (reviewed in ref. (62)). But, while fertility and immunity appear to be mutually antagonistic, both diminish with age. Advanced maternal age is a major cause of reduced human reproductive fitness (282). Immunosenescence, the loss of immune resistance with age, underlies increased morbidity and mortality in older organisms (217). Hence, age is an important consideration in the immunity−fertility dynamic, but the molecular mechanisms governing this tripartite relationship are poorly understood.

The nematode *Caenorhabditis elegans*, similar to other humans and other organisms, faces numerous stressors at the cellular (e.g., protein damage) and organismal (e.g., pathogens, high temperatures) levels, and responds via conserved, well-characterized systems such as the heat-shock response (HSR), oxidative stress response (OSR), hypoxia response (HR), unfolded protein response in the mitochondria (UPR^{mt}) or endoplasmic reticulum (UPR^{er}) and others (reviewed in refs. (283, 284)). The response to pathogen threat in *C. elegans* is spearheaded by an innate immune system that includes conserved signaling pathways such as the mitogen-activated protein kinase (MAPK) cascade (Fig. 1.3). The *C. elegans* p38 MAPK, PMK-1, is activated by pathogenic stimuli as well as other stressors, such as oxidative damage, and governs the activity of multiple transcription factors to facilitate pathogen-specific responses (79). Significant overlap exists between innate immune responders and other canonical stress-response factors. For instance, ATFS-1, SKN-1, HSF-1 and HIF-1, key mediators of UPR^{mt}, OSR, HSR and HR, respectively, also upregulate innate immunity genes and confer pathogen resistance (285-289). Many of these proteins, and other such stress-response mediators, also enhance

lifespan in *C. elegans* and other species (285, 286, 290-293). Additionally, their inactivation not only shortens lifespan but accelerates age-related decline in morphology, physiology, behavior, and other healthspan parameters (294, 295). So, while studying such factors has enriched our knowledge of stress-response mechanisms and longevity paradigms immensely, it has not advanced discovery of the molecular distinctions between the quantitative and qualitative measures of aging. This work identifies a role for TCER-1, *C. elegans* homolog of the human transcription elongation and splicing factor, TCERG1 (106, 107), in having discrete and opposite impacts on longevity and stress resilience. Of particular relevance are our discoveries here that suggest that TCER-1 represses immunity to divert resources towards fertility. This aligns with emerging concepts, as discussed in Chapter section 1.3, that distinct molecular mechanisms must coordinate the RIL dialogue and provide a molecular handle to understand them.

My graduate advisor first identified TCER-1 as a factor essential for the lifespan extension caused by germ line loss in *C. elegans* (109). In *C. elegans*, removal of a totipotent population of germline-stem cells increases lifespan in a manner dependent on a network of transcription factors including TCER-1 and the conserved longevity determinant, DAF-16/FOXO3A (reviewed in ref. (99)). TCER-1 overexpression increases the lifespan of normal, fertile animals underscoring its role as a pro-longevity gene (109). Our lab showed that TCER-1 and DAF-16 act coordinately to extend the lifespan of germline-less animals by preserving lipid homeostasis (110). We also discovered that, in normal fertile *C. elegans*, TCER-1 is critical for optimal reproduction as well as the prevention of age-related reproductive decline. *tcer-1* mutants produce fewer, and less viable, eggs than their wild type counterparts, and exhibit signs of premature reproductive senescence. Thus, TCER-1 promotes reproductive fitness under normal physiological conditions (110).

In this chapter, I highlight my contributions to the publication entitled "The longevity-promoting factor, TCER-1, widely represses stress resistance and innate immunity." This article demonstrated that TCER-1 inhibits resistance against multiple biotic and abiotic stressors, including immunoresistance against the opportunistic Gram-negative human pathogen, *Pseudomonas aeruginosa,* and Gram-positive pathogen, *Staphylococcus aureus* (Supp. Table 3.2-3.3). Preliminary experiments by Dr. Amrit revealed that *tcer-1* mutants have increased survival upon infection and, reciprocally, TCER-1 overexpression increases susceptibility towards *P. aeruginosa*. TCER-1 was also noted to act cell non-autonomously in somatic tissues to mediate both its anti-immunity and pro-longevity functions (Supp. Table 3.1) (10). Following these studies, my work showed that TCER-1 inhibits immunity during the fertile stages of life and not in post-reproductive animals, supporting that TCER-1 may repress immunity to promote reproductive fitness. This led to further findings that elevating TCER-1 levels protect animals from the decline in progeny production that follows infection. Numerous known, as well as novel, antibacterial genes suppressed by TCER-1 were also identified. My experimentation with these mutants then revealed that TCER-1 inhibits immunoresistance by repressing both PMK-1-dependennt and PMK-1-independent, innate immunity pathways. Taken together, this work reveals TCER-1 as a key factor governing the relationship between the linked processes of immunity, lifespan and fertility.

3.2 Methods

***C. elegans* Strains and Culture**: All strains were grown and maintained on standard nematode growth medium (NGM) at 20°C using E. coli strain OP50 as the food source. For

experiments involving RNAi, NGM plates supplemented with 1 ml per liter of 1 M IPTG (Isopropyl β-D-1-thiogalactopyranoside) and 1 ml per liter of 100 mg per ml ampicillin. The strains used in this study include N2 (wild type), CF2166 [tcer-1(tm1452) II], CF1038 [*daf-16(mu86)* I], CF1903 [*glp-1(e2144)* III], CF2154 [*tcer-1(tm1452) II; glp-1(e2144)* III], CF1880 [*daf-16(mu86) I; glp-1(e2144)* III], CF2858 [*tcer-1(tm1452); Ptcer*-1::TCER-1::GFP, *Podr-1::*RFP] AGP214 [*daf-16 (mu86) I; tcer-1(tm1452)* II], AGP215 [*daf-16(mu86) I; tcer-1(tm1452) II; glp-1 (e2144)* III], AGP1 {*glmIs [Ptcer-1::tcer-1::GFP+Podr-1::*RFP]} (generated by Dr. Amrit by integrating the transgene in CF2032 strain (109)), IT213 [*tcer-1 prom: tcer-1ORF:gfp:tcer-1 3'utr*](296), ZD1195 {*qdEx101[Poperon::islo-1::pmk-3::pmk-2::GFP::pmk-1::mCherry*]} (297), PRJ112 {*mutEx70 [pmk-1::GFP+rol-6(su1006)*]} (298), AGP97 [*pmk-1(km25)* IV] (299) (obtained by outcrossing to Ghazi lab N2), AGP213 [*tcer-1(tm1452) II; pmk-1 (km25)* IV], RB2356 [*dod-3(ok3202)* V], RB2478 [*irg-5(ok3418)* V], RB1994 [*dod- 24(ok2629)* IV], VC2496 [*ilys-3(ok3222)* V], AGP256 [*tcer-1(tm1452) II; ilys-3 (ok3222)* V], AGP258 [RB2356 {*dod-3(ok3202)* V} outcrossed to Ghazi lab N2], AGP257 [*tcer-1(tm1452) II; dod-3(ok3202)*V], GMC101{*dvIs100 (unc-54p::Aβ-1- 42::unc-54 3'-UTR+mtl-2p::GFP)*} and AGP275 [*tcer-1(tm1452) II; dvIs100 (unc- 54p::Aβ-1-42::unc-54 3'-UTR+mtl-2p::GFP)*]. Transgenic strains expressing TCER- 1 under control of tissue-specific promoters in different genetic backgrounds, generated by Dr. Amrit, are listed in Supp. Table 3.7.

Lifespan Assays: All lifespan experiments were conducted at 20°C on *E. coli* OP50 plates unless otherwise noted. Between 20-30 L4 hermaphrodites were transferred to each of ~5-6 plates per experiment and observed at 24-48hr intervals to document live, dead or censored (animals that exploded, bagged or could not be located) animals. Animals were scored as dead

when they failed to respond to gentle prodding with a platinum wire pick. Fertile strains were transferred every other day to fresh plates until progeny production ceased. For lifespan assays of strains with the temperature sensitive *glp-1* mutation, eggs were picked and maintained at 20°C for 2-4h, transferred to 25°C to induce sterility and then returned to 20°C on day 1 of adulthood (72h later) for lifespan analysis. For performing lifespan assays of transgenic strains with extrachromosomal arrays, eggs were picked onto fresh OP50 plates, incubated at the appropriate temperature and 48h later L4 animals were screened under a Leica M165FC microscope with a fluorescence attachment (Leica Microsystems, Wetzlar, Germany) for animals carrying the red co-injection marker labeling pharyngeal muscles. At the same time, a similar number of age-matched, non-transgenic siblings were collected for each strain and assayed for lifespan as internal controls in the experiment. Each lifespan was tested at least twice and often in 3-5 biological replicates. All survival data was plotted via the Kaplan–Meier method. Statistics were calculated using the non-parametric log-rank Mantel-Cox method using OASIS2 (https://sbi.postech.ac.kr/oasis2/) and subjected to multiplicity correction in experiments that involved more than two strains/conditions (244).

Pathogenic Stress Assays: Pathogenic bacterial strains used in this study include *Pseudomonas aeruginosa* (strains PA14 and PA01) and *Staphylococcus aureus* (NCTC8325). These strains were streaked from frozen stocks onto Luria Bertani (LB) agar (PA14 and PA01) or Brain Heart Infusion (BHI) agar (NCTC8325) plates, incubated at 37°C overnight and stored at 4°C for a week or less. For studies with PA14 and PA01, single colonies from the streaked plates were inoculated and grown in King's broth overnight at 37ºC with shaking. ~20µl of this broth culture was seeded onto slow killing (SK) plates (modified NGM plates containing 0.35%

peptone instead of 0.25%) and incubated for 24h at 37ºC. The plates were then left to sit at room temperature (RT) for 24h prior to use. Between 20-30 L4 hermaphrodites per strain were transferred to each of ~5-6 OP50 plates per experiment, incubated at 25ºC and monitored at 6-12h intervals to account for live, dead, or censored animals as described above. Using a variation of this paradigm, PA01 seeded onto standard NGM plates was also used for pathogen sensitivity assays. For studies with *S. aureus* (NCTC8352), single colonies from the streaked plate were inoculated and grown in BHI broth overnight at 37ºC with shaking and then ~10µL of this was spread onto BHI-agar plates. Plates were incubated overnight at 37°C for 24h followed by storage at RT for 24h. L4-stage animals were transferred to pathogenic plates, maintained at 25°C and monitored for survival every 24h. To analyze PA14 sensitivity of *C. elegans* strains at various stages of life, temporal assays were conducted by picking eggs of wild-type and *tcer-1* strains on OP50 plates, growing at 20°C and then transferring them onto PA14 SK plates at L4, day 2, day 4, day 6 or day 9 of adulthood and monitoring for survival at 25ºC as mentioned above. Reproductively active animals were transferred to fresh OP50 plates every day till the relevant day of PA14 exposure. To rule out the impact of internal hatching on experimental outcomes, wild-type and *tcer-1* L4 larval stage animals were treated with 100 µg per ml of 5-fluoro-2′-deoxyuridine (FUDR) on NGM plates with OP50. Exposing *C. elegans* to this treatment for 24h at 15°C before transferring to PA14 SK plates prevented the eggs from hatching. For RNAi experiments, animals were grown to the L4 stage on standard RNAi plates seeded with *E. coli* HT115 carrying an empty vector control (pAD12) or the relevant RNAi clone before transferring to PA14-seeded SK plates and assaying for survival at 25°C. Kaplan-Meier analysis and statistics were performed as described above for lifespan assays.

Fertility Assessment on OP50 and PA14: Gravid day 2 animals were allowed to lay eggs for a 2h period on OP50 plates. The eggs were allowed to hatch and develop at 20ºC for 65h till they are about to start laying eggs of their own. At this point the animals were transferred to single plates (10 plates per strain per experiment) and incubated at 20ºC. At the 4h timepoint the animals were transferred to fresh plates, moved back to 20ºC and eggs laid on the older plate counted. This was repeated at the 8h, 12h, 24h and 48h timepoints. To calculate percent reduction in egg laying upon pathogen stress the number of eggs laid by each strain on PA14 was normalized to its OP50 control at the same time point. The total brood size of each strain was calculated as the average of the total number of eggs laid per animal per strain during its lifetime. Unpaired t test was used to calculate statistical differences in egg-laying between strain/conditions.

Statistical analyses: All data in this article are expressed as mean (m) ± standard error of mean (sem) unless otherwise noted. Graphs were plotted and statistical analyses performed using Prism, OASIS2 or Microsoft Excel. Probability levels of 0.05 or below were considered statistically significant. Statistical significance of overlap between two groups of genes was calculated on Nemates (nemates.org/MA/progs/overlap_stats.html). The probability of overlapping genes was calculated by Dr. Amrit using the hypergeometric probability formula and the representation factor (RF) was calculated as the number of overlapping genes divided by the expected number of overlapping genes drawn from two independent groups.

Data Availability: Original text and full datasets from this study can be found in the publication, Amrit, Naim, et al 2020, Nature Communications. DOI: 10.1038/s41467-019-10759-z.

3.3 Results

3.3.1 TCER-1 does not repress immunity in post-reproductive adult

Like many other species, *C. elegans*' resistance against PA14 decreases with age. To determine if TCER-1/TCERG1's impact on immunity was age-dependent, I compared the PA14 resistance of *tcer-1* mutants as late L4 larvae (pre-adulthood), Day 2 adults (peak reproduction), Day 4 adults (reproductively active), Day 6 adults (vestigial reproduction) and Day 9 adults (post-reproductive) to that of age-matched WT controls (**Fig. 3.1a**). Both wild-type and *tcer-1* mutants showed a decline in survival time with increasing age, but *tcer-1* mutants survived significantly longer than their age-matched, wild-type counterparts when exposed to PA14 as L4 larvae, day 2, or day 4 adults. However, by day 6, when most animals cease egg-laying, *tcer-1* mutants were no longer more resistant than wild type (no statistical difference in 5/7 trials). By post-reproductive Day 9, *tcer-1* mutants were either equally susceptible to PA14 as wild-type animals, or even more sensitive (**Fig. 3.1a**, Supp. Table 3.5). Thus, *tcer-1* mutants exhibited increased survival on PA14 exclusively during the fertile stages of adulthood. The way TCER-1's effect and intensity matched the reproductive profile of the animal raised the possibility that TCER-1 fertility and immunity effects are interrelated.

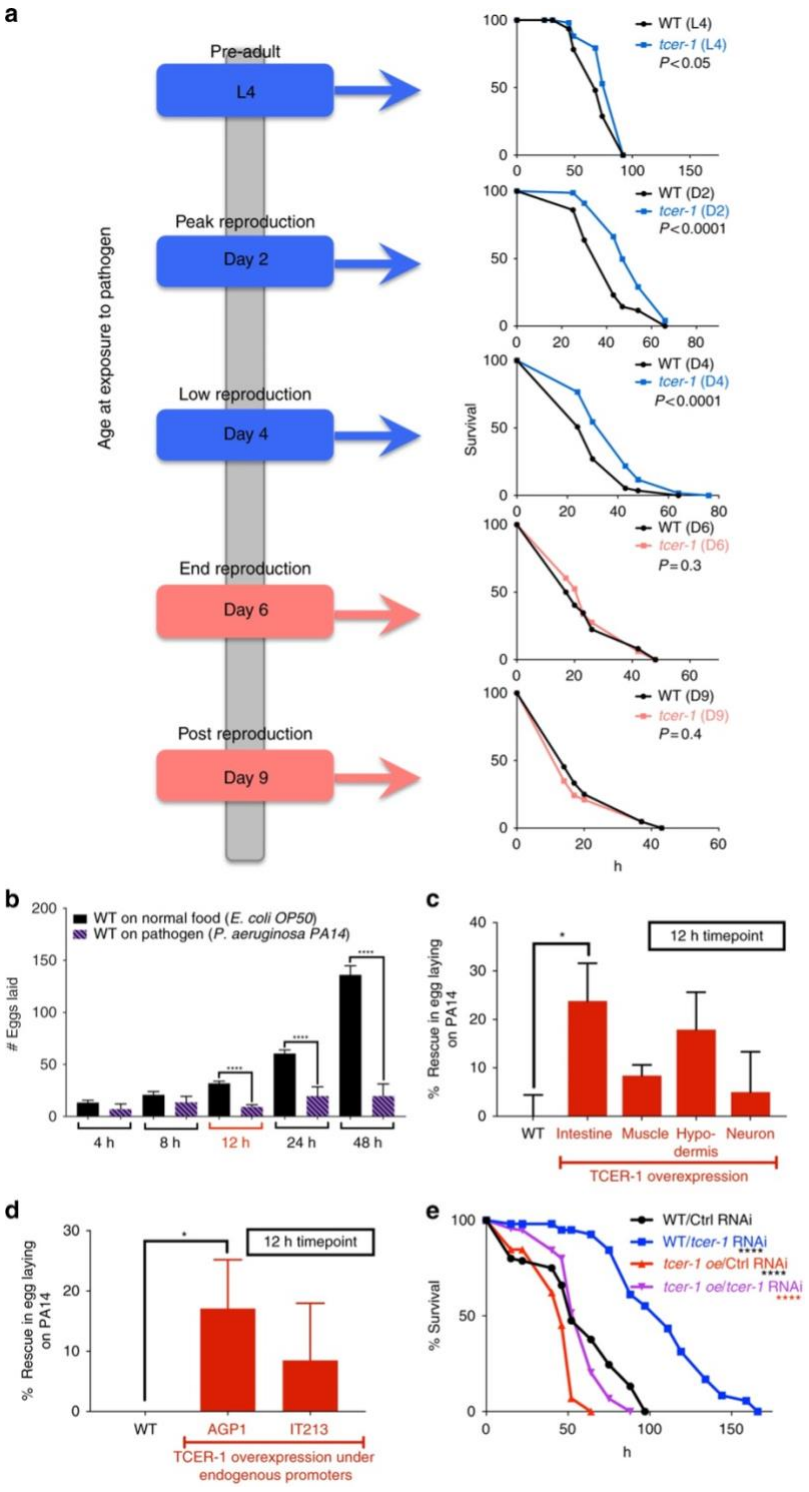

Figure 3.1 TCER-1 links fertility and immunity.

a TCER-1 does not inhibit immunity in post-reproductive adults. Schematic on left indicates age at which animals were transferred to PA14 plates. Mean survival (hours) upon PA14 exposure as

L4 larvae: wild type (WT, black: 71.69), *tcer-1* (blue: 79.97), reproductively active adults (blue): day 2: WT (40.89), *tcer-1* (51.36), day 4: WT (31.41), *tcer-1* (38.86) and at post-reproductive ages (pink): day 6: WT (24.82), *tcer-1* (26.17) or day 9: WT (20.91), *tcer-1* (19.6). **b** Fertility reduction caused by PA14. Egg-laying dynamics of late L4 larvae transferred to PA14 (purple, hashed) or control *E. coli* OP50 (black, solid). **c**, **d** Decline in egg laying caused by PA14 is limited by overexpressing TCER-1. *Y*-axes show percent rescue in egg laying 12 h after PA14 exposure by strains overexpressing TCER-1 (red bars, *X*-axes) in **c** individual somatic tissues or **d** under control of *tcer-1* endogenous promoters, as compared to the 65% reduction in egg laying shown by WT (baseline). To control for differences in brood sizes, number of eggs laid by each strain on PA14 was normalized to its brood size on OP50. For assays (**b**–**d**), data combined from 2 to 10 biological replicates with 10−20 animals per strain per replicate. Statistical significance calculated using two-tailed, unpaired *t* test. Error bars denote standard error. **e** TCER-1 overexpression increases PA14 susceptibility. Survival (hours) of wild-type on control vector (WT/Ctrl, black; $m = 57.47$, $n = 68/100$) or *tcer-1* RNAi (WT/*tcer-1*, blue, $m = 108.46$, $n = 100/100$) and endogenous promotor-driven TCER-1 transgenic strain (*tcer-1* o/e) on control (*tcer-1 oe*/Ctrl, red; $m = 43.46$, $n = 68/85$) or *tcer-1* RNAi (*tcer-1* oe/*tcer-1*, purple, $m = 57.96$, $n = 83/116$). Survival data analyzed using Kaplan−Meier test. Asterisks indicate statistical significance <0.05 (*), and <0.0001 (****) and color denotes the strain of comparison. *P* values adjusted for multiplicity where applicable. Details of number of animals in panel **a** and data from additional trials in Supp. Table 3.5. *Figure development and data collection for b-e by Francis RG Amrit*.

3.3.2 TCER-1 overexpression curbs PA14-induced fertility loss and increases susceptibility to infection.

Upon pathogen attack, fertility decline and reproductive arrest are usually one of the first consequences experienced by the host across species (52, 62). Overall, our previous work has shown TCER- 1 promotes reproductive fitness and germ line health in normal, fertile animals (110). In this study, TCER-1 appeared to exert the strongest immune repression during the animal's peak fertility, but not during the post-reproductive phase of life. Thus, we speculated that the TCER-1 protein repressed stress resistance to divert cellular resources towards progeny production. To test this, Dr. Amrit documented how PA14 effects *C. elegans* reproduction. Wild-type animals grown on normal food were assessed for a decline in egg-laying following transfer to PA14 or OP50 control plates. A decline in the number of eggs laid by infected animals became apparent in 8 h, and by 12 h infected *C. elegans* laid ~65% fewer eggs as compared to normal adults (**Fig. 3.1b**). We next asked if, and how, the dynamics of this decline would change upon elevating TCER-1 levels. The 12h post-infection timepoint was selected for these experiments as this stage was early enough to visualize a strong reduction in egg production well before the animal was overwhelmed by infection (48 h). We then compared the decline in egg laying upon PA14 exposure between wild-type adults and those overexpressing TCER-1 in the intestine, muscle, hypodermis, neurons or under control of the *tcer-1* endogenous promoter. While normal animals exhibited ~65% decline in the number of eggs laid 12 h post-infection, the decline in transgenic strains was only ~35−55% (**Fig. 3.1c, d**). The protective effect was strongest, and achieved statistical significance, in a strain overexpressing TCER-1 in intestinal cells and in one of two strains wherein TCER-1 was driven by its own promoter (**Fig. 3.1c, d**). Neuronal, hypodermal and muscle overexpression showed a consistent and perceptible rescue in

fertility, but did not achieve statistical significance. Thus, upregulating TCER-1 partly counteracted the fertility decline that followed pathogen attack in *C. elegans*. These observations support the premise that TCER-1 may promote the allocation of resources towards reproduction by repressing cellular investment in stress resilience.

If TCER-1 were indeed promoting reproduction by repressing immunity, we next wondered if TCER-1 overexpression would conversely increase susceptibility to pathogen. Interestingly, when TCER-1 was overexpressed in individual somatic tissues, no consistent alteration in PA14-sensitivity was observed (Supp. Table 3.4c). However, a transgenic strain overexpressing TCER-1 widely under control of its endogenous promoter showed high susceptibility to PA14 compared to the wild type (**Fig. 3.1e**) (296). This was despite having similar pharyngeal pumping rates as the wild-type and *tcer-1* mutants, which suggested that the TCER-1 overexpressing strain eats pathogen as frequently as wild type (Supp. Fig. 3.1a). The PA14 susceptibility of these TCER-1 overexpression strains was also abrogated upon *tcer-1* RNAi (**Fig. 3.1e**). In alignment with this established connection between TCER-1, fertility, and immunity, subsequent experiments showed that native TCER-1 levels are in turn lowered with the presence of pathogens and/or reproductive age. This was found by monitoring TCER-1::GFP expression in both the somatic tissues and germ cells, where Dr. Amrit detected a decrease in TCER-1 expression with both age and PA14 exposure (10). Overall, these data support TCER-1's validity as a regulator of reproduction versus immunity investments in animals, which innately responds to the environment and controls key processes accordingly.

3.3.3 TCER-1 represses both PMK-1 and PMK-1-independent genes in innate immunity

How does TCER-1 repress immunity? Comparative analysis of TCER-1 RNAseq data showed ~15% (42/295) of genes downregulated by TCER-1 were associated with immunity and stress resistance functions and half of this list was shown to be induced specifically upon PA14 exposure (Supp. Fig. 3.2a). Further, TCER-1-downregulated genes included the key immunity transcription factor, PMK-1/p38 MAPK. This led to quantitative PCR (Q-PCR) and translational reporter analysis, which showed both *pmk-1* mRNA and protein levels are suppressed by TCER-1 (10). Subsequent Q-PCRs and epistasis analysis revealed that several PMK-1-induced immunity targets are suppressed by TCER-1, yet, TCER-1 only partially suppresses immunity through PMK-1 (10). Dr. Amrit also identified four more PMK-1-independent immunity genes which were suppressed by TCER-1 in both normal and pathogenic conditions (10).

Since the molecular-genetic and epistasis tests suggested a partial influence of TCER-1 on the PMK-1 pathway, I sought to test whether the identified PMK-1-dependent or -independent genes repressed by TCER-1 had any functional roles in immunity. Thus, we obtained publicly available mutants of PMK-1-dependent genes, *dod-3*, *irg-5*, and *dod-24*, as well as the PMK-1-independent genes, *ilys-3*, and tested their resistance to PA14 upon *tcer-1* knockdown. L4-stage wild-type worms subjected to *tcer-1* RNAi through their development before PA14 exposure exhibited a significant increase in survival compared to control worms (**Fig. 3.2a-d**, Supp. Table 3.6a). However, *dod-3*, *irg-5*, *dod-24*, and *ilys-3* mutants did not exhibit any lifespan extension under the same conditions (**Fig. 3.2a-d**, Table 3.6a). I generated *tcer-1;dod-3* and *tcer-1;ilys-3* double mutants and found these also to be significantly more susceptible to PA14 than *tcer-1* mutants alone, confirming the observations made through RNAi-knockdown of these genes (**Fig. 3.2e-f**, Supp. Table 3.6b and 3.6c). Overall, these findings

indicate that TCER-1 represses the expression of multiple genes critical to PA14 resistance, and these include genes in the PMK-1 pathway and potentially novel immunity effectors.

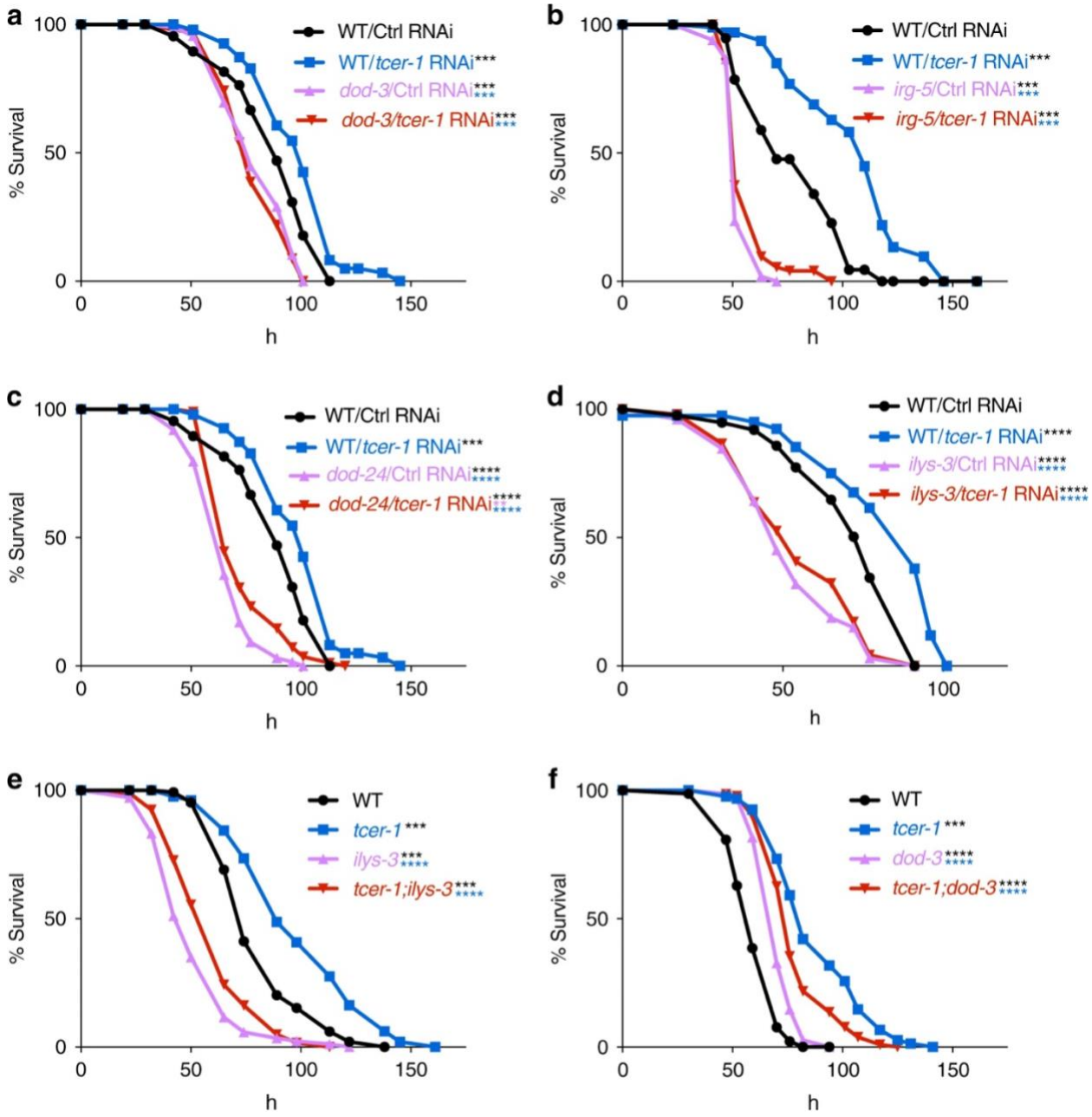

Figure 3.2 TCER-1-repressed genes are essential for resistance against PA14.

Survival of wild-type L4 animals grown from egg stage on empty control vector (black, WT/Ctrl) or *tcer-1* RNAi bacteria (blue, WT/*tcer-1*) and then transferred to PA14 plates compared to the survival of **a** *dod-3*, **b** *irg-5*, **c** *dod-24* or **d** *ilys-3* mutants grown on empty control vector (pink curves) or *tcer-1* RNAi bacteria (red). **a** WT/Ctrl ($m = 87.63 \pm 2.2$), WT/*tcer-1* ($m = 99.27 \pm 2.1$), *dod-3*/Ctrl ($m = 79.95 \pm 1.5$), *dod-3*/*tcer-*

1 ($m = 78.8 \pm 1.4$). **b** WT/Ctrl ($m = 77.67 \pm 3.0$), WT/*tcer-1* ($m = 104.62 \pm 2.7$), *irg-5*/Ctrl ($m = 53.07 \pm 0.7$), *irg-5/tcer-1* ($m = 56.69 \pm 1.2$). **c** WT/Ctrl ($m = 87.63 \pm 2.2$), WT/*tcer-1* ($m = 99.27 \pm 2.1$), *dod-24*/Ctrl ($m = 66.18 \pm 1.4$), *dod-24/tcer-1* ($m = 74.20 \pm 1.5$). **d** WT/Ctrl ($m = 72.12 \pm 2.3$), WT/*tcer-1* ($m = 81.33 \pm 2.5$), *ilys-3*/Ctrl ($m = 52.15 \pm 1.9$), *ilys-3/tcer-1* ($m = 55.21 \pm 2.0$). **e** Survival of wild type and mutants transferred to PA14 plates at L4 stage. WT (black, $m = 88.05 \pm 2.0$), *tcer-1* (blue, $m = 111.81 \pm 2.3$), *ilys-3* (pink, $m = 54.29 \pm 1.3$) and *tcer-1;ilys-3* ($m = 60.74 \pm 1.5$). **f** WT ($m = 60.06 \pm 0.8$), *tcer-1* ($m = 87.9 \pm 2.0$), *dod-3* ($m = 70.87 \pm 0.75$) and *tcer-1;dod-3* ($m = 79.06 \pm 1.3$). Survival estimated using the Kaplan−Meier analysis and shown as mean lifespan in hours (m) ± standard error of the mean (SEM). *P* values were adjusted for multiplicity where applicable. Asterisks indicate statistical significance <0.01 (**), <0.001 (***) and <0.0001 (****) and their color denotes the strain of comparison. Assays in panels (**a**) and (**c**) were performed in the same biological replicate so their controls are shared. Details of number of animals and data from additional trials are presented in Supp. Table 3.6.

3.4 Discussion

As discussed in Chapter section 1.1, infections reduce fertility, whereas increased reproduction is accompanied by immunosuppression in most species (62). Alterations to a woman's immune system are critical during pregnancy to tolerate fetal tissue, but are associated with increased susceptibility to infectious agents (52). In insects, infections reduce fecundity while mating diminishes infection resistance (62). Interestingly, my studies showed that TCER-1 immunosuppression only occurs during the reproductive phase of an animal's life. This

established a role for TCER-1 in the immunity-fertility dialogue, suggesting that this gene only suppresses immunity according to the animal's needs. Dr. Amrit's experiments, showing that TCER-1 overexpression could in-turn blunt the fertility loss caused by pathogen infection further supported this point. Ensuing findings on the pathways and multiple resistance paradigms through which TCER-1 suppresses immunity then revealed the breadth of immune mechanism impacted by this regulator, which led to my investigations in Chapter 4.0. Thus, this study's description of TCER-1 in lifespan, fertility, and immunity showcased its utility as a tool to study the complex RIL dialogue in animals.

The innate immune system is an ancient and conserved system of defense against pathogens, and PMK-1-directed MAPK signaling has a well-established role in driving transcriptional changes that mediate immunity (79). Our studies showed that TCER-1 may counter such changes directly or indirectly. First, Dr. Amrit identified PMK-1 to be a TCER-1-repressed gene and confirmed by both molecular and transgenic approaches. Several known PMK-1 targets were upregulated in *tcer-1* mutants. Yet, the *pmk-1* null mutation did not completely abrogate *tcer-1* mutants' resistance. The epistasis analyses for immune resistance which I conducted also noted TCER-1 to suppress immunity through both PMK-1-dependent and -independent targets. This suggests that TCER-1-mediated immunity suppression is only partially through PMK-1-repression. What other processes may be impacted by TCER-1 to impair immunity? Several cellular surveillance pathways are activated by pathogen exposure, either partially or completely independent of PMK-1 (285-289). In light of this, and TCER-1's role in inhibiting multiple stress modalities, a logical prospect is that cellular stress response factors may be inhibited by TCER-1. Indeed, several genes with roles in UPR^{mt} (e.g., mrps-5) and HR (e.g., *cysl-1*) were included in the TCER-1 DOWN group (110, 300, 301). *tcer-1*

mutants showed higher expression of the central UPR^{mt} regulator, *atfs-1*, the UPR^{mt} specific chaperone, *hsp-6* (Supp. Fig. 3.3a, b) and *hif-1*, the key HR mediator (Supp. Fig. 3.3c) (285, 286, 289, 302). Accordingly, we also noted a significant overlap between the TCER-1 DOWN genes and ATFS-1-regulated genes (Supp. Fig. 3.3d-f) (110, 285, 286).

Sequence-based computational approaches have led to the identification of numerous immune effectors in *C. elegans*, including conserved and invertebrate-specific lysozymes (LYS and ILYS proteins, respectively) that may digest bacterial cell walls (303, 304). TCER-1-repressed genes comprised some of these factors as well as novel proteins with predicted antibacterial functions. For instance, C50F7.5, a TCER-1-repressed gene upregulated >50-fold upon infection, encodes a protein that shares ~60% sequence similarity with a cell-surface glycoprotein in *Clostridium thermocellum* (10). Cell-surface glycoproteins function in pathogen recognition, the most well-known being the family of Toll-like receptors—receptors that sense pathogen associated molecular patterns expressed by infective agents (305). Notably, no pathogen-specific receptors have been identified yet in nematodes. Similarly, the TCER-1-repressed gene, *fbxa-59*, which encodes an F-Box protein, is highly upregulated upon PA14 exposure (10). F-Box proteins are E3 ligase components that mediate proteasomal protein degradation and influence longevity (306). Natural allelic variations of the HECT-domain E3 ligase, HECW-1, have been implicated in PA14 avoidance, and the CUL-6 E3 ligase complex is involved in the response to *Nematocida parisii* (307, 308). But, E3 ligases activated by *Pseudomonas* infection remain unknown. Characterization of the TCER-1- repressed transcriptome can reveal novel insights into the molecular repertoire of nematode immunity, which led to our studies in Chapter 4.0.

Cell non-autonomous mechanisms that govern longevity and stress resistance have been demonstrated recently in many contexts. In *C. elegans*, protein-folding imbalance in muscles induces transcellular chaperone signaling that evokes stress responses in intestine and neurons (309). XBP-1 and retrograde Wnt signaling act in neurons to coordinate the organismal UPR^{mt} and UPR^{ER} responses (reviewed in refs. (310, 311)) whereas intestinal DAF-16 expression is sufficient to confer longevity in germline-less mutants (235). Similarly, dFOXO activity in *Drosophila* fat body regulates brain insulin signaling as well as lifespan, whereas Activin disruption in muscles impacts systemic insulin metabolism (236, 312). In mice, Xbp1s activity in Pomc neurons is sufficient to improve hepatic glucose metabolism and protect against diet-induced obesity (313). An interesting finding of this study was also that TCER-1 can function in any of the four somatic tissues we tested to impact longevity and stress response. This differs greatly from our findings with the pro-longevity gene, NHR-49, in Chapter 2.0 which exerts highly tissue-specific effects on the two processes. Other experiments in this publication also found that expressing TCER-1 in any somatic tissue of *tcer-1* mutants suppressed their PA14 resistance. While it is possible that this is simply a consequence of toxicity caused by TCER-1 overexpression, the fact that these transgenes (a) do not cause lifespan shortening in normal animals fed either OP50 (Supp. Table 3.1) or PA14 (Supp. Table 3.4c), (b) do not shorten *glp-1* mutants longevity on OP50 (Supp. Table 3.1) and (c) extend the lifespan of *tcer-1;glp-1* mutants on OP50, supports TCER-1's non-autonomous mode of action in its anti-immunity and pro-longevity functions. It is indeed intriguing that TCER-1 overexpression has profoundly different consequences for the animal depending on consumption of benign food or noxious pathogen. It implies that TCER-1's presence in any somatic tissue can convert it into a coordinating center for orchestrating an animal-wide outcome, and that it may contextually direct the release of

vastly different signals from the same tissue. Such molecular versatility can be highly beneficial to an animal in the wild facing rapidly fluctuating conditions to coordinate different aspects of its physiology. The fact that TCER-1 does not exert tissue-specific effects on lifespan and immunity, like our findings with NHR-49 (Chapter 2.0), further supports the complexity of RIL regulation in animals.

TCER-1 is a longevity-promoting factor because it is essential for the lifespan extension conferred by germ line loss, and because its overexpression in normal, fertile adults increases their lifespan (109). Hence, the widespread, enhanced stress resistance of *tcer-1* mutants was surprising considering the strong correlation between longevity and stress tolerance (Supp. Table 3.2-3.3). It suggested that mechanisms that confer stress resistance do not directly confer longevity, although we cannot rule out this possibility for an as-yet untested stress modality. Though infrequently, mutations that increase thermal or oxidative stress resistance but do not increase lifespan (e.g., *pep-2*) as well as ones that enhance lifespan without improving stress endurance (e.g., *cep-1*) have been described (214, 215). Germline-less *daf-16* mutants are shorter-lived than wild type but exhibit greater thermotolerance, and *daf-2* mutants subjected to RNAi inactivation of the pro-longevity gene, *smk-1*, continue to exhibit increased thermotolerance (235). But, it is noteworthy that the instances of uncoupling reported so far have been exceptions and pro-longevity genes largely act as pro-stress-resistance factors. The thermotolerance uncoupling notwithstanding, *daf-16* and *smk-1* confer resistance against numerous stressors in long-lived and wild-type animals (34). Importantly, the knockdown of neither gene improves stress resistance, whereas *tcer-1* inactivation does, widely and consistently. *tcer-1* not only uncouples longevity from multiple stress modalities, it broadly antagonizes stress endurance. Additionally, while our previous study demonstrated that DAF-16

and TCER-1 collaborated to establish lipid homeostasis and promote longevity in germline-less adults (110), these data reveal that, TCER-1 and DAF-16 have an antagonistic relationship for stress resistance. They highlight the complexity of the links between lifespan and stress biology and suggest that the relationship is context-dependent and plastic.

It is also salient that while fertility and immunity appear to be mutually antagonistic, both diminish with age. In *C. elegans*, PMK-1 activity, which declines with age, is thought to underlie immunosenescence (314). Since TCER-1 acts, in part, to repress PMK-1, it is possible that the age-related loss of *tcer-1* mutants' PA14 resistance is linked to this reduction. Interestingly, the immune resistance of some sterile mutants is also reduced at post-reproductive ages, emphasizing that the association of immunity and fertility is multifaceted and governed by factors such as age and resource allocation (315). The fact that TCER-1 is essential for reproductive health and exerts a repressive influence on immunity only during the reproductive phase, and the observation that raising its levels allows the animal to escape some of the fertility loss inflicted by infection, suggest that TCER-1's primary molecular function may be to promote fertility. Indeed, further experiments by Dr. Amrit found that both somatic and germ line levels of TCER-1 are highest in young animals and decline with age. Interestingly, human oocytes also express high levels of TCERG1 mRNA and its levels decline in older oocytes, so it may have a conserved role in promoting reproductive fitness (316). Identification of both PMK-1-dependent and -independent TCER-1 immunity functions also implies that multiple pathways may suppress immunity in fertile animals, which led to my investigations in Chapter 4.0. In sum, this study showed TCER-1 can be a useful handle to decipher the mechanisms underlying RIL tradeoffs, a central finding of this thesis.

4.0 TCER-1 promotes siRNA production as a mechanism of immunosuppression

Mechanisms utilizing endogenous non-coding, small RNAs (smRNAs) are an ancient and conserved system for post-transcriptional gene regulation across species. Although the smRNA-directed silencing of complimentary transcripts is typically associated with viral resistance, emerging studies have implicated smRNA silencing strategies in immune responses to bacterial infections as well. Immune roles have particularly been described for the micro-RNA (miRNA) and piwi-RNA (piRNA) classes of smRNAs. Yet, a broader understanding of smRNA function in innate immunity, especially the small-interfering RNA (siRNA) class, remains unaddressed. As described in previous chapters, TCER-1, the *C. elegans* homolog of the human transcription elongation and splicing factor, TCERG-1, represses innate immunity in reproductively active worms, to possibly divert resources towards progeny production. In an effort to unravel TCER-1's mechanism of action, we discovered that TCER-1 promotes the biogenesis of a class of endogenous siRNAs, the 22G WAGO siRNAs, to mediate immune suppression. These discoveries constitute the focus of this chapter. We found that, similar to *tcer-1* mutants, multiple mutant strains for genes involved in siRNA amplification exhibited enhanced resistance to the human opportunistic pathogen, *Pseudomonas aeruginosa*. Our epistasis analyses revealed that many of these genes also act in the TCER-1 pathway to suppress immunity. Accordingly, smRNA sequencing found that *tcer-1* mutation caused a ~10% reduction in the levels of 22G siRNAs. Subsequent analyses of downstream targets then identified immune-impacting genes which are suppressed by TCER-1-directed siRNA silencing. Thus—as the siRNA class is rarely implicated in smRNA-directed immune control—this work describes a previously unrecognized pathway in antibacterial immunity.

4.1 Introduction

Small RNAs (smRNA) are short (~18-30nt) RNA molecules known for their ability to silence complimentary self and foreign genetic material, often through the process of RNA interference (RNAi). Since their first descriptions in *C. elegans*, host-produced smRNAs have been noted to control a panoply of biologic processes in a conserved manner across species, including development, fertility, and genomic stability (159, 317). Advances in technology, particularly deep sequencing, have revealed the existence of many distinct smRNA species in animals, and identified novel functions for each (161, 162). Notably, recent studies have shown smRNA regulation also impacts immunity to bacterial infection, however, the effects of diverse smRNA species on immune function remain largely understudied. This chapter discusses the regulation of innate-immune response by a class of endogenously-produced smRNAs acting genetically in concert with TCER-1, a major focus of this thesis. The *Caenorhabditis elegans* smRNA pathways are largely conserved with other species and hence offer a useful platform to dissect the complex functions of these smRNA species (160, 318).

In worms, as in other species, the main branches of endogenous smRNAs are the **microRNA (miRNA), small-interfering RNA (siRNA), and Piwi-interacting RNA (piRNA)** biosynthesis pathways, which regulate some shared, yet largely distinct, functions in organisms (Ch. 1.0, Fig. 1.4) (161). For instance, miRNAs, which may silence imperfectly-matching mRNAs outside of their heptameric "seed" sequence, regulate a diverse set of mRNA targets, most notably essential to development (163). piRNAs and siRNA are known for their conserved role in maintaining genome stability in animals, as they silence potentially interloping transposons in the germ line (164). Yet while piRNA activity is restricted to the germ line, additional roles of the siRNA pathway in the soma are still being explored (165).

Although smRNA regulation of immunity is typically associated with viral resistance (168, 319, 320), recent studies have begun to define roles for smRNA species in antibacterial immunity (170, 321). For instance, studies in both *C. elegans* and mammals have found miRNAs reshape immune response (169, 322). Mammalian studies attribute these effects mainly to miRNAs regulating genes expression in innate- and adaptive- immune cells. These effects include, but are not limited to, control of leukocyte development, immune cell activation, and inflammation (reviewed in (171)). However, recent work in *C. elegans*, which does not harbor dedicated immune cells, has shown that several miRNAs impact pathways involved in antibacterial immunity, such as the p38 MAPK axis and unfolded protein responses (172, 174, 318). Although less frequent, piRNA pathways have also been implicated in resistance to bacterial infection (323, 324). A role for the endogenous siRNA branch in antibacterial immunity has however been poorly described in worms and other metazoans (173, 325).

TCER-1 encodes the *C. elegans* homolog of the human transcription elongation and splicing factor, TCERG-1 that has been reported to both control alternative splicing of key mammalian genes such as Bcl2 and impact neuronal development (106). Studies from our laboratory collectively revealed that TCER-1 suppresses immunity in young, fertile, hermaphrodites to likely divert resources towards reproductive fitness (10, 109, 110). As described in Chapter 3.0, we found that TCER-1 promotes fertility and suppresses immunity exclusively during the worm's reproductive phase (10). TCER-1 overexpression also curbs *C. elegans* fertility loss upon infection and shortens pathogen survival. The unique ability of TCER-1 to suppress resistance to multiple pathogens and abiotic stressors further supports its extensive impact on immunity (10). Thus, experimental modulation of TCER-1 can be used a tool to identify wide-ranging mechanisms of immune suppression deployed by animals. The

conservation of this gene in promoting reproductive fitness is also supported by reports suggesting that TCERG1 expression in mouse and human oocytes declines with age (114, 326) as well as experimental observations from our collaborative studies (Brieno-Enriquez and Ghazi, unpublished). However, the mechanisms by which TCER-1 suppresses immune function is still being defined. Investigating immunosuppression pathways in *C. elegans*, an established model for innate immunity, has the potential to identify novel and conserved effectors in this process (79, 327).

Although many studies implicate miRNA and piRNA in the regulation of antibacterial immunity, siRNAs are seldom mentioned. Interestingly, a previous unbiased, whole-genome screen identified immune-suppressing TCER-1 as a gene essential for RNAi fidelity in *C. elegans*; a process that depends on functioning smRNA biosynthesis (176). Another study reported that *tcer-1* mutants have reduced endogenous siRNA activity (177). These evidences that TCER-1 promotes siRNA production provided an early indication that the immunoresistance of *tcer-1* mutants may be due to de-repression of transcripts normally silenced by siRNAs. The handful of studies which propose that immunity can be induced by the therapeutic introduction of exogenous siRNAs in patients suggest that endo-siRNA immune regulation in animals is plausible (328, 329). Similarly, studies in mammals showing endo-siRNAs can induce crucial antiviral immune components; and studies in plants finding siRNA responses improve bacterial defense, support this concept (reviewed in (325, 330)). Yet, few studies succinctly demonstrate the impact of siRNA regulation on antibacterial immunity in animals (328, 331). In support of this, *C. elegans* studies have identified many miRNA mutants with altered bacterial resistance (170, 332), but attempts to implicate siRNAs in immunity has mostly pointed back to the miRNA pathway, as certain biosynthesis genes operate in both of these pathways (173, 321). The

findings of this study, which consistently identify siRNA mutants with increased immunity to bacterial infection, are therefore unique.

In this study, we demonstrate that TCER-1's support of siRNA production likely contributes to the protein's role in repression of immunity against bacterial pathogens. *tcer-1* mutants exhibited a significant reduction in levels of a specific class of siRNAs, the 22G WAGO siRNAs. Much like *tcer-1* mutations, mutation of genes involved in siRNA biogenesis and amplification manifested enhanced resistance to the Gram-negative human pathogen, *Pseudomonas aeruginosa* strain PA14 (henceforth PA14). Epistatic analyses of mutations in genes involved in siRNA biosynthesis also suggested they acted in the same genetic pathway as TCER-1 to repress immunity. smRNA and mRNA transcriptional profiling of *tcer-1* mutants indicated overlaps with profiles of immunoresistant siRNA amplification mutants, further supporting their operation through the same pathway. In context with the established role of TCER-1, these findings uncover a role for 22G WAGO siRNAs in innate immunity, suggesting that TCER-1 promotes siRNA biogenesis, in part, to mediate immunosuppression.

4.2 Methods

***C. elegans* strains and culture:** *C. elegans* strains were grown and maintained using standard techniques on nematode growth medium (NGM) with *E. coli* strain OP50 as a food source (333). Experiments involving RNAi used NGM plates supplemented with 1 ml of 1 M IPTG (Isopropyl β-D-1-thiogalactopyranoside) and 1 ml 100 mg/ml Ampicillin per liter before seeding with HT115 *E. coli* containing RNAi constructs or an empty vector control (pAD12). Experiments using FUDR (5-fluoro-2′-deoxyuridine) to stop egg hatching involved

supplementing NGM with 100 μg/ml FUDR before seeding with OP50 (334). The main strains used in this study include N2 [wild type], CF2166 [*tcer-1(tm1452)*], and AGP278 [*tcer-1(glm27), crispr deletion*]. All strains are listed in Supp. Table 4.7. In survival analysis the L4 larval stage was counted as "time 0" or Day 0 of adulthood and living animals were transferred to new plates to separate parents from progeny. Animals that exploded, bagged, crawled off the plate or became contaminated were marked as censored upon observation. Statistical analysis of survival assays were done with the Online Application of Survival Analysis 2 (OASIS 2) program (244). P-Values were subsequently calculated using the log-rank Mantel-Cox test and results were graphed using GraphPad Prism (version 9).

Pathogen stress assays: To prepare a *Pseudomonas aeruginosa* (strain PA14) survival assay, PA14 plates were made by first streaking Luria Bertani (LB) agar plates with PA14 from -80°C glycerol stocks and incubating them at 37°C overnight for 4°C storage and use within one week. Single colonies from these PA14 streaks were then inoculated into 3mL King's Broth (Sigma) overnight (16–18 h) in a 37 °C shaking incubator. 20μL of this culture was then seeded onto slow-killing plates (modified NGM with 0.35% peptone), incubated at 37 °C for 24 h, then left at room temperature for 24 h before use (refs). In tandem, age-matched *C. elegans* strains were grown on OP50-NGM plates (or HT115-RNAi plates if specified) from egg-lay to the L4 stage for the transfer of 100+ animals (20-30 per plate) to five PA14 plates per strain. Survival on these plates at 25 °C (or 20 °C if specified) was then counted every 6–12 h to record the number of living, dead, and censored animals as described above. Surviving animals were also transferred to new PA14 plates each day for the first 3-4 days (48, 245). RNAi experiments used the same protocol except animals were grown from egg to the L4 stage on RNAi plates

(described above) before transfer to PA14 plates. FUDR treatments for designated assays additionally involved placing the L4 animals on FUDR plates (described above) for 24 h at 15 °C before transfer to PA14 plates (334). Kaplan−Meier analysis and statistics were performed as described above.

RNA isolation: Animals were synchronized by bleach treatment and hatched in M9 until arrested as L1 larvae. Synchronized larvae were plated on NGM plates containing OP50 and grown to gravid adult stage (72 hours post L1 synchronization). Animals were washed three times in M9 buffer, flash frozen in liquid nitrogen, and lysed in Trizol. RNA was isolated using two rounds of chloroform extraction followed by isopropanol precipitation.

mRNA-seq library preparation: rRNA was depleted using the Ribo-Zero rRNA Removal Kit (Human/Mouse/Rat, Illumina Cat # MRZH11124). rRNA-depleted RNA was DNase treated and size selected (>200 nucleotides) to remove 5S rRNA and tRNA using RNA the Clean & Concentrator-5 Kit (Zymo Research, Cat # R1015). RNA-seq libraries were prepared using the NEBNext Ultra II Directional RNA Library Prep Kit for Illumina (NEB, Cat # E7760S). Samples were sequenced on an Illumina HiSeq (Paired-End, 150 Cycles).

mRNA-seq data analysis: fastp was used to remove adapters and filter low quality data (fastp -w 16 -q 30 -u 70 -l 30 -r -W 4 -M 20) (335). Reads were mapped to the *C. elegans* genome (Wormbase release WS230) using STAR (336). Reads aligning to each annotated coding gene (WS230) were counted using RSEM (337). Differential expression analysis was done using DESeq2 (338).

sRNA-seq library preparation: 16-30-nt RNAs were size selected from total RNA on 17% denaturing polyacrylamide gels. smRNAs were treated with RNA polyphosphatase to reduce 5′ di- and triphosphates to monophosphates to enable 5′ adapter ligation. Sequencing libraries were prepared with the NEBNext Multiplex Small RNA Library Prep Set for Illumina (NEB, Cat # E7300S). Libraries were size selected on 10% polyacrylamide gels and sequenced on an Illumina NextSeq 500 sequencer (High Output Kit, Single-End, 75 Cycles).

sRNA-seq data analysis: smRNA sequences were parsed from adapters, quality filtered (reads with an average of Q < 30 were discarded), and mapped to the *C. elegans* genome (Wormbase release WS230) using CASHX v. 2.3 (339). Reads from specific features were counted using custom Perl scripts. smRNA features were classified as described in Brown et al (340). Multimapping reads were normalized by the number of matching genomic loci. Differentially expressed smRNAs were identified using DESeq2 (338).

GO analysis and overlap comparison: Genes which were classified as differentially regulated were separated into TCER-1-upregulated (UP) or TCER-1-downregulated (DOWN) groups ($p<0.05$, all gene lists). Relevant groups were then analyzed for gene class enrichment based on WormCat (wormcat.com) (246) and Wormbase Gene Set Enrichment Analysis tool (wormbase.org/tools/enrichment/tea/tea.cgi). The statistical significance of any overlaps between gene groups and representation factors was calculated using the Nemates program (nemates.org/MA/progs/overlap_stats.html).

Microscopy and fluorescence quantitation: GFP expression in transgenic strains was imaged using a Leica DM5500B compound scope with Leica (LAS X) imaging software and quantified using observational scoring of populations. For setup, progeny of transgenic mothers were grown to the young adult (L4) stage on *tcer-1* RNAi or empty vector control at 20°C, when fluorescent signal became clear. L4 transgenics were then transferred to PA14 or OP50 control plates and placed at 25°C for 16 h to later be imaged or scored for fluorescence. Animals subjected to imaging were immobilized using Levamisole (10mM) and imaged under set magnification and intensity settings, until >15 animals were imaged per condition. Animals subjected to fluorescence scoring were evaluated for their GFP intensity (high, medium, low) relatively across conditions in three biological replicates at an N > 50 per condition. Significance was calculated for differences between populations with 'high' GFP signal using a one-way ANVOA on PRISM software.

4.3 Results

4.3.1 TCER-1 suppresses immunity through PPW-1 and RRF-1 proteins of the siRNA pathway

TCER-1 is broadly expressed in somatic tissues and the germ line. Previously, we utilized tissue-specific TCER-1 expression to identify which tissues TCER-1 expression is sufficient in to repress immunoresistance. Our experiments showed that TCER-1 expression in any somatic tissue was sufficient to abolish the increased immunity of *tcer-1* mutants (10). Following this 'sufficiency' observation, we asked which tissue(s) TCER-1 was 'necessary' in to

repress immunity. To this end, we intended to perform site-specific RNAi inactivation of TCER-1 in somatic or germ-cells using the *ppw-1(pk1425)* and *rrf-1(ok589)* mutants, respectively. *ppw-1* encodes an Argonaute protein and *rrf-1* encodes an RNA-directed RNA polymerase; both proteins have well-described roles in siRNA biogenesis and have been extensively used in the *C. elegans* field to test the impact of soma-specific and germline-specific RNAi, respectively (341, 342). Surprisingly, we found that both *ppw-1* and *rrf-1* mutants survived significantly longer upon exposure to PA14 as compared to wild-type animals. Further, *tcer-1* RNAi knockdown did not enhance this effect (**Fig. 4.1A-B**, Supp. Table 4.1A). This led us to ask if these two siRNA biogenesis genes have a role in the PA14 immune response, and if they act in the same pathway as TCER-1 to perform these functions. To obviate potential RNAi-related confounding features, we introduced the *tcer-1(tm1452)* allele into the *ppw-1(pk1425)* and *rrf-1(ok589)* backgrounds and tested the survival of the strains upon PA14 infection. Similar to the RNAi experiment, both *ppw-1* and *rrf-1* mutants survived longer than wild type and neither mutation further enhanced the PA14 immunoresistance of the *tcer-1* mutant (**Fig. 4.1C-D**, Supp. Table 4.1B). To test the relationship between TCER-1 and these genes, we assessed TCER-1 expression in both mutants independently using a TCER-1::GFP strain. TCER-1-GFP levels were not altered in either mutant (**Fig. 4.1E**). Although *ppw-1* mRNA levels were not significantly altered in *tcer-1* mutants in our RNAseq analyses (described below), *rrf-1* mRNA levels showed a small, yet significant, ~1.5 fold-change decrease in *tcer-1* mutants (Supp. Table 4.2). While the epistatic relationship remains unclear, this expression data suggested that TCER-1 likely operates upstream of at least siRNA biosynthesis gene, RRF-1, to impair immune resistance (Supp. Fig. 4.1).

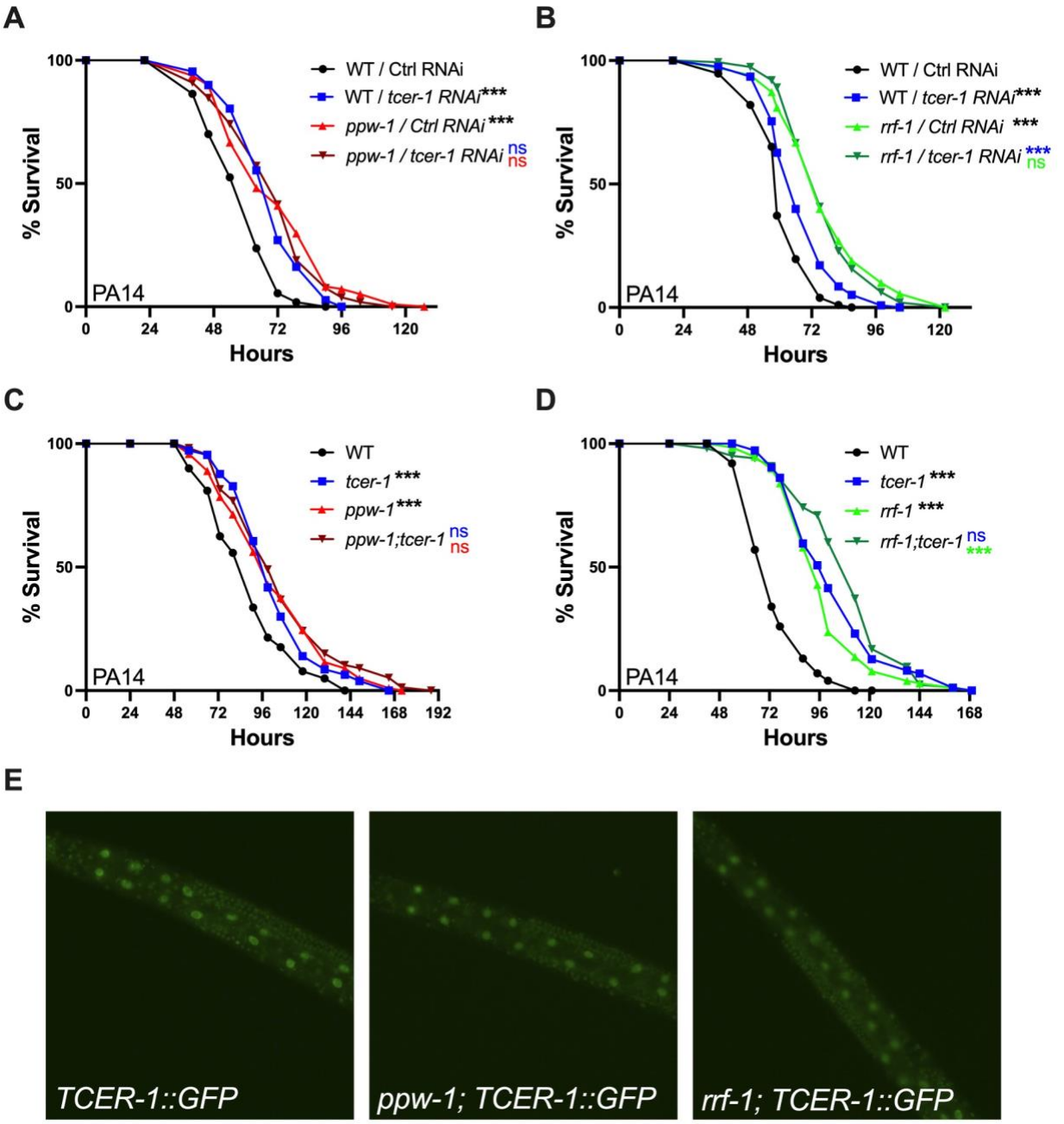

Figure 4.1 TCER-1 suppresses immunity through RRF-1 and PPW-1 proteins of the siRNA pathway.

(A-B) PA14 survival of wildtype (N2), *ppw-1(pk1425)*, and *rrf-1(ok589)* L4 animals grown from egg stage on *tcer-1* RNAi or empty vector control. (A) WT/Ctrl RNAi (m= 58.52 ± 1.48, n= 63/81), WT/*tcer-1* RNAi (m= 69.23 ± 1.48, n= 78/109), *ppw-1*/Ctrl RNAi (m= 71.2 ± 1.95, n=

99/112), *ppw-1*/*tcer-1* RNAi (m= 70.14 ± 1.62, n= 110/121). (B) WT/Ctrl RNAi (m= 60.93 ± 0.95, n= 110/134), WT/*tcer-1* RNAi (m= 67.91 ± 1.09, n= 129/157), *rrf-1*/Ctrl RNAi (m= 77.45 ± 1.67, n= 114/136), *rrf-1*/*tcer-1* RNAi (m= 77.3 ± 1.33, n= 117/154). (C-D) PA14 survival of wildtype (N2) and mutants grown in normal conditions and transferred to PA14 plates at the L4 stage. (C) WT (m= 88.97 ± 2.01, n= 116/143), *tcer-1(tm1452)* (m= 102.76 ± 2.3, n= 96/111), *ppw-1(pk1425)* (m= 102.95 ± 2.38, n= 134/148), *ppw-1(pk1425);tcer-1(tm1452)* (m= 106.68 ± 2.94, n= 95/116). (D) WT (m= 74.9 ± 1.34, n= 108/130), *tcer-1(tm1452)* (m= 103.91 ± 2.45, n= 91/120), *rrf-1(ok589)* (m= 97.99 ± 1.89, n= 113/137), *rrf-1(ok589);tcer-1(tm1452)* (m= 108.5 ± 2.55, n= 88/106). (E) Representative images of L4-stage TCER-1::GFP (IT213), *ppw-1(pk1425);* IT213, and *rrf-1(ok589);* IT213 strains. In A-D, mean survival following PA14 exposure shown in hours (m) ± SEM, n= observed/total (see Methods for details). Significance was calculated and using the log-rank method (Mantel Cox, OASIS2), and *p* values were adjusted for multiplicity. Statistical significance shown on each panel with the color of the asterisk indicating the strain being compared to. $p < 0.05$ (*), < 0.01 (**), <0.001 (***), not significant (ns). Data from additional trials are presented in Supp. Table 4.1A-B.

4.3.2 *tcer-1* mutants exhibit a reduction in WAGO siRNA levels.

The genetic epistasis observations above, and previous reports which imply a role for TCER-1 in smRNA biology (176, 177), led us to investigate the impact of TCER-1 in smRNA biogenesis. Hence, we employed a genomics approach to probe how TCER-1 influences smRNA biogenesis, and mRNA transcriptomic levels (**Fig. 4.2A**). Since the *tcer-1(tm1452)* (CF2166) mutant exhibits developmental asynchrony and this has been reported to increase 'noise' in the production of smRNA classes (343), we utilized an additional *tcer-1* mutant, *tcer-1(glm27)*

(AGP278), a gene deletion created using CRISPR in our laboratory that exhibits all the phenotypes shown by *tcer-1(tm1452),* including enhanced PA14 resistance (Amrit, Ghazi et al., unpublished). In collaboration with the laboratory of Tai Montgomery, we isolated RNA from age-matched CF2166, AGP278, and WT animals grown on normal *E. coli* OP50 food to the gravid stage (72h) (**Fig. 4.2A**). Then, to set up an smRNAseq, the Montgomery lab first size-selected isolated RNA for 16-30nt RNAs and treated these samples with RNA polyphosphatase (RNAP) to enable 5′ adapter ligation. Libraries were then prepared using the NEBNext Multiplex Small RNA Library Prep Set, size-selected, and sequenced on an Illumina NextSeq 500 sequencer (Single-End, 75bp). smRNA sequences were parsed from adapters, quality filtered, and mapped to the *C. elegans* genome using CASHX v. 2.3 (339). Following the counting of reads using custom Perl scripts, smRNAs were classified (as in (340)) with multi-mapping reads normalized by the number of matching genomic loci. Differentially-expressed smRNAs were then identified using DESeq2 (338). Analysis of where these differentially-expressed smRNAs map to the genome also allowed for important comparisons with subsequent mRNA-seq analyses, the details for which are described in the sections below.

smRNAseq revealed that various 22G WAGO siRNAs and piRNAs were reduced in both CF2166 and AGP278, as compared to WT animals, suggesting that TCER-1 promotes the biogenesis of these groups (TCER1-UP smRNAs) (**Fig. 4.2B-C**). In total, 481 smRNAs were significantly depleted in both *tcer-1* mutant worms compared to wild type (fold-change down >1.5, base mean >100) (**Fig. 4.2D**, Supplementary File 1). This high-confidence TCER1-UP smRNA group was later leveraged in subsequent analyses. Similarly, various miRNA and non-coding mRNA sequences were elevated in both CF2166 and AGP278, as compared to WT animals, suggesting that TCER-1 repressed the production of these groups (TCER1-DOWN

smRNAs). From this list, 600 TCER-1-DOWN smRNAs- were shared between CF2166 and AGP278 (**Fig. 4.2E**, Supp. File 1).

As a result of these findings, we focused on the TCER1-UP smRNA targets and asked if any major smRNA classes (e.g. miRNAs, piRNAs, different siRNA classes) were influenced more than others. We found that *tcer-1* mutations caused a ~10% reduction in the total production of one specific class of 22G siRNAs: the WAGO siRNAs (**Fig. 4.2F**, Supp. File 1). The total levels of other siRNA classes, including CSR-1 22Gs and ERGO-1 26Gs, were not altered nor were piRNA levels. However, total miRNA content was elevated ~30% (**Fig. 4.2F,** Supp. File 1). The prevalence of TCER1-UP smRNAs that belong to WAGO siRNA biogenesis-related classes (Supp. Table 4.3), the noted epistasis data, and specific reduction of 22G siRNAs in *tcer-1* mutants led us to hypothesize that TCER-1 suppressed immunity through promoting WAGO siRNA biogenesis.

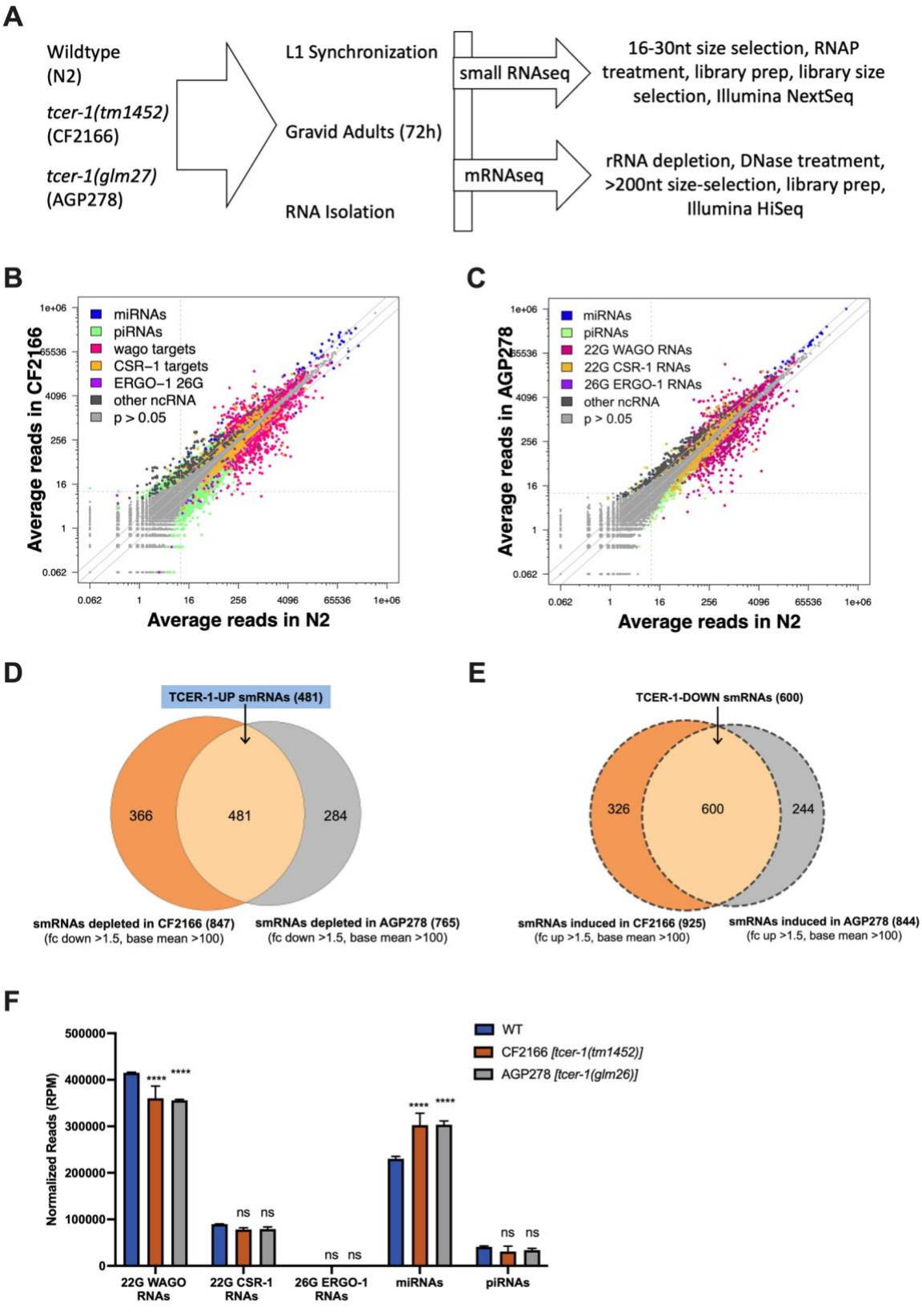

Figure 4.2 *tcer-1* mutation causes a ~10% reduction in total WAGO siRNAs.

(A) Schematic of growth and RNA isolation steps leading up to tandem smRNAseq-mRNAseq of wildtype (N2), *tcer-1(tm1452)* loss-of-function (CF2166), and CRISPR-generated *tcer-1(glm27)* deletion (AGP278) strains from three biological replicates. (B-C) Plots highlighting differentially regulated smRNA species in *tcer-1 null* (AGP278) and *tcer-1 lof* (CF2166) worms versus wildtype. (D) Overlap of 481 smRNAs between lists of smRNAs depleted (fold-change down >1.5, base mean > 100) in CF2166 and AGP278 strains in smRNAseq compared to N2 samples, yielding high-confidence list of 481 smRNAs likely upregulated by TCER-1 (TCER-1-UP smRNAs). List of 481 represented in blue in later figures. (E) Overlap of 600 smRNAs between lists of smRNAs induced (fold-change up >1.5, base mean > 100) in both CF2166 and AGP278 strains of smRNAseq implicated as suppressed by TCER-1 (TCER-1-DOWN smRNAs). Dotted lines around circles indicate negative regulation by TCER-1 protein. (F) Total normalized reads per smRNA class in wildtype (N2), *tcer-1(tm1452) lof* (CF2166). Error bars denote standard deviation. Statistical significance within each smRNA class is marked in relation to the WT control. p <0.0001 (****), p>0.05 not significant (ns). Statistical significance was calculated using a 2-way ANOVA on PRISM software. Full dataset and sequencing details presented in Supp. File 1.

4.3.3 Multiple mutations in genes mediating WAGO siRNA amplification phenocopy *tcer-1* mutants' increased immunity

Based on the smRNA profiles of *tcer-1* mutants and the genetic epistasis data, we examined the potential roles of other genes involved in biogenesis of the WAGO-class 22G siRNAs as well as ones functioning in miRNA or piRNA synthesis. Beyond the *ppw-1* and *rrf-1* mutants, we tested the survival on PA14 of 17 strains with mutations targeting 17 genes involved

in the biogenesis of different smRNA classes (**Fig. 4.3A**, Supp. Table 4.4A-B) particularly focusing on genes specific to miRNA, siRNA or piRNA biosynthesis. In accordance with our smRNAseq results, we found several additional mutants exclusively involved in siRNA biosynthesis had increased PA14 resistance similar to *tcer-1* mutants. Besides *rrf-1* and *ppw-1*, mutants for *Mutator* complex genes such as the *mut-14(pk738);smut-1(tm1301)* double mutant and *mut-7(pk720)* single mutant showed consistent and significantly enhanced PA14 survival (**Fig. 4.3B**). *Mutator* (*mut*) genes encode components of the Mutator Complex whose formation is critical for WAGO siRNA amplification and subsequent siRNA-mediated gene silencing (167). Similarly, the immune resistance of *mut-14;smut-1* double mutants was also assessed due to the functional redundantly of these genes in WAGO siRNA amplification (344). Hence, siRNA production is depleted by 95% and 85% in both *mut-14;smut-1* and *mut-7* strains, respectively (344). The observation that many WAGO siRNA amplification mutants phenocopy *tcer-1* mutants therefore reinforced our previous evidence that genes involved in WAGO siRNA production suppressed immunity. Other results showing sporadic increases, and deficiencies, in the immunoresistance of miRNA and piRNA mutants, further support this as the increased resistance of siRNA amplification mutants was consistent (Supp. Table 4.4A).

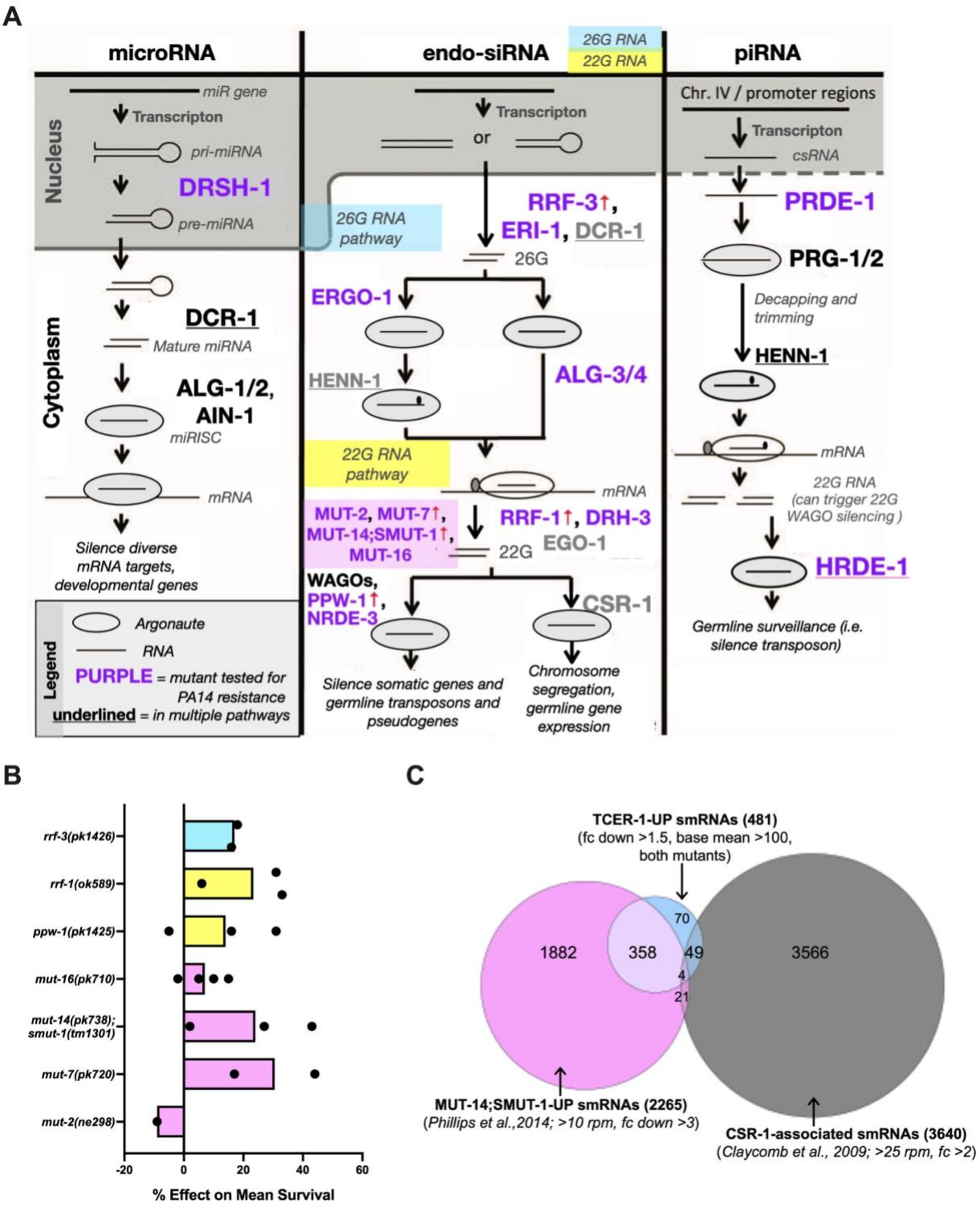

Figure 4.3 Mutation of genes involved in WAGO siRNA amplification phenocopy tcer-1 pathogen resistance.

(A) Schematic of endogenous micoRNA, siRNA, and piRNA pathways in *C. elegans*, including the additional 26G, and 22G siRNA classes that bind WAGO or CSR-1 argonautes. Biosynthesis genes written in purple indicates that the mutant was tested for PA14 resistance. Red arrows mark mutants with increased PA14 resistance. Pink box highlights tested mutants of the Mutator Complex, involved in WAGO siRNA amplification. Functional impacts of each smRNA class include, but are not limited to, the processes listed. Schematic adapted from Hoogstrate et al 2014 (161). (B) Percent effect on mean PA14 survival compared to wildtype control for select mutants involved in WAGO siRNA biogenesis. Points represent percent effect in individual trials. Details on the number of animals observed, mean survival, and standard error (SEM) within each trial and are presented in Supp. Table 4.4A-B. (C) Venn diagram of overlap between smRNA loci depleted >1.5x in both *tcer-1 lof* and *tcer-1* null mutants (481), siRNAs depleted in *mut-14(pk738);smut-1(tm1301)* (2265) (344), and CSR-associated siRNAs (3640) (345). TCER-1 vs MUT-14;SMUT-1: 362/481, Representation factor: 5.9, $p < 2.29e-225$. TCER-1 vs CSR-1: 53/481, Representation factor: 0.5, $p < 1.02e-08$. MUT-14;SMUT-1 vs CSR-1: 25 shared between 2265 and 3640, Representation factor: 0.1, $p < 7.40e-201$. Full overlap list can be found in Supp. File 3. Additional overlaps between TCER-1 and Mutator-regulated smRNAs and mRNAs can be found in Supp. Figure 4.3.

4.3.4 TCER-1-regulated smRNAs overlap strongly with WAGO siRNAs promoted by MUT factors

To examine whether TCER-1 suppresses immunity through the WAGO siRNA pathway we planned to conduct an epistasis with a *mut* mutant. Yet, no epistasis for immune resistance could include RNAi due to the effects of these WAGO-pathway mutants on dsRNA processing.

Then, although *mut-7* mutation has weaker impacts on siRNA production than *mut-14;smut-1* mutation, even efforts to introduce the *tcer-1* mutation into *mut-7* worms via mating yielded sterile double-mutants (Supp. Fig. 4.2) (344). Interestingly, single mutants for *mut-16* which display the most dramatic depletion of siRNAs among *mut* mutants, did not show increased survival, suggesting the involvement of specific Mutator Complex members (**Fig. 4.3B**) (344). To circumvent the challenges with genetic epistasis and examine potential interactions of TCER-1 with these specific WAGO amplification regulators, we compared the smRNA targets of TCER-1 and MUT genes where available (344). In particular, we asked if and to what extent, smRNAs upregulated by TCER-1 (TCER1-UP class) were also upregulated by MUTs. Out of 481 TCER1-UP smRNAs, we observed a striking 75% overlap with the smRNAs depleted in *mut-14;smut-1* mutants (362/481) (**Fig. 4.3C**, Supp. File 4). This high overlap was additionally maintained with the smRNAs depleted in *mut-16, mut-7*, and *mut-2* mutant worms (Supp. Fig. 4.3). Since MUT regulation is often used to define what smRNAs belong to the WAGO siRNA class (165), this suggests that TCER-1 smRNA regulation predominantly impacts WAGO siRNAs. Besides the WAGO siRNAs, CSR-1-associated siRNAs are a second class of 22G siRNA which act solely in the germ line, mostly to promote chromatin organization in mitosis and meiosis. When we compared the TCER1-UP list to CSR-1 siRNAs (345) we found a much smaller (~11%) yet statistically significant overlap. The immune resistance of *csr-1* mutants was not tested with the other altered smRNA biogenesis mutants due to concerns over its viability and poor health in normal conditions (345). Yet, it was recently shown that mutation of the *csr-1a* isoform also improved survival on PA14 (346). This suggests that the siRNA pathway, more broadly, acts to suppress immunity but TCER-1 does not act through CSR-1 pathway regulation.

4.3.5 TCER-1-dependent siRNA and mRNA profiles show poor overlap

Since the primary function attributed to 22G siRNAs is gene-expression silencing, a logical premise would be that TCER1-UP siRNAs would repress the expression of their respective complementary mRNA transcripts. The levels of such mRNAs would be predicted to be elevated in *tcer-1* mutants. To test this, we investigated the mRNAseq analyses conducted on the same samples of our three-strain smRNAseq. The Montgomery lab first prepared the library for this mRNAseq using the NEBNext Ultra II Directional RNA Library Prep Kit for Illumina following rRNA depletion, DNase treatment, and size-selection (>200nt) of isolated RNA. Sequencing was then performed on the llumina HiSeq seq platform (Paired-End, 150bp). After quality filtering with fastp (335), reads were then mapped using STAR (336), and counted using RSEM (337). Differentially-expressed mRNAs were then identified using DESeq2 (338). This revealed that 2615 and 2068 mRNAs were upregulated in CF2166 and AGP278, respectively, as compared to WT animals (**TCER1-DOWN mRNAs**) (Supp Fig. 4.4A, Supp. File 2). The shared 1500 mRNAs upregulated in both *tcer-1* mutants were allotted for subsequent analyses as a high-confidence TCER1-DOWN mRNA class. 976 and 264 mRNAs were also downregulated in CF2166 and AGP278, respectively, as compared to WT with 167 mRNA shared between these lists (**TCER1-UP mRNAs**) (Supp. Fig. 4.4B). Then, comparing the smRNA targets of TCER-1 with the mRNA targets showed no significant negative, or positive, correlation (R-squared= 0.051 and 0.0082 in CF2166 and AGP278 datasets, respectively) (**Fig. 4.4A-B**). In particular, of the 481 TCER1-UP siRNAs and 1500 TCER1-DOWN mRNAs, only 21 were shared (4%) (**Fig. 4.4C**; Supp. File 3). The overlap between the TCER1-DOWN smRNA and TCER1-UP mRNA groups was also minimal (11/481) (**Fig. 4.4D)**. These observations suggest that TCER-1's impact on the mRNA transcriptome is largely independent

of its effect on siRNA biogenesis, and its siRNA targets do not globally repress expression *tcer-1* target mRNAs. Interestingly, a similarly poor overlap has been reported between the smRNA and mRNA profiles of MUT factors such as MUT-16 (164).

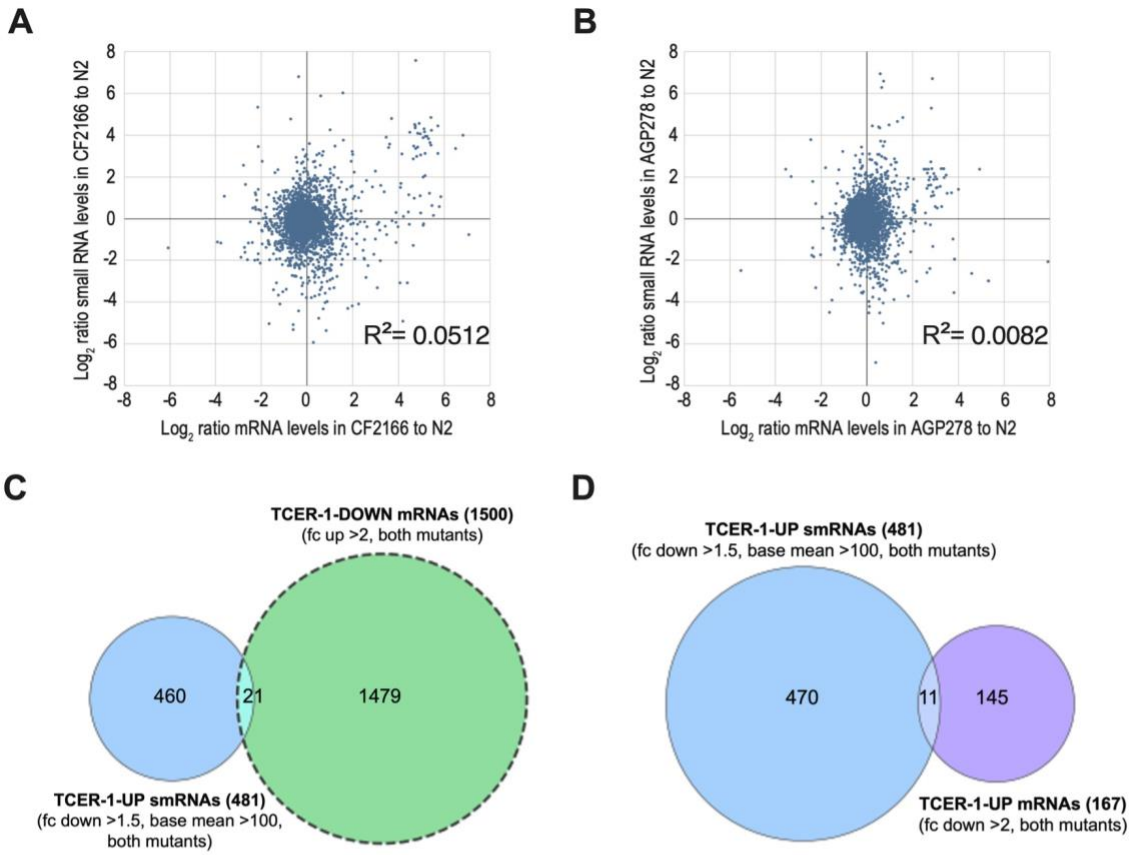

E

Gene	Identity	mRNA log2 FC in AGP278	mRNAseq Base Mean	smRNA log2 FC in AGP278	smRNAseq Base Mean
col-111	Extracellular material: collagen	1.8	136	-3.7	967
F15D4.5	Unknown	3.8	791	-3.5	16430
Y102A5C.36	Transmembrane protein: other	2.2	65	-3.0	1674
scrm-4	Metabolism: lipid: phospholipid	4.6	500	-2.6	586
T19A6.4	Transmembrane protein: other	1.4	89	-2.4	1023
rnh-1.3	mRNA functions: processing: nuclease	2.8	374	-2.4	12109
dmd-9	Transcription factor: ZF	1.3	204	-2.1	110
W06A11.4	Unknown	1.2	121	-2.1	2504
C38D9.2	Unknown	7.9	1881	-2.1	5744
col-38	Extracellular material: collagen	1.3	589	-2.0	312
F07E5.8	Unknown: reg by multiple stresses	2.9	18	-1.8	163
ser-5	Neuronal function: transcription factor	1.5	57	-1.7	445
C06A1.3	Signaling: phosphatase: other	1.9	75	-1.6	185
C08F11.7	Unknown: reg by multiple stresses	1.0	60	-1.3	1334
Y53F4B.11	Unknown: reg by multiple stresses	1.1	30	-1.1	723
dac-1	Transcription factor: other	1.2	34	-0.9	299
bigr-1	Metabolism: lipid: beta oxidation	1.2	46	-0.9	112
R04A9.9	Unknown: reg by multiple stresses	1.2	50	-0.8	246
F53B6.7	Signaling: phosphatase: other	1.3	68	-0.8	862
F31D5.1	Transmembrane transport	1.4	56	-0.6	207
col-60	Extracellular material: collagen	2.0	196	-0.6	466

Figure 4.4 TCER-1-dependent siRNA and mRNA profiles show poor overlap.

(A-B) Scatter plots displaying each annotated coding gene from mRNAseq of this study as a function of its corresponding log2 normalized smRNA read from our smRNAseq in (A) CF2166 and (B) AGP278 datasets. (C) Venn diagram of overlap between 481 TCER-1-UP smRNAs and 1500 TCER-1-DOWN mRNAs (mRNA fold-change up >2 in both *tcer-1* mutants, Fig. S4A). (D) Venn diagram of overlap between 481 TCER-1-UP smRNAs and 167 TCER-1-UP mRNAs (mRNA fold-change down >2 in both *tcer-1* mutants, Fig. S4B). TCER-1-UP smRNAs vs TCER-1-DOWN mRNAs: 21/481, Representation factor: 0.5, $p < 2.43e-04$; TCER-1-UP smRNAs vs TCER-1-UP mRNAs: 11/481, Representation factor: 2.4, $p < 0.006$. Dotted lines around circles indicate negative regulation by TCER-1 protein. (E) Organized list of 21 genes shared between TCER1-UP smRNAs and TCER1-DOWN mRNAs. The log2 fold-change (log2FC) of mRNA and smRNA levels in AGP278 mutants compared to wildtype, and the base mean in mRNAseq and smRNAseq analyses are displayed. Red text indicates the gene is also part of a list of smRNAs candidates in immunity, generated by sorting for highly TCER-1-upregulated smRNAs, largest base mean, and plausible function in immunity (Table S6). Full mRNAseq dataset can be found in Supplementary File 2. Full overlap list can be found in Supp. File 3.

4.3.6 Metabolic genes, s*crm-4* and *qdpr-1*, are potential factors through which TCER-1-upregulated smRNAs suppress immunity.

How do TCER-1-regulated siRNAs influence immune status? Given the plausible connection from our experiments that TCER-1 promotes WAGO siRNA production, which in turn suppresses immunity, we also sorted a list of the top smRNAs candidates through which

TCER-1 might suppress immune function. We first selected for smRNAs that are highly upregulated by TCER-1 based on data from both *tcer-1* mutants. We then sorted genes with the greatest base mean and plausible function in immunity to generate a candidate list for functional analyses (Supp. File 4, Supp. Table 4.6). Notably, 3/13 genes in this list were included in our list of 21 genes shared between TCER1-UP smRNAs and TCER1-DOWN mRNAs (**Fig. 4.4E**). Other encoded loci whose mRNAs were downregulated by *Mutator* activity, and ones reported to be induced by PA14 exposure were also considered strong candidates (Supp. Table 4.6, (148, 254, 344, 347), Amrit, Ghazi et al., unpublished). This approach therefore highlighted candidate targets for smRNA-directed immune suppression.

We then asked if RNAi- or mutation-based inactivation of any candidate genes impacted survival upon PA14 exposure. Among the top candidates tested, metabolic genes *scrm-4* and *qdpr-1* impacted immunity in a TCER-1 dependent manner (**Fig. 4.5**). SCRM-4 is a phospholipid scramblase responsible for phospholipid translocation in the membrane and is the ortholog of human Phospholipid Scramblase 3 (PLSCR3), noted to control mitochondrial structure, function, and apoptotic response (348)**.** smRNAs mapping to the *scrm-4* locus are significantly reduced in *tcer-1* mutants and corresponding mRNA expression is de-repressed in these mutants (log2FC: -2.6 and 4.6, respectively in AGP278) (**Fig. 4.5A**). Notably, *scrm-4* mutants exhibited impaired immune resistance upon PA14 exposure. RNAi knockdown of *tcer-1* did not increase survival of the mutants as it did in WT animals, indicating their functional relevance to TCER-1-mediated immune regulation (**Fig. 4.5B**, Supp. Table 4.5B).

The second gene, *qdpr-1*, encodes a reductase involved in biopterin synthesis and amino acid metabolism that is important for cuticle integrity (349). Mutation of its human ortholog, QDPR/DHPR, impairs phenylalanine processing leading to the amino acid buildup in

phenylketonuria (350). The smRNAs mapping to the *qdrpr-1* locus were decreased in *tcer-1* mutants and corresponding mRNA levels increased (log2FC: -2.4 and 0.96, respectively in AGP278) (**Fig. 4.5C**). We used a strain expressing a QDPR-1::GFP translational fusion reporter, (349) to assess expression changes *in vivo*. While PA14 exposure increased the protein levels as expected, supporting its role in immune response, we did not find this to be significantly impacted by *tcer-1* mutation. The reason underlying the mRNA vs. protein discrepancy remains unclear. But, our functional tests with PA14 exposure showed that *qdpr-1* mutants had modestly lower survival than WT, and *tcer-1* knockdown did not prolong their survival as in WT (**Fig. 4.5D**, Supp. Table 4.3) underscoring the role of the gene in the immune-resistance of *tcer-1* mutants. Together these data revealed at least two factors through which TCER-1-upregulated smRNAs suppress immunity. Although these genes are not generally implicated in immunity, genes with roles in amino acid metabolism and lipid metabolism have been increasingly noted in immune processes (351, 352).

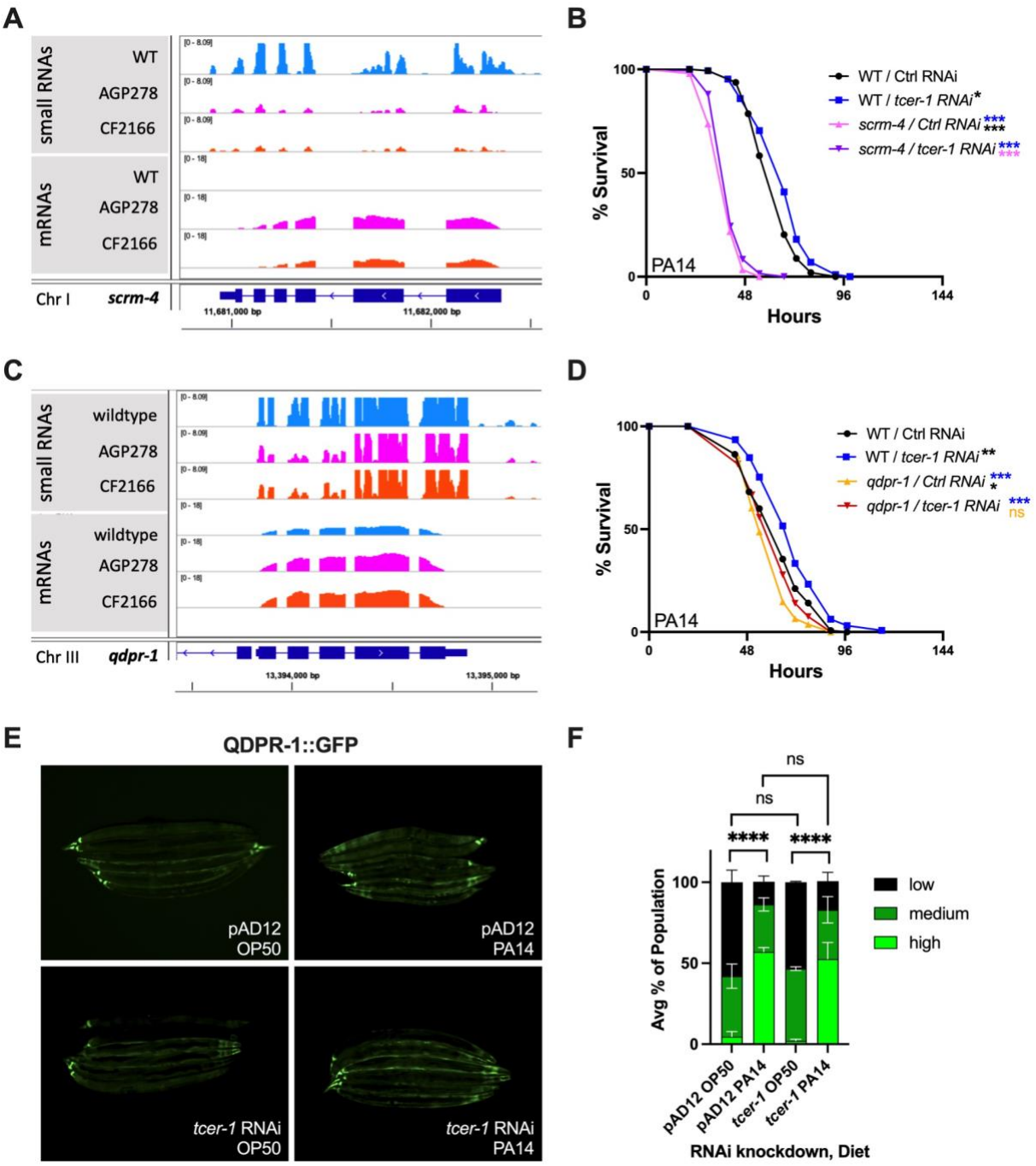

Figure 4.5 Metabolic genes, *scrm-4* and *qdpr-1*, are potential factors through which TCER-1-upregulated smRNAs suppress immunity.

(A) IGV genome browser view of smRNAseq (top) and mRNAseq (bottom) tracks, displaying the changes in smRNA and mRNA reads at the *scrm-4* locus in wildtype, *tcer-1 null*, and *tcer-1*

lof mutants. (B) PA14 survival of wildtype (N2) and *scrm-4(ok3596)* L4 animals grown from egg stage on *tcer-1* RNAi or empty vector control. WT/Ctrl RNAi (m= 62.42 ± 1.0, n= 118/150), WT/*tcer-1* RNAi (m= 66.42 ± 1.22, n= 112/157), *scrm-4*/Ctrl RNAi (m= 39.29 ± 0.57, n= 141/149), *scrm-4*/*tcer-1* RNAi (m= 41.86 ± 0.56, n= 144/150). (C) IGV genome browser view, as in A, at the *qdpr-1* locus. (D) PA14 survival of wildtype (N2) and *qdpr-1(tm2337)* L4 animals grown from egg stage on *tcer-1* RNAi or empty vector control. WT/Ctrl RNAi (m= 63.47 ± 1.23, n= 148/165), WT/*tcer-1* RNAi (m= 70.33 ± 1.37, n= 137.156), *qdpr-1*/Ctrl RNAi (m= 58.82 ± 0.98, n= 130/148), *qdpr-1*/*tcer-1* RNAi (m= 61.33 ± 1.31, n= 100/114). (E) Images of translational fusion reporter QDPR-1::GFP (CZ19215) strain grown to the L4 stage on *tcer-1* RNAi or empty vector control and exposed to PA14 or OP50 control plates at 25°C for 16 hours. (F) Fluorescence scoring of QDPR-1::GFP strains. Error bars show standard deviation among three biological replicates. Significance markings indicate differences between populations with 'high' GFP signal and were calculated using a one-way ANVOA on PRISM software. p <0.0001 (****), p>0.05 not significant (ns). Data from individual trials are presented in Supp. File 5. In B and D, mean survival following PA14 exposure shown in hours (m) ± SEM, n= observed/total (see Methods for details). Significance was calculated and using the log-rank method (Mantel Cox, OASIS2), and p values were adjusted for multiplicity. Statistical significance shown on each panel with the color of the asterisk indicating the strain being compared to. p <0.05 (*), < 0.01 (**), <0.001 (***), not significant (ns). Data from additional trials are presented in Supp. Table 4.5B.

4.4 Discussion

Endogenous smRNA mechanisms are an ancient and conserved system utilized for post-transcriptional gene regulation across species. In its established role as a regulator of immunity-fertility dialogue, TCER-1 directs the suppression of immunity in fertile animals. Our data suggests that TCER-1 promotes the production of siRNAs to suppress bacterial immunity. We identified siRNA biosynthesis genes which act in the same pathway as TCER-1 to suppress immunity. A specialized smRNAseq showed that *tcer-1* mutants have a ~10% reduction in siRNAs that bind WAGO argonautes. The discovery that other siRNA biosynthesis mutants, particularly in WAGO siRNA amplification, phenocopy TCER-1 immune resistance narrowed down this mechanism. The similarity of smRNA and mRNA regulation by TCER-1 and Mutator proteins supported this finding. Subsequent comparisons of TCER-1-dependent smRNA versus mRNA regulation generated a candidate list of genes in smRNA-directed immunosuppression. The finding that the downstream siRNA targets *scrm-4* and *qdpr-1* have mRNA levels that are upregulated in *tcer-1* mutants and promote immunity in a TCER-1 dependent manner proposed a means through which TCER-1-upregulated smRNAs suppress immunity.

One must question how else TCER-1 suppresses immunity. Our data suggests that TCER-1 promotes WAGO siRNA biosynthesis to suppress immunity. Yet mutation of *mut-16*, which encodes the core component of the Mutator Complex, did not increase immunity like other *mut* mutants. This surprising result is potentially due to the strong effects of *mut-16* loss of function causing confounding defects in pathogen-resistance experiments (353). Yet, TCER-1 smRNA and mRNA regulation overlapped strongly with regulation from all tested MUT factors, including MUT-16 (Supp. Fig. 4.3). Efforts to introduce a *tcer-1* mutation into a less-severe *mut* mutant, *mut-7*, nonetheless yielded a sterile double-mutant (Supp. Fig. 4.2). This suggested that

despite the strong regulatory overlap, TCER-1 impacts additional fitness pathways than MUTs. Our laboratory has already shown that TCER-1 suppresses immunity through both PMK-1/p38 MAPK-dependent and -independent mechanisms (10). Although smRNAs are also recorded to impact these processes, it is conceivable that smRNA regulation is one of several strategies used by TCER-1 to blunt immune response (172, 174, 318). Accordingly, our list of depleted smRNA levels in *tcer-1* mutants showed no strong enrichment in innate immunity GO terms (Supp. File 4). Yet, considering increasing evidence that lipid metabolic genes impact immunity, the presence of lipid metabolic annotations in this list supported TCER-1's smRNA-directed immune effects (351, 352).

Other studies propose that smRNAs enable pathogen avoidance as one bacterial survival strategy (324). Previous work in our lab has shown that increased pathogen survival in *tcer-1* mutants is not due to decreased pathogen uptake (10). To further test if TCER-1 regulation of smRNAs influences these generally piRNA-dependent avoidance mechanisms, we analyzed a *C. elegans* avoidance-associated smRNA profile following a 24-hour PA14 exposure in Moore *et. al*. The comparison of smRNAs that are downregulated in *tcer-1* mutants (481 loci) and avoidance-associated smRNAs that are downregulated following 24-hour PA14 exposure (700 loci) revealed a non-significant overlap between conditions (14 gene loci). In addition, while smRNAs downregulated in *tcer-1* mutants are predominantly of the WAGO siRNA-associated Mutator class (75%), smRNAs downregulated upon the 24-hour PA14 exposure are mainly piRNAs (66%) (Supp. File 3). This supports that TCER-1 regulation of smRNAs does not influence piRNA-dependent avoidance mechanisms, and instead alters siRNA biosynthesis.

Computation based classification of smRNA species in *C. elegans*, and identification of their mRNA targets, has led to the discovery of new roles for smRNAs. Our tandem smRNAseq-

mRNAseq approach allowed us to broadly assess transcriptomic changes and investigate trends in TCER-1-dependent smRNA silencing. This led to our generation of a candidate list of siRNA-targeted immune genes (Supp. Table 4.6) and ultimate identification of *qdpr-1* and *scrm-4*. Interestingly, all 13 genes in this list were annotated Mutator-dependent siRNAs (MUTs), half of which are shared with a list of mRNAs predicted to be silenced by MUT-16-promoted smRNAs (164). The fact that many of these strong candidates did not impact immunity (Supp. Table 4.5A-B) implies that smRNAs exert additional phenotypic effects in *tcer-1* mutants. For example, quantification of total smRNA classes in *tcer-1* mutants also revealed an increase in miRNA production (**Fig. 4.2F**). Given the diversity of genes that miRNAs silence, it is possible that these induced smRNAs contribute to the established fertility defects in *tcer-1* mutants. Thus, further characterization of the *tcer-1* transcriptome could supply novel insight on the molecular mechanisms employed by this immunosuppressing gene.

smRNA regulation of bacterial immune resistance is an emerging concept in human and animal studies. In humans, smRNAs have been particularly noted for their effects on innate immune cells and even mediating inflammatory response (354). Work in *C. elegans* has further uncovered smRNA effects on strongly conserved mechanisms, such as the p38 MAPK axis and unfolded protein response (172, 174, 318). Overall, *C. elegans'* endogenous smRNA pathways which exert these diverse regulatory effects are noted to be conserved (160, 355). However, the 'Worm-specific Argonaute Proteins' (WAGOs) in siRNA production are an evolutionarily-expanded protein family found exclusively in nematodes. For this reason, an interesting finding in this study was that TCER-1 immune suppression is linked to its promotion of WAGO siRNAs. Nonetheless, several studies argue that even if certain biosynthesis genes are not conserved, other animals will possess analogous mechanisms or overlapping smRNA pathways

(318, 356). This is partially supported by the fact downstream proteins in WAGO siRNA amplification, such as MUT-7, are conserved (167). Thus, whether TCER-1-dependent smRNA regulation is conserved for its total effects on the transcriptome is yet to be explored.

The pattern where increased fertility is accompanied by immunosuppression is a widespread problem in nature. The TCER-1 gene can be used as a tool to interrogate mechanisms of immune suppression deployed by animals. In previous work, our laboratory found TCER-1 uniquely suppresses immunity and promotes longevity, defying a common pattern that longevity mutations increase stress resistance (37). Our additional discovery that TCER-1 is essential for fertility and suppresses immunity only during the reproductive phase then established TCER-1's role as a regulator of fertility-immunity tradeoffs (10). These attributes led us to specifically probe how smRNAs suppress immunity in the larger context of TCER-1 control. Considering the additional connections between smRNAs and fertility regulation in literature, further studies may test if smRNAs cause the established fertility defects seen in *tcer-1* mutants (357, 358). With the goal to identify potential therapeutics, it would also be noteworthy to find if certain immune effectors can be de-repressed in animals though leveraging smRNA biology. Limitations of this study include the difficulty of validating more direct TCER-1 effects on smRNA-mRNA levels. Certain studies of Argonaute proteins which directly bind smRNAs use ChIP-seq techniques to validate these connections (345). In sum, this study uniquely describes the effects of the endogenous siRNA pathway in antibacterial immunity, displaying the overall transcriptomic and immunosuppressive effects of TCER-1 through these pathways. As my final study in a series of three chapters discussing the lifespan, fertility, and immunity effects of well-studied regulatory proteins, this chapter was particularly a deep-dive on the molecular mechanisms impacted by a regulator of the RIL dialogue.

5.0 Discussion and Concluding Remarks

The study of proteins in model organisms which mirror wider patterns in nature can provide insight to many biological mysteries. Indeed, the pro-longevity proteins NHR-49 and TCER-1 have served as useful tools in my study of the RIL dialogue. My work has identified (a) new functions for these well-described genes, (b) new mechanisms of context-dependent immune regulation by these genes, and (c) novel effectors of these pathways, supporting several emerging concepts in aging biology. Taken together, this work provides new insights on the distinct, yet interconnected, molecular mechanisms controlling immunity, fertility, and longevity.

Modulation of Longevity and Immunity by NHR-49: My study of NHR-49 in Chapter 2.0 displayed the importance of monitoring healthspan along with lifespan and the profound significance of site-of-action and biological context on gene function. Previously, NHR-49 was widely regarded as a gene beneficial for both lifespan and stress resistance. While confirming this, our study showed that NHR-49 exerts distinct control over lifespan and immune resistance. We discovered this upon expressing NHR-49 in specific tissues of normal or sterile *C. elegans* grown on control or *Pseudomonas* (PA14) plates. In normal and long-lived germline-less *nhr-49* mutant strains, NHR-49 re-expression from multiple tissues could improve longevity, while only neuronal NHR-49 consistently rescued immunity. NHR-49 re-expression in the hypodermis of *nhr-49* mutants—which rescues lifespan—was even shown to lower the immune resistance of these fertile strains, further supporting the existence of distinct lifespan vs. healthspan control. Assessment of known NHR-49 targets, *acs-2* and *fmo-2*, then showed NHR-49 controls

pathogen-specific transcriptional programs. This was because mutation of *acs-2* and *fmo-2*—which are upregulated >150 fold and ~1,000 fold to combat *S. aureus* infection, respectively—did not lower resistance to PA14 though NHR-49 promotes resistance against this pathogen as well (242, 271). Yet, the potential role of NHR-49 in resistance to natural *C. elegans* pathogens (e.g., oomycete *M. humicola*, microsporidia *N. parisii*, fungus *D. coniospora*) remains to be seen (359). In sum, this study supported the concept that the genetic pathways controlling lifespan and healthspan features are distinct and re-defined preexisting notions about the effects of a well-studied longevity gene.

There are many potential reasons that NHR-49 exerts tissue-specific control over immune resistance. It was particularly interesting that NHR-49 expression in the neurons and hypodermis caused very different immune effects (Fig. 2.4). Most bacterial pathogens consumed by worms are first perceived by the sensory neurons and infect through the digestive tract, whereas, fungal pathogens mostly attack through the cuticle and hypodermis. Thus, it is possible that these tissue specificities reflect the importance of NHR-49's presence in route-of-infection. We do not know if NHR-49 confers immunity against fungal pathogens or others that infect *C. elegans* by breaking skin barrier integrity, but it would be valuable to test this in future studies. Secondly, neuronal sensation not only causes changes in behavior such as pathogen avoidance, but neuronal signaling has also been implicated in immune regulation (reviewed in (80)). For example, dense core vesicle (DCV) secretion and neuronal TGF-β signaling has been shown to induce antimicrobial gene expression and resistance to *P. aeruginosa* and *D. coniospora*, respectively (360, 361). Also, among multiple examples, regulation from groups of neurons such as the ASH, CEP, and AQR neurons are noted for their cell non-autonomous effects on immune pathways such as the p38/PMK-1 MAPK axis (362-364). Our experiments involved NHR-49

expression in all neurons so whether NHR-49 acts in select neurons remains to be examined. Future studies could test this by genetic or laser ablation of specific neuronal groups on immunity in the strains expressing NHR-49 in neurons (as in (365) or (366)). Study of such phenotypes in different neuronal sensory-defective backgrounds is another potential strategy to identify neuronal signaling effects (367, 368).

Our work also raises important questions about NHR-49 activities in different tissues. What kind of genes' expression does it regulate upon infection and are these targets shared across tissues or distinct? It is conceivable that different downstream effectors are regulated by NHR-49 depending on tissue-of-expression. Indeed, adult tissues perform specific roles in pathogen defense as the hypodermis provides barrier integrity, the intestine serves as the main site of induction of immune genes, and neurons play key roles from pathogen detection to inter-tissue signaling (reviewed in (79, 80, 369)). So, it is feasible that NHR-49 in the hypodermis regulates genes that promote cuticle integrity, antibacterial genes in the intestine, and secreted signaling molecules in neurons which coordinate pathogen response. Yet, tissue-specific effectors of NHR-49 have not been identified and it is an important next step in deciphering NHR-49's mechanism of action. Tissue-specific RNAseq using fluorescent tagged strains has become achievable in worms in the last few years (370); the strains used in our study could be used to define NHR-49-directed tissue-specific transcriptomes under different conditions and genetic contexts. Interestingly, studies from our lab and others suggest that NHR-49 interacts with specific co-factors to regulate transcription in different contexts. It may utilize dedicated co-factors to govern the immune response in different tissues as well (277, 371). Though our experiments showed that RNAi knockdown of co-factor, *nhr-80,* only slightly altered PA14 resistance (Fig. 2.7l), we speculate that other NHR-49 partners including the 11 NHRs that

promote *glp-1* longevity (277) may reside in different tissues at different levels to cause these tissue-specific effects.

Given the major role of NHR-49 on immunity it remains critical that we identify tissue-specific NHR-49 immune targets. Previous work in our lab showed the NHR-49 promotes fatty acid β-oxidation and lipid desaturation as the mechanism by which it promotes longevity in germline-less and wild-type worms (104). For this reason, it is also important to consider the potential effects of NHR-49-dependent lipid metabolic regulation on immunity. NHR-49 is the homologue of a key human lipid metabolic regulator, PPARα, which is a major drug target for treating hypercholesteremia (101, 102). Interestingly, work from our laboratory and others have suggested that lipid metabolic genes impact immunity in both *C. elegans* and similar evidences are reported in mammals (10, 202-204). Our data open avenues for future studies to probe the role of PPARα and its downstream targets on immunity in mammalian studies. Identifying the potential role of PPARα in anti-pathogen response could have many implications, not only for potentially using PPARα agonists as immunostimulatory agents but for their unstudied effects on different tissues that would require development of tissue-targeted versions of these drugs (372).

Modulation of Fertility and Immunity by TCER-1: My study of TCER-1 with Dr. Francis RG Amrit in Chapter 3.0 established TCER-1's role as a regulator of RIL tradeoffs and identified several functional targets, indicating its associated immunosuppression pathways. Previous works from our lab had identified TCER-1 as a transcription factor needed for the long-life of the germline-less *glp-1* longevity model (109). Early on, this finding suggested that TCER-1 responds to the reproductive status of the animal to modulate other fitness traits accordingly. This was further supported by our study which described the mechanism by which

TCER-1 facilitated adaptation to germ line loss and showed this pro-longevity gene was also essential to reproductive health in fertile animals (110). Thus, our finding that TCER-1 additionally suppresses both stress resistance widely and immunity to several pathogens, revealed another layer of complexity in the function of this gene. Oftentimes, genes which promote lifespan also improve resistance to stress, underscoring the novelty of TCER-1's function (34). As a result, my experiments which showed TCER-1 exclusively suppressed immunity during the animal's fertile period raised the notion that TCER-1 suppresses immune resistance to promote reproduction in fertile animals. Subsequent observations that TCER-1 overexpression decreased resistance upon infection, and even protected against fertility loss, supported this further. My analysis of the immune resistance of mutants for TCER-1-suppressed genes then showed that TCER-1 suppresses immunity through the canonical p38 MAPK/PMK-1 pathway, and alternate pathways as well (10). These efforts ultimately revealed TCER-1's unique identity as an arbiter of the RIL dialogue, provided greater detail on its immune effects, and showcased this gene as a tool to understand functional tradeoffs in organisms.

The next logical step of this work is to determine the relevance of TCER-1's identified functions in reproduction, lifespan, and immunity in other organisms. One result of the extensive characterization of TCER-1 performed by our lab suggested that TCER-1 promotes fertility and TCER-1 levels decrease with age (10). This is mirrored by the fact mammalian TCERG1 is enriched in female human and mouse oocytes and this expression decreases with age (114, 326). Yet, the potential relevance of TCER-1/TCERG1 effects on lifespan, reproduction, and especially immunity, are largely unexplored. Our laboratory is currently engaged in a collaboration with *drosophila* biologists, Prof. Mariana Wolfner (Cornell) and Dr. Andrey Parkhitko (Univ. of Pittsburgh) to understand the role of the fly TCER-1 homologue, dTCER-1,

in fertility and immunity. If we observe that the dTCER1 indeed promotes fertility and suppresses stress resistance and immune function as observed in *C. elegans*, this would provide additional rationale to explore mammalian TCERG1 effects. Homozygous mouse *Tcerg1* mutants are known to exhibit preweaning lethality (373). Preliminary RNAseq analysis of *TCERG1* knockdown in mammalian cell lines could therefore be used to test for TCERG1 effects on immunity-associated genes. Our lab is also examining the reproductive expression and function of mouse TCERG1 in reproduction in collaboration with the Brieno-Enriquez lab (Univ. of Pittsburgh). Further studies could assess TCERG1 expression and the impact of TCERG1 knockdown in immune cells *in vivo* to define potential TCERG1 effects on the immune system. The maturation of these findings could then suggest if and how TCERG1 impacts human health.

An important question arising from my work pertains to the mechanism by which TCER-1 modulates fertility and immunity. Previous studies in our lab have shown that TCER-1 regulates many lipid metabolic genes and promotes longevity by contributing to the establishment of lipid homeostasis following germ line loss (110). Beyond the implication that lipid metabolic genes play roles in immunity (discussed in section 1.3.2), studies from our lab have further hypothesized that *C. elegans* experience trade-offs between immunity and fertility due to TCER-1 allocation of limited lipid resources to either process. This is because both immunity and reproduction are energy-intensive processes shown to utilize stored lipids (10, 202-204). Preliminary data in our lab showing that TCER-1 controls lipid-hydrolysis genes to govern the deposition of fats into embryos further supports this point (Bahr, Amrit, and Ghazi, unpublished). This is potentially why TCER-1 overexpression through the intestine (Fig. 3.1c) blunted fertility loss upon pathogen exposure compared to overexpression through other tissues. Future studies on this topic will involve the characterization of TCER-1 effects on lipid storage

in maternal versus embryonic tissues upon infection (Bahr, Amrit, and Ghazi, unpublished). If *tcer-1* mutants have reduced fat storage in embryonic tissues compared to wild type animals as preliminary data suggests, this model can be used to understand how TCER-1 regulation of lipid metabolism may control the RIL axis.

TCER-1 Control of smRNA Pathways to Modulate Immunity: My detailed characterizations in Chapter 4.0 investigated small RNA (smRNA) mechanisms as one strategy by which TCER-1 suppresses immunity. With a focus on TCER-1 immunosuppressive effects, this study confirmed early evidence that TCER-1 promotes the production of smRNAs and notably demonstrated the influence of the siRNA pathway in immune suppression (176, 177). This is novel because, unlike miRNAs and piRNAs, the siRNA pathway has rarely been implicated as a regulator of antibacterial immunity. In comparison to previous studies which implicated siRNA effects on immunity (173, 321), this study identified that several biogenesis mutants— consistently targeting genes involved in siRNA amplification—possessed increased immunity. Our tandem, collaborative, smRNAseq-mRNAseq approach then allowed us to broadly assess transcriptomic changes and screen for trends in TCER-1-dependent smRNA silencing. This revealed that *tcer-1* mutation causes a ~10% reduction in the production of certain siRNAs. Subsequent analyses then suggested that TCER-1 acts through the same genetic pathway as siRNAs to suppress immunity and demonstrated a similarity in smRNA regulation by TCER-1 and immunoresistant siRNA amplification mutants. Further investigation of downstream targets then identified candidate immune-impacting genes which are suppressed by TCER-1-directed siRNA silencing. Taken together, these findings proposed a mechanism thorough which TCER-1-upregulated smRNAs suppress immunity, revealing the role of siRNAs

in this process. Further assessment of TCER-1-dependent smRNA regulation may uncover why TCER-1 induces immunosuppression in context with TCER-1's additional roles in the RIL axis.

Considering the TCER-1 immune impacts revealed by our studies, it is important to note that TCER-1 effects against natural pathogens (e.g. oomycete *M. humicola*, microsporidia *N. parisii*, fungus *D. coniospora*) are yet to be tested (359). Similarly, although siRNA pathways in worms are typically associated with viral resistance (168, 319, 320), we do not know the effects of TCER-1-directed smRNA regulation on resistance to natural viral infection, such as the intracellular Orsay virus (152). As discussed in Chapter 3.0, our data indeed suggests that TCER-1 suppresses stress resistance widely, as *tcer-1* mutants have increased resistance to multiple stressors (e.g. resistance to heat, oxidative stress, and DNA damage). TCER-1 also suppresses resistance to multiple Gram-positive (*P. aeruginosa* strain PA14 and PA01) and Gram-negative bacteria (*S. aureus* and *E. faecalis*) (10). Thus, we speculate that *tcer-1* mutants would likely have increased resistance to natural bacterial pathogens. We also hypothesize that *tcer-1* mutants would have increased resistance to natural viral pathogens despite their lower levels of total siRNAs. This is because, as suggested by our smRNAseq in Chapter 4.0, TCER-1 does not influence total siRNA levels but instead promotes the production of a small and select subset of siRNAs. So, it is possible that this small subset also includes siRNAs deployed in immune-suppression. Testing the impact of smRNA-dependent and -independent TCER-1 effects on antiviral immunity would therefore be an interesting next step of this work. The likely possibility that TCER-1-dependent smRNA regulation varies in different *C. elegans* tissues may also play a role in these effects (297, 322, 374).

Our findings that TCER-1 impacts the production of various smRNA species also brings forth questions on how TCER-1 expression is regulated. Other experiments from our publication

additionally showed that somatic and germ line levels of TCER-1 are highest in young animals and decline with age (10). We speculated this downregulation was the mechanism by which TCER-1, a pro-fertility regulator of immunity-fertility investments, no longer promotes fertility in post-reproductive worms. Yet, precisely how this change in expression occurs is a key area of interest to our studies. For example, our smRNAseq results showed total miRNAs are increased in *tcer-1* mutants (Fig. 4.2f) and suggest a possibility that TCER-1 regulation of smRNAs might cause the downregulation of TCER-1 levels with age. Although we did not find that the *tcer-1* locus (or the one known upstream regulator, *kri-1* (109)) was explicitly targeted by these miRNAs, it is possible that TCER-1-DOWN smRNAs might silence unidentified genes that promote TCER-1 expression (Supp. File 1). One approach to identify additional factors which regulate TCER-1 expression could therefore utilize an RNAi screen to find genes which change TCER-1-GFP signal following knockdown. If TCER-1 downregulation with age is independent of smRNA regulation, these findings could alternatively indicate whether TCER-1 levels decline due to age-dependent expression changes, particularly if any hits are noted to change in published analyses of aged *C. elegans* transcriptomes (i.e., (375, 376)). Yet, TCER-1 regulated miRNAs might not silence *tcer-1* expression itself, but instead suppress genes characteristic of the *tcer-1* mutant phenotype. For instance, TCER-1-DOWN miRNAs may instead cause *tcer-1* mutant's fertility deficits, as miRNA pathways are found to impact various reproduction-associated processes in both worms and mammals (357, 377, 378). Probing the mechanisms by which TCER-1 levels decline with age may therefore reveal more about its regulation of and responses to RIL changes to better define its effects.

Despite some evidence that TCER-1 does not exert tissue-specific effects on lifespan and immunity, the question of heterogenous TCER-1 effects remain open for speculation. For

instance, our laboratory found that TCER-1 is broadly expressed in somatic tissues and the germ line. Unlike NHR-49 tissue-specific effects on immunity, additional experiments from our 2019 publication showed that TCER-1 expression from any somatic tissue was sufficient to rescue its immunosuppressive effects to wild-type levels (10). In reaction to these findings, our study of TCER-1 effects on smRNA pathways began because we wanted to test where TCER-1 expression was necessary to suppress immunity. Yet, since the results of this necessity experiment were unclear, due to the additional immune effects of soma and germ line-specific knockdown strains (341, 342), TCER-1 tissue-specific regulation remains a possibility. Single-cell RNAseq is a useful technique which could be utilized to define tissue-specific gene expression changes dictated by TCER-1 (379, 380). We speculate that TCER-1 will regulate different gene sets in the germline versus soma because TCER-1 exerts opposite effects on reproduction and immunity, which are vastly different processes separately associated with germline and somatic tissues, respectively. Understanding additional stress-specific mechanisms of TCER-1 action is another avenue for exploration for our work. Thus far, our laboratory has performed RNAseq analysis of TCER-1 effects in *glp-1* mutants and upon PA14 infection, and identified transcriptomic differences ((110) and (Amrit, Ghazi et al., unpublished)) yet it would be interesting to understand how TCER-1 controls transcriptomic response to other stresses such as heat, oxidative stress, or infection by natural pathogens and whether these responses are unique.

Conclusion: How and why animals experience tradeoffs between key functions like reproduction, immune function, and longevity is a question of fundamental importance in biology and medicine. Emerging studies, and the work of this thesis, have uncovered gene-

regulators which can respond to organismal needs and mediate these processes accordingly. Such genes can further be used as a tool to understand the RIL dialogue, due to the likely conservation of the molecular mechanisms underlying their effects. The tractable *C. elegans* nematode model provides an invaluable platform to dissect genetic pathways and discern reproductive, immunity, and longevity impacts. Altogether, this thesis has demonstrated the context-specific effects of two RIL regulators, characterized their regulatory strategies, and identified their effectors particularly in conserved immunity pathways. In the future, these findings are likely to contribute to understanding mechanisms by which immunity is suppressed during human pregnancy, how lifespan may be impacted differently than immunity, and how immune activation curbs fertility with the potential to reveal a means to modulate RIL traits for biomedical advancement.

Appendix A Chapter 2.0 Supplementary Figures

(S1a) Strains compared by RNA-Seq in present study

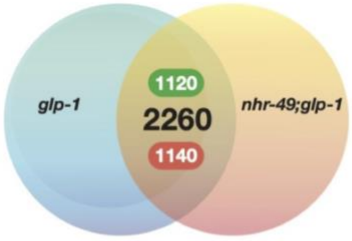

(S1b) Comparison of NHR-49 targets with DAF-16 and TCER-1 targets in *glp-1* mutants

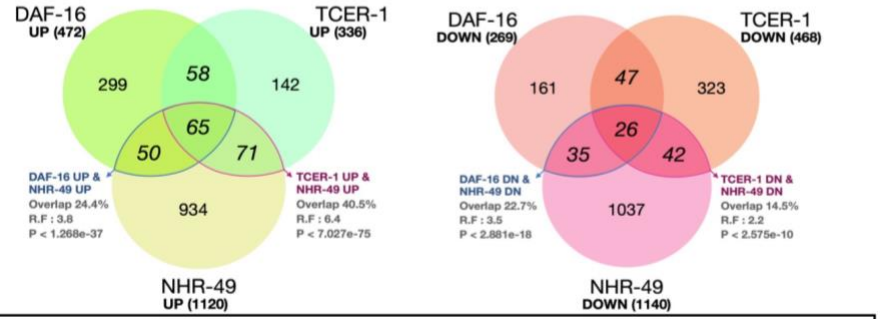

(S1c) NHR-49 UP genes (this study) with previously-identified roles in *glp-1* longevity *(Amrit et al., PLoS Gen. 2016)*

Wormbase Gene ID	Public Name	Overlapping Group	Avg. % Suppression of Lifespan
WBGene00000966	*dhs-2*	DAF-16 & TCER-1 UP	-14
WBGene00000981	*dhs-18*	DAF-16 & TCER-1 UP	-12
WBGene00001387	*far-3*	DAF-16 & TCER-1 UP	-12
WBGene00001500	*ftn-1*	DAF-16 & TCER-1 UP	-18
WBGene00001777	*gst-29*	DAF-16 & TCER-1 UP	-15
WBGene00004818	*skr-12*	DAF-16 & TCER-1 UP	-22
WBGene00004994	*spp-9*	DAF-16 & TCER-1 UP	-12
WBGene00004997	*spp-12*	DAF-16 & TCER-1 UP	-14
WBGene00007140	*cyp-29A4*	DAF-16 & TCER-1 UP	-15
WBGene00010706	*cyp-14A2*	DAF-16 & TCER-1 UP	-17
WBGene00011362	*cest-1.1*	DAF-16 & TCER-1 UP	-19
WBGene00013904	*ugt-6*	DAF-16 & TCER-1 UP	-21
WBGene00017390	F12A10.1	DAF-16 & TCER-1 UP	-11
WBGene00020413	T10E9.3	DAF-16 & TCER-1 UP	-22
WBGene00020909	W01A11.1	DAF-16 & TCER-1 UP	-17
WBGene00000975	*dhs-12*	DAF-16 UP	-17
WBGene00003473	*mtl-1*	DAF-16 UP	-22
WBGene00012404	Y6G8.2	DAF-16 UP	-18
WBGene00014030	*glb-1*	DAF-16 UP	-15
WBGene00021491	*comt-4*	DAF-16 UP	-11
WBGene00000982	*dhs-19*	TCER-1 UP	-22
WBGene00000986	*dhs-23*	TCER-1 UP	-20
WBGene00000988	*dhs-25*	TCER-1 UP	-21
WBGene00007362	*cyp-35C1*	TCER-1 UP	-17
WBGene00007848	*cytb-5.1*	TCER-1 UP	-21
WBGene00007963	*cyp-25A1*	TCER-1 UP	-10
WBGene00008499	*cyp-37A1*	TCER-1 UP	-22
WBGene00010659	K08D8.5	TCER-1 UP	-15
WBGene00011830	*cyp-29A2*	TCER-1 UP	-10
WBGene00013594	Y872A.2	TCER-1 UP	-15
WBGene00015400	*cyp-35A2*	TCER-1 UP	-16
WBGene00015692	*ugt-25*	TCER-1 UP	-14
WBGene00016786	*cyp-35A4*	TCER-1 UP	-20
WBGene00018958	*cest-27*	TCER-1 UP	-11
WBGene00019473	*cyp-35A5*	TCER-1 UP	-13

Supplementary Figure 2.1 Strains compared by RNA-seq in present study and comparison of NHR-49 targets with DAF-16 and TCER-1 targets in *glp-1* mutants.

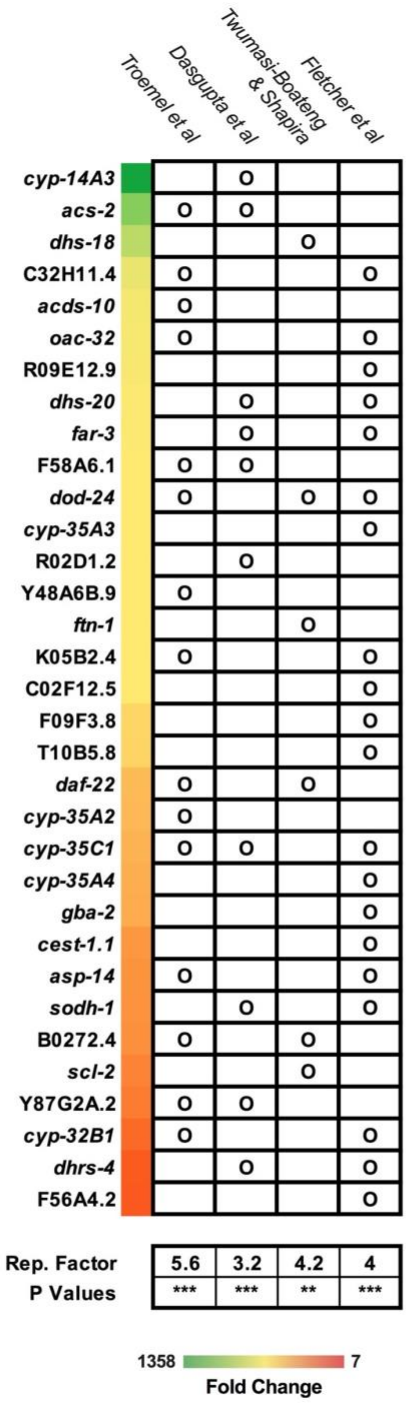

(S2) - Comparison of the top 100 UP NHR-49 targets with studies examining transcriptomic changes upon PA14 exposure (Troemel et al., 2006; Dasgupta et al., 2020; Twumasi-Boateng and Shapira, 2012; Fletcher et al., 2019).

Supplementary Figure 2.2 Comparison of the top 100 UP NHR-49 targets with studies examining transcriptomic changes upon PA14 exposure.

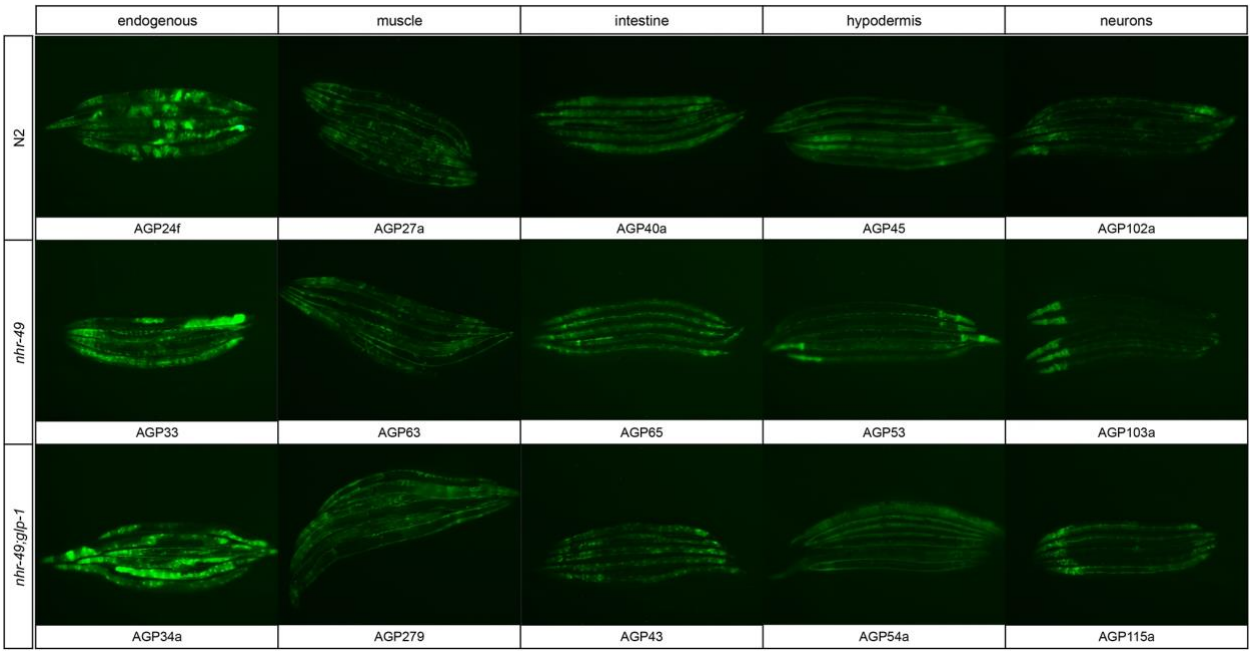

Supplementary Figure 2.3 Images of transgenic strains.

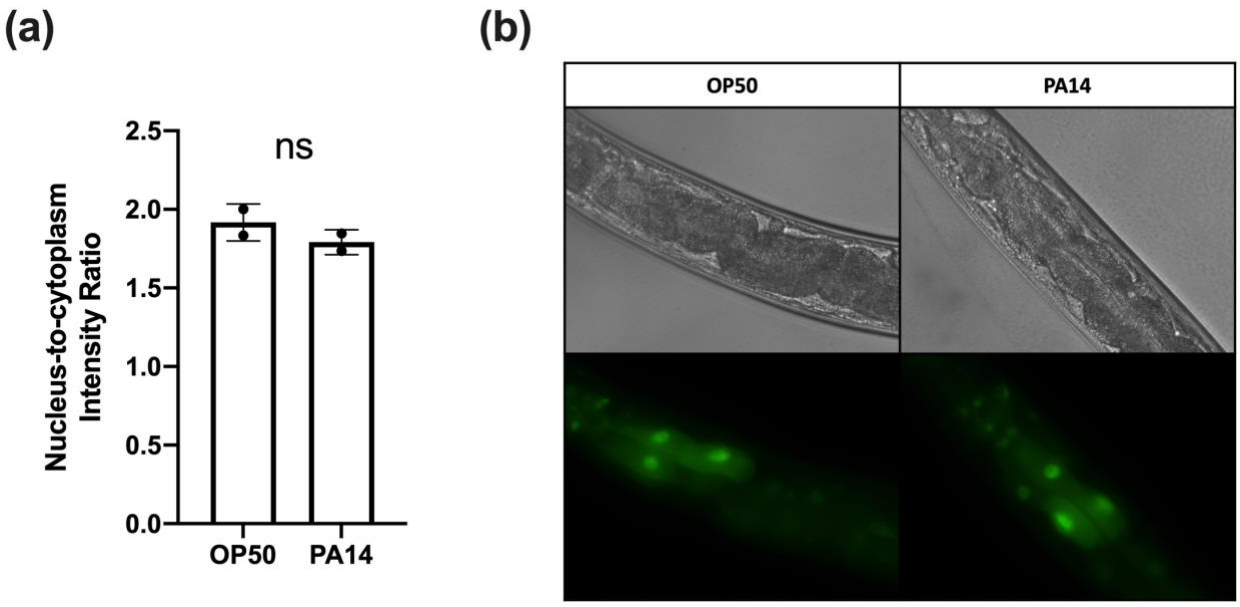

Supplementary Figure 2.4 Exposure to PA14 does not alter NHR-49 nuclear localization.

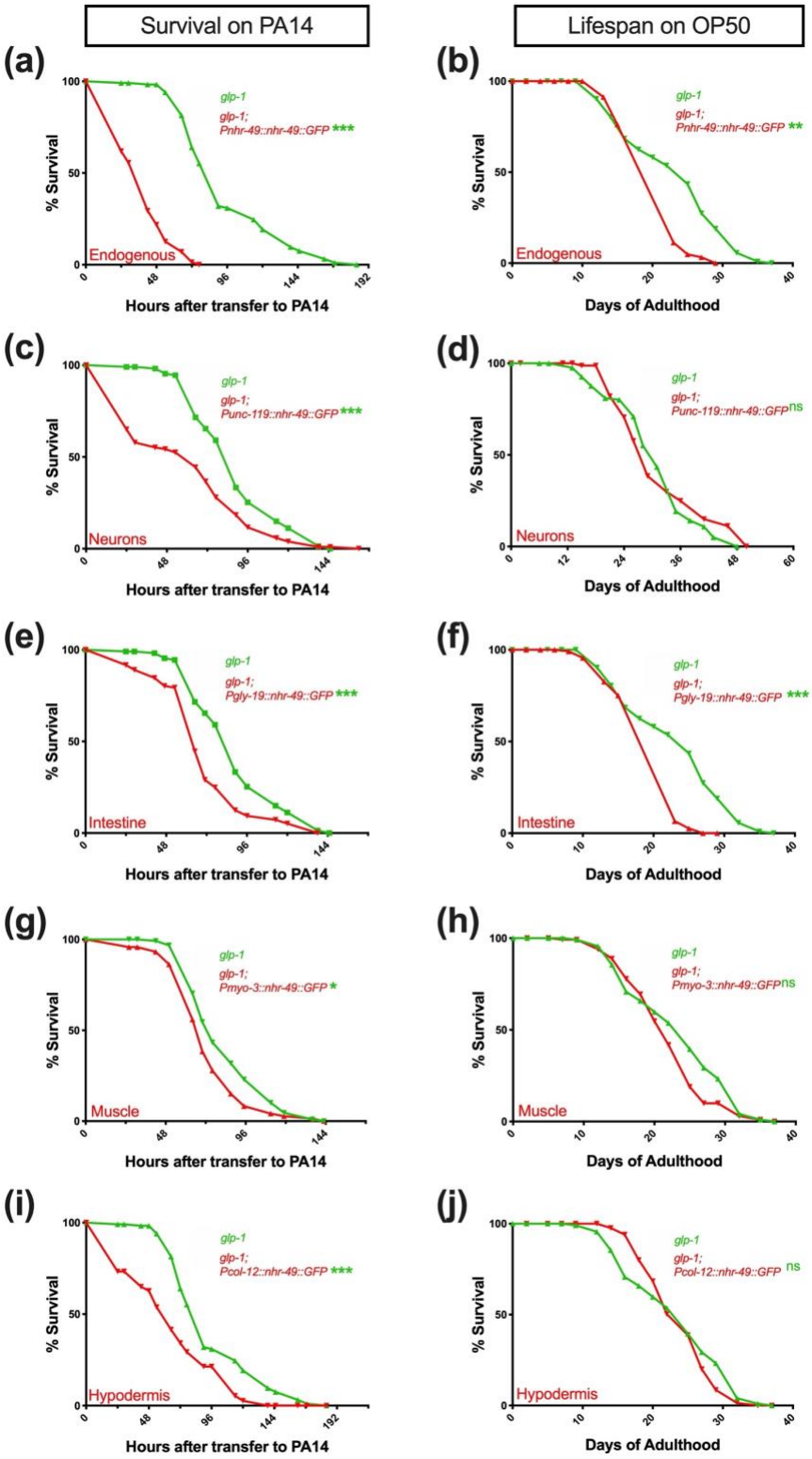

Supplementary Figure 2.5 Impact of tissue-specific overexpression of NHR-49 in *glp-1* mutants on lifespan and PA14 survival.

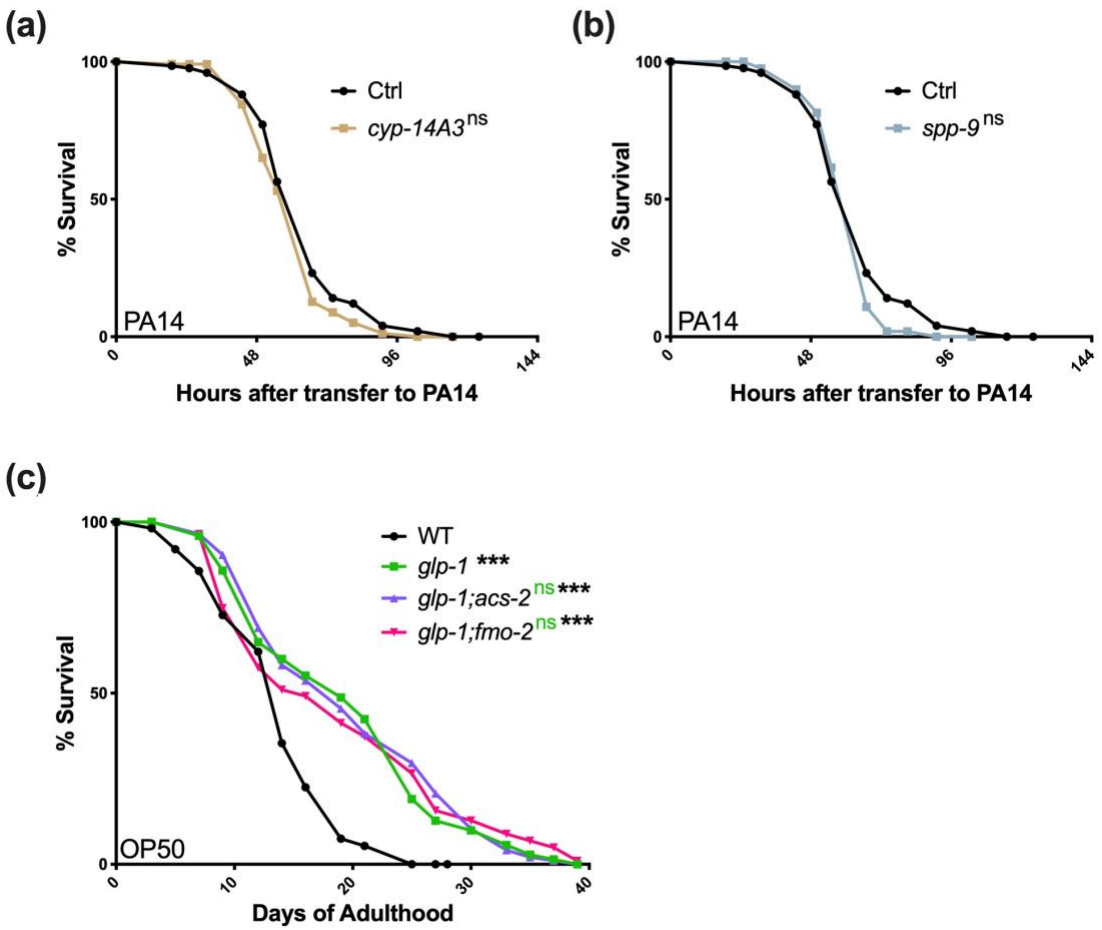

Supplementary Figure 2.6 NHR-49 targets, *cyp-14A3* and *spp-9*, do not alter PA14 immunity; mutation of canonical NHR-49 targets, *acs*-2 and *fmo-2*, does not lower the *glp-1* lifespan.

Appendix A.1 Chapter 2.0 Supplementary Tables

Supplementary Table 2.1 RNA-seq results of *nhr-49;glp-1* and *glp-1* strains

(D-Scholarship Link)

Supplementary Table 2.2 Impact of *nhr-49(et7)* allele and Fenofibrate treatment on survival

Table S2a: Impact of *nhr-49(et7)* on PA14 survival (A.1) and OP50 lifespan (A.2)

Table S2a.1: SURVIVAL ON PA14

Genotype	Trial 1			Bonferroni P value
	n = obs/ total	Mean (h)	SE +/-	P *(vs* N2)
WT	126 / 145	54.32	1.09	
nhr-49(et7) gof	94 / 136	62.79	1.31	<0.0001
Trial 2				
WT	60 / 117	78.4	2.66	
nhr-49(et7) gof	79 / 110	74.68	3.67	0.4354
Trial 3				
WT	102 / 129	76.98	2.25	
nhr-49(et7) gof	73 / 118	76.09	2.57	1
Trial 4#				
WT	87 / 150	77.36	1.79	
nhr-49(et7) gof	60 / 130	89.35	2.22	<0.0001
Trial 5~				
WT	94 / 120	75.16	2.74	
nhr-49(et7) gof	94 / 140	76.77	2.3	1
Trial 6$				
WT	78 / 106	67.46	2.15	
nhr-49(et7) gof	93 / 125	77.88	1.85	0.0002

Table S2a.2: SURVIVAL ON OP50

Genotype	Trial 1◇			Bonferroni P value
	n = obs/ total	Mean (h)	SE +/-	P *(vs* N2)
WT	99 / 120	15.61	0.46	
nhr-49(et7) gof	78 / 118	16.75	0.54	0.4299
Trial 2†				
WT	103 / 136	16.49	0.44	
nhr-49(et7) gof	86 / 117	13.46	0.66	0.0422

Special characters #, ~, $, ◇, † on trial headings denote the trial was performed alongside similarly-labeled experiments in Table S6A.
Underlined Trials in S2a and S2b shown in Figs. 2b and 2c, respectively.

Table S2b: Impact of Fenofibrate on survival upon PA14 exposure

SURVIVAL ON PA14

Genotype	Treatment	Trial 1			Bonferroni P-value	
		n = obs/ total	Mean (h)	SE +/-	P *(vs* WT Control)	P *(vs* FF Control)
WT	Control	103 / 129	56.81	1.08		
	Fenofibrate	93 / 135	62.1	1.26	0.0041	0.0041
nhr-49	Control	107 / 134	47.69	0.98	<0.0001	
	Fenofibrate	104 / 134	45.33	0.89	<0.0001	0.072
Trial 2						
WT	Control	82 / 131	61.69	0.99		
	Fenofibrate	78 / 137	65.92	1.78	< 0.0001	< 0.0001
nhr-49	Control	83 / 130	41.33	0.71	< 0.0001	
	Fenofibrate	94 / 131	41.36	0.8	< 0.0001	0.0004
Trial 3						
WT	Control	103 / 150	59.21	1.09		
	Fenofibrate	104 / 150	63.16	1.43	0.0187	0.0187
nhr-49	Control	62 / 119	44.82	0.76	< 0.0001	
	Fenofibrate	110 / 149	40.99	0.83	< 0.0001	1
Trial 4						
WT	Control	131 / 160	66	1.19		
	Fenofibrate	148 / 160	71.86	1.11	0.0006	0.0006
nhr-49	Control	126 / 160	47.92	0.7	< 0.0001	
	Fenofibrate	152 / 161	47.44	0.71	< 0.0001	1
Trial 5						
WT	Control	108 / 150	66.75	1.37		
	Fenofibrate	90 / 145	64.73	1.32	1	1
nhr-49	Control	116 / 122	50.49	0.99	< 0.0001	
	Fenofibrate	110 / 120	51.3	0.95	< 0.0001	1
Trial 6						
WT	Control	103 / 120	78.28	1.73		
	Fenofibrate	84 / 120	70.11	1.42	0.0017	0.0017
nhr-49	Control	150 / 159	51.94	0.72	< 0.0001	
	Fenofibrate	148 / 160	52.91	0.77	< 0.0001	1
Trial 7						
WT	Control	95 / 146	61.37	1.46		
	Fenofibrate	91 / 139	63.24	1.66	0.041	0.041
nhr-49	Control	102 / 146	46.38	0.88	< 0.0001	
	Fenofibrate	123 / 151	48.08	0.65	< 0.0001	< 0.0001
Trial 8						
WT	Control	53/150	70.09	2.47		
	Fenofibrate	65/150	61.58	2.17	0.0066	0.0066
nhr-49	Control	127/150	46.82	0.76	< 0.0001	
	Fenofibrate	108/150	41.86	0.49	< 0.0001	< 0.0001

Supplementary Table 2.3 a-e Impact of tissue-specific promoter-driven NHR-49 expression on *nhr-49;glp-1* mutants' survival of PA14 or OP50.

Table S3a: Impact of endogenous promoter-driven NHR-49 expression on survival of *nhr-49;glp-1* mutants on PA14 (a.1) or OP50 (a.2)

Table S3a.1: SURVIVAL ON PA14

Strain	Background/Genotype	Trial 1*			Bonferroni P-value		
		n = obs/ total	Mean (h)	SE +/-	P *(vs* N2)	P *(vs nhr-49; glp-1)*	P *(vs glp-1)*
WT	Wild type	100 / 122	59.17	1.14			
AGP22	*nhr-49;glp-1*	111 / 121	56.25	1.42	0.7488		
CF1903	*glp-1*	117 / 124	80.71	1.62	<0.0001	<0.0001	
AGP34	*nhr-49;glp-1 glmEx5 [Pnhr-49::nhr-49::GFP + Pmyo-2::mCh]*	79 / 113	43.77	1.36	<0.0001	<0.0001	<0.0001
Trial 2#							
WT	Wild type	68/120	72.12	2.14			
AGP22	*nhr-49;glp-1*	108/120	57.92	1.35	<0.0001		
CF1903	*glp-1*	105/120	82.88	2.08	0.0042	<0.0001	
AGP34	*nhr-49;glp-1 glmEx5 [Pnhr-49::nhr-49::GFP + Pmyo-2::mCh]*	95/120	43.33	1.74	<0.0001	<0.0001	<0.0001
Trial 3^							
WT	Wild type	67 / 114	75.62	1.71			
AGP22	*nhr-49;glp-1*	98 / 111	53.32	1.26	<0.0001		
CF1903	*glp-1*	104 / 108	89.65	2.83	0.0429	<0.0001	
AGP34	*nhr-49;glp-1 glmEx5 [Pnhr-49::nhr-49::GFP + Pmyo-2::mCh]*	69 / 78	35.59	1.37	<0.0001	<0.0001	<0.0001
Trial 4$							
WT	Wild type	88 / 128	92.05	1.99			
AGP22	*nhr-49;glp-1*	106 / 132	69.89	1.69	<0.0001		
CF1903	*glp-1*	101 / 131	106.42	2.74	0.0004	<0.0001	
AGP34	*nhr-49;glp-1 glmEx5 [Pnhr-49::nhr-49::GFP + Pmyo-2::mCh]*	80 / 111	54.13	2.67	<0.0001	<0.0001	<0.0001

Table S3a.2: SURVIVAL ON OP50

Strain	Background Genotype	Trial 1@			Bonferroni P-value		
		n = obs/ total	Mean (days)	SE +/-	P *(vs* N2)	P *(vs nhr-49;glp-1)*	P *(vs glp-1)*
AGP22	*nhr-49;glp-1*	72/72	11.27	0.26			
CF1903	*glp-1*	65/77	25.78	0.98		<0.0001	
AGP34	*nhr-49;glp-1 glmEx5 [Pnhr-49::nhr-49::GFP + Pmyo-2::mCh]*	14/26	24.6	1.39		<0.0001	1
Trial 2&							
WT	Wild type	52/71	16.26	0.91			
AGP22	*nhr-49;glp-1*	55/72	11.28	0.26	0.0002		
CF1903	*glp-1*	51/70	24.43	1.08	<0.0001	<0.0001	
AGP34	*nhr-49;glp-1 glmEx5 [Pnhr-49::nhr-49::GFP + Pmyo-2::mCh]*	59/60	23.72	1.32	<0.0001	<0.0001	1
Trial 3~							
AGP22	*nhr-49;glp-1*	125 / 142	9.96	0.07			
CF1903	*glp-1*	100 / 107	18.49	0.53		<0.0001	
AGP34	*nhr-49;glp-1 glmEx5 [Pnhr-49::nhr-49::GFP + Pmyo-2::mCh]*	102 / 124	15.61	0.58		<0.0001	0.0046

*, #, ^, $, & and ~ on different tabs/sub-sections of Table S3 denote trials performed at the same time
Underlined Trials shown in Fig. 3

Supplementary Table 2.3 (continued)

Table S3b: Impact of neuronal (*unc-119*) promoter-driven NHR-49 expression on survival of *nhr-49;glp-1* mutants on PA14 (b.1) or OP50 (b.2)

Table S3b. 1: SURVIVAL ON PA14

Strain	Background/Genotype	Trial 1*			Bonferroni P-value		
		n = obs/ total	Mean (h)	SE +/-	P *(vs* N2)	P *(vs nhr-49;glp-1*)	P *(vs glp-1*)
WT	Wild type	100 / 122	59.17	1.14			
AGP22	*nhr-49;glp-1*	111 / 121	56.25	1.42	0.7488		
CF1903	*glp-1*	117 / 124	80.71	1.62	<0.0001	<0.0001	
AGP115	*nhr-49;glp-1 glmEx29 [Punc-119:: nhr-49::GFP + Pmyo-2::mCh]*	107 / 120	74.76	2.92	<0.0001	<0.0001	1
Trial 2#							
WT	Wild type	68/120	72.12	2.14			
AGP22	*nhr-49;glp-1*	108/120	57.92	1.35	<0.0001		
CF1903	*glp-1*	105/120	82.88	2.08	0.0042	<0.0001	
AGP115	*nhr-49;glp-1 glmEx29 [Punc-119:: nhr-49::GFP + Pmyo-2::mCh]*	104/120	77.91	3.28	0.1476	<0.0001	1
Trial 3^							
WT	Wild type	67 / 114	75.62	1.71			
AGP22	*nhr-49;glp-1*	98 / 111	53.32	1.26	<0.0001		
CF1903	*glp-1*	104 / 108	89.65	2.83	0.0429	<0.0001	
AGP115	*nhr-49;glp-1 glmEx29 [Punc-119:: nhr-49::GFP + Pmyo-2::mCh]*	90 / 102	92.09	3.49	0.0028	<0.0001	1

Table Sb.2: SURVIVAL ON OP50

Strain	Background Genotype	Trial 1&			Bonferroni P-value		
		n = obs/ total	Mean (days)	SE +/-	P *(vs* N2)	P *(vs nhr-49;glp-1*)	P *(vs glp-1*)
WT	Wild type	52/71	16.26	0.91			
AGP22	*nhr-49;glp-1*	55/72	11.28	0.26	0.0002		
CF1903	*glp-1*	51/70	24.43	1.08	<0.0001	<0.0001	
AGP115	*nhr-49;glp-1 glmEx29 [Punc-119:: nhr-49::GFP + Pmyo-2::mCh]*	66/71	24.41	1.04	<0.0001	<0.0001	1
Trial 2							
WT	Wild type	71 / 100	23.8	0.58			
AGP22	*nhr-49;glp-1*	110 / 145	11.38	0.19	<0.0001		
CF1903	*glp-1*	83 / 84	22.58	1.06	1	<0.0001	
AGP115	*nhr-49;glp-1 glmEx29 [Punc-119:: nhr-49::GFP + Pmyo-2::mCh]*	67 / 92	23.97	0.45	1	<0.0001	1
Trial 3							
WT	Wild type	71 / 82	17.99	0.58			
AGP22	*nhr-49;glp-1*	63 / 65	11.11	0.33	<0.0001		
CF1903	*glp-1*	109 / 121	24.25	0.91	<0.0001	<0.0001	
AGP115	*nhr-49;glp-1 glmEx29 [Punc-119:: nhr-49::GFP + Pmyo-2::mCh]*	83 / 103	24.9	0.55	<0.0001	<0.0001	1

*, #, ^, $, & and ~ on different tabs/sub-sections of Table S3 denote trials performed at the same time
Underlined Trials shown in Fig. 3

Supplementary Table 2.3 (continued)

Table S3c: Impact of intestinal (*gly-19*) promoter-driven NHR-49 expression on survival of *nhr-49;glp-1* mutants on PA14 (c.1) and OP50 (c.2)

Table S3c. 1: SURVIVAL ON PA14

Strain	Background/Genotype	Trial 1*			Bonferroni P-value		
		n = obs/ total	Mean (h)	SE +/-	P *(vs* N2)	P *(vs nhr-49;glp-1)*	P *(vs glp-1)*
WT	Wildtype	100 / 122	59.17	1.14			
AGP22	*nhr-49;glp-1*	111 / 121	56.25	1.42	0.7488		
CF1903	*glp-1*	117 / 124	80.71	1.62	<0.0001	<0.0001	
AGP43	*nhr-49;glp-1 glmEx10 [Pgly-19::nhr-49::GFP + Pmyo-2::mCherry]*	68 / 79	47.82	2.57	0.0026	0.0693	<0.0001
Trial 2$							
WT	Wildtype	88 / 128	92.05	1.99			
AGP22	*nhr-49;glp-1*	106 / 132	69.89	1.69	<0.0001		
CF1903	*glp-1(e2144)*	101 / 131	106.42	2.74	0.0004	<0.0001	
AGP43	*nhr-49;glp-1 glmEx10 [Pgly-19::nhr-49::GFP + Pmyo-2::mCherry]*	86 / 140	77.36	3.45	0.0086	0.0726	<0.0001
Trial 3							
WT	Wildtype	94 / 135	89.9	2.17			
AGP22	*nhr-49;glp-1*	124 / 139	61.35	1.3	<0.0001		
CF1903	*glp-1(e2144)*	94 / 139	93.57	2.96	1	<0.0001	
AGP43	*nhr-49;glp-1 glmEx10 [Pgly-19::nhr-49::GFP + Pmyo-2::mCherry]*	93 / 140	61.68	2.39	<0.0001	1	<0.0001

Table S3c.2: SURVIVAL ON OP50

Strain	Background Genotype	Trial 1@			Bonferroni P-value		
		n = obs/ total	Mean (days)	SE +/-	P *(vs* N2)	P *(vs nhr-49;glp-1)*	P *(vs glp-1)*
AGP22	*nhr-49;glp-1*	72/72	11.27	0.26			
CF1903	*glp-1(e2144)*	65/77	25.78	0.98		<0.0001	
AGP43	*nhr-49;glp-1 glmEx10 [Pgly-19::nhr-49::GFP + Pmyo-2::mCherry]*	41/63	19.79	0.95		<0.0001	0.0002
Trial 2~							
AGP22	*nhr-49;glp-1*	125 / 142	9.96	0.07			
CF1903	*glp-1(e2144)*	100 / 107	18.49	0.53		<0.0001	
AGP43	*nhr-49;glp-1 glmEx10 [Pgly-19::nhr-49::GFP + Pmyo-2::mCherry]*	118 / 137	16.55	0.2		<0.0001	0.0011

*, #, ^, $, & and ~ on different tabs/sub-sections of Table S3 denote trials performed at the same time
Underlined Trials shown in Fig. 3

Supplementary Table 2.3 (continued)

Table S3d: Impact of muscle (*myo-3*) promoter-driven NHR-49 expression on survival of *nhr-49;glp-1* mutants on PA14 (d.1) and OP50 (d.2)

Table S3d. 1: SURVIVAL ON PA14

Strain	Background/Genotype	Trial 1*			Bonferroni P-value		
		n = obs/ total	Mean (h)	SE +/-	P *(vs* N2)	P *(vs nhr-49;glp-1)*	P *(vs glp-1)*
WT	Wildtype	100 / 122	59.17	1.14			
AGP22	*nhr-49;glp-1*	111 / 121	56.25	1.42	0.7488		
CF1903	*glp-1*	117 / 124	80.71	1.62	<0.0001	<0.0001	
AGP279	*nhr-49;glp-1 glmEx7 [Pmyo-3::nhr-49::GFP + Pmyo-2::mCherry]*	109 / 115	52.44	1.67	0.3334	1	<0.0001
	Trial 2#						
WT	Wildtype	68/120	72.12	2.14			
AGP22	*nhr-49;glp-1*	108/120	57.92	1.35	<0.0001		
CF1903	*glp-1*	105/120	82.88	2.08	0.0042	<0.0001	
AGP279	*nhr-49;glp-1 glmEx7 [Pmyo-3::nhr-49::GFP + Pmyo-2::mCherry]*	108/120	62.52	2.29	0.1479	<0.0001	<0.0001
	Trial 3^						
WT	Wildtype	67 / 114	75.62	1.71			
AGP22	*nhr-49;glp-1*	98 / 111	53.32	1.26	<0.0001		
CF1903	*glp-1*	104 / 108	89.65	2.83	0.0429	<0.0001	
AGP279	*nhr-49;glp-1 glmEx7 [Pmyo-3::nhr-49::GFP + Pmyo-2::mCherry]*	105 / 115	63.53	1.76	<0.0001	<0.0001	<0.0001

Table S3d.2: SURVIVAL ON OP50

Strain	Background Genotype	Trial 1@			Bonferroni P-value		
		n = obs/ total	Mean (days)	SE +/-	P *(vs* N2)	P *(vs nhr-49;glp-1)*	P *(vs glp-1)*
AGP22	*nhr-49;glp-1*	72/72	11.27	0.26			
CF1903	*glp-1*	65/77	25.78	0.98		<0.0001	
AGP279	*nhr-49;glp-1 glmEx7 [Pmyo-3::nhr-49::GFP + Pmyo-2::mCherry]*	34/59	21.4	1.02		<0.0001	0.0113
	Trial 2~						
AGP22	*nhr-49;glp-1*	125 / 142	9.96	0.07			
CF1903	*glp-1*	100 / 107	18.49	0.53		<0.0001	
AGP279	*nhr-49;glp-1 glmEx7 [Pmyo-3::nhr-49::GFP + Pmyo-2::mCherry]*	109 / 116	17.71	0.33		<0.0001	1

*, #, ^, $, & and ~ on different tabs/sub-sections of Table S3 denote trials performed at the same time
Underlined Trials shown in Fig. 3

Supplementary Table 2.3 (continued)

Table S3e: Impact of hypodermal (*col-12*) promoter-driven NHR-49 expression on survival of *nhr-49;glp-1* mutants on PA14 (e.1) and OP50 (e.2)

Table S3e.1: SURVIVAL ON PA14

Strain	Background/Genotype	Trial 1*			Bonferroni P-value		
		n = obs/ total	Mean (h)	SE +/-	P (*vs* N2)	P (*vs nhr-49;glp-1*)	P (*vs glp-1*)
WT	Wildtype	100 / 122	59.17	1.14			
AGP22	*nhr-49;glp-1*	111 / 121	56.25	1.42	0.7488		
CF1903	*glp-1*	117 / 124	80.71	1.62	<0.0001	<0.0001	
AGP54	*nhr-49;glp-1 glmEx11 [Pcol-12::nhr-49::GFP + Pmyo-2::mCherry]*	97 / 115	57.83	2.42	1	1	<0.0001
	Trial 2#						
WT	Wildtype	68/120	72.12	2.14			
AGP22	*nhr-49;glp-1*	108/120	57.92	1.35	<0.0001		
CF1903	*glp-1*	105/120	82.88	2.08	0.0042	<0.0001	
AGP54	*nhr-49;glp-1 glmEx11 [Pcol-12::nhr-49::GFP + Pmyo-2::mCherry]*	96/120	56.06	2.53	0.0004	1	<0.0001
	Trial 3^						
WT	Wildtype	67 / 114	75.62	1.71			
AGP22	*nhr-49;glp-1*	98 / 111	53.32	1.26	<0.0001		
CF1903	*glp-1*	104 / 108	89.65	2.83	0.0429	<0.0001	
AGP54	*nhr-49;glp-1 glmEx11 [Pcol-12::nhr-49::GFP + Pmyo-2::mCherry]*	89 / 104	66.00	2.7	0.0508	<0.0001	<0.0001

Table S3e.2: SURVIVAL ON OP50

Strain	Background Genotype	Trial 1@			Bonferroni P-value		
		n = obs/ total	Mean (days)	SE +/-	P (*vs* N2)	P (*vs nhr-49;glp-1*)	P (*vs glp-1*)
AGP22	*nhr-49;glp-1*	72/72	11.27	0.26			
CF1903	*glp-1*	65/77	25.78	0.98		<0.0001	
AGP54	*nhr-49;glp-1 glmEx11 [Pcol-12::nhr-49::GFP + Pmyo-2::mCherry]*	28/42	21.06	1.36		<0.0001	0.0593
	Trial 2~						
AGP22	*nhr-49;glp-1*	125 / 142	9.96	0.07			
CF1903	*glp-1*	100 / 107	18.49	0.53		<0.0001	
AGP54	*nhr-49;glp-1 glmEx11 [Pcol-12::nhr-49::GFP + Pmyo-2::mCherry]*	118 / 136	16.61	0.13		<0.0001	0.0009

*, #, ^, $, & and ~ on different tabs/sub-sections of Table S3 denote trials performed at the same time
Underlined Trials shown in Fig. 3

Supplementary Table 2.4 a-e Impact of tissue-specific promoter-driven NHR-49 expression on *nhr-49* mutants' survival of PA14 or OP50.

Table S4a: Impact of endogenous promoter-driven NHR-49 expression on survival of *nhr-49* mutants on PA14 (a.1) and OP50 (a.2)

Table S4a.1: SURVIVAL ON PA14

Strain	Background/Genotype	Trial 1*			Bonferroni P-value	
		n = obs/ total	Mean (h)	SE +/-	P *(vs* N2)	P *(vs nhr-49)*
WT	Wildtype	125 / 155	67.25	1.86		
AGP12a	*nhr-49*	145 / 167	51.89	1.41	<0.0001	
AGP33	*nhr-49 glmEx5 [Pnhr-49::nhr-49::GFP + Pmyo-2::mCh]*	115 / 131	46.68	2.12	<0.0001	0.506
Trial 2#						
WT	Wildtype	93/150	68.58	2.05		
AGP12a	*nhr-49*	126/150	64.63	1.81	0.6022	
AGP33	*nhr-49 glmEx5 [Pnhr-49::nhr-49::GFP + Pmyo-2::mCh]*	87/100	74.96	3.35	0.7647	0.0101
Trial 3^						
WT	Wildtype	63/125	78.24	2.57		
AGP12a	*nhr-49*	99/127	58	1.44	<0.0001	
AGP33	*nhr-49 glmEx5 [Pnhr-49::nhr-49::GFP + Pmyo-2::mCh]*	87/127	94.98	3.08	0.002	<0.0001
Trial 4$						
WT	Wildtype	55/90	84.82	2.63		
AGP12a	*nhr-49*	102/113	60.24	1.52	0.0001	
AGP33	*nhr-49 glmEx5 [Pnhr-49::nhr-49::GFP + Pmyo-2::mCh]*	100/125	84.35	2.17	1	0.0001

Table S4a.2:SURVIVAL ON OP50

Strain	Background/Genotype	Trial 1@			Bonferroni P-value	
		n = obs/ total	Mean (h)	SE +/-	P *(vs* N2)	P *(vs nhr-49)*
WT	Wildtype	67/73	16.67	0.65		
AGP12a	*nhr-49*	33/77	14.39	0.69	0.1514	
AGP33	*nhr-49 glmEx5 [Pnhr-49::nhr-49::GFP + Pmyo-2::mCh]*	56/69	18.99	0.71	0.1646	0.0001
Trial 2&						
WT	Wildtype	89 / 122	15.42	0.49		
AGP12a	*nhr-49*	110 / 119	12.5	0.36	<0.0001	
AGP33	*nhr-49 glmEx5 [Pnhr-49::nhr-49::GFP + Pmyo-2::mCh]*	97 / 112	18	0.57	0.0424	<0.0001

*, #, ^, $, & on different tabs/sub-sections of Table S4 denote trials performed at the same time
Underlined Trials shown in Fig.4

Supplementary Table 2.4 (continued)

Table S4b: Impact of neuronal (*unc-119*) promoter-driven NHR-49 expression on survival of *nhr-49* mutants on PA14 (b.1) and OP50 (b.2)

Table S4b. 1: SURVIVAL ON PA14

Strain	Background/Genotype	Trial 1*			Bonferroni P-value	
		n = obs/ total	Mean (h)	SE +/-	P (*vs* N2)	P (*vs nhr-49*)
WT	Wildtype	125 / 155	67.25	1.86		
AGP12a	*nhr-49*	145 / 167	51.89	1.41	<0.0001	
AGP103a	*nhr-49 glmEx20 [Punc-119:: nhr-49::GFP + Pmyo-2::mCh]*	113 / 124	57.87	2.82	0.9996	0.0017
Trial 2#						
WT	Wildtype	93/150	68.58	2.05		
AGP12a	*nhr-49*	126/150	64.63	1.81	0.6022	
AGP103a	*nhr-49 glmEx20 [Punc-119:: nhr-49::GFP + Pmyo-2::mCh]*	86/130	77.42	3.34	<0.0001	0.0002
Trial 3^						
WT	Wildtype	63/125	78.24	2.57		
AGP12a	*nhr-49*	99/127	58	1.44	<0.0001	
AGP103a	*nhr-49 glmEx20 [Punc-119:: nhr-49::GFP + Pmyo-2::mCh]*	96/125	81.54	3.19	0.7738	<0.0001
Trial 4$						
WT	Wildtype	55/90	84.82	2.63		
AGP12a	*nhr-49*	102/113	60.24	1.52	0.0001	
AGP103a	*nhr-49 glmEx20 [Punc-119:: nhr-49::GFP + Pmyo-2::mCh]*	95/110	84.44	2.73	1	0.0001

Table S4b.2: SURVIVAL ON OP50

Strain	Background/Genotype	Trial 1@			Bonferroni P-value	
		n = obs/ total	Mean (h)	SE +/-	P (*vs* N2)	P (*vs nhr-49*)
WT	Wildtype	67/73	16.67	0.65		
AGP12a	*nhr-49*	33/77	14.39	0.69	0.1514	
AGP103a	*nhr-49 glmEx20 [Punc-119:: nhr-49::GFP + Pmyo-2::mCh]*	48/57	14.58	0.63	0.1326	1
Trial 2						
WT	Wildtype	74 / 91	24.2	0.55		
AGP12a	*nhr-49*	70 / 75	14.29	0.22	<0.0001	
AGP103a	*nhr-49 glmEx20 [Punc-119:: nhr-49::GFP + Pmyo-2::mCh]*	87 / 95	13.98	0.2	<0.0001	1
Trial 3						
WT	Wildtype	71 / 100	23.8	0.58		
AGP12a	*nhr-49*	41 / 72	9.23	0.31	<0.0001	
AGP103a	*nhr-49 glmEx20 [Punc-119:: nhr-49::GFP + Pmyo-2::mCh]*	73 / 91	15.37	0.57	<0.0001	<0.0001
Trial 4						
WT	Wildtype	71 / 82	17.99	0.58		
AGP12a	*nhr-49*	63 / 65	11.11	0.33	<0.0001	
AGP103a	*nhr-49 glmEx20 [Punc-119:: nhr-49::GFP + Pmyo-2::mCh]*	33 / 76	22.23	0.71	0.0006	0.0002

*, #, ^, $, & on different tabs/sub-sections of Table S4 denote trials performed at the same time

Underlined Trials shown in Fig.4

Supplementary Table 2.4 (continued)

Table S4c: Impact of intestinal (*gly-19*) promoter-driven NHR-49 expression on survival of *nhr-49* mutants on PA14 (c.1) and OP50 (c.2)

Table S4c. 1: SURVIVAL ON PA14

Strain	Background/Genotype	Trial 1*			Bonferroni P-value	
		n = obs/ total	Mean (h)	SE +/-	P *(vs* N2)	P *(vs nhr-49*)
WT	Wildtype	125 / 155	67.25	1.86		
AGP12a	*nhr-49*	145 / 167	51.89	1.41	<0.0001	
AGP65	*nhr-49 glmEx9 [Pgly-19:: nhr-49 ::GFP + Pmyo-2::mCh]*	107 / 132	50.82	2.14	<0.0001	1
	Trial 2#					
WT	Wildtype	93/150	68.58	2.05		
AGP12a	*nhr-49*	126/150	64.63	1.81	0.6022	
AGP65	*nhr-49 glmEx9 [Pgly-19:: nhr-49 ::GFP + Pmyo-2::mCh]*	89/150	73.78	2.92	1	0.0201
	Trial 3^					
WT	Wildtype	63/125	78.24	2.57		
AGP12a	*nhr-49*	99/127	58	1.44	<0.0001	
AGP65	*nhr-49 glmEx9 [Pgly-19:: nhr-49 ::GFP + Pmyo-2::mCh]*	87/125	77.6	2.73	1	<0.0001
	Trial 4$					
WT	Wildtype	55/90	84.82	2.63		
AGP12a	*nhr-49*	102/113	60.24	1.52	0.0001	
AGP65	*nhr-49 glmEx9 [Pgly-19:: nhr-49 ::GFP + Pmyo-2::mCh]*	100/116	75.5	2.37	0.2823	0.0001

Table S4c.2: Survival on SURVIVAL ON OP50

Strain	Background/Genotype	Trial 1@			Bonferroni P-value	
		n = obs/ total	Mean (h)	SE +/-	P *(vs* N2)	P *(vs nhr-49*)
WT	Wildtype	67/73	16.67	0.65		
AGP12a	*nhr-49*	33/77	14.39	0.69	0.1514	
AGP65	*nhr-49 glmEx9 [Pgly-19:: nhr-49 ::GFP + Pmyo-2::mCh]*	47/56	15.85	0.71	1	1
	Trial 2&					
WT	Wildtype	89 / 122	15.42	0.49		
AGP12a	*nhr-49*	110 / 119	12.5	0.36	<0.0001	
AGP65	*nhr-49 glmEx9 [Pgly-19:: nhr-49 ::GFP + Pmyo-2::mCh]*	97 / 118	15.25	0.4	1	<0.0001

*, #, ^, $, & on different tabs/sub-sections of Table S4 denote trials performed at the same time
Underlined Trials shown in Fig.4

Supplementary Table 2.4 (continued)

Table S4d: Impact of muscle (*myo-3*) promoter-driven NHR-49 expression on survival of *nhr-49* mutants on PA14 (d.1) and OP50 (d.2)

Table S4d. 1: SURVIVAL ON PA14

Strain	Background/Genotype	Trial 1*			Bonferroni P-value	
		n = obs/ total	Mean (h)	SE +/-	P *(vs* N2)	P *(vs nhr-49*)
WT	Wildtype	125 / 155	67.25	1.86		
AGP12a	*nhr-49*	145 / 167	51.89	1.41	<0.0001	
AGP63	*nhr-49 glmEx8 [Pmyo-3::nhr-49 ::GFP + Pmyo-2::mCh]*	137 / 153	44.92	1.55	<0.0001	0.0819
	Trial 2#					
WT	Wildtype	93/150	68.58	2.05		
AGP12a	*nhr-49*	126/150	64.63	1.81	0.6022	
AGP63	*nhr-49 glmEx8 [Pmyo-3::nhr-49 ::GFP + Pmyo-2::mCh]*	115/150	65.11	1.73	1	1
	Trial 3^					
WT	Wildtype	63/125	78.24	2.57		
AGP12a	*nhr-49*	99/127	58	1.44	<0.0001	
AGP63	*nhr-49 glmEx8 [Pmyo-3::nhr-49 ::GFP + Pmyo-2::mCh]*	91/126	68.06	1.59	0.0124	<0.0001
	Trial 4$					
WT	Wildtype	55/90	84.82	2.63		
AGP12a	*nhr-49*	102/113	60.24	1.52	0.0001	
AGP63	*nhr-49 glmEx8 [Pmyo-3::nhr-49 ::GFP + Pmyo-2::mCh]*	105/119	65.73	1.27	0.0001	0.0991

Table S4d.2: SURVIVAL ON OP50

Strain	Background/Genotype	Trial 1@			Bonferroni P-value	
		n = obs/ total	Mean (h)	SE +/-	P *(vs* N2)	P *(vs nhr-49*)
WT	Wildtype	67/73	16.67	0.65		
AGP12a	*nhr-49*	33/77	14.39	0.69	0.1514	
AGP63	*nhr-49 glmEx8 [Pmyo-3::nhr-49 ::GFP + Pmyo-2::mCh]*	73/75	11.84	0.54	0.0001	0.0893
	Trial 2&					
WT	Wildtype	89 / 122	15.42	0.49		
AGP12a	*nhr-49*	110 / 119	12.5	0.36	<0.0001	
AGP63	*nhr-49 glmEx8 [Pmyo-3::nhr-49 ::GFP + Pmyo-2::mCh]*	75 / 80	12.01	0.71	0.0001	1

*, #, ^, $, & on different tabs/sub-sections of Table S4 denote trials performed at the same time
Underlined Trials shown in Fig.4

Supplementary Table 2.4 (continued)

Table S4e: Impact of hypodermal (*col-12*) promoter-driven NHR-49 expression on survival of *nhr-49* mutants on PA14 (e.1) and OP50 (e.2)

Table S4e. 1: SURVIVAL ON PA14

Strain	Background/Genotype	Trial 1*			Bonferroni P-value	
		n = obs/ total	Mean (h)	SE +/-	P *(vs* N2)	P *(vs nhr 49)*
WT	Wildtype	125 / 155	67.25	1.86		
AGP12a	*nhr-49*	145 / 167	51.89	1.41	<0.0001	
AGP53	*nhr-49 glmEx11 [Pcol-12::nhr-49::GFP + Pmyo-2::mCh]*	138 / 150	30.21	1.77	<0.0001	<0.0001
Trial 2#						
WT	Wildtype	93/150	68.58	2.05		
AGP12a	*nhr-49*	126/150	64.63	1.81	0.6022	
AGP63	*nhr-49 glmEx8 [Pmyo-3::nhr-49::GFP + Pmyo-2::mCh]*	90/128	48.55	2.56	<0.0001	0.0001
Trial 3^						
WT	Wildtype	63/125	78.24	2.57		
AGP12a	*nhr-49*	99/127	58	1.44	<0.0001	
AGP53	*nhr-49 glmEx11 [Pcol-12::nhr-49::GFP + Pmyo-2::mCh]*	79/100	46.27	2.72	<0.0001	0.0415
Trial 4$						
WT	Wildtype	55/90	84.82	2.63		
AGP12a	*nhr-49*	102/113	60.24	1.52	0.0001	
AGP53	*nhr-49 glmEx11 [Pcol-12::nhr-49::GFP + Pmyo-2::mCh]*	28/32	48.62	4.65	0.0001	0.146

Table S4e.2: SURVIVAL ON OP50

Strain	Background/Genotype	Trial 1@			Bonferroni P-value	
		n = obs/ total	Mean (h)	SE +/-	P *(vs* N2)	P *(vs nhr 49)*
WT	Wildtype	67/73	16.67	0.65		
AGP12a	*nhr-49*	33/77	14.39	0.69	0.1514	
AGP53	*nhr-49 glmEx11 [Pcol-12::nhr-49::GFP + Pmyo-2::mCh]*	59/70	16.89	0.65	1	0.0926
Trial 2&						
WT	Wildtype	89 / 122	15.42	0.49		
AGP12a	*nhr-49*	110 / 119	12.5	0.36	<0.0001	
AGP53	*nhr-49 glmEx11 [Pcol-12::nhr-49::GFP + Pmyo-2::mCh]*	131 / 141	14.86	0.45	1	<0.0001

*, #, ^, $, & on different tabs/sub-sections of Table S4 denote trials performed at the same time
Underlined Trials shown in Fig.4

Supplementary Table 2.5 a-e Impact of tissue-specific promoter-driven NHR-49 overexpression on wild-type *C. elegans* survival of PA14 or OP50.

Table S5a: Impact of endogenous promoter-driven NHR-49 overexpression on survival of wild-type *C. elegans* on PA14 (a.1) and OP50 (a.2)

Table S5a. 1: SURVIVAL ON PA14

Strain	Background/Genotype	Trial 1*			Bonferroni P-value	Non-Bonferroni P-value
		n = obs/ total	Mean (h)	SE +/-		
WT	Wild type	126 / 145	54.32	1.09		
AGP24f	*glmEx5 [Pnhr-49::nhr-49::GFP + Pmyo-2::mCh]*	123 / 153	68.14	1.7	<0.0001	<0.0001
Trial 2#						
WT	Wild type	60 / 117	78.4	2.66		
AGP24f	*glmEx5 [Pnhr-49::nhr-49::GFP + Pmyo-2::mCh]*	61 / 110	71.05	3.78	0.229	0.0286
Trial 3^						
WT	Wild type	102 / 129	76.98	2.25		
AGP24f	*glmEx5 [Pnhr-49::nhr-49::GFP + Pmyo-2::mCh]*	75 / 121	76.89	3.06	1	0.895

Table S5a.2: SURVIVAL ON OP50

Strain	Background/Genotype	Trial 1@			Bonferroni P-value (*vs* N2)	Non-Bonferroni P (*vs* N2)
		n = obs/ total	Mean (h)	SE +/-		
WT	Wild type	67 / 73	16.67	0.65		
AGP12a	*nhr-49*	33 / 77	14.39	0.69	0.1514	
AGP24f	*glmEx5 [Pnhr-49::nhr-49::GFP + Pmyo-2::mCh]*	35 / 44	20.83	1.01	0.0109	0.0016
Trial 2~						
WT	Wild type	73 / 121	17.81	0.56		
AGP12a	*nhr-49*	69 / 76	14.6	0.54	0.0003	
AGP24f	*glmEx5 [Pnhr-49::nhr-49::GFP + Pmyo-2::mCh]*	70 / 115	17.58	0.75	1	0.603

*, #, ^, &, @, ~ on different tabs/sub-sections of Table S5 denote trials performed at the same time
Underlined Trials shown in Fig. 5

Supplementary Table 2.5 (continued)

Table S5b: Impact of neuronal (*unc-119*) promoter-driven NHR-49 overexpression on survival of wild-type *C. elegans* on PA14 (b.1) and OP50 (b.2)

Table S5B. 1: SURVIVAL ON PA14

Strain	Background/Genotype	Trial 1*			Bonferroni P-value	Non-Bonferroni P-value
		n = obs/ total	Mean (h)	SE +/-		
WT	Wild type	126 / 145	54.32	1.09		
AGP102	*glmEx20 [Pnhr-49::unc-119::GFP + Pmyo-2::mCh]*	114 / 136	73.72	1.61	<0.0001	<0.0001
Trial 2#						
WT	Wild type	60 / 117	78.4	2.66		
AGP102	*glmEx20 [Pnhr-49::unc-119::GFP + Pmyo-2::mCh]*	88/120	70.79	2.11	0.093	0.0116
Trial 3^						
WT	Wild type	102 / 129	76.98	2.25		
AGP102	*glmEx20 [Pnhr-49::unc-119::GFP + Pmyo-2::mCh]*	96/127	86.37	2.44	0.0333	0.0135

Table S5B.2: SURVIVAL ON OP50

Strain	Background/Genotype	Trial 1@			Bonferroni P-value	Non-Bonferroni P-value
		n = obs/ total	Mean (h)	SE +/-		
WT	Wild type	67 / 73	16.67	0.65		
AGP102	*glmEx20 [Pnhr-49::unc-119::GFP + Pmyo-2::mCh]*	39/57	19.31	0.75	0.0651	0.0093
Trial 2						
WT	Wild type	74 / 91	24.2	0.55		
AGP102	*glmEx20 [Pnhr-49::unc-119::GFP + Pmyo-2::mCh]*	57 / 94	22.35	0.6	0.4163	0.0416
Trial 3						
WT	Wild type	71 / 100	23.8	0.58		
AGP102	*glmEx20 [Pnhr-49::unc-119::GFP + Pmyo-2::mCh]*	40 / 71	21.53	0.81	0.074	0.0092
Trial 4						
WT	Wildtype	71 / 82	17.99	0.58		
AGP102	*glmEx20 [Pnhr-49::unc-119::GFP + Pmyo-2::mCh]*	32 / 70	23.23	0.97	<0.0001	<0.0001

*, #, ^, &, @, ~ on different tabs/sub-sections of Table S5 denote trials performed at the same time
Underlined Trials shown in Fig. 5

Supplementary Table 2.5 (continued)

Table S5c: Impact of Intestinal (*gly-19*) promoter-driven NHR-49 overexpression on survival of wild-type *C. elegans* on PA14 (c.1) or OP50 (c.2)

Table S5c. 1: SURVIVAL ON PA14

Strain	Background/Genotype	Trial 1*			Bonferroni P-value	Non-Bonferroni P-value
		n = obs/ total	Mean (h)	SE +/-		
WT	Wild type	126 / 145	54.32	1.09		
AGP40	*glmEx9 [Pgly-19::nhr-49::GFP + Pmyo-2::mCherry]*	117 / 131	73.6	1.83	<0.0001	<0.0001
Trial 2#						
WT	Wild type	60/117	78.4	2.66		
AGP40	*glmEx9 [Pgly-19::nhr-49::GFP + Pmyo-2::mCherry]*	92/128	94.83	2.72	0.0007	0.0001
Trial 3^						
WT	Wildtype	102/129	76.98	2.25		
AGP40	*glmEx9 [Pgly-19::nhr-49::GFP + Pmyo-2::mCherry]*	96/124	91.97	2.65	0.0002	0.0001

Table S5c.2: SURVIVAL ON OP50

Strain	Background Genotype	Trial 1@			Bonferroni P-value (*vs* N2)	Non-Bonferroni P (*vs* N2)
		n = obs/ total	Mean (days)	SE +/-		
WT	Wild type	67/73	16.67	0.65		
AGP12a	*nhr-49*	33/77	14.39	0.69	0.1514	
AGP40	*glmEx9 [Pgly-19::nhr-49::GFP + Pmyo-2::mCherry]*	64/67	18.49	0.82	0.6491	0.0927
Trial 2~						
WT	Wild type	73 / 121	17.81	0.56		
AGP12a	*nhr-49*	69 / 76	14.6	0.54	0.0003	
AGP40	*glmEx9 [Pgly-19::nhr-49::GFP + Pmyo-2::mCherry]*	86 / 116	19.06	0.4	1	0.202

*, #, ^, &, @, ~ on different tabs/sub-sections of Table S5 denote trials performed at the same time
Underlined Trials shown in Fig. 5

Supplementary Table 2.5 (continued)

Table S5d: Impact of muscle (*myo-3*) promoter-driven NHR-49 overexpression on survival of wild-type *C. elegans* on PA14 (d.1) or OP50 (d.2)

Table S5d. 1: SURVIVAL ON PA14

Strain	Background/Genotype	Trial 1*			Bonferroni P-value	Non-Bonferroni P-value
		n = obs/ total	Mean (h)	SE +/-		
WT	Wild type	126 / 145	54.32	1.09		
AGP27	*glmEx9 [Pmyo-3::nhr-49 ::GFP + Pmyo-2::mCherry]*	106 / 126	61.12	2.11	0.0007	0.0001
	Trial 2#					
WT	Wild type	60/117	78.4	2.66		
AGP27	*glmEx9 [Pmyo-3::nhr-49 ::GFP + Pmyo-2::mCherry]*	61/100	72.85	4.25	1	0.289
	Trial 3^					
WT	Wild type	102/129	76.98	2.25		
AGP27	*glmEx9 [Pmyo-3::nhr-49 ::GFP + Pmyo-2::mCherry]*	66/100	72.11	4.28	1	0.363

Table S5d.2: SURVIVAL ON OP50

Strain	Background Genotype	Trial 1@			Bonferroni P-value (*vs* N2)	Non-Bonferroni P (*vs* N2)
		n = obs/ total	Mean (days)	SE +/-		
WT	Wild type	67/73	16.67	0.65		
AGP12a	*nhr-49*	33/77	14.39	0.69	0.1514	
AGP27	*glmEx9 [Pmyo-3::nhr-49 ::GFP + Pmyo-2::mCherry]*	39/52	14.6	0.55	0.5331	0.0762
	Trial 2~					
WT	Wild type	73 / 121	17.81	0.56		
AGP12a	*nhr-49*	69 / 76	14.6	0.54	0.0003	
AGP27	*glmEx9 [Pmyo-3::nhr-49 ::GFP + Pmyo-2::mCherry]*	84 / 109	19.89	0.68	0.0389	0.0065

*, #, ^, &, @, ~ on different tabs/sub-sections of Table S5 denote trials performed at the same time
Underlined Trials shown in Fig. 5

Supplementary Table 2.5 (continued)

Table S5e: Impact of hypodermal *(col-12)* promoter-driven NHR-49 overexpression on survival of wild-type *C. elegans* on PA14 (e.1) or OP50 (e.2)

Table S5e. 1: SURVIVAL ON PA14

Strain	Background/Genotype	Trial 1*			Bonferroni P-value	Non-Bonferroni P-value
		n = obs/ total	Mean (h)	SE +/-		
WT	Wild type	126 / 145	54.32	1.09		
AGP45	*glmEx11 [Pcol-12::nhr-49::GFP + Pmyo-2::mCherry]*	117 / 137	77.16	1.44	<0.0001	<0.0001
Trial 2#						
WT	Wild type	60/117	78.4	2.66		
AGP45	*glmEx11 [Pcol-12::nhr-49::GFP + Pmyo-2::mCherry]*	77/125	85.91	3.67	1	0.326
Trial 3^						
WT	Wildtype	102/129	76.98	2.25		
AGP45	*glmEx11 [Pcol-12::nhr-49::GFP + Pmyo-2::mCherry]*	63/97	82.68	2.65	0.3504	0.013

Table S5e.2: SURVIVAL ON OP50

Strain	Background Genotype	Trial 1@			Bonferroni P-value (*vs* N2)	Non-Bonferroni P (*vs* N2)
		n = obs/ total	Mean (days)	SE +/-		
WT	Wild type	67/73	16.67	0.65		
AGP12a	*nhr-49*	33/77	14.39	0.69	0.1514	
AGP45	*glmEx11 [Pcol-12::nhr-49::GFP + Pmyo-2::mCherry]*	57/66	17.27	0.67	1	0.4482
Trial 2~						
WT	Wild type	73 / 121	17.81	0.56		
AGP12a	*nhr-49*	69 / 76	14.6	0.54	0.0003	
AGP45	*glmEx11 [Pcol-12::nhr-49::GFP + Pmyo-2::mCherry]*	95 / 120	18.3	0.53	1	0.468

*, #, ^, &, @, ~ on different tabs/sub-sections of Table S5 denote trials performed at the same time

Underlined Trials shown in Fig. 5

Supplementary Table 2.6 (a) Impact of tissue-specific expression of *nhr-49(et7)* on survival of PA14 or OP50; (b) Impact of Fenofibrate supplementation on PA14 survival of *nhr-49* mutants expressing NHR-49 in muscles or hypodermis.

Table S6a: Impact of tissue-specific expression of *nhr-49(et7)* on survival on PA14 (a.1) and lifespan on OP50 (a.2)

Table S6a.1: SURVIVAL ON PA14

Tissue of Expression	Background / Genotype	Trial 1#			Bonferroni P-value	
		n = obs/ total	Mean (h)	SE +/-	P (vs N2)	P (vs *nhr-49*)
	Wildtype	87 / 150	77.36	1.79		
	nhr-49(nr2041) lof	116 / 150	62.34	1.07	<0.0001	
Neurons	*Punc-119::nhr-49(et7)::GFP + Pmyo-2::mCherry*	68 / 125	67.18	1.46	0.0003	0.026
Hypodermis	*Pcol-12::nhr-49(et7)::GFP + Pmyo-2::mCherry*	73 / 125	74.5	2.4	1	<0.0001
Neurons	*nhr-49;[Punc-119::nhr-49(et7)::GFP + Pmyo-2::mCherry]*	72 / 115	63.45	1.57	<0.0001	1
Trial 2~						
	Wildtype	94 / 120	75.16	2.74		
	nhr-49(nr2041) lof	117 / 130	53.73	1.54	<0.0001	
Neurons	*Punc-119::nhr-49(et7)::GFP + Pmyo-2::mCherry*	98 / 125	62.92	1.59	0.0017	0.0037
Hypodermis	*Pcol-12::nhr-49(et7)::GFP + Pmyo-2::mCherry*	118 / 145	55.46	2.11	<0.0001	1
Neurons	*nhr-49;[Punc-119::nhr-49(et7)::GFP + Pmyo-2::mCherry]*	123 / 136	58.22	1.12	<0.0001	0.59
Trial 3$						
	Wildtype	78 / 106	67.46	2.15		
	nhr-49(nr2041) lof	94 / 105	52.23	1.69	> 0.0001	
Neurons	*Punc-119::nhr-49(et7)::GFP + Pmyo-2::mCherry*	73 / 107	57.15	1.71	0.0002	0.0197
Hypodermis	*Pcol-12::nhr-49(et7)::GFP + Pmyo-2::mCherry*	69 / 105	60.24	2.22	0.0647	0.0013
Neurons	*nhr-49;[Punc-119::nhr-49 (et7)::GFP + Pmyo-2::mCherry]*	89 / 111	61.77	1.71	0.0316	> 0.0001

Table S6a.2: SURVIVAL ON OP50

Tissue of Expression	Background / Genotype	Trial 1◇			Bonferroni P-value	
		n = obs/ total	Mean (h)	SE +/-	P (vs N2)	P (vs *nhr-49*)
	Wildtype	99 / 120	15.61	0.46		
	nhr-49(nr2041) lof	101 / 119	7.66	0.2	< 0.0001	
Neurons	*Punc-119::nhr-49(et7)::GFP + Pmyo-2::mCherry*	61 / 80	12.63	0.76	0.023	< 0.0001
Hypodermis	*Pcol-12::nhr-49(et7)::GFP + Pmyo-2::mCherry*	82 / 100	11.11	0.63	< 0.0001	< 0.0001
Neurons	*nhr-49;[Punc-119::nhr-49(et7)::GFP + Pmyo-2::mCherry]*	69 / 89	9.31	0.38	< 0.0001	0.0004
Trial 2†						
	Wildtype	103 / 136	16.49	0.44		
	nhr-49(nr2041) lof	119 / 130	7.31	0.18	< 0.0001	
Neurons	*Punc-119::nhr-49(et7)::GFP + Pmyo-2::mCherry*	28 / 60	10.23	0.74	< 0.0001	< 0.0001
Hypodermis	*Pcol-12::nhr-49(et7)::GFP + Pmyo-2::mCherry*	60 / 90	9.09	0.53	< 0.0001	0.0003
Neurons	*nhr-49;[Punc-119::nhr-49(et7)::GFP + Pmyo-2::mCherry]*	98 / 134	8.75	0.23	< 0.0001	< 0.0001

Special characters #, ~, $, ◇, † on trial headings denote the trial was performed at the same time as correspondingly-labeled trials in Table S2A. Underlined Trials shown in Fig. 6.

Supplementary Table 2.6 (continued)

Table S6b: Impact of Fenofibrate supplementation on PA14 survival of *nhr-49* mutants expressing NHR-49 in muscles (*myo-3*) or hypodermis (*col-12*)

SURVIVAL ON PA14						
Tissue of Expression	Genotype	Treatment	Trial 1			Bonferroni P value
			n = obs/ total	Mean (h)	SE +/-	P (vs Control)
Muscle	*nhr-49;[Pmyo-3::nhr-49::GFP + Pmyo-2::mCherry]*	Control	62 / 88	57.88	1.55	
		Fenofibrate	66 / 100	59.35	1.36	1
Hypodermis	*nhr-49;[Pcol-12::nhr-49::GFP + Pmyo-2::mCherry]*	Control	100 / 133	63.59	0.93	
		Fenofibrate	111 / 135	62.56	1.07	1
Trial 2						
Muscle	*nhr-49;[Pmyo-3::nhr-49::GFP + Pmyo-2::mCherry]*	Control	57 / 71	52.76	1.48	
		Fenofibrate	117 / 120	55.35	1.29	0.6649
Hypodermis	*nhr-49;[Pcol-12::nhr-49::GFP + Pmyo-2::mCherry]*	Control	94 / 120	61.2	1.37	
		Fenofibrate	89 / 105	64.22	1.24	1
Trial 3						
Muscle	*nhr-49;[Pmyo-3::nhr-49::GFP + Pmyo-2::mCherry]*	Control	43 / 45	60.47	2.38	
		Fenofibrate	54 / 58	66.54	1.53	0.6314
Hypodermis	*nhr-49;[Pcol-12::nhr-49::GFP + Pmyo-2::mCherry]*	Control	63 / 81	68.34	1.46	
		Fenofibrate	126 / 154	68.89	1.07	1
Trial 4						
Muscle	*nhr-49;[Pmyo-3::nhr-49::GFP + Pmyo-2::mCherry]*	Control	132 / 150	60.41	1.07	
		Fenofibrate	127 / 149	59.22	1	1
Hypodermis	*nhr-49;[Pcol-12::nhr-49::GFP + Pmyo-2::mCherry]*	Control	114 / 152	61.42	1.42	
		Fenofibrate	130 / 151	58.43	1.03	1
Trial 5						
Muscle	*nhr-49;[Pmyo-3::nhr-49::GFP + Pmyo-2::mCherry]*	Control	135/150	55.43	1.08	
		Fenofibrate	124/153	52.82	1.05	0.9918
Hypodermis	*nhr-49;[Pcol-12::nhr-49::GFP + Pmyo-2::mCherry]*	Control	112/151	55.04	1.24	
		Fenofibrate	120/150	53.38	1.12	1

Supplementary Table 2.7 a-e Impact of tissue-specific promoter-driven NHR-49 expression on *glp-1* mutant's survival of PA14 or OP50.

Table S7a: Impact of endogenous promoter-driven NHR-49 expression on survival of *glp-1* mutants on PA14 (a.1) and OP50 (a.2)

Table S7a. 1: SURVIVAL ON PA14

Strain	Background/Genotype	Trial 1*			Bonferroni P-value	
		n = obs/ total	Mean (h)	SE +/-	P *(vs* N2)	P *(vs glp-1)*
WT	Wildtype	83 / 105	67.31	1.37		
CF1903	*glp-1*	116 / 127	83.68	2.04	<0.0001	
AGP29	*glp-1 glmEx6 [Pnhr-49::nhr-49 ::GFP + Pmyo-2::mCh]*	105 / 112	38.6	1.57	<0.0001	<0.0001
Trial 2#						
WT	Wildtype	61/112	72.21	3.63		
CF1903	*glp-1*	95/109	88.89	2.57	0.001	
AGP29	*glp-1 glmEx6 [Pnhr-49::nhr-49 ::GFP + Pmyo-2::mCh]*	98/115	44.15	1.92	<0.0001	<0.0001
Trial 3^						
WT	Wildtype	68 / 120	68.39	2.2		
CF1903	*glp-1*	102 / 117	94.91	3.2	0.0001	
AGP29	*glp-1 glmEx6 [Pnhr-49::nhr-49 ::GFP + Pmyo-2::mCh]*	94 / 105	39.35	1.56	0.0001	0.0001
Trial 4						
WT	Wildtype	88 / 128	92.05	1.99		
CF1903	*glp-1*	101 / 131	106.42	2.74	0.0004	
AGP29	*glp-1 glmEx6 [Pnhr-49::nhr-49 ::GFP + Pmyo-2::mCh]*	132 / 156	53.58	2.18	<0.0001	<0.0001

Table S7a.2: SURVIVAL ON OP50

Strain	Background/Genotype	Trial 1@			Bonferroni P-value	
		n = obs/ total	Mean (h)	SE +/-	P *(vs* N2)	P *(vs glp-1)*
AGP22	*nhr-49;glp-1*	72/72	11.27	0.26		<0.0001
CF1903	*glp-1*	65/77	25.78	0.98		
AGP29	*glp-1 glmEx6 [Pnhr-49::nhr-49 ::GFP + Pmyo-2::mCh]*	13/14	22.62	1.85		0.0755
Trial 2~						
WT	Wildtype	82 / 122	15.53	0.58		
CF1903	*glp-1*	112 / 124	22.98	0.67	<0.0001	
AGP29	*glp-1 glmEx6 [Pnhr-49::nhr-49 ::GFP + Pmyo-2::mCh]*	94 / 108	21.31	0.42	<0.0001	0.003
Trial 3$						
WT	Wildtype	73 / 121	17.81	0.56		
CF1903	*glp-1*	101 / 114	23.35	0.69	<0.0001	
AGP29	*glp-1 glmEx6 [Pnhr-49::nhr-49 ::GFP + Pmyo-2::mCh]*	55 / 120	21.71	0.53	<0.0001	0.3082

Special characters *, #, ^, &, @, ~ on different tabs/sub-sections of Table S7 denote trials performed at the same time. Underlined Trials shown in Fig. S5

Supplementary Table 2.7 (continued)

Table S7b: Impact of neuronal (*unc-119*) promoter-driven NHR-49 expression on survival of *glp-1* mutants on PA14 (b.1) and OP50 (b.2)

Table S7a.1: SURVIVAL ON PA14

Strain	Background/Genotype	Trial 1*			Bonferroni P-value	
		n = obs/ total	Mean (h)	SE +/-	P *(vs* N2)	P *(vs glp 1*)
WT	Wildtype	83 / 105	67.31	1.37		
CF1903	*glp-1*	116 / 127	83.68	2.04	<0.0001	
AGP105	*glp-1 glmEx20 [Punc-119::nhr-49::GFP + Pmyo-2::mCh]*	97 / 117	70.81	2.96	0.0174	0.242
Trial 2#						
WT	Wildtype	61/112	72.21	3.63		
CF1903	*glp-1*	95/109	88.89	2.57	0.001	
AGP105	*glp-1 glmEx20 [Punc-119::nhr-49::GFP + Pmyo-2::mCh]*	111/120	59.86	3.3	0.1603	<0.0001
Trial 3^						
WT	Wildtype	68 / 120	68.39	2.2		
CF1903	*glp-1*	102 / 117	94.91	3.2	0.0001	
AGP105	*glp-1 glmEx20 [Punc-119::nhr-49::GFP + Pmyo-2::mCh]*	73 / 80	73.22	4.93	1	0.0582

Table S7b.2: SURVIVAL ON OP50

Strain	Background/Genotype	Trial 1			Bonferroni P-value	
		n = obs/ total	Mean (h)	SE +/-	P *(vs* N2)	P *(vs glp 1*)
WT	Wildtype	52/71	16.26	0.91		
CF1903	*glp-1*	51/70	24.43	1.08	<0.0001	
AGP105	*glp-1 glmEx20 [Punc-119::nhr-49::GFP + Pmyo-2::mCh]*	29 / 42	21.78	1.86	0.01	1
Trial 2						
WT	Wildtype	74 / 91	24.2	0.55		
CF1903	*glp-1*	120 / 124	30.54	0.79	<0.0001	
AGP105	*glp-1 glmEx20 [Punc-119::nhr-49::GFP + Pmyo-2::mCh]*	70 / 80	31.4	1.1	<0.0001	1
Trial 3						
WT	Wildtype	71 / 100	23.8	0.58		
CF1903	*glp-1*	83 / 84	22.58	1.06	1	
AGP105	*glp-1 glmEx20 [Punc-119::nhr-49::GFP + Pmyo-2::mCh]*	51 / 63	26.69	0.74	0.1157	1
Trial 4						
WT	Wildtype	71 / 82	17.99	0.58		
CF1903	*glp-1*	109 / 121	24.25	0.91	<0.0001	
AGP105	*glp-1 glmEx20 [Punc-119::nhr-49::GFP + Pmyo-2::mCh]*	99 / 120	28.14	0.89	<0.0001	0.38

Special characters *, #, ^, &, @, ~ on different tabs/sub-sections of Table S7 denote trials performed at the same time. Underlined Trials shown in Fig. S5

Supplementary Table 2.7 (continued)

Table S7c: Impact of intestinal (*gly-19*) promoter-driven NHR-49 expression on survival of *glp-1* mutants on PA14 (c.1) and OP50 (c.2)

Table S7c. 1: SURVIVAL ON PA14

Strain	Background/Genotype	Trial 1*			Bonferroni P-value	
		n = obs/ total	Mean (h)	SE +/-	P *(vs* N2)	P *(vs glp 1)*
WT	Wildtype	83 / 105	67.31	1.37		
CF1903	*glp-1*	116 / 127	83.68	2.04	<0.0001	
AGP44	*glp-1 glmEx10 [Pgly-19::nhr-49::GFP + Pmyo-2::mCh]*	89 / 108	80.91	2.67	<0.0001	1
Trial 2#						
WT	Wildtype	61/112	72.21	3.63		
CF1903	*glp-1*	95/109	88.89	2.57	0.001	
AGP44	*glp-1 glmEx10 [Pgly-19::nhr-49::GFP + Pmyo-2::mCh]*	106/120	69.98	2.52	1	<0.0001
Trial 3^						
WT	Wildtype	68 / 120	68.39	2.2		
CF1903	*glp-1*	102 / 117	94.91	3.2	0.0001	
AGP44	*glp-1 glmEx10 [Pgly-19::nhr-49::GFP + Pmyo-2::mCh]*	97 / 115	82.13	2.71	0.0044	0.0086

Table S7c.2: SURVIVAL ON OP50

Strain	Background/Genotype	Trial 1@			Bonferroni P-value	
		n = obs/ total	Mean (h)	SE +/-	P *(vs* N2)	P *(vs glp 1)*
AGP22	*nhr-49;glp-1*	72/72	11.27	0.26		<0.0001
CF1903	*glp-1*	65/77	25.78	0.98		
AGP44	*glp-1 glmEx10 [Pgly-19::nhr-49::GFP + Pmyo-2::mCh]*	26/27	20.06	1.09		0.0003
Trial 2~						
WT	Wildtype	82 / 122	15.53	0.58		
CF1903	*glp-1*	112 / 124	22.98	0.67	<0.0001	
AGP44	*glp-1 glmEx10 [Pgly-19::nhr-49::GFP + Pmyo-2::mCh]*	105 / 122	20.69	0.44	<0.0001	0.0002
Trial 3$						
WT	Wildtype	73 / 121	17.81	0.56		
CF1903	*glp-1*	101 / 114	23.35	0.69	<0.0001	
AGP44	*glp-1 glmEx10 [Pgly-19::nhr-49::GFP + Pmyo-2::mCh]*	101 / 116	20.93	0.41	0.0004	0.0004

Special characters *, #, ^, &, @, ~ on different tabs/sub-sections of Table S7 denote trials performed at the same time. Underlined Trials shown in Fig. S5

Supplementary Table 2.7 (continued)

Table S7d: Impact of muscle (*myo-3*) promoter-driven NHR-49 expression on survival of *glp-1* mutants on PA14 (d.1) and OP50 (d.2)

Table S7d. 1: SURVIVAL ON PA14

Strain	Background/Genotype	Trial 1*			Bonferroni P-value	
		n = obs/ total	Mean (h)	SE +/-	P *(vs* N2)	P *(vs glp-1*)
WT	Wildtype	83 / 105	67.31	1.37		
CF1903	*glp-1*	116 / 127	83.68	2.04	<0.0001	
AGP36	*glp-1 glmEx7 [Pmyo-3::nhr-49::GFP + Pmyo-2::mCh]*	96 / 118	73.05	2.12	0.0378	0.0107
Trial 2#						
WT	Wildtype	61/112	72.21	3.63		
CF1903	*glp-1*	95/109	88.89	2.57	0.001	
AGP36	*glp-1 glmEx7 [Pmyo-3::nhr-49::GFP + Pmyo-2::mCh]*	110/120	80.21	2.84	0.3629	0.6544
Trial 3^						
WT	Wildtype	68 / 120	68.39	2.2		
CF1903	*glp-1*	102 / 117	94.91	3.2	0.0001	
AGP36	*glp-1 glmEx7 [Pmyo-3::nhr-49::GFP + Pmyo-2::mCh]*	110 / 120	88.62	2.93	<0.0001	0.747

Table S7d.2: SURVIVAL ON OP50

Strain	Background/Genotype	Trial 1@			Bonferroni P-value	
		n = obs/ total	Mean (h)	SE +/-	P *(vs* N2)	P *(vs glp-1*)
AGP22	*nhr-49;glp-1*	72/72	11.27	0.26		<0.0001
CF1903	*glp-1*	65/77	25.78	0.98		
AGP36	*glp-1 glmEx7 [Pmyo-3::nhr-49::GFP + Pmyo-2::mCh]*	46/83	24.65	0.98		1
Trial 2$						
WT	Wildtype	73 / 121	17.81	0.56		
CF1903	*glp-1*	101 / 114	23.35	0.69	<0.0001	
AGP36	*glp-1 glmEx7 [Pmyo-3::nhr-49::GFP + Pmyo-2::mCh]*	104 / 121	21.89	0.55	<0.0001	0.3937

Special characters *, #, ^, &, @, ~ on different tabs/sub-sections of Table S7 denote trials performed at the same time. Underlined Trials shown in Fig. S5

Supplementary Table 2.7 (continued)

Table S7e: Impact of hypodermal (*col-12*) promoter-driven NHR-49 expression on survival of *glp-1* mutants on PA14 (e.1) and OP50 (e.2)

Table S7e.1: SURVIVAL ON PA14

Strain	Background/Genotype	Trial 1*			Bonferroni P-value	
		n = obs/ total	Mean (h)	SE +/-	P *(vs* N2)	P *(vs glp-1*)
WT	Wildtype	83 / 105	67.31	1.37		
CF1903	*glp-1*	116 / 127	83.68	2.04	<0.0001	
AGP41	*glp-1 glmEx11 [Pcol-12::nhr-49::GFP + Pmyo-2::mCh]*	80 / 98	69.92	2.58	0.0674	0.009
	Trial 2#					
WT	Wildtype	61/112	72.21	3.63		
CF1903	*glp-1*	95/109	88.89	2.57	0.001	
AGP36	*glp-1 glmEx7 [Pmyo-3::nhr-49::GFP + Pmyo-2::mCh]*	12./13	79.72	9.95	1	1
	Trial 3^					
WT	Wildtype	68 / 120	68.39	2.2		
CF1903	*glp-1*	102 / 117	94.91	3.2	0.0001	
AGP41	*glp-1 glmEx11 [Pcol-12::nhr-49::GFP + Pmyo-2::mCh]*	47 / 60	65.17	4.78	1	<0.0001

Table S7e.2: SURVIVAL ON OP50

Strain	Background/Genotype	Trial 1@			Bonferroni P-value	
		n = obs/ total	Mean (h)	SE +/-	P *(vs* N2)	P *(vs glp-1*)
AGP22	*nhr-49;glp-1*	72/72	11.27	0.26		<0.0001
CF1903	*glp-1*	65/77	25.78	0.98		
AGP41	*glp-1 glmEx11 [Pcol-12::nhr-49::GFP + Pmyo-2::mCh]*	28/42	24.06	0.83		0.0611
	Trial 2$					
WT	Wildtype	73 / 121	17.81	0.56		
CF1903	*glp-1*	101 / 114	23.35	0.69	<0.0001	
AGP41	*glp-1 glmEx11 [Pcol-12::nhr-49::GFP + Pmyo-2::mCh]*	84 / 102	23.79	0.54	<0.0001	1

Special characters *, #, ^, &, @, ~ on different tabs/sub-sections of Table S7 denote trials performed at the same time. Underlined Trials shown in Fig. S5

Supplementary Table 2.8 Comparison of lipid-catabolic genes regulated by NHR-49 in *glp-1* mutants and upon PA14 infection.

Lipolysis Process	Gene	Wormbase Gene ID	Impact of Germline Loss [dependence on DAF-16 (D16), TCER-1 (T1) *(Amrit et al., 2016)* &/or NHR-49 (N49 *(Ratnappan et al., 2014)*]	Studies documenting PA14-induced gene-expression changes			
				Troemel et al., 2006	*Dasgupta et al., 2020* (only UP reported)	*Twumasi-Boateng & Shapira, 2012*	*Fletcher et al., 2019*
Mitochondrial β-oxidation	*acs-2*	WBGene00009221	UP (D16, T1, N49)	UP	UP		
	acs-22	WBGene00017012	UP (T1, N49)				DOWN
	cpt-5	WBGene00008629	UP (N49)				DOWN
	acdh-1	WBGene00016943	UP (N49)	DOWN	DOWN		DOWN
	acdh-2	WBGene00015894	UP (N49)				DOWN
	acdh-9	WBGene00017874	DOWN (T1, N49)				
	acdh-11	WBGene00012860	UP (T1, N49)				DOWN
	ech-1.1	WBGene00001150	UP (N49)				
	ech-7	WBGene00001156	UP (D16, T1, N49)				DOWN
	hacd-1	WBGene00019978	UP (D16, T1, N49)	DOWN		DOWN	DOWN
	B0272.3	WBGene00007129	UP (N49)				
	acaa-2	WBGene00009952	UP (D16, T1, N49)				DOWN
	kat-1	WBGene00002183	UP (N49)				DOWN
Peroxisomal β-Oxidation	*F08A8.2*	WBGene00008565	UP (D16, T1, N49)	DOWN			
	F08A8.3	WBGene00008566	UP (T1, N49)	DOWN		DOWN	
	F08A8.4/a	WBGene00008567	UP (T1, N49)	DOWN		DOWN	
	acox-1.1	WBGene00008564	UP (D16, T1, N49)	UP	UP	UP	UP
	ech-9	WBGene00001158	DOWN (N49)	UP	UP	UP	UP
Lipases and Lipase-like Proteins	*lipl-1*	WBGene00010062	UP (D16, T1, N49)	UP	UP		UP
	lipl-2	WBGene00009773	UP (D16, T1, N49)		UP		
	lipl-3	WBGene00020016	UP (N49)				DOWN
	lipl-4	WBGene00019376	UP (N49)				
	lipl-5	WBGene00022642	UP (D16, T1, N49)	DOWN		DOWN	DOWN
	lipl-6	WBGene00021963	UP (N49)				
	lips-5	WBGene00011725	UP (N49)				UP
	lips-14	WBGene00019208	UP (D16, T1, N49)	DOWN			DOWN
	lips-17	WBGene00019939	UP (N49)				
	fil-1	WBGene00011321	DOWN (N49)	UP	UP		UP

UP: Gene upregulated; DOWN: Gene downregulated; Genes similarly changed in *glp-1* vs. PA14 are highlighted in green and oppositely changes ones in red.

Supplementary Table 2.9 Impact of RNAi knockdown on NHR-49-target lipid-metabolic genes and partner NHRs on survival of wildtype animals on PA14

RNAi treatment	Trial 1			P-value
	n = obs/ total	Mean (h)	SE +/-	P (*vs* Control)
Control	100 / 130	63.8	1.51	
nhr-80	82 / 131	57.9	1.35	0.003
nhr-71	111 / 143	70.1	1.55	0.005
nhr-13	104 / 124	61.14	1.19	0.093
acox-1.1	99 / 114	66.81	1.13	0.445
hacd-1	89 / 133	61.39	1.31	0.147
Trial 2				
Control	96 / 125	65.56	1.26	
nhr-80	103 / 125	62.2	1.26	0.062
nhr-71	88 / 125	67.6	1.57	0.188
nhr-13	95 / 125	65.89	1.16	0.909
acox-1.1	95 / 105	66.45	1.57	0.475
hacd-1	88 / 107	70.05	1.88	0.016

Supplementary Table 2.10 Strains used in this study

Strain	Genotype	Source
N2	Wild type, Ghazi Lab	
CF1903	*glp-1(e2144ts)*	
AGP12a	*nhr-49(nr2041)I* Outcrossed Ghazi Lab N2 3x	
AGP22	*nhr-49(nr2041)I; glp-1(e2141ts)III*	
AGP110	*nhr-49(et7).* Outcrossed *nhr-49(et7)* to Ghazi Lab N2 4x	This study
VC1668	*fmo-2(ok2147)*	CGC
RB1899	*acs-2 (ok2457)*	CGC
EB271	*fmo-2p::gfp + rol-6(su1006)*	CGC
WBM170	*wbmEx57 [acs-2p::GFP + rol-6(su1006)]*	*Burkewitz et al., 2015*
AGP309	*glp-1(e2144ts);fmo-2(ok2147)*	This study
AGP308	*glp-1(e2144ts);acs-2(ok2457)*	This study
NHR-49 Transgenic Strains		
Wild Type Background		
AGP24f	*glmEx5[Pnhr-49::nhr-49::gfp + Pmyo-2::mCherry]*	*Ratnappan et al., 2014*
AGP27a	*glmEx7[Pmyo-3::nhr-49::GFP + Pmyo-2::mCherry]*	This study
AGP40a	*glmEx9[Pgly-19::nhr-49::GFP + Pmyo-2::mCherry]*	This study
AGP45	*glmEx11[Pcol-12::nhr-49::GFP + Pmyo-2::mCherry]*	This study
AGP102a	*glmEx20[Punc-119::nhr-49::GFP + Pmyo-2::mCherry]*	This study
***nhr-49* Mutant Background**		
AGP33a	*nhr-49(nr2041)I;glmEx5 [Pnhr-49::nhr-49::GFP + Pmyo-2::mCherry]*	This study
AGP63	*nhr-49(nr2041)I;glmEx8 [Pmyo-3::nhr-49::GFP + Pmyo-2::mCherry]*	This study
AGP65	*nhr-49(nr2041)I;glmEx9 [Pgly-19::nhr-49::GFP + Pmyo-2::mCherry]*	This study
AGP53	*nhr-49(nr2041)I;glmEx11 [Pcol-12::nhr-49::GFP + Pmyo-2::mCherry]*	This study
AGP103a	*nhr-49(nr2014)I;glmEx20[Punc-119::nhr-49::GFP + Pmyo-2::mCherry]*	This study
***glp-1* Mutant Background**		
AGP29d	*glp-1(e2141ts)III;glmEx6[Pnhr-49::nhr-49::GFP + Pmyo-2::mCherry].* Obtained by crossing AGP28a x CF1903.	This study
AGP36a	*glp-1(e2141ts)III;glmEx7[Pmyo-3::nhr-49::GFP + Pmyo-2::mCherry]*	This study
AGP44	*glp-1(e2141ts)III;glmEx10 [Pgly-19::nhr-49::GFP + Pmyo-2::mCherry]*	This study
AGP41a/b	*glp-1(e2141ts) III;glmEx11[Pcol-12::nhr-49::GFP + Pmyo-2::mCherry]*	This study
AGP105a/b	*glp-1(e2141)III;glmEx20[Punc-119::nhr-49::GFP + Pmyo-2::mCherry]*	This study
***nhr-49;glp-1* Mutant Background**		
AGP34a	*nhr-49(nr2041)I;glp-1(e2141ts)III;glmEx5 [Pnhr-49::nhr-49::GFP + Pmyo-2::mCherry]*	This study
AGP279	*nhr-49(nr2041)I;glp-1(e2141ts)III;glmEx7 [Pmyo-3::nhr-49::GFP + Pmyo-2::mCherry].* Obtained by crossing AGP36 x AGP12a	This study
AGP43	*nhr-49(nr2041)I;glp-1(e2141)III;glmEx10 [Pgly-19::nhr-49::GFP + Pmyo-2::mCherry]*	This study
AGP54a	*nhr-49(nr2041);glp-1(e2141);glmEx11 [Pcol-12::nhr-49::GFP + Pmyo-2::mCherry]*	This study
AGP70a/b	*nhr-49(nr2041);glp-1(e2141);glmEx13 [Prgef-1::nhr-49::GFP + Pmyo-2::mCherry]*	This study
AGP115a/b	*nhr-49(nr2041);glp-1(e2141);glmEx29 [Punc-119::nhr-49::GFP + Pmyo-2::mCherry]*	This study
Tissue-specific *nhr-49(et7) gof* Expressing Strains		
AGP311	*glm21 [Pcol-12::nhr-49(et7)::gfp + Pmyo-2::mCherry]*	This study
AGP312	*glm22 [Punc-119::nhr-49(et7)::gfp + Pmyo-2::mCherry]*	This study
AGP313	*nhr-49(nr2041)I; glm22 [Punc-119::nhr-49(et7)::gfp + Pmyo-2::mCherry]*	This study

Appendix B Chapter 3.0 Supplementary Figures

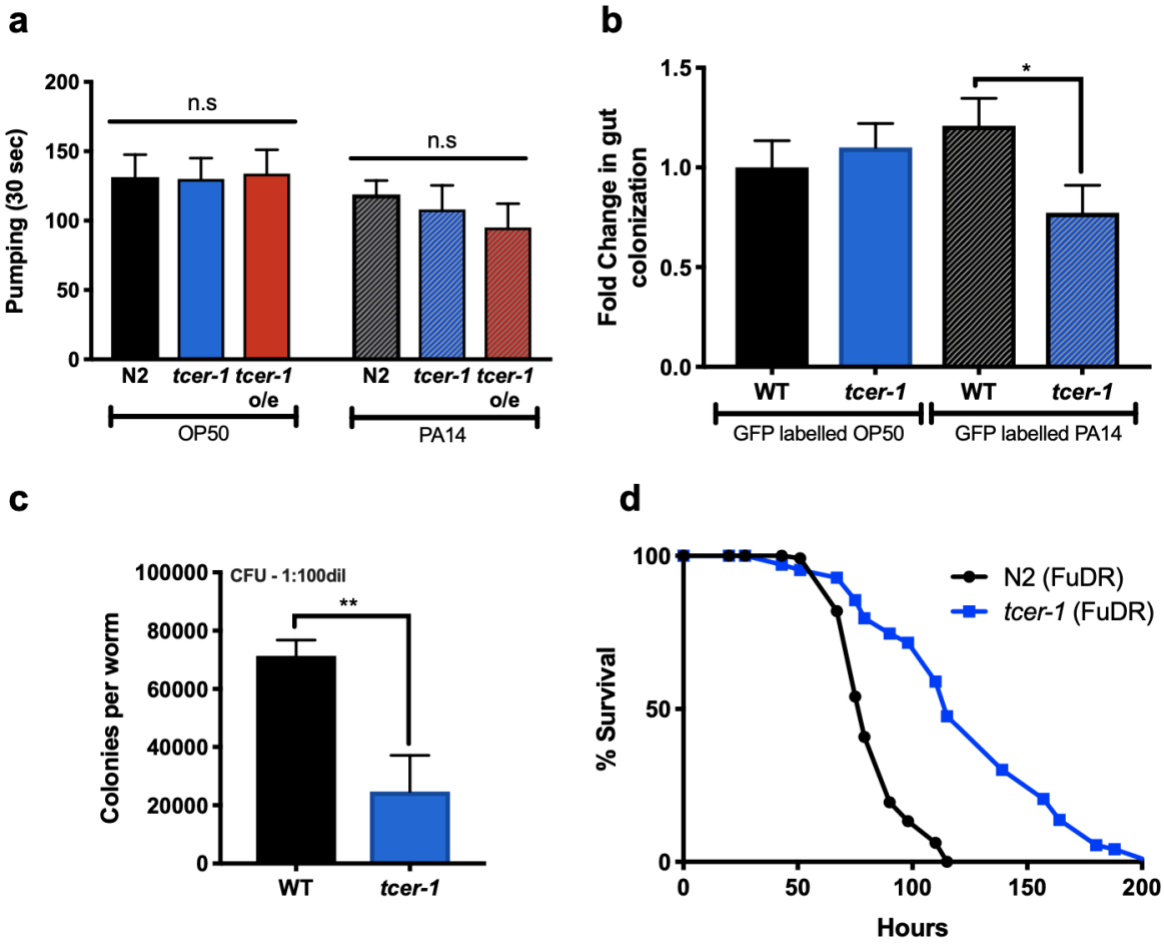

Supplementary Figure 3.1 Increased PA14-resistance of *tcer-1* mutants is not due to aberrant feeding or matricide.

(a) Pharyngeal pumping. The pumping rate between wild type (WT, black), *tcer-1* mutants (blue) and a TCER-1- overexpressing strain (red) showed no significant difference using the ordinary one-way ANOVA statistical test on normal OP50 and pathogenic PA14 food source. Data shown is combined from three independent biological replicates with 15-20 animals tested per strain, per replicate. **(b)** Measurement of bacterial ingestion. GFP in intestinal lumens of

wild-type (WT, black) and *tcer-1* mutants (blue) was measured 24h after transfers of age-matched L4 larvae to GFP labelled OP50 or PA14. Significance was calculated using the unpaired one-tailed t test * $P<0.05$ **(c)** CFU Analysis. Number of colonies (CFU) generated by bacteria isolated from wild-type (black) or *tcer-1* mutants (blue) exposed to PA14. Significance was calculated using the unpaired two-tailed t test ** $P<0.01$. **(d)** Effect of bagging/matricide on PA14 resistance. L4-stage animals exposed to 100 μg/ml FuDR-containing plates for 24h followed by transfer to PA14 plates**.** WT (m = 59.35 ± 1.3, n = 89/106) and *tcer-1* (m = 98.6 ± 3.5, n = 83/109, P vs WT <0.0001) (m = 114.18 ± 3.9, n = 81/106, P vs *glp-1* <0.001). Survival was calculated using the Kaplan Meier statistical analysis and data shown as mean (m) + standard error of the mean (SEM).

a. Subset of TCER-1 DOWN genes predicted to be invovled in immunity and stress related functiions as per the associated GO terms

WB Gene ID	Gene Description	GO Term	PMK-1 dependent (Troemel et al. 2006)	Identified as Induced by PA14
WBGene00003099	LYSozyme (*lys-10*)	Increased pathogene susceptability	Troemel et al	X
WBGene00016669	Invertebrate LYSozyme (*ilys-2*)	lysozyme activity, Defense to Gram-ve Bacterium		X
WBGene00005003	SaPosin-like Protein family (*spp-18*)	Innate Immune Response		X X
WBGene00016670	Invertebrate LYSozyme (*ilys-3*)	lysozyme activity		X
WBGene00015759	hypothetical protein (*C14C6.5*)	Innate Immune Response	Troemel et al	X
WBGene00003093	LYSozyme (*lys-4*)	lysozyme activity		
WBGene00007875	Downstream Of DAF-16 (regulated by DAF-16) (*dod-24*)	Innate Immune Response, Defense to Gram-ve Bacterium	Troemel et al	X X X
WBGene00009813	Histidine ammonia-lyase (*haly-1*)	Stress Response to Zinc Ion		X
WBGene00019779	hypothetical protein (*M60.2*)	Innate Immune Response, Defense to Gram-ve Bacterium		X
WBGene00003096	LYSozyme (*lys-7*)	Innate Immune Response, Defense to Gram-ve Bacterium		
WBGene00000556	CaeNaCin (Caenorhabditis bacteriocin) (*cnc-2*)	Innate Immune Response, Defense to Gram-ve Bacterium		
WBGene00001772	Glutathione S-Transferase (*gst-24*)	Innate Immune Response		X
WBGene00010124	hypothetical protein (*F55G11.4*)	Defense to Gram-ve Bacterium	Troemel et al	X
WBGene00020455	F-box A protein (*fbxa-59*)	Innate Immune Response		X X
WBGene00000599	Cuticle collagen 10 (*col-10*)	Response to Oxidative stress		
WBGene00020658	hypothetical protein (*T21F4.1*)	Innate Immune Response		X
WBGene00016542	hypothetical protein (*C39H7.4*)	Innate Immune Response		X X
WBGene00003877	Peptide transporter family 1 (*pept-1*)	Response to oxidative stress		
WBGene00002024	Heat Shock Protein (*hsp-43*)	Stress Response		
WBGene00015052	C-type LECtin (*clec-52*)	Defense to Gram-ve Bacterium		X
WBGene00009433	hypothetical protein (*F35E12.9*)	Innate Immune Response, Defense to Gram-ve Bacterium		X X
WBGene00009429	hypothetical protein (*F35E12.5*)	Innate Immune Response, Defense to Gram-ve Bacterium	Troemel et al	X
WBGene00018910	hypothetical protein (*F56A4.2*)	Innate Immune Response		X
WBGene00021224	C-type LECtin (*clec-209*)	Innate Immune Response		X
WBGene00000717	COLlagen (*col-144*)	Response to Oxidative stress		
WBGene00009213	THaumatiN family (*thn-1*)	Innate Immune Response		
WBGene00018384	hypothetical protein (*F43C11.7*)	Innate Immune Response, Defense to Gram-ve Bacterium		
WBGene00016769	hypothetical protein (*C49C8.5*)	Innate Immune Response		X X X
WBGene00022645	hypothetical protein (*ZK6.11*)	Innate Immune Response	Troemel et al	X
WBGene00011647	Non-centrosomal microtubule array protein 1 (*noca-1*)	Apoptotic Process		
WBGene00022644	Downstream Of DAF-16 (regulated by DAF-16) (*dod-19*)	Innate Immune Response	Troemel et al	X X
WBGene00008199	hypothetical protein (*C49C3.9*)	Innate Immune Response, Defense to Gram-ve Bacterium		X X X
WBGene00004055	Mitogen-activated protein kinase pmk-1 (*pmk-1*)	Innate Immune Response, Defense to Gram-ve Bacterium		
WBGene00019427	Autophagic-related protein 16.2 (*atg-16.2*)	Defense to Gram-ve Bacterium		
WBGene00000900	Cell surface receptor *daf-4* (*daf-4*)	Innate Immune Response		
WBGene00008634	hypothetical protein (*F10A3.4*)	Innate Immune Response		
WBGene00001333	Ezrin/Radixin/Moesin (*erm-1*)	Apoptotic Process		
WBGene00002008	Heat Shock Protein (*hsp-4*)	Apoptotic Process, Stress Response		
WBGene00018760	Infection Response Gene (*irg-3*)	Innate Immune Response		X X X
WBGene00017262	hypothetical protein (*F08F3.4*)	Innate Immune Response		X
WBGene00001029	DNaJ domain (prokaryotic heat shock protein) (*dnj-11*)	Stress Response		
WBGene00020549	Glycylpeptide N-tetradecanoyltransferase (*nmt-1*)	Apoptotic Process		

X = Induced by PA14 (Curated from Wormbase); X = Troemel et al 2006; X = Shapira et al 2006; X = Twumasi-Boeteng and Shapira 2012

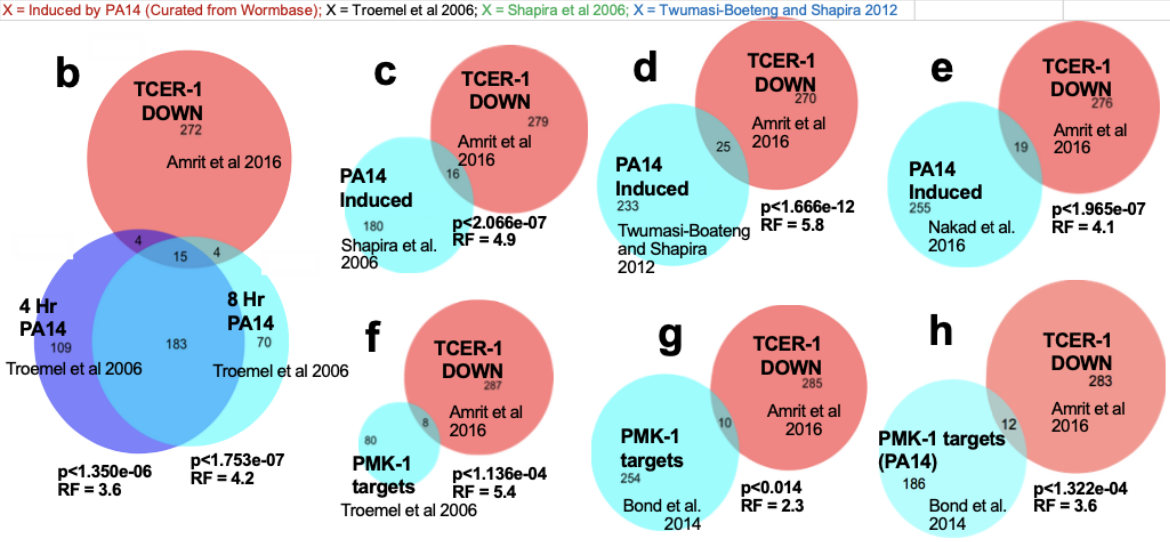

Supplementary Figure 3.2 TCER-1-repressed genes are enriched for roles involved in immunity and stress resistance.

(a) Of the 295 genes predicted to be down regulated >1.5 fold by TCER-1 (TCER-1 'DOWN' class), 42 listed here have reported immunity and/or stress-related functions based on the associated GO terms. Of these, many have been shown to be upregulated upon infection by PA14 and/or under PMK-1 control (shown in column three, key under table). **(b-e)** Graphical representation of the comparison of overlap between TCER-1 'DOWN' genes with lists from previous studies that identified genes induced upon PA14 infection. **(f-h)** Graphical representation of the comparison of overlap between TCER-1 'DOWN' genes with studies that identified PMK-1 targets. The statistical significance of the overlap observed between the DOWN group and each gene lists are shown under the respective panels as is with the degree of over- enrichment, calculated as representation factor (RF) on Nemates (nemates.org/MA/progs/overlap_stats.html).

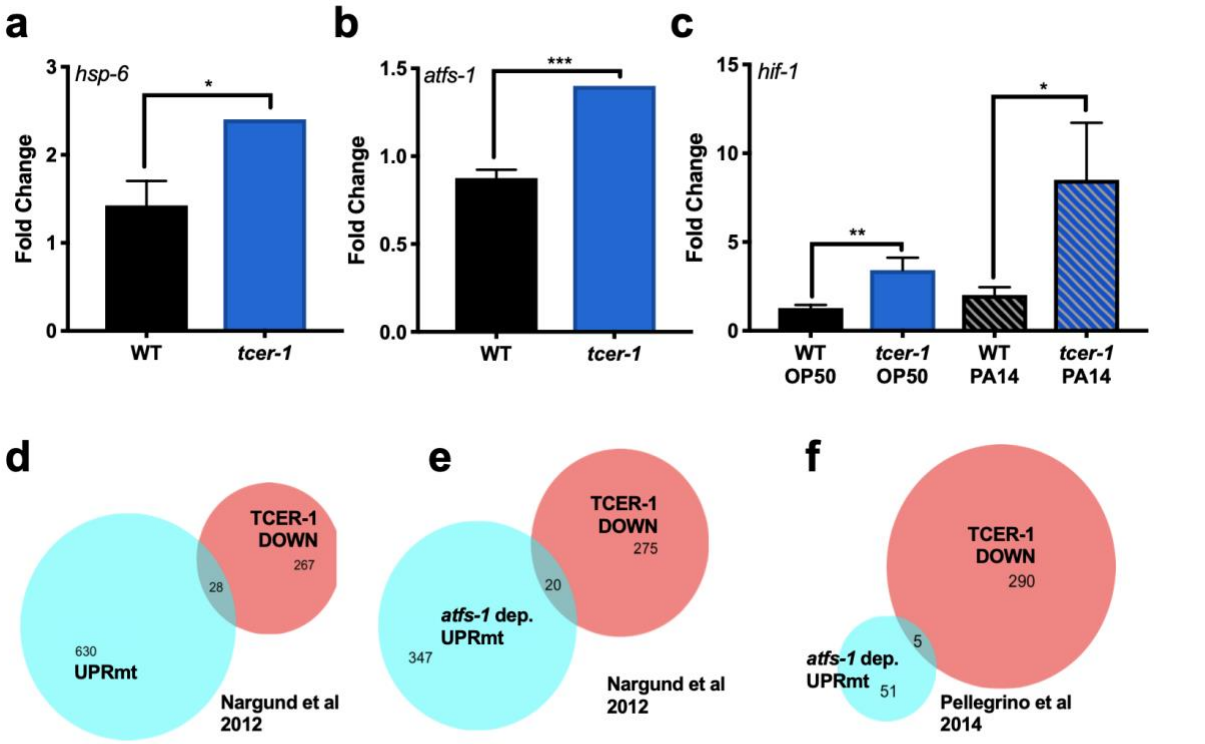

Fig	RNA-Seq Gene Class	Comparison Study	Details	Statistical Significance	Representation Factor
d	TCER-1 Downregulated	Nargund et al.	Mito UPR Targets	p < 6.282e-06	2.5
e	TCER-1 Downregulated	Nargund et al.	atfs dependent Mito UPR Targets	p < 4.091e-06	3.3
f	TCER-1 Downregulated	Pellegrino et al.	Mito UPR Targets and PA14 shared	p < 0.002	5.3

Supplementary Figure 3.3 TCER-1 represses expression of key transcription factors mediating UPR^{mt} and hypoxia response.

(a-c) mRNA levels of *hsp-6*, *atfs-1* and *hif-1* compared between day 1 wild-type (WT, black), *tcer-1* (blue) maintained on OP50 (solid bars) or exposed as L4s to PA14 for 8 hours (hashed bars in c). Data combined from 2-5 independent biological replicates, each including three technical replicates. Error bars denote standard error of the mean. Asterisks represent the statistical significance of differences observed in an unpaired, one-tailed t-test with P values 0.05 (*) or 0.01(***). **(d-f)** Graphical representation of the comparison of overlap between TCER-1 'DOWN' class with lists from previous genomic studies identifying UPR^{mt} genes. P values for

associated probability/overlap and representation factor (RF) were calculated on Nemates (nemates.org/MA/progs/overlap_stats.html).

Appendix B.1 Chapter 3.0 Supplementary Tables

Supplementary Table 3.1 (a-e) Effect of transgenic TCER-1 expression driven by tissue-specific promoters on lifespan of different strains on *E. coli* OP50 diet

(D-Scholar Link)

The impact of TCER-1 expression in individual tissues on the lifespan of wild-type animals as well as *tcer-1*, *glp-1* and *tcer-1;glp-1* mutants. TCER-1 was driven under control of (1A) *tcer-1* endogenous promoter (1B) intestine-specific promotor (1C) Neuron-specific promotor (1D) muscle-specific promotor and (1E) hypodermis-specific promotor.

Supplementary Table 3.2 Survival of wildtype and *tcer-1* mutants exposed to *P. aeruginosa* PA01 and *S. aureus* NCTC8325

2A. Survival of wildtype and *tcer-1* mutants exposed to PA01 on SK plates and NGM plates							
Plate Type	Pathogen	Strain	Genotype	Trial 1[#]			
				n = obs/ total	Mean	SE ^	p (*vs* N2)
SK	PA01	N2	Wildtype	118 / 142	126.43	+/- 2.38	
SK	PA01	CF2166	*tcer-1*	143 / 173	139.98	+/- 2.65	**0.001**
Trial 2							
SK	PA01	N2	Wildtype	105 / 127	110.80	+/- 3.1	
SK	PA01	CF2166	*tcer-1*	111 / 133	110.10	+/- 3.14	**0.931**
Trial 3							
SK	PA01	N2	Wildtype	112 / 124	121.27	+/- 2.89	
SK	PA01	CF2166	*tcer-1*	83 / 129	131.64	+/- 3.75	**0.03**
Trial 4							
NGM	PA01	N2	Wildtype	83 / 99	155.56	+/- 4.43	
NGM	PA01	CF2166	*tcer-1*	50 / 111	151.76	+/- 6.12	**0.8**
Trial 5							
NGM	PA01	N2	Wildtype	124 / 147	136.19	+/- 2.33	
NGM	PA01	CF2166	*tcer-1*	110 / 149	143.96	+/- 3.92	**0.013**
Trial 6							
NGM	PA01	N2	Wildtype	118 / 138	122.73	+/- 2.66	
NGM	PA01	CF2166	*tcer-1*	116 / 154	125.94	+/- 2.92	**0.4**
2B. Survival of wildtype and tcer-1 mutants exposed to *S. aureus* (NCTC8325) on BHI plates							
Trial 1[#]							
BHI	*S. aureus* (NCTC8325)	N2	Wildtype	97 / 111	94.67	+/- 1.44	
BHI	*S. aureus* (NCTC8325)	CF2166	*tcer-1*	145 / 169	109.27	+/- 1.5	**0.001**
Trial 2							
BHI	*S. aureus* (NCTC8325)	N2	Wildtype	110 / 120	105.14	+/- 2.27	
BHI	*S. aureus* (NCTC8325)	CF2166	*tcer-1*	98 / 116	115.05	+/- 2.69	**0.001**

[#] Data from Tables 2A (Trial 1) and 2B (Trial 1) represented in Figs. 1b and 1c respectively.

Supplementary Table 3.3 Effect of *tcer-1* mutation on resistance against oxidative and ER stress

3A. Survival of wild type and mutant strains upon exposure to tBOOH						
Strain	Genotype	Trial 1[#]			Bonferroni P values	
		n = obs/ total	Mean	SE ^	p *(vs* N2)	p *(vs glp-1)*
N2	Wildtype	57/98	17.32	+/- 1.05		
CF2166	*tcer-1*	33/100	25.65	+/- 1.65	0.0001	
CF1903	*glp-1*	79/100	27.88	+/- 1.46	0.0001	
CF2154	*tcer-1;glp-1*	29/100	56.31	+/- 5.06	0.0001	0.0001
		Trial 2			Bonferroni P values	
N2	Wildtype	28/90	15.19	+/- 1.3		
CF2166	*tcer-1*	33/100	25.78	+/- 3.32	0.0248	
CF1903	*glp-1*	51/100	50.59	+/- 3.28	0.001	
CF2154	*tcer-1;glp-1*	38/100	30.84	+/- 3.59	0.0009	0.0001
		Trial 3			Bonferroni P values	
N2	Wildtype	44/80	17.81	+/- 1.37		
CF2166	*tcer-1*	38/80	23.37	+/- 1.3	0.1637	
CF1903	*glp-1*	69/80	33.51	+/- 2.24	0.0008	
CF2154	*tcer-1;glp-1*	56/80	49.83	+/- 4.81	0.0097	0.0092
3B. Survival of wild type and mutant strains upon exposure to Tunicamycin						
		Trial 1			Bonferroni P values	
N2	Wildtype	89/100	16.58	+/- 0.65		
CF2166	*tcer-1*	91/101	16.01	+/- 0.56	1	
CF1903	*glp-1*	107/107	18.41	+/- 1.27	1	
CF2154	*tcer-1;glp-1*	79/100	21.73	+/- 1.25	0.0012	0.3749
		Trial 2			Bonferroni P values	
N2	Wildtype	91/104	18.13	+/- 0.64		
CF2166	*tcer-1*	87/104	17.27	+/- 0.67	1	
CF1903	*glp-1*	96/108	18.81	+/- 1.03	1	
CF2154	*tcer-1;glp-1*	100/101	24.91	+/- 2.96	0.0021	0.1118
		Trial 3			Bonferroni P values	
N2	Wildtype	57/79	17.66	+/- 0.73		
CF2166	*tcer-1*	100/102	16.7	+/- 0.7	1	
CF1903	*glp-1*	99/111	21.91	+/- 1.16	0.0018	
CF2154	*tcer-1;glp-1*	87/106	20.83	+/- 1.3	0.401	1

[#]Data from Table 3A (Trial 1) represented in Fig. 1e.

Supplementary Table 3.4 (a-c) Effect of TCER-1 expression in different tissues on resistance against *P. aeruginosa* PA14

4A. Survival of strains expressing TCER-1 in different tissues of *tcer-1* mutants upon exposure to *P. aeruginosa* PA14								
Strain	Genotype	Tissue of TCER-1 expression (promoter)	Trial 1[#]			Bonferroni P-value		
			n = obs/ total	Mean	SE ^	P (*vs* N2)	P (*vs glp-1*)	P (*vs tcer-1*)
N2	Wildtype	Control	87/111	60.68	+/- 0.95			
CF1903	*glp-1*	Control	98/104	79.22	+/- 2.11	0.001		
CF2154	*tcer-1;glp-1*	Control	55/78	80.3	+/- 3.3	0.001	1	
CF2166	*tcer-1*	Control	53/102	96.31	+/- 2.74	0.001	0.0001	
AGP173	*tcer-1*	*tcer-1 (Endogenous promoter)*	48/63	70.91	+/- 3.4	0.002	0.7498	0.0001
AGP194	*tcer-1*	*Muscle (myo-3)*	88/100	64	+/- 2.7	0.144	0.003	0.001
AGP120	*tcer-1*	*Hypodermis (col-12)*	72/102	71.67	+/- 3.11	0.0001	1	0.0001
AGP92	*tcer-1*	*Intestine (gly-19)*	77/99	55.33	+/- 3.08	1	0.0001	0.001
AGP170	*tcer-1*	*Neurons (rgef-1)*	85/107	62.32	+/- 1.9	1	0.0001	0.001
Trial 2						**Bonferroni P-value**		
N2	Wildtype	Control	75/102	63.75	+/- 1.03			
CF1903	*glp-1*	Control	96/118	84.79	+/- 2.72	0.001		
CF2154	*tcer-1;glp-1*	Control	49/75	86.07	+/- 4.44	0.0005	1	
CF2166	*tcer-1*	Control	33/100	102.04	+/- 3.14	0.001	0.0001	
AGP194	*tcer-1*	*Muscle (myo-3)*	70/100	73.95	+/- 3.9	0.1159	0.3085	0.0001
AGP120	*tcer-1*	*Hypodermis (col-12)*	55/100	87.29	+/- 4.64	0.0001	1	0.0087
AGP92	*tcer-1*	*Intestine (gly-19)*	50/100	71.83	+/- 4.41	1	0.1522	0.0001
AGP170	*tcer-1*	*Neurons (rgef-1)*	87/100	59.16	+/- 1.71	0.3631	0.001	0.001
Trial 3						**Bonferroni P-value**		
N2	Wildtype	Control	54/65	85.93	+/- 2.07			
CF2166	*tcer-1*	Control	86/106	113.03	+/- 3.28	0.001		
CF2858	*tcer-1*	*tcer-1 (Endogenous promoter)*	88/101	100.88	+/- 2.6	0.0001		0.0098
Trial 4						**Bonferroni P-value**		
N2	Wildtype	Control	74/86	84.68	+/- 1.88			
CF2166	*tcer-1*	Control	64/91	115.73	+/- 3.98	0.001		
CF2858	*tcer-1*	*tcer-1 (Endogenous promoter)*	78/93	101.12	+/- 4.08	0.0047		0.0394
Trial 5						**Bonferroni P-value**		
N2	Wildtype	Control	66/81	79.56	+/- 1.52			0.001
CF2166	*tcer-1*	Control	46/75	113.11	+/- 2.96	0.001		
AGP170	*tcer-1*	*Neurons (rgef-1)*	100/110	78.65	+/- 1.14	1		0.001
Trial 6						**Bonferroni P-value**		
N2	Wildtype	Control	59/73	61.92	+/- 2.4			0.001
CF2166	*tcer-1*	Control	65/77	85.37	+/- 2.7	0.001		
AGP170	*tcer-1*	*Neurons (rgef-1)*	101/112	53.68	+/- 1.14	0.0012		0.001

Supplementary Table 3.4 (continued)

4B. Survival of strains expressing TCER-1 in different tissues of *tcer-1;glp-1* mutants upon exposure to *P. aeruginosa* PA14								
Strain	Genotype	Expression	Trial 1			Bonferroni P-value		
			n = obs/ total	Mean	SE ^	P *(vs* N2)	P *(vs glp-1)*	P *(vs tcer-1;glp-1)*
N2	Wildtype	Control	52/60	46.6	+/- 1.23			
CF1903	*glp-1*	Control	47/60	68.48	+/- 2.39	0.001		
CF2154	*tcer-1;glp-1*	Control	43/60	63.84	+/- 4.86	0.0001	0.6025	
AGP172	*tcer-1;glp-1*	*tcer-1 (Endogenous promoter)*	36/60	82.26	+/- 6.29	0.0001	0.4028	0.3869
AGP79	*tcer-1;glp-1*	*Muscle (myo-3)*	40/50	33.23	+/- 2.26	0.0001	0.001	0.001
AGP122	*tcer-1;glp-1*	*Hypodermis (col-12)*	17/29	63.02	+/- 9.87	1	1	1
AGP91	*tcer-1;glp-1*	*Intestine (gly-19)*	47/75	36.27	+/- 4.7	0.0001	0.001	0.0001
AGP171	*tcer-1;glp-1*	*Neurons (rgef-1)*	39/61	56.5	+/- 5.28	1	0.2669	0.6632
Trial 2#						**Bonferroni P-value**		
N2	Wildtype	Control	63/82	47.61	+/- 1.29			
CF1903	*glp-1*	Control	73/82	59.52	+/- 1.91	0.0001		
CF2154	*tcer-1;glp-1*	Control	50/80	67.98	+/- 4.46	0.0003	0.3984	
AGP172	*tcer-1;glp-1*	*tcer-1 (Endogenous promoter)*	09/˜10	26.3	+/- 6.79	0.0004	0.0001	0.0001
AGP79	*tcer-1;glp-1*	*Muscle (myo-3)*	66/80	25.03	+/- 1.64	0.001	0.001	0.001
AGP122	*tcer-1;glp-1*	*Hypodermis (col-12)*	39/60	47.15	+/- 3.29	1	0.0594	0.0068
AGP91	*tcer-1;glp-1*	*Intestine (gly-19)*	64/80	22.45	+/- 1.23	0.001	0.001	0.001
AGP171	*tcer-1;glp-1*	*Neurons (rgef-1)*	53/80	54.08	+/- 3.61	0.7272	1	0.0992
Trial 3#						**Bonferroni P-value**		
N2	Wildtype	Control	87/111	60.68	+/- 0.95			
CF1903	*glp-1*	Control	98/104	79.22	+/- 2.11	0.001		
CF2154	*tcer-1;glp-1*	Control	55/78	80.3	+/- 3.3	0.001	1	
AGP172	*tcer-1;glp-1*	*tcer-1 (Endogenous promoter)*	58/66	44	+/- 3.32	0.0002	0.0001	0.001
Trial 4#						Bonferroni P-value		
N2	Wildtype	Control	83/91	75.3	+/- 2.94			
CF1903	*glp-1*	Control	91/92	102.34	+/- 2.86	0.0001		
CF2154	*tcer-1;glp-1*	Control	59/85	126.59	+/- 6.16	0.001	0.0001	
AGP171	*tcer-1;glp-1*	*Neurons (rgef-1)*	82/102	84.31	+/- 5.42	0.1357	0.9185	0.0001
Trial 5						Bonferroni P-value		
N2	Wildtype	Control	68/86	71.77	-2.68			
CF1903	*glp-1*	Control	88/99	98.35	-2.99	0.001		
CF2154	*tcer-1;glp-1*	Control	50/80	129.12	-6.11	0.001	0.0001	
AGP171	*tcer-1;glp-1*	*Neurons (rgef-1)*	65/78	90.72	-6.65	0.012	1	0.0008

4C. Survival of strains expressing TCER-1 in different tissues in wildtype animals upon exposure to *P. aeruginosa* PA14							
Strain	Genotype	Tissue of TCER-1 expression (promoter)	Trial 1			Bonferroni P-value	
			n = obs/ total	Mean	SE ^	P *(vs* N2)	P *(vs tcer-1)*
N2	Wildtype	Control	66/75	94.25	+/- 2.31		0.0039
CF2166	*tcer-1*	Control	38/50	110.04	+/- 4.07	0.0039	
AGP75	Wildtype	*tcer-1 (Endogenous promoter)*	24/25	83.03	+/- 2.53	0.0156	0.001
AGP76	Wildtype	*Muscle (myo-3)*	41/42	76.92	+/- 3.35	0.0013	0.001
AGP77	Wildtype	*Intestine (gly-19)*	60/80	82.38	+/- 2.33	0.008	0.001
AGP132	Wildtype	*Neurons (rgef-1)*	49/60	75.14	+/- 2.01	0.001	0.001
AGP108	Wildtype	*Hypodermis (col-12)*	61/76	88.84	+/- 2.39	0.7878	0.0001
Trial 2						**Bonferroni P-value**	
N2	Wildtype	Control	80/95	83.7	+/- 1.94		0.001
CF2166	*tcer-1*	Control	34/60	115.18	+/- 5.53	0.001	
AGP75	Wildtype	*tcer-1 (Endogenous promoter)*	17/23	81.65	+/- 5.15	1	0.0011
AGP76	Wildtype	*Muscle (myo-3)*	58/67	78.55	+/- 2.35	1	0.001
AGP77	Wildtype	*Intestine (gly-19)*	94/111	83.79	+/- 1.76	1	0.001
AGP132	Wildtype	*Neurons (rgef-1)*	73/83	77.32	+/- 2.4	0.303	0.001
AGP108	Wildtype	*Hypodermis (col-12)*	72/80	85.88	+/- 1.98	1	0.001
Trial 3						**Bonferroni P-value**	
N2	Wildtype	Control	66/81	79.56	+/- 1.52		0.001
CF2166	*tcer-1*	Control	46/75	113.11	+/- 2.96	0.001	
AGP75	Wildtype	*tcer-1 (Endogenous promoter)*	51/65	77.01	+/- 2.21	1	0.001
Trial 4						**Bonferroni P-value**	
N2	Wildtype	Control	59/73	61.92	+/- 2.4		0.001
CF2166	*tcer-1*	Control	65/77	85.37	+/- 2.7	0.001	
AGP75	Wildtype	*tcer-1 (Endogenous promoter)*	68/80	55.82	+/- 2.24	0.1456	0.001

#Data from Table 4A (Trial 1) represented in Fig. 2 (a-e).

#Data from Table 4B (Trial 3), (Trial 2) and (Trial 4) represented in Fig. 2(f), Fig. 2(g,l and j) and Fig. 2(h) respectively.

Supplementary Table 3.5 Survival of wild type worms and *tcer-1* mutants exposed to *P. aeruginosa* PA14 at different ages

Strain	Genotype	Stage of PA14 Exposure	Trial 1			
			n = obs/ total	Mean (hrs)	SE ^	P (*vs* N2)
N2	Wildtype	L4	84 / 105	85.96	+/- 1.78	
CF2166	*tcer-1*	L4	27 / 90	108.65	+/- 5.69	**0.0001**
N2	Wildtype	Day 2	92 / 100	44.18	+/- 1.97	
CF2166	*tcer-1*	Day 2	64 / 113	65.52	+/- 2.15	**0.001**
N2	Wildtype	Day 4	89 / 101	18.22	+/- 1.84	
CF2166	*tcer-1*	Day 4	101 / 102	17.3	+/- 1.38	**0.8361**
N2	Wildtype	Day 6	84 / 102	41.02	+/- 2.47	
CF2166	*tcer-1*	Day 6	97 / 100	20.42	+/- 0.98	**0.001**
N2	Wildtype	Day 9	91 / 100	25.16	+/- 1.9	
CF2166	*tcer-1*	Day 9	92 / 101	10.5	+/- 0.98	**0.001**
Trial 2						
N2	Wildtype	L4	87 / 100	47.63	+/- 4.14	
CF2166	*tcer-1*	L4	53 / 100	84.01	+/- 3.74	**0.0001**
N2	Wildtype	Day 2	77 / 104	46.5	+/- 1.44	
CF2166	*tcer-1*	Day 2	97 / 123	74.5	+/- 2.45	**0.001**
N2	Wildtype	Day 4	85 / 108	28	+/- 0.83	
CF2166	*tcer-1*	Day 4	108 / 125	36.66	+/- 1.48	**0.0001**
N2	Wildtype	Day 6	98 / 105	21.95	+/- 1.19	
CF2166	*tcer-1*	Day 6	87 / 105	15.84	+/- 0.76	**0.0001**
N2	Wildtype	Day 9	93 / 100	13.81	+/- 1.42	
CF2166	*tcer-1*	Day 9	95 / 100	13.01	+/- 0.9	**0.8798**
Trial 3						
N2	Wildtype	L4	110 / 120	73.38	+/- 1.62	
CF2166	*tcer-1*	L4	91 / 145	100.18	+/- 2.54	**0.0001**
N2	Wildtype	Day 2	77 / 81	32.35	+/- 1.55	
CF2166	*tcer-1*	Day 2	108 / 113	59.26	+/- 2.29	**0.001**
N2	Wildtype	Day 4	160 / 170	30.59	+/- 1.24	
CF2166	*tcer-1*	Day 4	162 / 183	41.06	+/- 1.57	**0.001**
N2	Wildtype	Day 6	126 / 158	36.98	+/- 1.51	
CF2166	*tcer-1*	Day 6	158 / 179	26.04	+/- 1.25	**0.0001**
N2	Wildtype	Day 9	98 / 98	16.95	+/- 1.32	
CF2166	*tcer-1*	Day 9	146 / 146	16.99	+/- 0.94	**0.8193**
Trial 4[#]						
N2	Wildtype	L4	36 / 100	71.69	+/- 2.39	
CF2166	*tcer-1*	L4	10 / 100	79.97	+/- 3.96	**0.051**
N2	Wildtype	Day 2	59 / 100	40.89	+/- 1.53	
CF2166	*tcer-1*	Day 2	30 / 80	51.36	+/- 1.91	**0.0001**
N2	Wildtype	Day 4	89 / 120	31.41	+/- 1.1	
CF2166	*tcer-1*	Day 4	66 / 76	38.86	+/- 1.56	**0.0001**
N2	Wildtype	Day 6	76 / 102	24.82	+/- 1.32	
CF2166	*tcer-1*	Day 6	99 / 106	26.17	+/- 1.09	**0.3852**
N2	Wildtype	Day 9	84 / 86	20.91	+/- 1.11	
CF2166	*tcer-1*	Day 9	65 / 66	19.64	+/- 1.21	**0.4315**
Trial 5						
N2	Wildtype	L4	40 / 117	72.5	+/- 2.21	
CF2166	*tcer-1*	L4	20 / 100	77.54	+/- 1.91	**0.0449**
N2	Wildtype	Day 2	66 / 141	42.79	+/- 1.05	
CF2166	*tcer-1*	Day 2	25 / 145	56.84	+/- 1.91	**0.001**
N2	Wildtype	Day 4	81 / 113	22.41	+/- 1.08	
CF2166	*tcer-1*	Day 4	88 / 118	34.08	+/- 1.52	**0.001**
N2	Wildtype	Day 6	85 / 98	16.95	+/- 1.01	
CF2166	*tcer-1*	Day 6	89 / 95	15.68	+/- 0.39	**0.1052**
N2	Wildtype	Day 9	39 / 50	18.72	+/- 1.69	
CF2166	*tcer-1*	Day 9	26 / 30	17.4	+/- 1.63	**0.4938**
Trial 6						
N2	Wildtype	L4	48 / 122	52.58	+/- 1.08	
CF2166	*tcer-1*	L4	12 / 124	77.92	+/- 3.75	**0.001**
N2	Wildtype	Day 2	70 / 123	30.03	+/- 0.85	
CF2166	*tcer-1*	Day 2	60 / 160	43.18	+/- 1.66	**0.001**
N2	Wildtype	Day 4	114 / 144	29.97	+/- 0.9	
CF2166	*tcer-1*	Day 4	130 / 150	31.92	+/- 0.71	**0.0505**
N2	Wildtype	Day 6	136 / 139	12.08	+/- 0.35	
CF2166	*tcer-1*	Day 6	138 / 140	11.85	+/- 0.24	**0.7772**
N2	Wildtype	Day 9	108 / 112	6.67	+/- 0.57	
CF2166	*tcer-1*	Day 9	98 / 103	9.56	+/- 0.81	**0.002**
Trial 7						
N2	Wildtype	L4	91 / 108	42.08	+/- 3.84	
CF2166	*tcer-1*	L4	68 / 108	46.7	+/- 4.06	**0.5215**
N2	Wildtype	Day 2	73 / 118	50.5	+/- 1.97	
CF2166	*tcer-1*	Day 2	65 / 112	59.65	+/- 1.74	**0.003**
N2	Wildtype	Day 4	54 / 75	38.91	+/- 1.93	
CF2166	*tcer-1*	Day 4	78 / 101	31.22	+/- 1.64	**0.0023**
N2	Wildtype	Day 6	68 / 71	19	+/- 1.51	
CF2166	*tcer-1*	Day 6	46 / 51	16.97	+/- 2.00	**0.9215**
N2	Wildtype	Day 9	39 / 57	16.24	+/- 2.78	
CF2166	*tcer-1*	Day 9	55 / 58	11.74	+/- 1.66	**0.1904**

[#]Data from Table 5 (Trial 4) represented in Fig. 3a.

Supplementary Table 3.6 (a-c) Impact of TCER-1-repressed genes on *P. aeruginosa* PA14 resistance

6A. Effect of mutations in TCER-1-repressed genes on PA14 resistance induced by *tcer-1* RNAi								
Strain	Genotype	RNAi	Trial 1#			Bonferroni P-value		
			n = obs/ total	Mean	SE ^	P (*vs* N2 on Ctrl)	P (*vs* N2 on *tcer-1* RNAi)	P (*vs* mutant on Ctrl)
N2	Wildtype	*Ctrl*	47/65	77.67	+/- 3.01			
N2	*Wildtype*	*tcer-1*	85/101	104.62	+/- 2.68	0.001		
RB2478	*irg-5(ok3418)]*	*Ctrl*	74/90	53.07	+/- 0.71	0.001	0.001	
RB2478	*irg-5(ok3418)]*	*tcer-1*	78/90	56.69	+/- 1.21	0.001	0.001	0.164
Trial 2#						Bonferroni P-value		
N2	Wildtype	*Ctrl*	67/100	87.63	+/- 2.23			
N2	Wildtype	*tcer-1*	80/105	99.27	+/- 2.05	0.0006		
RB1994	*dod-24(ok2629)*	*Ctrl*	71/90	66.18	+/- 1.42	0.0001	0.0001	
RB1994	*dod-24(ok2629)*	*tcer-1*	88/105	74.20	+/- 1.49	0.0001	0.0001	0.0015
RB2356	*dod-3(ok3202)*	*Ctrl*	74/100	79.95	+/- 1.58	0.0027	0.001	
RB2356	*dod-3(ok3202)*	*tcer-1*	83/100	78.89	+/- 1.45	0.0001	0.001	1
Trial 3						Bonferroni P-value		
N2	Wildtype	*Ctrl*	68/100	57.47	+/- 3.04			
N2	Wildtype	*tcer-1*	53/105	108.46	+/- 3.91	0.001		
VC2496	*ilys-3(ok3222)*	*Ctrl*	56/103	54.53	+/- 2.07	0.929	0.001	
VC2496	*ilys-3(ok3222)*	*tcer-1*	65/101	55.51	+/- 1.67	0.568	0.001	1
RB1994	*dod-24(ok2629)*	*Ctrl*	36/40	35.15	+/- 3.37	0.0001	0.001	
RB1994	*dod-24(ok2629)*	*tcer-1*	62/77	62.42	+/- 2.33	1	0.0001	0.0001
RB2356	*dod-3(ok3202)*	*Ctrl*	47/70	72.57	+/- 3.5	0.0082	0.001	
RB2356	*dod-3(ok3202)*	*tcer-1*	55/95	62.64	+/- 3.87	0.5273	0.001	0.4335
Trial 4						Bonferroni P-value		
N2	Wildtype	*Ctrl*	75 / 89	70.93	+/- 1.8			
N2	Wildtype	*tcer-1*	46 / 58	75.99	+/- 1.57	0.2074		
RB2478	*irg-5(ok3418)]*	*Ctrl*	76 / 90	45.96	+/- 2.29	0.001	0.001	
RB2478	*irg-5(ok3418)]*	*tcer-1*	50 / 58	45.68	+/- 2.3	0.001	0.001	1
Trial 5#						Bonferroni P-value		
N2	Wildtype	*Ctrl*	50/85	72.12	+/- 2.3			
N2	Wildtype	*tcer-1*	59/81	81.33	+/- 2.45	0.0002		
VC2496	*ilys-3(ok3222)*	*Ctrl*	66/103	52.15	+/- 1.94	0.0001	0.0001	
VC2496	*ilys-3(ok3222)*	*tcer-1*	66/100	55.21	+/- 2.03	0.0001	0.0001	1

6B. Survival of *tcer-1;ilys-3* and *tcer-1;dod-3* double mutants upon exposure to PA14						
Strain	Genotype	Trial 1#			Bonferroni P-value	
		n = obs/ total	Mean	SE ^	P (*vs* N2)	P (*vs tcer-1*)
N2	Wildtype	91 / 119	88.05	+/- 2.08		
CF2166	*tcer-1*	86 / 119	111.81	+/- 2.35	0.001	
VC2496	*ilys-3*	106 / 112	54.29	+/- 1.3	0.001	0.0001
AGP256	*tcer-1;ilys-3*	84 / 89	60.74	+/- 1.54	0.001	0.0001
Trial 2					Bonferroni P-value	
N2	Wildtype	129 / 150	81.61	+/- 1.68		
CF2166	*tcer-1*	112 / 132	99.18	+/- 2.54	0.0001	
VC2496	*ilys-3*	103 / 113	52.06	+/- 1.81	0.001	0.001
AGP256	*tcer-1;ilys-3*	81 / 93	60.58	+/- 2.05	0.001	0.001

6C. Survival of *dod-3;tcer-1* double mutants upon exposure to *P. aeruginosa* PA14							
Strain	Genotype	Trial 1			Corrected P value		
		n = obs/ total	Mean	SE ^	P (*vs* N2)	P (*vs tcer-1*)	P (*vs dod-3*)
N2	Wildtype	129 / 156	78.34	1.77			
CF2166	*tcer-1*	70 / 107	103.14	2.16	0.0001		
AGP258	*dod-3*	114 / 147	82.36	1.92	0.4726	0.0001	
AGP257	*tcer-1;dod-3*	97 / 118	90.33	2.01	0.0001	0.0001	0.0137
Trial 2#					Corrected P value		
N2	Wildtype	139 / 151	60.06	0.86			
CF2166	*tcer-1*	93 / 126	87.90	2.04	0.0001		
AGP258	*dod-3*	120 / 131	70.87	0.75	0.0001	0.0001	
AGP257	*tcer-1;dod-3*	113 / 138	79.06	1.36	0.0001	0.0005	0.0001

#Data from Table 6A (Trial 2), (Trial 1) and (Trial 5) represented in Fig. 7(a,c), Fig. 7(b) and Fig. 7(d) respectively.

#Data from Tables 6B (Trial 1) and 6C (Trial 2) represented in Figs. 7e and 7f respectively.

Supplementary Table 3.7 Transgenic strains used in this study

Strain	Genotype	Transgene	Tissue of TCER-1 expression (promoter)
AGP75	*N2*	*glmEx15 [Ptcer-1::TCER-1::GFP + Pmyo-2::mCherry]*	endogenous (*tcer-1*)
AGP77	*N2*	*glmEx17 [Pgly-19::TCER-1::GFP + Pmyo-2::mCh]*	intestine
AGP132	*N2*	*glmEx25 [Prgef-1::TCER-1::GFP + Pmyo-2::mCh]*	neurons
AGP76	*N2*	*glmEx16 [Pmyo-3::TCER-1::GFP + Pmyo-2::mCh]*	muscles
AGP108	*N2*	*glmEx18 [Pcol12::tcer-1::GFP and Pmyo-2::mCh]*	hypodermis
AGP173	*tcer-1*	*glmEx15 [Ptcer-1::TCER1::GFP; Pmyo-2::mCherry] injected in CF2166*	endogenous (*tcer-1*)
AGP92	*tcer-1*	*glmEx17 [Pgly-19::TCER-1::GFP + Pmyo-2::mCh] injected in CF2166*	intestine
AGP170	*tcer-1*	*glmEx25 [Prgef-1::TCER-1::GFP + Pmyo-2::mCh] injected in CF2166*	neurons
AGP194	*tcer-1*	*glmEx16 [Pmyo-3::TCER-1::GFP + Pmyo-2::mCh] injected in CF2166*	muscles
AGP120	*tcer-1*	*glmEx18 [Pcol12::tcer-1::GFP and Pmyo-2::mCh] injected in CF2166*	hypodermis
AGP80	*glp-1*	*glmEx15 [Ptcer-1::TCER-1::GFP + Pmyo-2::mCherry] injected in CF1903*	endogenous (*tcer-1*)
AGP78	*glp-1*	*glmEx17 [Pgly-19::TCER-1::GFP + Pmyo-2::mCh] injected in CF1903*	intestine
AGP133	*glp-1*	*glmEx25 [Prgef-1::TCER-1::GFP + Pmyo-2::mCh] injected in CF1903*	neurons
AGP194	*glp-1*	*glmEx16 [Pmyo-3::TCER-1::GFP + Pmyo-2::mCh] injected in CF1903*	muscles
AGP121	*glp-1*	*glmEx18 [Pcol12::tcer-1::GFP and Pmyo-2::mCh] injected in CF1903*	hypodermis
AGP172	*tcer-1;glp-1*	*glmEx15 [Ptcer-1::TCER1::GFP; Pmyo-2::mCherry] injected in CF2154*	endogenous (*tcer-1*)
AGP91	*tcer-1;glp-1*	*glmEx17 [Pgly-19::TCER-1::GFP + Pmyo-2::mCh] injected in CF2154*	intestine
AGP171	*tcer-1;glp-1*	*glmEx25 [Prgef-1::TCER-1::GFP + Pmyo-2::mCh] injected in CF2154*	neurons
AGP79	*tcer-1;glp-1*	*glmEx16 [Pmyo-3::TCER-1::GFP + Pmyo-2::mCh] injected in CF2154*	muscles
AGP122	*tcer-1;glp-1*	*glmEx18 [Pcol12::tcer-1::GFP and Pmyo-2::mCh] injected in CF2154*	hypodermis

Appendix C Chapter 4.0 Supplementary Figures

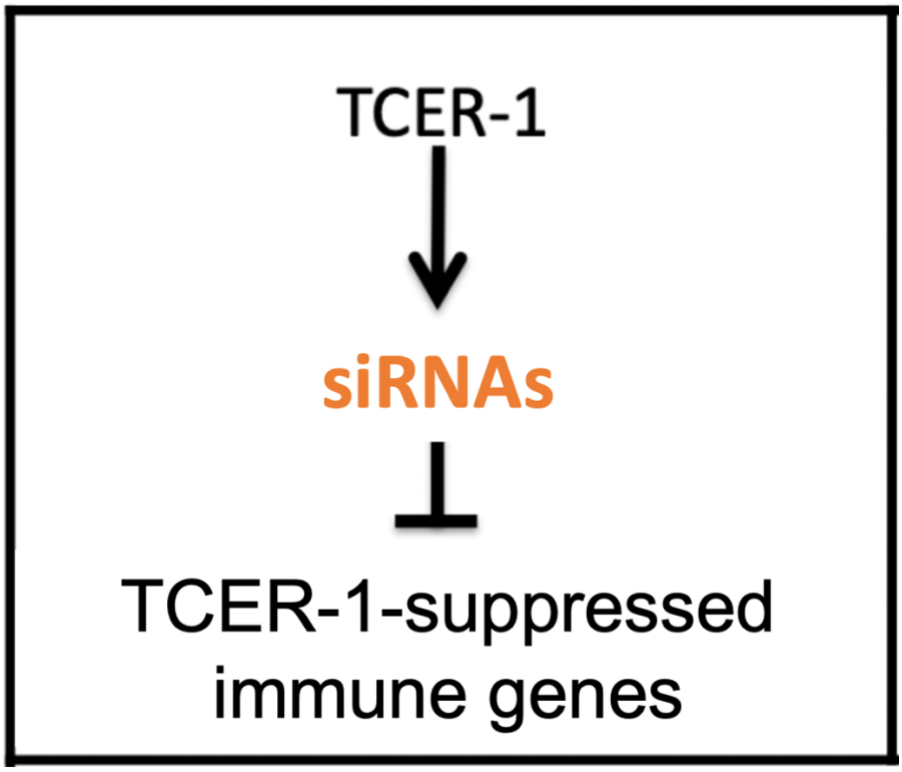

Supplementary Figure 4.1 Schematic of hypothesized endo-siRNA-directed mechanism of TCER-1-immunosuppression.

Schematic proposing that TCER-1 suppresses immunity by promoting siRNA biosynthesis, which in turn, silence complementary mRNAs of immune genes.

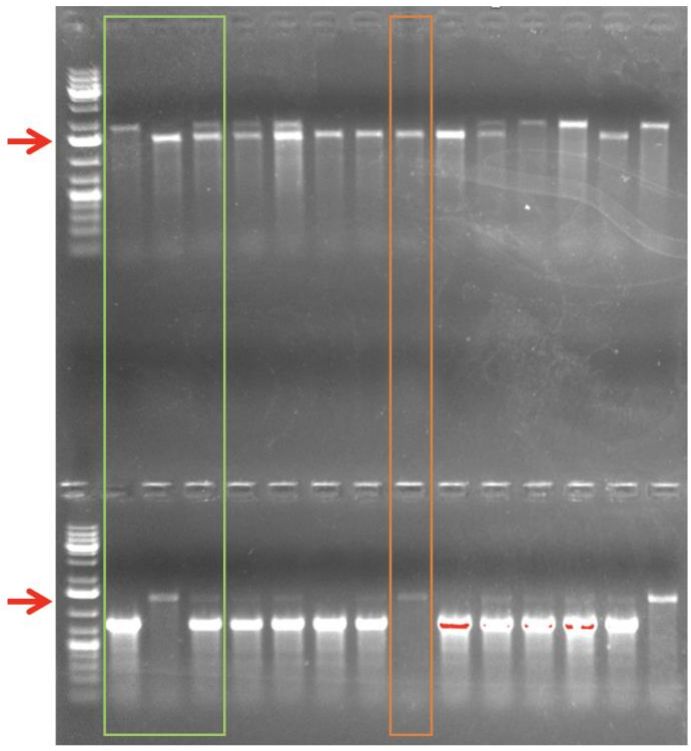

Supplementary Figure 4.2 Introducing the *tcer-1(tm1452)* mutation into *mut-7(pk720)* mutants yielded a sterile line

Genotyping of F2-generation single-worm lines from a cross between *tcer-1(tm1452)* and *mut-7(pk720)* mutants. Top row shows PCR results from use of *tcer-1* primers (expect 1.7kb in WT and 1.4kb band in mutant). Bottom row shows PCR results from use of *mut-7* primers (expect 830bp in WT and 1.4kb band in mutant). Expected mutant band size compared to GeneRuler 1 kb Plus DNA Ladder shown by red arrows on left. (Column 2-4, Green Box) wildtype control, mutant control, heterozygous control. (Column 5-15) F2-generation single-worm lines; orange box denotes sterile double-mutant. Genotyping primers used for *tcer-1(tm1452)* (top row): F_gccaattctggttgagtgac, R_tccatcagtcaagacga. Genotyping primers used for *mut-7(pk720)* (bottom row): F_ttggtgagacccatcttgg, F2_gggtatcgtattagcatgacg, R_aattgctgtatgctcgtgg.

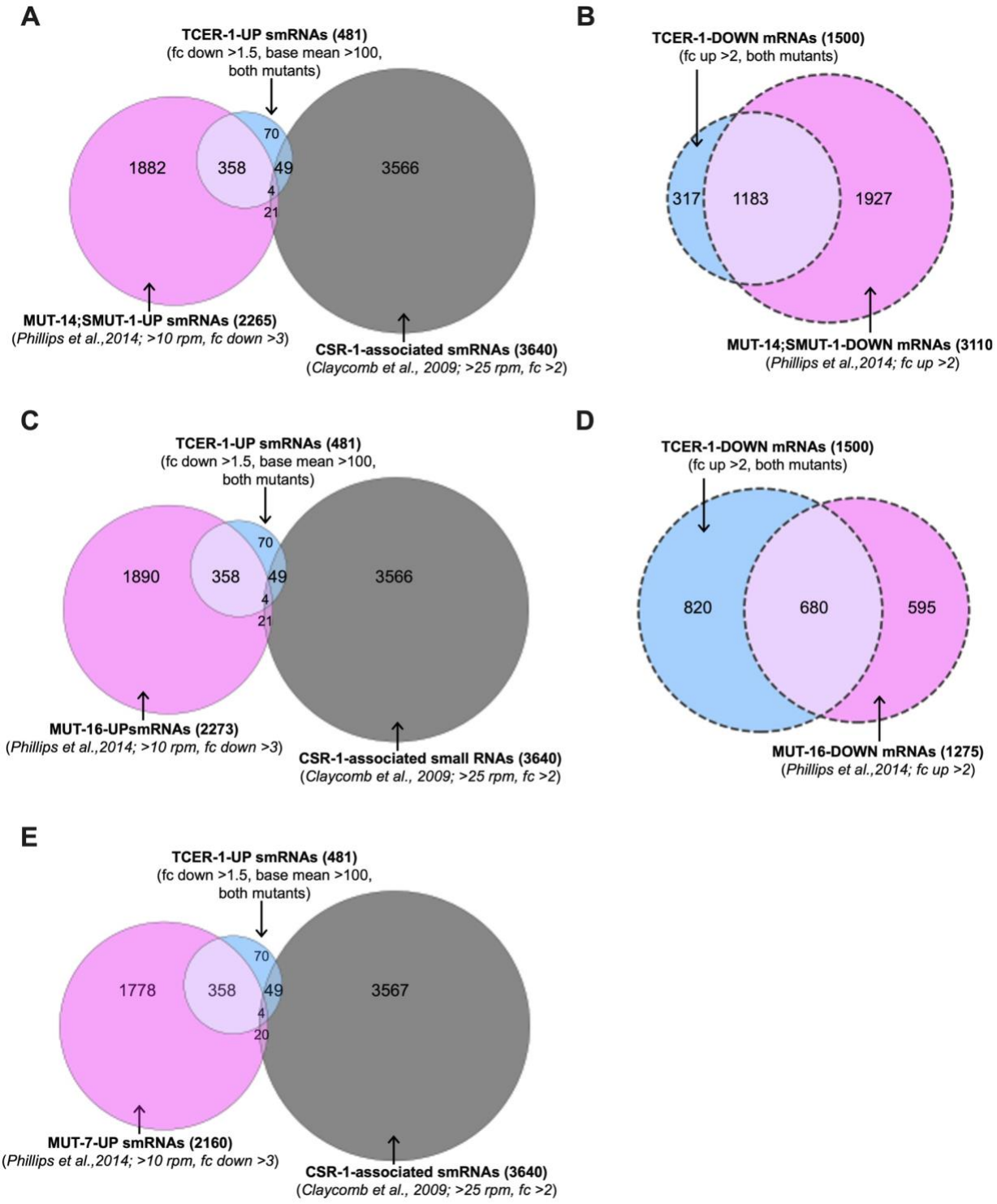

Supplementary Figure 4.3 Similarities between TCER-1 and Mutator-regulated smRNA and mRNA profiles.

(A, C, E) Overlap between smRNAs depleted in Mutator mutants, TCER-1-UP smRNAs, and CSR-1-associated smRNAs. (B, D) Overlap between mRNAs induced in Mutator mutants and TCER-1-DOWN mRNAs. Dotted lines around circles indicate negative regulation by protein. 'A' also shown in main figures as Fig. 4.3C.

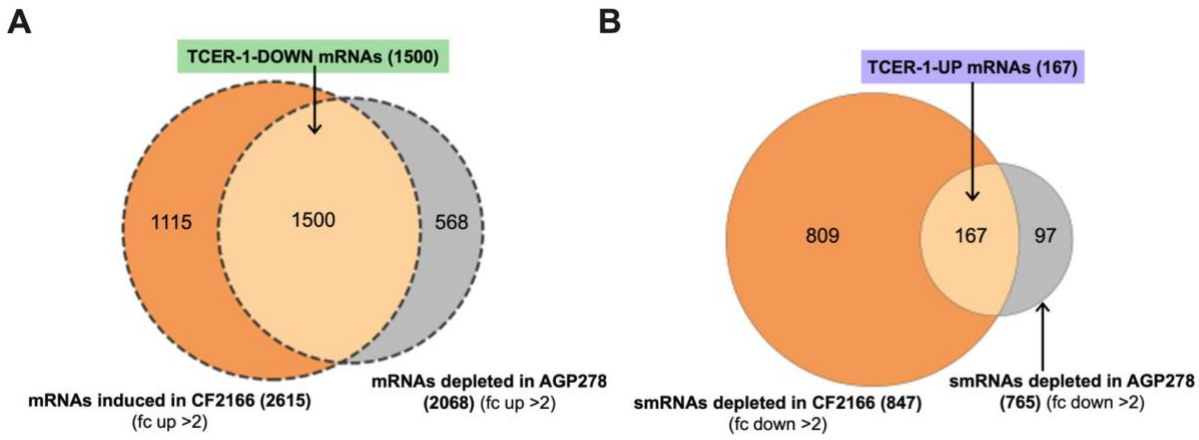

Supplementary Figure 4.4 TCER-1-DOWN and TCER-1-UP mRNA lists, defined by mRNA changes in CF2166 and AGP278 mutants.

(A) Overlap between lists of mRNAs induced at a fold-change >2 in CF2166 and AGP278 strains in mRNAseq comparison to N2 samples, yielding high-confidence list of 1500 mRNAs likely downregulated by TCER-1 (TCER-1-DOWN mRNAs, represented in green in other figures). Dotted lines around circles indicate negative regulation by TCER-1 protein. (B) Overlap between lists of mRNAs depleted at a fold-change >2 in CF2166 and AGP278 strains in mRNAseq comparison to N2 samples, yielding list of 167 mRNAs likely downregulated by TCER-1 (TCER-1-DOWN mRNAs, represented in purple in other figures).

Appendix C.1 Chapter 4.0 Supplementary Tables

Supplementary Table 4.1 Impact of *tcer-1* knockdown (a) and loss-of-function mutation (b) on *ppw-1* and *rrf-1* mutant PA14 survival

Table S1A: Impact of *tcer-1* knockdown on *ppw-1* and *rrf-1* mutant PA14 survival

Strain	Genotype	RNAi treatment	Trial 1			Bonferroni P-value	
			n = obs/ total	Mean (h)	SE +/-	P *(vs* N2 pAD12)	P *(vs pAD12 control)*
N2	Wildtype	pAD12	99 / 112	64.21	1.73		
N2	Wildtype	*tcer-1*	92 / 97	78.73	1.39		>0.001
RB798	*rrf-1(ok589)*	pAD12	100 / 115	78.17	2.8	>0.001	
RB798	*rrf-1(ok589)*	*tcer-1*	126 / 140	93.07	2.4		0.0076
NL3511	*ppw-1(pk1425)*	pAD12	82 / 123	86.34	2.54	>0.001	
NL3511	*ppw-1(pk1425)*	*tcer-1*	149 / 180	91.81	1.83		0.6764
Trial 2							
N2	Wildtype	pAD12	87 / 113	56.61	1.36		
N2	Wildtype	*tcer-1*	86 / 114	64.57	1.51		>0.001
RB798	*rrf-1(ok589)*	pAD12	97 / 117	75.99	2.25	>0.001	
RB798	*rrf-1(ok589)*	*tcer-1*	119 / 136	83.89	1.75		0.3887
NL3511	*ppw-1(pk1425)*	pAD12	118 / 126	76.33	1.77	>0.001	
NL3511	*ppw-1(pk1425)*	*tcer-1*	132 / 148	70	1.32		0.0197
Trial 3*							
N2	Wildtype	pAD12	110 / 134	60.93	0.95		
N2	Wildtype	*tcer-1*	129 / 157	67.91	1.09		>0.001
RB798	*rrf-1(ok589)*	pAD12	114 / 136	77.45	1.67	>0.001	
RB798	*rrf-1(ok589)*	*tcer-1*	117 / 154	77.3	1.33		1
NL3511	*ppw-1(pk1425)*	pAD12	123 / 144	72.14	1.46	>0.001	
NL3511	*ppw-1(pk1425)*	*tcer-1*	1412 / 154	72.46	1.2		1
Trial 4*							
N2	Wildtype	pAD12	63 / 81	58.52	1.48		
N2	Wildtype	*tcer-1*	78 / 109	69.23	1.48		>0.001
RB798	*rrf-1(ok589)*	pAD12	93 / 108	83.39	2.16	>0.001	
RB798	*rrf-1(ok589)*	*tcer-1*	104 / 131	88.44	2.12		0.3968
NL3511	*ppw-1(pk1425)*	pAD12	99 / 112	71.2	1.95	>0.001	
NL3511	*ppw-1(pk1425)*	*tcer-1*	110 / 121	70.14	1.62		1
Trial 5							
N2	Wildtype	pAD12	131 / 167	59.33	1.16		
N2	Wildtype	*tcer-1*	143 / 161	76.23	1.52		>0.001
RB798	*rrf-1(ok589)*	pAD12	137 / 170	79.77	1.63	>0.001	
RB798	*rrf-1(ok589)*	*tcer-1*	144 / 164	82.62	1.69		0.807
NL3511	*ppw-1(pk1425)*	pAD12	144 / 157	84.43	1.74	>0.001	
NL3511	*ppw-1(pk1425)*	*tcer-1*	134 / 151	87.16	1.99		1
Trial 6							
N2	Wildtype	pAD12	75/151	57.93	1.09		
N2	Wildtype	*tcer-1*	73/175	77.06	1.8		>0.001
RB798	*rrf-1(ok589)*	pAD12	97/155	81.81	2.1	>0.001	
RB798	*rrf-1(ok589)*	*tcer-1*	123/160	82.11	1.24		0.2123
NL3511	*ppw-1(pk1425)*	pAD12	71/140	70.34	2.11	>0.001	
NL3511	*ppw-1(pk1425)*	*tcer-1*	111/155	78.32	1.32		0.0019

*asterisk denotes that trail is displayed in main text

Supplementary Table 4.1 (continued)

Table S1B: Impact of tcer-1 loss-of-function mutation on *ppw-1* and *rrf-1* mutant PA14 suvival						
Strain	**Genotype**	**Trial 1**			**Bonferroni P-value**	
		n = obs/ total	**Mean (h)**	**SE +/-**	**P *(vs* N2)**	**P *(vs single mutant*)**
N2	Wildtype	149 / 181	90.81	1.65		
CF1266	*tcer-1(tm1452)*	113 / 163	97.57	1.74	0.0354	
NL3511	*ppw-1(pk1425)*	141 / 180	86.38	1.44	0.0624	
AGP274	*ppw-1;tcer-1*	127 / 181	93.08	1.75	1	0.0023
RB798	*rrf-1(ok589)*	134 / 180	96.04	1.51	0.3229	
AGP273	*rrf-1;tcer-1*	103 / 154	99.44	1.76	0.007	0.3859
Trial 2*						
N2	Wildtype	116 / 143	88.97	2.01		
CF1266	*tcer-1(tm1452)*	96 / 111	102.76	2.3	>0.001	
NL3511	*ppw-1(pk1425)*	134 / 148	102.95	2.38	>0.001	
AGP274	*ppw-1;tcer-1*	95 / 116	106.68	2.94	>0.001	1
RB798	*rrf-1(ok589)*	120 / 140	118.33	2.88	>0.001	
AGP273	*rrf-1;tcer-1*	127 / 148	102.84	2.38	>0.001	>0.001
Trial 3*						
N2	Wildtype	108 / 130	74.9	1.34		
CF1266	*tcer-1(tm1452)*	91 / 120	103.91	2.45	>0.001	
NL3511	*ppw-1(pk1425)*	119 / 146	97.77	1.96	>0.001	
AGP274	*ppw-1;tcer-1*	99 / 123	112.97	2.94	>0.001	>0.001
RB798	*rrf-1(ok589)*	113 / 137	97.99	1.89	>0.001	
AGP273	*rrf-1;tcer-1*	88 / 106	108.5	2.55	>0.001	>0.001

Supplementary Table 4.2 Small RNA biosynthesis gene mRNA levels from mRNAseq of *tcer-1* mutants (this study)

Table S2: Small RNA biosynthesis gene mRNA levels from mRNAseq of *tcer-1* mutants (this study)							
Strains Compared	Gene	baseMean	log2FoldChange	lfcSE	stat	pvalue	padj
AGP278 v N2	*ppw-1*	6248.56	-0.16	0.06	-2.70	0.007	0.015
CF2166 v N2	*ppw-1*	6248.56	-0.08	0.06	-1.33	0.183	0.259
AGP278 v N2	*rrf-1*	4262.61	-0.52	0.06	-8.59	9.07E-18	1.18E-16
CF2166 v N2	*rrf-1*	4262.61	-0.67	0.06	-11.13	9.24E-29	1.45E-27
AGP278 v N2	*mut-16*	3572.80	-0.62	0.06	-10.23	1.48E-24	3.29E-23
CF2166 v N2	*mut-16*	3572.80	-0.55	0.06	-9.02	1.90E-19	1.82E-18
AGP278 v N2	*mut-14*	1504.13	-0.44	0.07	-6.38	1.77E-10	1.10E-09
CF2166 v N2	*mut-14*	1504.13	-0.24	0.07	-3.49	0.00048	0.00114
AGP278 v N2	*mut-7*	3103.85	-0.39	0.06	-7.03	2.13E-12	1.62E-11
CF2166 v N2	*mut-7*	3103.85	-0.23	0.06	-4.19	2.74E-05	7.63E-05

Supplementary Table 4.3 Class distribution of TCER-1-UP (left) and TCER-1-DOWN (right) smRNAs

Small RNA classes depleted in *tcer-1* mutants (481)		
Type	# of DE smRNAs	Percent
CSR	53	11%
MUT	380	79%
ncRNA	12	2%
piRNA	36	7%
miRNA	0	0%
TOTAL	481	100%

Small RNA classes induced in *tcer-1* mutants (600)		
Type	# of DE smRNAs	Percent
CSR	62	10%
MUT	290	48%
ncRNA	171	29%
piRNA	9	2%
miRNA	68	11%
TOTAL	600	100%

Supplementary Table 4.4 Impact of small RNA biogenesis mutations on PA14 survival at (a) standard temperature of 25 °C degrees and (b) 20°C.

Table S4A: Impact of small RNA biogenesis mutations on PA14 survival (PA14 exposure at standard temperature of 25 degrees)					
Strain	Genotype	Trial 1			Bonferroni P-value
		n = obs/ total	Mean (h)	SE +/-	P *(vs* N2)
N2	Wildtype	108 / 130	74.9	1.34	
CF2166	*tcer-1 (tm1452)*	91 / 120	103.91	2.45	<0.001
VC1138	*drsh-1(ok369)*	28 / 30	100.99	3.15	<0.001
WM206	*drh-3(ne4253)*	90 / 111	67.84	2.52	0.085
NL2099	*rrf-3 (pk1426)*	94 / 110	88.46	2.36	<0.001
SX2499	*prde-1(mj207)*	71 / 104	75.84	2	1
Trial 2					
N2	Wildtype	57 / 125	78.44	2.41	
CF2166	*tcer-1 (tm1452)*	78 / 128	99.16	2.38	<0.001
WM158	*ergo-1 (tm1860)*	103 / 141	80.99	2.13	1
NL2099	*rrf-3 (pk1426)*	98 / 127	91.04	2.24	0.0015
Trial 3					
N2	Wildtype	93 / 112	66.28	1.36	
CF2166	*tcer-1 (tm1452)*	70 / 113	99.1	3.2	<0.001
WM300	*alg-3(tm1155);alg-4(ok1041)*	111 / 130	69.7	1.71	0.3487
YY538	*hrde-1(tm1200)*	113 / 138	58.91	1.29	0.0018
YY158	*nrde-3(gg66)*	106 / 120	69.46	1.18	0.2682
Trial 4					
N2	Wildtype	120 / 150	67.43	1.3	
CF2166	*tcer-1 (tm1452)*	79 / 132	102.39	2.27	<0.001
GR1373	*eri-1(mg366)*	109 / 140	71.83	1.22	0.1188
YY166	*ergo-1(gg98)*	92 / 140	70.24	1.34	0.7856
YY158	*nrde-3(gg66)*	112 / 150	72.11	1.36	0.0463
Trial 5					
N2	Wildtype	99/ 138	58.56	1.53	
CF2166	*tcer-1 (tm1452)*	52 / 136	77.52	2.93	<0.001
NL1810	*mut-16(pk710)*	121 / 135	64.21	1.39	0.0309
GR1946	*mut-14(pk738);smut-1(tm1301)*	115 / 138	59.46	1.66	1

Supplementary Table 4.4 (continued)

Table S4B: Impact of small RNA biogenesis mutations on PA14 survival (PA14 exposure at 20 degrees)					
Strain	Genotype	Trial 1			Bonferroni P-value
		n = obs/ total	Mean (h)	SE +/-	P *(vs* N2)
N2	Wildtype	112 / 162	111.47	1.92	
CF2166	*tcer-1 (tm1452)*	120 / 201	151.35	4.2	<0.001
NL1810	*mut-16(pk710)*	110 / 141	116.67	3.14	0.6114
GR1946	*mut-14(pk738);smut-1(tm1301)*	134 / 160	141.88	3.7	<0.001
NL1820	*mut-7(pk720)*	89 / 115	160.94	5.52	<0.001
WM30	*mut-2(ne298)*	124 / 153	101.24	1.64	<0.001
Trial 2					
N2	Wildtype	137 / 155	118.27	2.7	
CF2166	*tcer-1 (tm1452)*	119 / 170	183.11	4.35	<0.001
NL1810	*mut-16(pk710)*	127 / 145	135.95	2.95	<0.001
GR1946	*mut-14(pk738);smut-1(tm1301)*	139 / 159	169.7	4.52	<0.001
NL1820	mut-7(pk720)	129 / 149	138.18	4.44	<0.001
Trial 3					
N2	Wildtype	117 /158	137.64	3.34	
CF2166	*tcer-1 (tm1452)*	94 / 167	166.53	4.48	<0.001
NL1810	*mut-16(pk710)*	80 / 122	134.79	3.51	1
DCL565	*rde-1(mkc36)*	115 / 164	127.83	3.04	0.1937
WM45	*rde-1(ne300)*	105 / 134	102.26	1.27	<0.001
WM27	rde-1(ne219)	105 / 135	115.25	2.01	<0.001

Supplementary Table 4.5 (a) Impact of gene knockdown on *tcer-1* mutant PA14 survival;

(b) Impact of *tcer-1* knockdown on candidate mutants' PA14 survival

Table S5A: Impact of gene knockdown on *tcer-1* mutant PA14 survival

Strain	Genotype	RNAi Treatment	Trial 1			Bonferroni P-value	
			n = obs/ total	Mean (h)	SE +/-	P *(vs WT pAD12)*	P *(vs tcer-1 pAD12)*
N2	Wildtype	pAD12	70 / 118	68.32	1.61		
CF2166	*tcer-1 (tm1452)*	pAD12	90 / 144	97.17	1.69	< 0.0001	
CF2166	*tcer-1 (tm1452)*	*egl-20*	115 / 160	98.17	1.56	< 0.0001	1
CF2166	*tcer-1 (tm1452)*	F15D4.5	91 / 143	93.28	1.56	< 0.0001	0.624
CF2166	*tcer-1 (tm1452)*	T28D6.4	100 / 151	95.42	1.66	< 0.0001	1
CF2166	*tcer-1 (tm1452)*	Y69A2AR.31	95 / 150	91.19	1.55	< 0.0001	0.0369

Table S5B: Impact of *tcer-1* knockdown on candidate mutants' PA14 survival

Strain	Genotype	RNAi Treatment	Trial 1*			Bonferroni P-value	
			n = obs/ total	Mean (h)	SE +/-	P *(vs WT pAD12)*	P *(vs pAD12 ctrl)*
N2	Wildtype	pAD12	148 / 165	63.47	1.23		
N2	Wildtype	*tcer-1*	137 / 156	70.33	1.37	0.0017	0.0017
RB2015	*acs-5(ok2668)*	pAD12	113 / 123	60.26	1.29	0.8756	
RB2015	*acs-5(ok2668)*	*tcer-1*	114 / 131	63.5	1.42	1	0.1870
	asah-1(tm495)	pAD12	153 / 165	66.22	1.19	1	
	asah-1(tm495)	*tcer-1*	116 / 134	72.08	1.54	<0.001	0.0082
LC87	*qdpr-1(tm2337)*	pAD12	130 / 148	58.82	0.98	0.0270	
LC87	*qdpr-1(tm2337)*	*tcer-1*	100 / 114	61.33	1.31	1	0.2215
Trial 2*							
N2	Wildtype	pAD12	118 / 150	62.42	1.00		
N2	Wildtype	*tcer-1*	112 / 157	66.42	1.22	0.0247	0.0247
	F15D4.5(tm7964)	pAD12	125 / 150	73.01	1.64	<0.001	
	F15D4.5(tm7964)	*tcer-1*	123 / 142	73.44	1.56	<0.001	1
LC87	*qdpr-1(tm2337)*	pAD12	71 / 111	58.73	1.63	1	
LC87	*qdpr-1(tm2337)*	*tcer-1*	96 / 128	58.94	1.37	1	1
RB2584	*scrm-4(ok3596)*	pAD12	141 / 149	39.29	0.57	<0.001	
RB2584	*scrm-4(ok3596)*	*tcer-1*	144 / 150	41.86	0.56	<0.001	<0.001
	T28D6.4(tm926)	pAD12	94 / 112	59.87	1.45	1	
	T28D6.4(tm926)	*tcer-1*	98 / 125	67.05	1.44	0.0026	0.0043
Trial 3							
N2	Wildtype	pAD12	133 / 152	62.73	0.87		
N2	Wildtype	*tcer-1*	116 / 147	66.24	1.1	<0.001	<0.001
	F15D4.5(tm7964)	pAD12	106 / 125	73.03	1.51	<0.001	
	F15D4.5(tm7964)	*tcer-1*	111 / 148	75.16	1.83	<0.001	0.4472
LC87	*qdpr-1(tm2337)*	pAD12	108 / 138	65.29	1.29	0.0085	
LC87	*qdpr-1(tm2337)*	*tcer-1*	106 / 135	62.23	1.11	1	1

*asterisk denotes that trail is displayed in main text

Supplementary Table 4.6 Top smRNAs candidates through which TCER-1 might suppress immunity

smRNA target gene	Locus	smRNA class	Target descriptor	smRNA log2FC in AGP278	smRNAseq Base Mean	mRNA log2FC in AGP278	UP in at least one PA14 study?*	mRNA FoldChange in *mut-14 smut-1* (*Phillips et al., 2014*)
F15D4.5	F15D4.5	mut	Unknown	-3.5	17139	3.81	no	63.5
qdpr-1	T03F6.1	mut	Metabolism: amino acid breakdown	-2.4	10569	0.96	no	1.3
Y102A5C.36	Y102A5C.36	mut	Transmembrane protein: other	-3.0	1737	2.12	no	3.2
T28D6.4	T28D6.4	mut	Unknown	-6.9	2717	0.39	no	1.7
Y69A2AR.31	Y69A2AR.31	mut	Transmembrane protein: signaling receptor	-3.7	2467	0.25	no	2.0
scrm-4	F11A6.2	mut	Metabolism: lipid: phospholipid scramblase	-2.6	606	4.59	no	5.7
ZK973.8	ZK973.8	mut	Unknown: regulated by multiple stresses	-2.3	1189	0.96	no	4.2
acs-5	Y76A2B.3	mut	Metabolism: lipid: fatty acid biosynthesis	-4.5	1945	0.57	no	1.3
Y69A2AL.2	Y69A2AL.2	mut	Signaling: lipid: phospholipase A	-4.0	667	0.07	yes	1.3
egl-20	W08D2.1	mut	Signaling: WNT	-5.7	656	0.38	no	2.1
grd-16	Y69A2AL.1	mut	Signaling: hedgehog-like	-6.4	417	-0.69	no	2.4
cutl-10	Y53H1B.1	mut	Extracellular material: cuticlin	-7.1	345	-0.78	no	4.4
asah-1	K11D2.2	mut	Metabolism: lipid: sphingolipid	-5.0	105	0.71	yes	1.1

Genes labeled "mut" indicate their correspondance to differentially regulated Mutator-dependent siRNAs
RED means gene is also upregulated >2 fc in *tcer-1* mRNAseq (list of 1500).
*UP in at least one PA14 study: comparison to Shapira, M., et al. (2006), Troemel, E. R., et al. (2006); Twumasi-Boateng, K. and M. Shapira (2012); and Amrit et al., unpublished

Supplementary Table 4.7 *C. elegans* strains used in this study

Name	Genotype
N2	Wild type, Ghazi Lab
CF2166	*tcer-1(tm1452)* II
AGP278	*tcer-1(glm27)* II CRISPR deletion (*Amrit, Ghazi, et al., unpublished*)
IT213	*[tcer-1 prom::tcer-1ORF::gfp::tcer-1 3'utr] (Pushpa et al., 2013)*
AGP272	*ppw-1(pk1425)* I*; IT213*
AGP271	*rrf-1(ok589)* I*; IT213*
CZ19215	QDPR-1::GFP translational fusion reporter (*Loer et al. 2015*)
Small RNA Biosynthesis Mutants	
NL3511	*ppw-1(pk1425)* I
AGP274	*ppw-1(pk1425)* I*; tcer-1(tm1452)* II
RB798	*rrf-1(ok589)* I
AGP273	*rrf-1(ok589)* I*; tcer-1(tm1452)* II
VC1138	*drsh-1(ok369* I
WM206	*drh-3(ne4253)* I
NL2099	*rrf-3 (pk1426)* II
SX2499	*prde-1(mj207)* V
WM158	*ergo-1(tm1860)* V
WM300	*alg-4(ok1041)* III*; alg-3(tm1155)* IV
YY538	*hrde-1(tm1200)* III
YY158	*nrde-3(gg66)* X
GR1373	*eri-1(mg366)* IV
YY166	*ergo-1(gg98)* V
NL1810	*mut-16(pk710)* I
GR1946	*mut-14(pk738)* V*;smut-1(tm1301)* V
NL1820	*mut-7(pk720)* III
WM30	*mut-2(ne298)* I
DCL565	*rde-1(mkc36)* V
WM45	*rde-1(ne300)* V
WM27	*rde-1(ne219)* V
Mutants for Candidate Immune-Impacting Genes	
NBRP*	*F15D4.5(tm7964)* II
LC87	*qdpr-1(tm2337)* III
NBRP*	*T28D6.4(tm926)* III
RB2584	*scrm-4(ok3596)* I
RB2015	*acs-5(ok2668)* III
NBRP*	*asah-1(tm495)* I

*NBRP label denotes *C. elegans* strains from the National BioResource Project of Japan

Appendix C.2 Chapter 4.0 Supplementary Files

Supplementary File 1 smRNAseq of *tcer-1* mutants

(D-Scholarship Link)

Supplementary File 2 mRNAseq of *tcer-1* mutants

(D-Scholarship Link)

Supplementary File 3 Overlap analysis of smRNAseq and mRNAseq datasets

(D-Scholarship Link)

Supplementary File 4 Selection of smRNA candidates through which TCER-1 might suppress immunity.

(D-Scholarship Link)

Supplementary File 5 Fluorescence scoring of QDPR-1::GFP strains.

(D-Scholarship Link)

Bibliography

1.Flatt T, Heyland A. Mechanisms of life history evolution : the genetics and physiology of life history traits and trade-offs. Oxford ; New York: Oxford University Press; 2011. xxv, 478 p. p.

2.Stearns SC. The evolution of life histories / Stephen C. Stearns. Oxford ; New York: Oxford University Press; 1992.

3.Luu H, Tate AT. Recovery and immune priming modulate the evolutionary trajectory of infection-induced reproductive strategies. J Evol Biol. 2017;30(9):1748-62. Epub 2017/07/02. doi: 10.1111/jeb.13138. PubMed PMID: 28667661.

4.Brazdova A, Senechal H, Peltre G, Poncet P. Immune Aspects of Female Infertility. Int J Fertil Steril. 2016;10(1):1-10. Epub 2016/04/29. doi: 10.22074/ijfs.2016.4762. PubMed PMID: 27123194; PMCID: PMC4845518.

5.Kwak-Kim J, Bao S, Lee SK, Kim JW, Gilman-Sachs A. Immunological modes of pregnancy loss: inflammation, immune effectors, and stress. Am J Reprod Immunol. 2014;72(2):129-40. Epub 2014/03/26. doi: 10.1111/aji.12234. PubMed PMID: 24661472.

6.Abu-Raya B, Michalski C, Sadarangani M, Lavoie PM. Maternal Immunological Adaptation During Normal Pregnancy. Front Immunol. 2020;11:575197. Epub 2020/11/03. doi: 10.3389/fimmu.2020.575197. PubMed PMID: 33133091; PMCID: PMC7579415.

7.Maklakov AA, Chapman T. Evolution of ageing as a tangle of trade-offs: energy versus function. Proc Biol Sci. 2019;286(1911):20191604. Epub 2019/09/19. doi: 10.1098/rspb.2019.1604. PubMed PMID: 31530150; PMCID: PMC6784717.

8.Naim N, Amrit FRG, Ratnappan R, DelBuono N, Loose JA, Ghazi A. Cell nonautonomous roles of NHR-49 in promoting longevity and innate immunity. Aging Cell. 2021;20(7):e13413. Epub 2021/06/23. doi: 10.1111/acel.13413. PubMed PMID: 34156142; PMCID: PMC8282243.

9.Naim N, Amrit FRG, McClendon TB, Yanowitz JL, Ghazi A. The molecular tug of war between immunity and fertility: Emergence of conserved signaling pathways and regulatory mechanisms. Bioessays. 2020;42(12):e2000103. Epub 2020/11/11. doi: 10.1002/bies.202000103. PubMed PMID: 33169418; PMCID: PMC8219210.

10.Amrit FRG, Naim N, Ratnappan R, Loose J, Mason C, Steenberge L, McClendon BT, Wang G, Driscoll M, Yanowitz JL, Ghazi A. The Longevity-Promoting Factor, TCER-1, Widely Represses Stress Resistance and Innate Immunity. Nature Communications. 2019;10(1):3042. Epub 2019/07/19. doi: 10.1038/s41467-019-10759-z. PubMed PMID: 31316054; PMCID: PMC6637209.

11.Healy K, Ezard THG, Jones OR, Salguero-Gomez R, Buckley YM. Animal life history is shaped by the pace of life and the distribution of age-specific mortality and reproduction. Nat Ecol Evol. 2019;3(8):1217-24. Epub 2019/07/10. doi: 10.1038/s41559-019-0938-7. PubMed PMID: 31285573.

12.Travers LM, Garcia-Gonzalez F, Simmons LW. Live fast die young life history in females: evolutionary trade-off between early life mating and lifespan in female Drosophila melanogaster. Sci Rep. 2015;5:15469. Epub 2015/10/21. doi: 10.1038/srep15469. PubMed PMID: 26482533; PMCID: PMC4612512.

13.Zhu Q, Fu S, Zhang Q, Tian J, Zhao Y, Yao Y. Female Fertility Has a Negative Relationship With Longevity in Chinese Oldest-Old Population: A Cross-Sectional Study. Front Endocrinol (Lausanne). 2021;11(1101). doi: 10.3389/fendo.2020.616207.

14.Barnes AI, Boone JM, Jacobson J, Partridge L, Chapman T. No extension of lifespan by ablation of germ line in Drosophila. Proc Biol Sci. 2006;273(1589):939-47. Epub 2006/04/22. doi: 10.1098/rspb.2005.3388. PubMed PMID: 16627279; PMCID: PMC1560242.

15.Benedusi V, Martini E, Kallikourdis M, Villa A, Meda C, Maggi A. Ovariectomy shortens the life span of female mice. Oncotarget. 2015;6(13):10801-11. Epub 2015/02/27. doi: 10.18632/oncotarget.2984. PubMed PMID: 25719423; PMCID: PMC4484420.

16.Galvez D, Chapuisat M. Immune priming and pathogen resistance in ant queens. Ecol Evol. 2014;4(10):1761-7. Epub 2014/06/26. doi: 10.1002/ece3.1070. PubMed PMID: 24963375; PMCID: PMC4063474.

17.Barribeau SM, Schmid-Hempel P. Sexual healing: mating induces a protective immune response in bumblebees. J Evol Biol. 2017;30(1):202-9. Epub 2016/08/20. doi: 10.1111/jeb.12964. PubMed PMID: 27538716.

18.Speakman JR, Garratt M. Oxidative stress as a cost of reproduction: beyond the simplistic trade-off model. Bioessays. 2014;36(1):93-106. Epub 2013/11/29. doi: 10.1002/bies.201300108. PubMed PMID: 24285005.

19.Low BS, Hazel A, Parker N, Welch KB. Influences on Women's Reproductive Lives: Unexpected Ecological Underpinnings. Cross-Cultural Research. 2008;42(3):201-19. doi: 10.1177/1069397108317669.

20.Zwaan B, Bijlsma R, Hoekstra RF. Direct Selection on Life Span in Drosophila Melanogaster. Evolution. 1995;49(4):649-59. Epub 1995/08/01. doi: 10.1111/j.1558-5646.1995.tb02301.x. PubMed PMID: 28565142.

21.Rose MR. Laboratory Evolution of Postponed Senescence in Drosophila Melanogaster. Evolution. 1984;38(5):1004-10. Epub 1984/09/01. doi: 10.1111/j.1558-5646.1984.tb00370.x. PubMed PMID: 28555803.

22.Partridge L, Prowse N, Pignatelli P. Another set of responses and correlated responses to selection on age at reproduction in Drosophila melanogaster. Proc Biol Sci. 1999;266(1416):255-

61. Epub 1999/03/19. doi: 10.1098/rspb.1999.0630. PubMed PMID: 10081162; PMCID: PMC1689678.

23.Flatt T, Min KJ, D'Alterio C, Villa-Cuesta E, Cumbers J, Lehmann R, Jones DL, Tatar M. Drosophila germ-line modulation of insulin signaling and lifespan. Proc Natl Acad Sci U S A. 2008;105(17):6368-73. Epub 2008/04/25. doi: 10.1073/pnas.0709128105. PubMed PMID: 18434551; PMCID: PMC2359818.

24.Min KJ, Lee CK, Park HN. The lifespan of Korean eunuchs. Curr Biol. 2012;22(18):R792-3. Epub 2012/09/29. doi: 10.1016/j.cub.2012.06.036. PubMed PMID: 23017989.

25.Hsin H, Kenyon C. Signals from the reproductive system regulate the lifespan of C. elegans. Nature. 1999;399(6734):362-6. Epub 1999/06/09. doi: 10.1038/20694. PubMed PMID: 10360574.

26.Arantes-Oliveira N, Apfeld J, Dillin A, Kenyon C. Regulation of life-span by germ-line stem cells in Caenorhabditis elegans. Science. 2002;295(5554):502-5. Epub 2002/01/19. doi: 10.1126/science.1065768. PubMed PMID: 11799246.

27.Partridge L, Gems D, Withers DJ. Sex and Death: What Is the Connection? Cell. 2005;120(4):461-72. doi: https://doi.org/10.1016/j.cell.2005.01.026.

28.Blacher P, Huggins TJ, Bourke AFG. Evolution of ageing, costs of reproduction and the fecundity-longevity trade-off in eusocial insects. Proc Biol Sci. 2017;284(1858). Epub 2017/07/14. doi: 10.1098/rspb.2017.0380. PubMed PMID: 28701554; PMCID: PMC5524490.

29.Dammann P, Sumbera R, Massmann C, Scherag A, Burda H. Extended longevity of reproductives appears to be common in Fukomys mole-rats (Rodentia, Bathyergidae). PLoS One. 2011;6(4):e18757. Epub 2011/05/03. doi: 10.1371/journal.pone.0018757. PubMed PMID: 21533255; PMCID: PMC3076438.

30.Mason JB, Cargill SL, Anderson GB, Carey JR. Transplantation of young ovaries to old mice increased life span in transplant recipients. J Gerontol A Biol Sci Med Sci. 2009;64(12):1207-11. Epub 2009/09/25. doi: 10.1093/gerona/glp134. PubMed PMID: 19776215; PMCID: PMC2773817.

31.Choy JT, Eisenberg ML. Comprehensive men's health and male infertility. Transl Androl Urol. 2020;9(Suppl 2):S239-S43. Epub 2020/04/08. doi: 10.21037/tau.2019.08.35. PubMed PMID: 32257864; PMCID: PMC7108997.

32.Podfigurna-Stopa A, Czyzyk A, Grymowicz M, Smolarczyk R, Katulski K, Czajkowski K, Meczekalski B. Premature ovarian insufficiency: the context of long-term effects. J Endocrinol Invest. 2016;39(9):983-90. Epub 2016/04/20. doi: 10.1007/s40618-016-0467-z. PubMed PMID: 27091671; PMCID: PMC4987394.

33.Barnes AI, Boone JM, Jacobson J, Partridge L, Chapman T. No extension of lifespan by ablation of germ line in Drosophila. Proceedings Biological sciences. 2006;273(1589):939-47. doi: 10.1098/rspb.2005.3388. PubMed PMID: 16627279.

34.Zhou KI, Pincus Z, Slack FJ. Longevity and stress in Caenorhabditis elegans. Aging (Albany NY). 2011;3(8):733-53. Epub 2011/09/23. doi: 10.18632/aging.100367. PubMed PMID: 21937765; PMCID: PMC3184976.

35.Johnson TE, de Castro E, Hegi de Castro S, Cypser J, Henderson S, Tedesco P. Relationship between increased longevity and stress resistance as assessed through gerontogene mutations in Caenorhabditis elegans. Exp Gerontol. 2001;36(10):1609-17. Epub 2001/10/24. doi: 10.1016/s0531-5565(01)00144-9. PubMed PMID: 11672983.

36.Murakami S. Stress resistance in long-lived mouse models. Exp Gerontol. 2006;41(10):1014-9. Epub 2006/09/12. doi: 10.1016/j.exger.2006.06.061. PubMed PMID: 16962277.

37.Epel ES, Lithgow GJ. Stress biology and aging mechanisms: toward understanding the deep connection between adaptation to stress and longevity. J Gerontol A Biol Sci Med Sci. 2014;69 Suppl 1:S10-6. Epub 2014/05/17. doi: 10.1093/gerona/glu055. PubMed PMID: 24833580; PMCID: PMC4022128.

38.Wang HD, Kazemi-Esfarjani P, Benzer S. Multiple-stress analysis for isolation of Drosophila longevity genes. Proc Natl Acad Sci U S A. 2004;101(34):12610-5. Epub 2004/08/17. doi: 10.1073/pnas.0404648101. PubMed PMID: 15308776; PMCID: PMC515105.

39.Collins JJ, Huang C, Hughes S, Kornfeld K. The measurement and analysis of age-related changes in Caenorhabditis elegans. WormBook. 2008:1-21. Epub 2008/04/03. doi: 10.1895/wormbook.1.137.1. PubMed PMID: 18381800; PMCID: PMC4781475.

40.Fabian DK, Garschall K, Klepsatel P, Santos-Matos G, Sucena E, Kapun M, Lemaitre B, Schlotterer C, Arking R, Flatt T. Evolution of longevity improves immunity in Drosophila. Evol Lett. 2018;2(6):567-79. Epub 2018/12/20. doi: 10.1002/evl3.89. PubMed PMID: 30564440; PMCID: PMC6292704.

41.Xia J, Gravato-Nobre M, Ligoxygakis P. Convergence of longevity and immunity: lessons from animal models. Biogerontology. 2019;20(3):271-8. Epub 2019/02/24. doi: 10.1007/s10522-019-09801-w. PubMed PMID: 30796710; PMCID: PMC6535424.

42.Bansal A, Zhu LJ, Yen K, Tissenbaum HA. Uncoupling lifespan and healthspan in Caenorhabditis elegans longevity mutants. Proc Natl Acad Sci U S A. 2015;112(3):E277-86. Epub 2015/01/07. doi: 10.1073/pnas.1412192112. PubMed PMID: 25561524; PMCID: PMC4311797.

43.Alper S, McElwee MK, Apfeld J, Lackford B, Freedman JH, Schwartz DA. The Caenorhabditis elegans germ line regulates distinct signaling pathways to control lifespan and innate immunity. J Biol Chem. 2010;285(3):1822-8. Epub 2009/11/20. doi: 10.1074/jbc.M109.057323. PubMed PMID: 19923212; PMCID: PMC2804340.

44.Yamawaki TM, Arantes-Oliveira N, Berman JR, Zhang P, Kenyon C. Distinct activities of the germline and somatic reproductive tissues in the regulation of Caenorhabditis elegans' longevity. Genetics. 2008;178(1):513-26. Epub 2008/01/19. doi: 10.1534/genetics.107.083253. PubMed PMID: 18202391; PMCID: PMC2206098.

45.Dues DJ, Andrews EK, Senchuk MM, Van Raamsdonk JM. Resistance to Stress Can Be Experimentally Dissociated From Longevity. J Gerontol A Biol Sci Med Sci. 2019;74(8):1206-14. Epub 2018/09/25. doi: 10.1093/gerona/gly213. PubMed PMID: 30247515; PMCID: PMC6625593.

46.Lin YJ, Seroude L, Benzer S. Extended life-span and stress resistance in the Drosophila mutant methuselah. Science. 1998;282(5390):943-6. Epub 1998/10/30. doi: 10.1126/science.282.5390.943. PubMed PMID: 9794765.

47.TeKippe M, Aballay A. C. elegans germline-deficient mutants respond to pathogen infection using shared and distinct mechanisms. PLoS One. 2010;5(7):e11777. Epub 2010/07/30. doi: 10.1371/journal.pone.0011777. PubMed PMID: 20668681; PMCID: PMC2909909.

48.Keith SA, Amrit FR, Ratnappan R, Ghazi A. The C. elegans healthspan and stress-resistance assay toolkit. Methods. 2014;68(3):476-86. Epub 2014/04/15. doi: 10.1016/j.ymeth.2014.04.003. PubMed PMID: 24727065.

49.Kourtis AP, Read JS, Jamieson DJ. Pregnancy and infection. N Engl J Med. 2014;371(11):1077. Epub 2014/09/11. doi: 10.1056/NEJMc1408436. PubMed PMID: 25207782.

50.Littauer EQ, Esser ES, Antao OQ, Vassilieva EV, Compans RW, Skountzou I. H1N1 influenza virus infection results in adverse pregnancy outcomes by disrupting tissue-specific hormonal regulation. PLoS Pathog. 2017;13(11):e1006757. Epub 2017/11/28. doi: 10.1371/journal.ppat.1006757. PubMed PMID: 29176767; PMCID: PMC5720832.

51.Rowe JH, Ertelt JM, Aguilera MN, Farrar MA, Way SS. Foxp3(+) regulatory T cell expansion required for sustaining pregnancy compromises host defense against prenatal bacterial pathogens. Cell Host Microbe. 2011;10(1):54-64. Epub 2011/07/20. doi: 10.1016/j.chom.2011.06.005. PubMed PMID: 21767812; PMCID: PMC3140139.

52.Robinson DP, Klein SL. Pregnancy and pregnancy-associated hormones alter immune responses and disease pathogenesis. Horm Behav. 2012;62(3):263-71. Epub 2012/03/13. doi: 10.1016/j.yhbeh.2012.02.023. PubMed PMID: 22406114; PMCID: PMC3376705.

53.Patas K, Engler JB, Friese MA, Gold SM. Pregnancy and multiple sclerosis: feto-maternal immune cross talk and its implications for disease activity. J Reprod Immunol. 2013;97(1):140-6. Epub 2013/02/26. doi: 10.1016/j.jri.2012.10.005. PubMed PMID: 23432880.

54.Krishnan L, Nguyen T, McComb S. From mice to women: the conundrum of immunity to infection during pregnancy. J Reprod Immunol. 2013;97(1):62-73. Epub 2013/02/26. doi: 10.1016/j.jri.2012.10.015. PubMed PMID: 23432873; PMCID: PMC3748615.

55.Blackwell AD. Helminth infection during pregnancy: insights from evolutionary ecology. Int J Womens Health. 2016;8:651-61. Epub 2016/12/14. doi: 10.2147/IJWH.S103529. PubMed PMID: 27956844; PMCID: PMC5113914.

56.Szekeres-Bartho J. The Role of Progesterone in Feto-Maternal Immunological Cross Talk. Med Princ Pract. 2018;27(4):301-7. Epub 2018/06/28. doi: 10.1159/000491576. PubMed PMID: 29949797; PMCID: PMC6167700.

57.Sen A, Kushnir VA, Barad DH, Gleicher N. Endocrine autoimmune diseases and female infertility. Nat Rev Endocrinol. 2014;10(1):37-50. Epub 2013/11/06. doi: 10.1038/nrendo.2013.212. PubMed PMID: 24189508.

58.Wang WJ, Hao CF, Yi L, Yin GJ, Bao SH, Qiu LH, Lin QD. Increased prevalence of T helper 17 (Th17) cells in peripheral blood and decidua in unexplained recurrent spontaneous abortion patients. J Reprod Immunol. 2010;84(2):164-70. Epub 2010/01/29. doi: 10.1016/j.jri.2009.12.003. PubMed PMID: 20106535.

59.Knutson AO, Watters JJ. All roads lead to inflammation: Is maternal immune activation a common culprit behind environmental factors impacting offspring neural control of breathing? Respir Physiol Neurobiol. 2020;274:103361. Epub 2019/12/25. doi: 10.1016/j.resp.2019.103361. PubMed PMID: 31874263; PMCID: PMC6952303.

60.Cappelletti M, Della Bella S, Ferrazzi E, Mavilio D, Divanovic S. Inflammation and preterm birth. J Leukoc Biol. 2016;99(1):67-78. Epub 2015/11/06. doi: 10.1189/jlb.3MR0615-272RR. PubMed PMID: 26538528.

61.Makhseed M, Raghupathy R, Azizieh F, Omu A, Al-Shamali E, Ashkanani L. Th1 and Th2 cytokine profiles in recurrent aborters with successful pregnancy and with subsequent abortions. Hum Reprod. 2001;16(10):2219-26. Epub 2001/09/28. doi: 10.1093/humrep/16.10.2219. PubMed PMID: 11574519.

62.Schwenke RA, Lazzaro BP, Wolfner MF. Reproduction-Immunity Trade-Offs in Insects. Annu Rev Entomol. 2016;61:239-56. Epub 2015/12/17. doi: 10.1146/annurev-ento-010715-023924. PubMed PMID: 26667271; PMCID: PMC5231921.

63.Mylonakis E, Ausubel FM, Perfect JR, Heitman J, Calderwood SB. Killing of Caenorhabditis elegans by Cryptococcus neoformans as a model of yeast pathogenesis. Proceedings of the National Academy of Sciences. 2002;99(24):15675-80. doi: 10.1073/pnas.232568599.

64.Hwang S-B, Choi J-G, Wei S, Park B-J, Chelliah R, Oh D-H. In vivo screening platform for shiga toxin-producing Escherichia coli (STEC) using Caenorhabditis elegans as a model. PloS one. 2018;13(2):e0193277-e. doi: 10.1371/journal.pone.0193277. PubMed PMID: 29489863.

65.Tang RJ, Breger J, Idnurm A, Gerik KJ, Lodge JK, Heitman J, Calderwood SB, Mylonakis E. Cryptococcus neoformans gene involved in mammalian pathogenesis identified by a Caenorhabditis elegans progeny-based approach. Infect Immun. 2005;73(12):8219-25. Epub 2005/11/22. doi: 10.1128/IAI.73.12.8219-8225.2005. PubMed PMID: 16299318; PMCID: PMC1307092.

66.Bonney EA. Immune Regulation in Pregnancy: A Matter of Perspective? Obstet Gynecol Clin North Am. 2016;43(4):679-98. Epub 2016/11/07. doi: 10.1016/j.ogc.2016.07.004. PubMed PMID: 27816154; PMCID: PMC5527289.

67.Howick VM, Lazzaro BP. Genotype and diet shape resistance and tolerance across distinct phases of bacterial infection. BMC Evol Biol. 2014;14(1):56. Epub 2014/03/25. doi: 10.1186/1471-2148-14-56. PubMed PMID: 24655914; PMCID: PMC3997931.

68.Oku KP, T. A. R.; Wedell, N. Does mating negatively affect female immune defences in insects? Animal Biology. 2019;69(1):117-36. doi: https://doi.org/10.1163/15707563-20191082.

69.Short SM, Lazzaro BP. Female and male genetic contributions to post-mating immune defence in female Drosophila melanogaster. Proc Biol Sci. 2010;277(1700):3649-57. Epub 2010/06/25. doi: 10.1098/rspb.2010.0937. PubMed PMID: 20573620; PMCID: PMC2982248.

70.Short SM, Wolfner MF, Lazzaro BP. Female Drosophila melanogaster suffer reduced defense against infection due to seminal fluid components. J Insect Physiol. 2012;58(9):1192-201. Epub 2012/06/16. doi: 10.1016/j.jinsphys.2012.06.002. PubMed PMID: 22698822; PMCID: PMC3423548.

71.Maures TJ, Booth LN, Benayoun BA, Izrayelit Y, Schroeder FC, Brunet A. Males shorten the life span of C. elegans hermaphrodites via secreted compounds. Science. 2014;343(6170):541-4. Epub 2013/12/03. doi: 10.1126/science.1244160. PubMed PMID: 24292626; PMCID: PMC4126796.

72.Chapman T, Liddle LF, Kalb JM, Wolfner MF, Partridge L. Cost of mating in Drosophila melanogaster females is mediated by male accessory gland products. Nature. 1995;373(6511):241-4. Epub 1995/01/19. doi: 10.1038/373241a0. PubMed PMID: 7816137.

73.Schedl T. Developmental Genetics of the Germ Line. In: nd, Riddle DL, Blumenthal T, Meyer BJ, Priess JR, editors. C elegans II. Cold Spring Harbor (NY)1997.

74.Lui DY, Colaiacovo MP. Meiotic development in Caenorhabditis elegans. Adv Exp Med Biol. 2013;757:133-70. Epub 2012/08/09. doi: 10.1007/978-1-4614-4015-4_6. PubMed PMID: 22872477; PMCID: PMC3764601.

75.Templeman NM, Luo S, Kaletsky R, Shi C, Ashraf J, Keyes W, Murphy CT. Insulin Signaling Regulates Oocyte Quality Maintenance with Age via Cathepsin B Activity. Curr Biol. 2018;28(5):753-60 e4. Epub 2018/02/27. doi: 10.1016/j.cub.2018.01.052. PubMed PMID: 29478855; PMCID: PMC5893159.

76.Perez MF, Lehner B. Vitellogenins - Yolk Gene Function and Regulation in Caenorhabditis elegans. Front Physiol. 2019;10:1067. Epub 2019/09/26. doi: 10.3389/fphys.2019.01067. PubMed PMID: 31551797; PMCID: PMC6736625.

77.Corsi AK, Wightman B, Chalfie M. A Transparent window into biology: A primer on Caenorhabditis elegans. WormBook. 2015:1-31. Epub 2015/06/19. doi: 10.1895/wormbook.1.177.1. PubMed PMID: 26087236; PMCID: PMC4781331.

78.Yuen GJ, Ausubel FM. Both live and dead Enterococci activate Caenorhabditis elegans host defense via immune and stress pathways. Virulence. 2018;9(1):683-99. Epub 2018/02/14. doi: 10.1080/21505594.2018.1438025. PubMed PMID: 29436902; PMCID: PMC5955442.

79.Kim DH, Ewbank JJ. Signaling in the innate immune response. WormBook. 2018;2018:1-35. Epub 2015/12/24. doi: 10.1895/wormbook.1.83.2. PubMed PMID: 26694508; PMCID: PMC6369418.

80.Liu Y, Sun J. Detection of Pathogens and Regulation of Immunity by the Caenorhabditis elegans Nervous System. mBio. 2021;12(2). Epub 2021/04/01. doi: 10.1128/mBio.02301-20. PubMed PMID: 33785621; PMCID: PMC8092265.

81.Lai CH, Chou CY, Ch'ang LY, Liu CS, Lin W. Identification of novel human genes evolutionarily conserved in Caenorhabditis elegans by comparative proteomics. Genome Research. 2000;10(5):703-13. Epub 2000/05/16. doi: 10.1101/gr.10.5.703. PubMed PMID: 10810093; PMCID: PMC310876.

82.Dowen RH. CEH-60/PBX and UNC-62/MEIS Coordinate a Metabolic Switch that Supports Reproduction in C. elegans. Dev Cell. 2019;49(2):235-50 e7. Epub 2019/04/09. doi: 10.1016/j.devcel.2019.03.002. PubMed PMID: 30956009.

83.Klass MR. Aging in the nematode Caenorhabditis elegans: major biological and environmental factors influencing life span. Mech Ageing Dev. 1977;6(6):413-29. Epub 1977/11/01. doi: 10.1016/0047-6374(77)90043-4. PubMed PMID: 926867.

84.Mathew MD, Mathew ND, Ebert PR. WormScan: a technique for high-throughput phenotypic analysis of Caenorhabditis elegans. PLoS One. 2012;7(3):e33483. Epub 2012/03/30. doi: 10.1371/journal.pone.0033483. PubMed PMID: 22457766; PMCID: PMC3311640.

85.Garcia Garvi A, Puchalt JC, Layana Castro PE, Navarro Moya F, Sanchez-Salmeron AJ. Towards Lifespan Automation for Caenorhabditis elegans Based on Deep Learning: Analysing Convolutional and Recurrent Neural Networks for Dead or Live Classification. Sensors (Basel). 2021;21(14). Epub 2021/07/25. doi: 10.3390/s21144943. PubMed PMID: 34300683; PMCID: PMC8309694.

86.Klass MR. A method for the isolation of longevity mutants in the nematode Caenorhabditis elegans and initial results. Mech Ageing Dev. 1983;22(3-4):279-86. Epub 1983/07/01. doi: 10.1016/0047-6374(83)90082-9. PubMed PMID: 6632998.

87.Friedman DB, Johnson TE. A mutation in the age-1 gene in Caenorhabditis elegans lengthens life and reduces hermaphrodite fertility. Genetics. 1988;118(1):75-86. Epub 1988/01/01. doi: 10.1093/genetics/118.1.75. PubMed PMID: 8608934; PMCID: PMC1203268.

88.Tissenbaum HA. Using C. elegans for aging research. Invertebrate reproduction & development. 2015;59(sup1):59-63. Epub 2014/12/09. doi: 10.1080/07924259.2014.940470. PubMed PMID: 26136622.

89.Kenyon C, Chang J, Gensch E, Rudner A, Tabtiang R. A C. elegans mutant that lives twice as long as wild type. Nature. 1993;366(6454):461-4. doi: 10.1038/366461a0.

90.Kenyon C. The first long-lived mutants: discovery of the insulin/IGF-1 pathway for ageing. Philos Trans R Soc Lond B Biol Sci. 2011;366(1561):9-16. Epub 2010/12/01. doi: 10.1098/rstb.2010.0276. PubMed PMID: 21115525; PMCID: PMC3001308.

91.Murphy CT, McCarroll SA, Bargmann CI, Fraser A, Kamath RS, Ahringer J, Li H, Kenyon C. Genes that act downstream of DAF-16 to influence the lifespan of Caenorhabditis elegans. Nature. 2003;424(6946):277-83. Epub 2003/07/08. doi: 10.1038/nature01789. PubMed PMID: 12845331.

92.Oh SW, Mukhopadhyay A, Dixit BL, Raha T, Green MR, Tissenbaum HA. Identification of direct DAF-16 targets controlling longevity, metabolism and diapause by chromatin immunoprecipitation. Nat Genet. 2006;38(2):251-7. Epub 2005/12/29. doi: 10.1038/ng1723. PubMed PMID: 16380712.

93.Bartke A. Insulin and aging. Cell Cycle. 2008;7(21):3338-43. Epub 2008/10/25. doi: 10.4161/cc.7.21.7012. PubMed PMID: 18948730.

94.Mathew R, Pal Bhadra M, Bhadra U. Insulin/insulin-like growth factor-1 signalling (IIS) based regulation of lifespan across species. Biogerontology. 2017;18(1):35-53. Epub 2017/01/20. doi: 10.1007/s10522-016-9670-8. PubMed PMID: 28101820.

95.Willcox BJ, Donlon TA, He Q, Chen R, Grove JS, Yano K, Masaki KH, Willcox DC, Rodriguez B, Curb JD. FOXO3A genotype is strongly associated with human longevity. Proc Natl Acad Sci U S A. 2008;105(37):13987-92. Epub 2008/09/04. doi: 10.1073/pnas.0801030105. PubMed PMID: 18765803; PMCID: PMC2544566.

96.Suh Y, Atzmon G, Cho MO, Hwang D, Liu B, Leahy DJ, Barzilai N, Cohen P. Functionally significant insulin-like growth factor I receptor mutations in centenarians. Proc Natl Acad Sci U S A. 2008;105(9):3438-42. Epub 2008/03/05. doi: 10.1073/pnas.0705467105. PubMed PMID: 18316725; PMCID: PMC2265137.

97.Morley JF, Morimoto RI. Regulation of longevity in Caenorhabditis elegans by heat shock factor and molecular chaperones. Mol Biol Cell. 2004;15(2):657-64. Epub 2003/12/12. doi: 10.1091/mbc.e03-07-0532. PubMed PMID: 14668486; PMCID: PMC329286.

98.Austin J, Kimble J. glp-1 is required in the germ line for regulation of the decision between mitosis and meiosis in C. elegans. Cell. 1987;51(4):589-99. Epub 1987/11/20. doi: 10.1016/0092-8674(87)90128-0. PubMed PMID: 3677168.

99.Amrit FRG, Ghazi A. Influences of Germline Cells on Organismal Lifespan and Healthspan. In: Olsen A, Gill MS, editors. Ageing: Lessons from C elegans. Cham: Springer International Publishing; 2017. p. 109-35.

100.Taubert S, Ward JD, Yamamoto KR. Nuclear hormone receptors in nematodes: evolution and function. Mol Cell Endocrinol. 2011;334(1-2):49-55. Epub 2010/05/05. doi: 10.1016/j.mce.2010.04.021. PubMed PMID: 20438802; PMCID: PMC3042524.

101.Kersten S, Stienstra R. The role and regulation of the peroxisome proliferator activated receptor alpha in human liver. Biochimie. 2017;136:75-84. Epub 2017/01/13. doi: 10.1016/j.biochi.2016.12.019. PubMed PMID: 28077274.

102.Tenenbaum A, Fisman EZ. Fibrates are an essential part of modern anti-dyslipidemic arsenal: spotlight on atherogenic dyslipidemia and residual risk reduction. Cardiovasc Diabetol. 2012;11:125. Epub 2012/10/13. doi: 10.1186/1475-2840-11-125. PubMed PMID: 23057687; PMCID: PMC3489608.

103.Taubert S, Van Gilst MR, Hansen M, Yamamoto KR. A Mediator subunit, MDT-15, integrates regulation of fatty acid metabolism by NHR-49-dependent and -independent pathways in C. elegans. Genes Dev. 2006;20(9):1137-49. Epub 2006/05/03. doi: 10.1101/gad.1395406. PubMed PMID: 16651656; PMCID: PMC1472473.

104.Ratnappan R, Amrit FR, Chen SW, Gill H, Holden K, Ward J, Yamamoto KR, Olsen CP, Ghazi A. Germline signals deploy NHR-49 to modulate fatty-acid beta-oxidation and desaturation in somatic tissues of C. elegans. PLoS Genet. 2014;10(12):e1004829. Epub 2014/12/05. doi: 10.1371/journal.pgen.1004829. PubMed PMID: 25474470; PMCID: PMC4256272.

105.Goh GYS, Winter JJ, Bhanshali F, Doering KRS, Lai R, Lee K, Veal EA, Taubert S. NHR-49/HNF4 integrates regulation of fatty acid metabolism with a protective transcriptional response to oxidative stress and fasting. Aging Cell. 2018;17(3):e12743. Epub 2018/03/07. doi: 10.1111/acel.12743. PubMed PMID: 29508513; PMCID: PMC5946062.

106.Sanchez-Hernandez N, Boireau S, Schmidt U, Munoz-Cobo JP, Hernandez-Munain C, Bertrand E, Sune C. The in vivo dynamics of TCERG1, a factor that couples transcriptional elongation with splicing. RNA. 2016;22(4):571-82. Epub 2016/02/14. doi: 10.1261/rna.052795.115. PubMed PMID: 26873599; PMCID: PMC4793212.

107.Coiras M, Montes M, Montanuy I, Lopez-Huertas MR, Mateos E, Le Sommer C, Garcia-Blanco MA, Hernandez-Munain C, Alcami J, Sune C. Transcription elongation regulator 1 (TCERG1) regulates competent RNA polymerase II-mediated elongation of HIV-1 transcription and facilitates efficient viral replication. Retrovirology. 2013;10:124. Epub 2013/10/30. doi: 10.1186/1742-4690-10-124. PubMed PMID: 24165037; PMCID: PMC3874760.

108.Holbert S, Denghien I, Kiechle T, Rosenblatt A, Wellington C, Hayden MR, Margolis RL, Ross CA, Dausset J, Ferrante RJ, Neri C. The Gln-Ala repeat transcriptional activator CA150 interacts with huntingtin: neuropathologic and genetic evidence for a role in Huntington's disease pathogenesis. Proc Natl Acad Sci U S A. 2001;98(4):1811-6. Epub 2001/02/15. doi: 10.1073/pnas.041566798. PubMed PMID: 11172033; PMCID: PMC29339.

109.Ghazi A, Henis-Korenblit S, Kenyon C. A transcription elongation factor that links signals from the reproductive system to lifespan extension in Caenorhabditis elegans. PLoS Genet. 2009;5(9):e1000639. Epub 2009/09/15. doi: 10.1371/journal.pgen.1000639. PubMed PMID: 19749979; PMCID: PMC2729384.

110.Amrit FR, Steenkiste EM, Ratnappan R, Chen SW, McClendon TB, Kostka D, Yanowitz J, Olsen CP, Ghazi A. DAF-16 and TCER-1 Facilitate Adaptation to Germline Loss by Restoring Lipid Homeostasis and Repressing Reproductive Physiology in C. elegans. PLoS Genet. 2016;12(2):e1005788. Epub 2016/02/11. doi: 10.1371/journal.pgen.1005788. PubMed PMID: 26862916; PMCID: PMC4749232.

111.Kocabas AM, Crosby J, Ross PJ, Otu HH, Beyhan Z, Can H, Tam W-L, Rosa GJM, Halgren RG, Lim B, Fernandez E, Cibelli JB. The transcriptome of human oocytes. Proceedings of the National Academy of Sciences. 2006;103(38):14027-32. doi: 10.1073/pnas.0603227103.

112.Zheng X, Pedersen LC, Gabel SA, Mueller GA, DeRose EF, London RE. Unfolding the HIV-1 reverse transcriptase RNase H domain--how to lose a molecular tug-of-war. Nucleic Acids Res. 2016;44(4):1776-88. Epub 2016/01/17. doi: 10.1093/nar/gkv1538. PubMed PMID: 26773054; PMCID: PMC4770237.

113.Zheng P, Patel B, McMenamin M, Moran E, Paprocki AM, Kihara M, Schramm RD, Latham KE. Effects of Follicle Size and Oocyte Maturation Conditions on Maternal Messenger RNA Regulation and Gene Expression in Rhesus Monkey Oocytes and Embryos1. Biology of Reproduction. 2005;72(4):890-7. doi: 10.1095/biolreprod.104.035881.

114.Steuerwald NM, Bermudez, M.G., Wells, D., Munne, S., Cohen, J. Maternal age-related differential global expression profiles observed in human oocytes. Reproductive BioMedicine Online,. 2007;14(6):700-8. doi: doi:10.1016/S1472-6483(10)60671-2.

115.Corsi AK, Wightman B, Chalfie M. A Transparent Window into Biology: A Primer on Caenorhabditis elegans. Genetics. 2015;200(2):387-407. Epub 2015/06/20. doi: 10.1534/genetics.115.176099. PubMed PMID: 26088431; PMCID: PMC4492366.

116.Argon Y, Ward S. Caenorhabditis elegans fertilization-defective mutants with abnormal sperm. Genetics. 1980;96(2):413-33. Epub 1980/10/01. doi: 10.1093/genetics/96.2.413. PubMed PMID: 7196361; PMCID: PMC1214308.

117.Kadandale P, Singson A. Oocyte production and sperm utilization patterns in semi-fertile strains of Caenorhabditis elegans. BMC Dev Biol. 2004;4:3. Epub 2004/04/17. doi: 10.1186/1471-213X-4-3. PubMed PMID: 15086962; PMCID: PMC404374.

118.Graham PL, Schedl T, Kimble J. More mog genes that influence the switch from spermatogenesis to oogenesis in the hermaphrodite germ line of Caenorhabditis elegans. Dev Genet. 1993;14(6):471-84. Epub 1993/01/01. doi: 10.1002/dvg.1020140608. PubMed PMID: 8111975.

119.Hubbard EJ, Greenstein D. The Caenorhabditis elegans gonad: a test tube for cell and developmental biology. Dev Dyn. 2000;218(1):2-22. Epub 2000/05/24. doi: 10.1002/(SICI)1097-0177(200005)218:1<2::AID-DVDY2>3.0.CO;2-W. PubMed PMID: 10822256.

120.Rog O, Dernburg AF. Chromosome pairing and synapsis during Caenorhabditis elegans meiosis. Curr Opin Cell Biol. 2013;25(3):349-56. Epub 2013/04/13. doi: 10.1016/j.ceb.2013.03.003. PubMed PMID: 23578368; PMCID: PMC3694717.

121.Kitagawa R. Key players in chromosome segregation in Caenorhabditis elegans. Front Biosci (Landmark Ed). 2009;14:1529-57. Epub 2009/03/11. doi: 10.2741/3323. PubMed PMID: 19273145; PMCID: PMC2745088.

122.Goodwin EB, Ellis RE. Turning clustering loops: sex determination in Caenorhabditis elegans. Curr Biol. 2002;12(3):R111-20. Epub 2002/02/13. doi: 10.1016/s0960-9822(02)00675-9. PubMed PMID: 11839294.

123.Luo S, Kleemann GA, Ashraf JM, Shaw WM, Murphy CT. TGF-beta and insulin signaling regulate reproductive aging via oocyte and germline quality maintenance. Cell. 2010;143(2):299-312. Epub 2010/10/16. doi: 10.1016/j.cell.2010.09.013. PubMed PMID: 20946987; PMCID: PMC2955983.

124.Luo S, Shaw WM, Ashraf J, Murphy CT. TGF-beta Sma/Mab signaling mutations uncouple reproductive aging from somatic aging. PLoS Genet. 2009;5(12):e1000789. Epub 2009/12/31. doi: 10.1371/journal.pgen.1000789. PubMed PMID: 20041217; PMCID: PMC2791159.

125.Hughes SE, Evason K, Xiong C, Kornfeld K. Genetic and pharmacological factors that influence reproductive aging in nematodes. PLoS Genetics. 2005;preprint(2006). doi: 10.1371/journal.pgen.0030025.eor.

126.Samaddar M, Goudeau J, Sanchez M, Hall DH, Bohnert KA, Ingaramo M, Kenyon C. A genetic screen identifies new steps in oocyte maturation that enhance proteostasis in the immortal germ lineage. Elife. 2021;10. Epub 2021/04/14. doi: 10.7554/eLife.62653. PubMed PMID: 33848238; PMCID: PMC8043744.

127.Han SM, Cottee PA, Miller MA. Sperm and oocyte communication mechanisms controlling C. elegans fertility. Dev Dyn. 2010;239(5):1265-81. Epub 2009/12/25. doi: 10.1002/dvdy.22202. PubMed PMID: 20034089; PMCID: PMC2963114.

128.Luo S, Murphy CT. Caenorhabditis elegans reproductive aging: Regulation and underlying mechanisms. Genesis (New York, NY : 2000). 2011;49(2):53-65. Epub 2010/11/26. doi: 10.1002/dvg.20694. PubMed PMID: 21105070.

129.Hughes SE, Evason K, Xiong C, Kornfeld K. Genetic and pharmacological factors that influence reproductive aging in nematodes. PLoS Genet. 2007;3(2):e25. Epub 2007/02/20. doi: 10.1371/journal.pgen.0030025. PubMed PMID: 17305431; PMCID: PMC1797816.

130.Huang C, Xiong C, Kornfeld K. Measurements of age-related changes of physiological processes that predict lifespan of Caenorhabditis elegans. Proc Natl Acad Sci U S A. 2004;101(21):8084-9. Epub 2004/05/14. doi: 10.1073/pnas.0400848101. PubMed PMID: 15141086; PMCID: PMC419561.

131.Carranza-Garcia E, Navarro RE. Insights Into the Hypometabolic Stage Caused by Prolonged Starvation in L4-Adult Caenorhabditis elegans Hermaphrodites. Front Cell Dev Biol. 2020;8:124. Epub 2020/03/27. doi: 10.3389/fcell.2020.00124. PubMed PMID: 32211406; PMCID: PMC7057233.

132.Schaffler A, Scholmerich J. Innate immunity and adipose tissue biology. Trends Immunol. 2010;31(6):228-35. Epub 2010/05/04. doi: 10.1016/j.it.2010.03.001. PubMed PMID: 20434953.

133.Vrablik TL, Watts JL. Polyunsaturated fatty acid derived signaling in reproduction and development: insights from Caenorhabditis elegans and Drosophila melanogaster. Mol Reprod Dev. 2013;80(4):244-59. Epub 2013/02/27. doi: 10.1002/mrd.22167. PubMed PMID: 23440886; PMCID: PMC4350910.

134.Lynn DA, Dalton HM, Sowa JN, Wang MC, Soukas AA, Curran SP. Omega-3 and -6 fatty acids allocate somatic and germline lipids to ensure fitness during nutrient and oxidative stress in Caenorhabditis elegans. Proc Natl Acad Sci U S A. 2015;112(50):15378-83. Epub 2015/12/02. doi: 10.1073/pnas.1514012112. PubMed PMID: 26621724; PMCID: PMC4687584.

135.Matsuoka S, Armstrong AR, Sampson LL, Laws KM, Drummond-Barbosa D. Adipocyte Metabolic Pathways Regulated by Diet Control the Female Germline Stem Cell Lineage in Drosophila melanogaster. Genetics. 2017;206(2):953-71. Epub 2017/04/12. doi: 10.1534/genetics.117.201921. PubMed PMID: 28396508; PMCID: PMC5499197.

136.Sun C, Zhang S. Immune-Relevant and Antioxidant Activities of Vitellogenin and Yolk Proteins in Fish. Nutrients. 2015;7(10):8818-29. Epub 2015/10/28. doi: 10.3390/nu7105432. PubMed PMID: 26506386; PMCID: PMC4632452.

137.Fischer M, Regitz C, Kull R, Boll M, Wenzel U. Vitellogenins increase stress resistance of Caenorhabditis elegans after Photorhabdus luminescens infection depending on the steroid-signaling pathway. Microbes Infect. 2013;15(8-9):569-78. Epub 2013/06/04. doi: 10.1016/j.micinf.2013.05.002. PubMed PMID: 23727258.

138.Alper S, McBride SJ, Lackford B, Freedman JH, Schwartz DA. Specificity and complexity of the Caenorhabditis elegans innate immune response. Mol Cell Biol. 2007;27(15):5544-53. Epub 2007/05/29. doi: 10.1128/MCB.02070-06. PubMed PMID: 17526726; PMCID: PMC1952075.

139.Wong D, Bazopoulou D, Pujol N, Tavernarakis N, Ewbank JJ. Genome-wide investigation reveals pathogen-specific and shared signatures in the response of Caenorhabditis elegans to infection. Genome Biol. 2007;8(9):R194. Epub 2007/09/19. doi: 10.1186/gb-2007-8-9-r194. PubMed PMID: 17875205; PMCID: PMC2375032.

140.Pukkila-Worley R, Ausubel FM. Immune defense mechanisms in the Caenorhabditis elegans intestinal epithelium. Curr Opin Immunol. 2012;24(1):3-9. Epub 2012/01/13. doi: 10.1016/j.coi.2011.10.004. PubMed PMID: 22236697; PMCID: PMC3660727.

141.Ermolaeva MA, Schumacher B. Insights from the worm: the C. elegans model for innate immunity. Semin Immunol. 2014;26(4):303-9. Epub 2014/05/27. doi: 10.1016/j.smim.2014.04.005. PubMed PMID: 24856329; PMCID: PMC4248339.

142.Dierking K, Yang W, Schulenburg H. Antimicrobial effectors in the nematode Caenorhabditis elegans: an outgroup to the Arthropoda. Philos Trans R Soc Lond B Biol Sci. 2016;371(1695). Epub 2016/05/11. doi: 10.1098/rstb.2015.0299. PubMed PMID: 27160601; PMCID: PMC4874396.

143.Pukkila-Worley R. Surveillance Immunity: An Emerging Paradigm of Innate Defense Activation in Caenorhabditis elegans. PLoS Pathog. 2016;12(9):e1005795. Epub 2016/09/16. doi: 10.1371/journal.ppat.1005795. PubMed PMID: 27631629; PMCID: PMC5025020.

144.Cohen LB, Troemel ER. Microbial pathogenesis and host defense in the nematode C. elegans. Curr Opin Microbiol. 2015;23:94-101. Epub 2014/12/03. doi: 10.1016/j.mib.2014.11.009. PubMed PMID: 25461579; PMCID: PMC4324121.

145.Soares-Silva M, Diniz FF, Gomes GN, Bahia D. The Mitogen-Activated Protein Kinase (MAPK) Pathway: Role in Immune Evasion by Trypanosomatids. Front Microbiol. 2016;7:183. Epub 2016/03/05. doi: 10.3389/fmicb.2016.00183. PubMed PMID: 26941717; PMCID: PMC4764696.

146.Kim DH, Feinbaum R, Alloing G, Emerson FE, Garsin DA, Inoue H, Tanaka-Hino M, Hisamoto N, Matsumoto K, Tan MW, Ausubel FM. A conserved p38 MAP kinase pathway in Caenorhabditis elegans innate immunity. Science. 2002;297(5581):623-6. Epub 2002/07/27. doi: 10.1126/science.1073759. PubMed PMID: 12142542.

147.Fletcher M, Tillman EJ, Butty VL, Levine SS, Kim DH. Global transcriptional regulation of innate immunity by ATF-7 in C. elegans. PLoS Genet. 2019;15(2):e1007830. Epub 2019/02/23. doi: 10.1371/journal.pgen.1007830. PubMed PMID: 30789901; PMCID: PMC6400416.

148.Troemel ER, Chu SW, Reinke V, Lee SS, Ausubel FM, Kim DH. p38 MAPK regulates expression of immune response genes and contributes to longevity in C. elegans. PLoS Genet. 2006;2(11):e183. Epub 2006/11/14. doi: 10.1371/journal.pgen.0020183. PubMed PMID: 17096597; PMCID: PMC1635533.

149.Kim DH, Liberati NT, Mizuno T, Inoue H, Hisamoto N, Matsumoto K, Ausubel FM. Integration of Caenorhabditis elegans MAPK pathways mediating immunity and stress resistance by MEK-1 MAPK kinase and VHP-1 MAPK phosphatase. Proc Natl Acad Sci U S A. 2004;101(30):10990-4. Epub 2004/07/17. doi: 10.1073/pnas.0403546101. PubMed PMID: 15256594; PMCID: PMC503731.

150.Mallo GV, Kurz CL, Couillault C, Pujol N, Granjeaud S, Kohara Y, Ewbank JJ. Inducible antibacterial defense system in C. elegans. Curr Biol. 2002;12(14):1209-14. Epub 2002/08/15. doi: 10.1016/s0960-9822(02)00928-4. PubMed PMID: 12176330.

151.Gumienny TL, Savage-Dunn C. TGF-beta signaling in C. elegans. WormBook. 2013:1-34. Epub 2013/08/03. doi: 10.1895/wormbook.1.22.2. PubMed PMID: 23908056; PMCID: PMC5081272.

152.Reddy KC, Dror T, Sowa JN, Panek J, Chen K, Lim ES, Wang D, Troemel ER. An Intracellular Pathogen Response Pathway Promotes Proteostasis in C. elegans. Curr Biol. 2017;27(22):3544-53 e5. Epub 2017/11/07. doi: 10.1016/j.cub.2017.10.009. PubMed PMID: 29103937; PMCID: PMC5698132.

153.Reddy KC, Dror T, Underwood RS, Osman GA, Elder CR, Desjardins CA, Cuomo CA, Barkoulas M, Troemel ER. Antagonistic paralogs control a switch between growth and pathogen resistance in C. elegans. PLoS Pathog. 2019;15(1):e1007528. Epub 2019/01/15. doi: 10.1371/journal.ppat.1007528. PubMed PMID: 30640956; PMCID: PMC6347328.

154.Garsin DA, Villanueva JM, Begun J, Kim DH, Sifri CD, Calderwood SB, Ruvkun G, Ausubel FM. Long-lived C. elegans daf-2 mutants are resistant to bacterial pathogens. Science. 2003;300(5627):1921. Epub 2003/06/21. doi: 10.1126/science.1080147. PubMed PMID: 12817143.

155.Murphy CT, Hu PJ. Insulin/insulin-like growth factor signaling in C. elegans. WormBook. 2013:1-43. Epub 2014/01/08. doi: 10.1895/wormbook.1.164.1. PubMed PMID: 24395814; PMCID: PMC4780952.

156.Roselli M, Schifano E, Guantario B, Zinno P, Uccelletti D, Devirgiliis C. Caenorhabditis Elegans and Probiotics Interactions from a Prolongevity Perspective. Int J Mol Sci. 2019;20(20). Epub 2019/10/30. doi: 10.3390/ijms20205020. PubMed PMID: 31658751; PMCID: PMC6834311.

157.Ewbank JJ. Signaling in the immune response. WormBook. 2006:1-12. Epub 2007/12/01. doi: 10.1895/wormbook.1.83.1. PubMed PMID: 18050470; PMCID: PMC4781569.

158.Hamilton AJ, Baulcombe DC. A species of small antisense RNA in posttranscriptional gene silencing in plants. Science. 1999;286(5441):950-2. Epub 1999/11/05. doi: 10.1126/science.286.5441.950. PubMed PMID: 10542148.

159.Castel SE, Martienssen RA. RNA interference in the nucleus: roles for small RNAs in transcription, epigenetics and beyond. Nat Rev Genet. 2013;14(2):100-12. Epub 2013/01/19. doi: 10.1038/nrg3355. PubMed PMID: 23329111; PMCID: PMC4205957.

160.Youngman EM, Claycomb JM. From early lessons to new frontiers: the worm as a treasure trove of small RNA biology. Front Genet. 2014;5:416. Epub 2014/12/17. doi: 10.3389/fgene.2014.00416. PubMed PMID: 25505902; PMCID: PMC4245922.

161.Hoogstrate SW, Volkers RJ, Sterken MG, Kammenga JE, Snoek LB. Nematode endogenous small RNA pathways. Worm. 2014;3:e28234. Epub 2014/10/24. doi: 10.4161/worm.28234. PubMed PMID: 25340013; PMCID: PMC4205135.

162.Ruby JG, Jan C, Player C, Axtell MJ, Lee W, Nusbaum C, Ge H, Bartel DP. Large-scale sequencing reveals 21U-RNAs and additional microRNAs and endogenous siRNAs in C. elegans. Cell. 2006;127(6):1193-207. Epub 2006/12/19. doi: 10.1016/j.cell.2006.10.040. PubMed PMID: 17174894.

163.Bouasker S, Simard MJ. The slicing activity of miRNA-specific Argonautes is essential for the miRNA pathway in C. elegans. Nucleic Acids Res. 2012;40(20):10452-62. Epub 2012/08/21. doi: 10.1093/nar/gks748. PubMed PMID: 22904066; PMCID: PMC3488219.

164.Reed KJ, Svendsen JM, Brown KC, Montgomery BE, Marks TN, Vijayasarathy T, Parker DM, Nishimura EO, Updike DL, Montgomery TA. Widespread roles for piRNAs and WAGO-class siRNAs in shaping the germline transcriptome of Caenorhabditis elegans. Nucleic Acids Res. 2020;48(4):1811-27. Epub 2019/12/25. doi: 10.1093/nar/gkz1178. PubMed PMID: 31872227; PMCID: PMC7038979.

165.Zhang C, Montgomery TA, Gabel HW, Fischer SE, Phillips CM, Fahlgren N, Sullivan CM, Carrington JC, Ruvkun G. mut-16 and other mutator class genes modulate 22G and 26G siRNA pathways in Caenorhabditis elegans. Proc Natl Acad Sci U S A. 2011;108(4):1201-8. Epub 2011/01/20. doi: 10.1073/pnas.1018695108. PubMed PMID: 21245313; PMCID: PMC3029761.

166.Knutson AK, Egelhofer T, Rechtsteiner A, Strome S. Germ Granules Prevent Accumulation of Somatic Transcripts in the Adult Caenorhabditis elegans Germline. Genetics. 2017;206(1):163-78. Epub 2017/03/05. doi: 10.1534/genetics.116.198549. PubMed PMID: 28258184; PMCID: PMC5419467.

167.Phillips CM, Montgomery TA, Breen PC, Ruvkun G. MUT-16 promotes formation of perinuclear mutator foci required for RNA silencing in the C. elegans germline. Genes Dev. 2012;26(13):1433-44. Epub 2012/06/21. doi: 10.1101/gad.193904.112. PubMed PMID: 22713602; PMCID: PMC3403012.

168.Gammon DB. Caenorhabditis elegans as an Emerging Model for Virus-Host Interactions. J Virol. 2017;91(23). Epub 2017/09/22. doi: 10.1128/JVI.00509-17. PubMed PMID: 28931683; PMCID: PMC5686719.

169.Zhou X, Li X, Wu M. miRNAs reshape immunity and inflammatory responses in bacterial infection. Signal Transduct Target Ther. 2018;3:14. Epub 2018/05/31. doi: 10.1038/s41392-018-0006-9. PubMed PMID: 29844933; PMCID: PMC5968033.

170.Sun L, Zhi L, Shakoor S, Liao K, Wang D. microRNAs Involved in the Control of Innate Immunity in Candida Infected Caenorhabditis elegans. Sci Rep. 2016;6:36036. Epub 2016/11/01. doi: 10.1038/srep36036. PubMed PMID: 27796366; PMCID: PMC5086856.

171.Drury RE, O'Connor D, Pollard AJ. The Clinical Application of MicroRNAs in Infectious Disease. Front Immunol. 2017;8:1182. Epub 2017/10/11. doi: 10.3389/fimmu.2017.01182. PubMed PMID: 28993774; PMCID: PMC5622146.

172.Aalto AP, Nicastro IA, Broughton JP, Chipman LB, Schreiner WP, Chen JS, Pasquinelli AE. Opposing roles of microRNA Argonautes during Caenorhabditis elegans aging. PLoS

Genet. 2018;14(6):e1007379. Epub 2018/06/22. doi: 10.1371/journal.pgen.1007379. PubMed PMID: 29927939; PMCID: PMC6013023.

173.Welker NC, Habig JW, Bass BL. Genes misregulated in C. elegans deficient in Dicer, RDE-4, or RDE-1 are enriched for innate immunity genes. RNA. 2007;13(7):1090-102. Epub 2007/05/29. doi: 10.1261/rna.542107. PubMed PMID: 17526642; PMCID: PMC1894926.

174.Zhi L, Yu Y, Li X, Wang D, Wang D. Molecular Control of Innate Immune Response to Pseudomonas aeruginosa Infection by Intestinal let-7 in Caenorhabditis elegans. PLoS Pathog. 2017;13(1):e1006152. Epub 2017/01/18. doi: 10.1371/journal.ppat.1006152. PubMed PMID: 28095464; PMCID: PMC5271417.

175.Dai LL, Gao JX, Zou CG, Ma YC, Zhang KQ. mir-233 modulates the unfolded protein response in C. elegans during Pseudomonas aeruginosa infection. PLoS Pathog. 2015;11(1):e1004606. Epub 2015/01/09. doi: 10.1371/journal.ppat.1004606. PubMed PMID: 25569229; PMCID: PMC4287614.

176.Kim JK, Gabel HW, Kamath RS, Tewari M, Pasquinelli A, Rual JF, Kennedy S, Dybbs M, Bertin N, Kaplan JM, Vidal M, Ruvkun G. Functional genomic analysis of RNA interference in C. elegans. Science. 2005;308(5725):1164-7. Epub 2005/03/26. doi: 10.1126/science.1109267. PubMed PMID: 15790806.

177.Montgomery TA, Rim YS, Zhang C, Dowen RH, Phillips CM, Fischer SE, Ruvkun G. PIWI associated siRNAs and piRNAs specifically require the Caenorhabditis elegans HEN1 ortholog henn-1. PLoS Genet. 2012;8(4):e1002616. Epub 2012/04/27. doi: 10.1371/journal.pgen.1002616. PubMed PMID: 22536158; PMCID: PMC3334881.

178.Bonney EA. Demystifying animal models of adverse pregnancy outcomes: touching bench and bedside. Am J Reprod Immunol. 2013;69(6):567-84. Epub 2013/03/02. doi: 10.1111/aji.12102. PubMed PMID: 23448345; PMCID: PMC4301576.

179.Robertson SA, Care AS, Moldenhauer LM. Regulatory T cells in embryo implantation and the immune response to pregnancy. J Clin Invest. 2018;128(10):4224-35. Epub 2018/10/03. doi: 10.1172/JCI122182. PubMed PMID: 30272581; PMCID: PMC6159994.

180.Tsetsarkin KA, Maximova OA, Liu G, Kenney H, Teterina N, Bloom ME, Grabowski JM, Mlera L, Nagata BM, Moore I, Martens C, Amaro-Carambot E, Lamirande EW, Whitehead SS, Pletnev AG. Routes of Zika virus dissemination in the testis and epididymis of immunodeficient mice. Nat Commun. 2018;9(1):5350. Epub 2018/12/19. doi: 10.1038/s41467-018-07782-x. PubMed PMID: 30559387; PMCID: PMC6297220.

181.Lee KA. Linking immune defenses and life history at the levels of the individual and the species. Integr Comp Biol. 2006;46(6):1000-15. Epub 2006/12/01. doi: 10.1093/icb/icl049. PubMed PMID: 21672803.

182.Lee G-Y, Sohn J, Lee S-JV. Combinatorial Approach Using Caenorhabditis elegans and Mammalian Systems for Aging Research. Molecules and cells. 2021;44(7):425-32. doi: 10.14348/molcells.2021.0080. PubMed PMID: 34248055.

183.Hiruma K, Kaneko Y. Hormonal regulation of insect metamorphosis with special reference to juvenile hormone biosynthesis. Curr Top Dev Biol. 2013;103:73-100. Epub 2013/01/26. doi: 10.1016/B978-0-12-385979-2.00003-4. PubMed PMID: 23347516.

184.Yamanaka N, Rewitz KF, O'Connor MB. Ecdysone control of developmental transitions: lessons from Drosophila research. Annu Rev Entomol. 2013;58:497-516. Epub 2012/10/18. doi: 10.1146/annurev-ento-120811-153608. PubMed PMID: 23072462; PMCID: PMC4060523.

185.Allard JB, Duan C. Comparative endocrinology of aging and longevity regulation. Front Endocrinol (Lausanne). 2011;2:75-. doi: 10.3389/fendo.2011.00075. PubMed PMID: 22654825.

186.Schwenke RA, Lazzaro BP. Juvenile Hormone Suppresses Resistance to Infection in Mated Female Drosophila melanogaster. Curr Biol. 2017;27(4):596-601. Epub 2017/02/14. doi: 10.1016/j.cub.2017.01.004. PubMed PMID: 28190728; PMCID: PMC5319889.

187.Zera AJ, Zhao Z. Effect of a juvenile hormone analogue on lipid metabolism in a wing-polymorphic cricket: implications for the endocrine-biochemical bases of life-history trade-offs. Physiol Biochem Zool. 2004;77(2):255-66. Epub 2004/04/20. doi: 10.1086/383500. PubMed PMID: 15095245.

188.Yamamoto R, Bai H, Dolezal AG, Amdam G, Tatar M. Juvenile hormone regulation of Drosophila aging. BMC Biol. 2013;11:85. Epub 2013/07/20. doi: 10.1186/1741-7007-11-85. PubMed PMID: 23866071; PMCID: PMC3726347.

189.Zhang L, Cheng L, Chapman JW, Sappington TW, Liu J, Cheng Y, Jiang X. Juvenile hormone regulates the shift from migrants to residents in adult oriental armyworm, Mythimna separata. Sci Rep. 2020;10(1):11626. Epub 2020/07/17. doi: 10.1038/s41598-020-66973-z. PubMed PMID: 32669571; PMCID: PMC7363820.

190.Templeman NM, Murphy CT. Regulation of reproduction and longevity by nutrient-sensing pathways. J Cell Biol. 2018;217(1):93-106. Epub 2017/10/28. doi: 10.1083/jcb.201707168. PubMed PMID: 29074705; PMCID: PMC5748989.

191.Tu MP, Yin CM, Tatar M. Mutations in insulin signaling pathway alter juvenile hormone synthesis in Drosophila melanogaster. Gen Comp Endocrinol. 2005;142(3):347-56. Epub 2005/06/07. doi: 10.1016/j.ygcen.2005.02.009. PubMed PMID: 15935161.

192.Lopez AL, 3rd, Chen J, Joo HJ, Drake M, Shidate M, Kseib C, Arur S. DAF-2 and ERK couple nutrient availability to meiotic progression during Caenorhabditis elegans oogenesis. Dev Cell. 2013;27(2):227-40. Epub 2013/10/15. doi: 10.1016/j.devcel.2013.09.008. PubMed PMID: 24120884; PMCID: PMC3829605.

193.Edmonds JW, Prasain JK, Dorand D, Yang Y, Hoang HD, Vibbert J, Kubagawa HM, Miller MA. Insulin/FOXO signaling regulates ovarian prostaglandins critical for reproduction. Dev Cell. 2010;19(6):858-71. Epub 2010/12/15. doi: 10.1016/j.devcel.2010.11.005. PubMed PMID: 21145501; PMCID: PMC3026445.

194.Wang MC, Bohmann D, Jasper H. JNK extends life span and limits growth by antagonizing cellular and organism-wide responses to insulin signaling. Cell. 2005;121(1):115-25. Epub 2005/04/12. doi: 10.1016/j.cell.2005.02.030. PubMed PMID: 15820683.

195.Salinas LS, Maldonado E, Navarro RE. Stress-induced germ cell apoptosis by a p53 independent pathway in Caenorhabditis elegans. Cell Death Differ. 2006;13(12):2129-39. Epub 2006/05/27. doi: 10.1038/sj.cdd.4401976. PubMed PMID: 16729024.

196.Aballay A, Drenkard E, Hilbun LR, Ausubel FM. Caenorhabditis elegans innate immune response triggered by Salmonella enterica requires intact LPS and is mediated by a MAPK signaling pathway. Curr Biol. 2003;13(1):47-52. Epub 2003/01/16. doi: 10.1016/s0960-9822(02)01396-9. PubMed PMID: 12526744.

197.Chen J, Xie C, Tian L, Hong L, Wu X, Han J. Participation of the p38 pathway in Drosophila host defense against pathogenic bacteria and fungi. Proc Natl Acad Sci U S A. 2010;107(48):20774-9. Epub 2010/11/16. doi: 10.1073/pnas.1009223107. PubMed PMID: 21076039; PMCID: PMC2996427.

198.Clark RI, Woodcock KJ, Geissmann F, Trouillet C, Dionne MS. Multiple TGF-beta superfamily signals modulate the adult Drosophila immune response. Curr Biol. 2011;21(19):1672-7. Epub 2011/10/04. doi: 10.1016/j.cub.2011.08.048. PubMed PMID: 21962711; PMCID: PMC3191266.

199.Suzanne M, Irie K, Glise B, Agnes F, Mori E, Matsumoto K, Noselli S. The Drosophila p38 MAPK pathway is required during oogenesis for egg asymmetric development. Genes Dev. 1999;13(11):1464-74. Epub 1999/06/11. doi: 10.1101/gad.13.11.1464. PubMed PMID: 10364162; PMCID: PMC316763.

200.Monsivais D, Matzuk MM, Pangas SA. The TGF-beta Family in the Reproductive Tract. Cold Spring Harb Perspect Biol. 2017;9(10). Epub 2017/02/15. doi: 10.1101/cshperspect.a022251. PubMed PMID: 28193725; PMCID: PMC5554737.

201.Becker T, Loch G, Beyer M, Zinke I, Aschenbrenner AC, Carrera P, Inhester T, Schultze JL, Hoch M. FOXO-dependent regulation of innate immune homeostasis. Nature. 2010;463(7279):369-73. Epub 2010/01/22. doi: 10.1038/nature08698. PubMed PMID: 20090753.

202.Hubler MJ, Kennedy AJ. Role of lipids in the metabolism and activation of immune cells. J Nutr Biochem. 2016;34:1-7. Epub 2016/07/18. doi: 10.1016/j.jnutbio.2015.11.002. PubMed PMID: 27424223; PMCID: PMC5694687.

203.Dolezal T, Krejcova G, Bajgar A, Nedbalova P, Strasser P. Molecular regulations of metabolism during immune response in insects. Insect Biochem Mol Biol. 2019;109:31-42. Epub 2019/04/09. doi: 10.1016/j.ibmb.2019.04.005. PubMed PMID: 30959109.

204.Nhan JD, Turner CD, Anderson SM, Yen CA, Dalton HM, Cheesman HK, Ruter DL, Uma Naresh N, Haynes CM, Soukas AA, Pukkila-Worley R, Curran SP. Redirection of SKN-1 abates the negative metabolic outcomes of a perceived pathogen infection. Proc Natl Acad Sci U S A.

2019;116(44):22322-30. Epub 2019/10/16. doi: 10.1073/pnas.1909666116. PubMed PMID: 31611372; PMCID: PMC6825279.

205.Santos CG, Humann FC, Hartfelder K. Juvenile hormone signaling in insect oogenesis. Curr Opin Insect Sci. 2019;31:43-8. Epub 2019/05/22. doi: 10.1016/j.cois.2018.07.010. PubMed PMID: 31109672.

206.DiAngelo JR, Bland ML, Bambina S, Cherry S, Birnbaum MJ. The immune response attenuates growth and nutrient storage in Drosophila by reducing insulin signaling. Proc Natl Acad Sci U S A. 2009;106(49):20853-8. Epub 2009/10/29. doi: 10.1073/pnas.0906749106. PubMed PMID: 19861550; PMCID: PMC2791644.

207.Van Gilst MR, Hadjivassiliou H, Yamamoto KR. A Caenorhabditis elegans nutrient response system partially dependent on nuclear receptor NHR-49. Proc Natl Acad Sci U S A. 2005;102(38):13496-501. Epub 2005/09/15. doi: 10.1073/pnas.0506234102. PubMed PMID: 16157872; PMCID: PMC1201344.

208.Richardson A, Fischer KE, Speakman JR, de Cabo R, Mitchell SJ, Peterson CA, Rabinovitch P, Chiao YA, Taffet G, Miller RA, Renteria RC, Bower J, Ingram DK, Ladiges WC, Ikeno Y, Sierra F, Austad SN. Measures of Healthspan as Indices of Aging in Mice-A Recommendation. J Gerontol A Biol Sci Med Sci. 2016;71(4):427-30. Epub 2015/08/25. doi: 10.1093/gerona/glv080. PubMed PMID: 26297941; PMCID: PMC4834833.

209.Richardson A, Fischer KE, Speakman JR, de Cabo R, Mitchell SJ, Peterson CA, Rabinovitch P, Chiao YA, Taffet G, Miller RA, Rentería RC, Bower J, Ingram DK, Ladiges WC, Ikeno Y, Sierra F, Austad SN. Measures of Healthspan as Indices of Aging in Mice-A Recommendation. The journals of gerontology Series A, Biological sciences and medical sciences. 2016;71(4):427-30. Epub 2015/08/22. doi: 10.1093/gerona/glv080. PubMed PMID: 26297941.

210.Melov S. Geroscience approaches to increase healthspan and slow aging. F1000Res. 2016;5. Epub 2016/05/10. doi: 10.12688/f1000research.7583.1. PubMed PMID: 27158475; PMCID: PMC4856109.

211.Sierra F. The Emergence of Geroscience as an Interdisciplinary Approach to the Enhancement of Health Span and Life Span. Cold Spring Harb Perspect Med. 2016;6(4):a025163-a. doi: 10.1101/cshperspect.a025163. PubMed PMID: 26931460.

212.Kirkwood TL, Kapahi P, Shanley DP. Evolution, stress, and longevity. J Anat. 2000;197 Pt 4:587-90. Epub 2001/02/24. doi: 10.1046/j.1469-7580.2000.19740587.x. PubMed PMID: 11197532; PMCID: PMC1468174.

213.Dues DJ, Schaar CE, Johnson BK, Bowman MJ, Winn ME, Senchuk MM, Van Raamsdonk JM. Uncoupling of oxidative stress resistance and lifespan in long-lived isp-1 mitochondrial mutants in Caenorhabditis elegans. Free Radic Biol Med. 2017;108:362-73. Epub 2017/04/11. doi: 10.1016/j.freeradbiomed.2017.04.004. PubMed PMID: 28392283; PMCID: PMC5493208.

214.Meissner B, Boll M, Daniel H, Baumeister R. Deletion of the intestinal peptide transporter affects insulin and TOR signaling in Caenorhabditis elegans. J Biol Chem. 2004;279(35):36739-45. Epub 2004/05/25. doi: 10.1074/jbc.M403415200. PubMed PMID: 15155758.

215.Arum O, Johnson TE. Reduced expression of the Caenorhabditis elegans p53 ortholog cep-1 results in increased longevity. J Gerontol A Biol Sci Med Sci. 2007;62(9):951-9. Epub 2007/09/27. doi: 10.1093/gerona/62.9.951. PubMed PMID: 17895432.

216.Kew C, Huang W, Fischer J, Ganesan R, Robinson N, Antebi A. Evolutionarily conserved regulation of immunity by the splicing factor RNP-6/PUF60. Elife. 2020;9. Epub 2020/06/17. doi: 10.7554/eLife.57591. PubMed PMID: 32538777; PMCID: PMC7332298.

217.Nikolich-Zugich J. The twilight of immunity: emerging concepts in aging of the immune system. Nat Immunol. 2018;19(1):10-9. Epub 2017/12/16. doi: 10.1038/s41590-017-0006-x. PubMed PMID: 29242543.

218.Cunha LL, Perazzio SF, Azzi J, Cravedi P, Riella LV. Remodeling of the Immune Response With Aging: Immunosenescence and Its Potential Impact on COVID-19 Immune Response. Front Immunol. 2020;11:1748. Epub 2020/08/28. doi: 10.3389/fimmu.2020.01748. PubMed PMID: 32849623; PMCID: PMC7427491.

219.Fulop T, Larbi A, Witkowski JM. Human Inflammaging. Gerontology. 2019;65(5):495-504. Epub 2019/05/06. doi: 10.1159/000497375. PubMed PMID: 31055573.

220.Fulop T, Witkowski JM, Olivieri F, Larbi A. The integration of inflammaging in age-related diseases. Semin Immunol. 2018;40:17-35. Epub 2018/10/06. doi: 10.1016/j.smim.2018.09.003. PubMed PMID: 30287177.

221.Franceschi C, Campisi J. Chronic inflammation (inflammaging) and its potential contribution to age-associated diseases. J Gerontol A Biol Sci Med Sci. 2014;69 Suppl 1:S4-9. Epub 2014/05/17. doi: 10.1093/gerona/glu057. PubMed PMID: 24833586.

222.Lee JC, Espéli M, Anderson CA, Linterman MA, Pocock JM, Williams NJ, Roberts R, Viatte S, Fu B, Peshu N, Hien TT, Phu NH, Wesley E, Edwards C, Ahmad T, Mansfield JC, Gearry R, Dunstan S, Williams TN, Barton A, Vinuesa CG, Parkes M, Lyons PA, Smith KG. Human SNP links differential outcomes in inflammatory and infectious disease to a FOXO3-regulated pathway. Cell. 2013;155(1):57-69. Epub 2013/09/17. doi: 10.1016/j.cell.2013.08.034. PubMed PMID: 24035192; PMCID: PMC3790457.

223.Leavy O. Muscling in on repair. Nature Reviews Immunology. 2014;14(2):63-. doi: 10.1038/nri3602.

224.Bharath LP, Agrawal M, McCambridge G, Nicholas DA, Hasturk H, Liu J, Jiang K, Liu R, Guo Z, Deeney J, Apovian CM, Snyder-Cappione J, Hawk GS, Fleeman RM, Pihl RMF, Thompson K, Belkina AC, Cui L, Proctor EA, Kern PA, Nikolajczyk BS. Metformin Enhances Autophagy and Normalizes Mitochondrial Function to Alleviate Aging-Associated Inflammation. Cell Metab. 2020;32(1):44-55.e6. Epub 2020/05/14. doi: 10.1016/j.cmet.2020.04.015. PubMed PMID: 32402267; PMCID: PMC7217133.

225.Ziv E, Hu D. Genetic variation in insulin/IGF-1 signaling pathways and longevity. Ageing Res Rev. 2011;10(2):201-4. Epub 2010/09/28. doi: 10.1016/j.arr.2010.09.002. PubMed PMID: 20868776.

226.Cargill SL, Carey JR, Muller HG, Anderson G. Age of ovary determines remaining life expectancy in old ovariectomized mice. Aging Cell. 2003;2(3):185-90. Epub 2003/07/29. doi: 10.1046/j.1474-9728.2003.00049.x. PubMed PMID: 12882411; PMCID: PMC2386250.

227.Levine ME, Lu AT, Chen BH, Hernandez DG, Singleton AB, Ferrucci L, Bandinelli S, Salfati E, Manson JE, Quach A, Kusters CD, Kuh D, Wong A, Teschendorff AE, Widschwendter M, Ritz BR, Absher D, Assimes TL, Horvath S. Menopause accelerates biological aging. Proc Natl Acad Sci U S A. 2016;113(33):9327-32. Epub 2016/07/28. doi: 10.1073/pnas.1604558113. PubMed PMID: 27457926; PMCID: PMC4995944.

228.Pelosi E, Omari S, Michel M, Ding J, Amano T, Forabosco A, Schlessinger D, Ottolenghi C. Constitutively active Foxo3 in oocytes preserves ovarian reserve in mice. Nat Commun. 2013;4:1843. Epub 2013/05/16. doi: 10.1038/ncomms2861. PubMed PMID: 23673628; PMCID: PMC4504230.

229.Lunetta KL, D'Agostino RB, Sr., Karasik D, Benjamin EJ, Guo CY, Govindaraju R, Kiel DP, Kelly-Hayes M, Massaro JM, Pencina MJ, Seshadri S, Murabito JM. Genetic correlates of longevity and selected age-related phenotypes: a genome-wide association study in the Framingham Study. BMC Med Genet. 2007;8 Suppl 1:S13. Epub 2007/10/16. doi: 10.1186/1471-2350-8-S1-S13. PubMed PMID: 17903295; PMCID: PMC1995604.

230.Vilchez D, Boyer L, Morantte I, Lutz M, Merkwirth C, Joyce D, Spencer B, Page L, Masliah E, Berggren WT, Gage FH, Dillin A. Increased proteasome activity in human embryonic stem cells is regulated by PSMD11. Nature. 2012;489(7415):304-8. Epub 2012/09/14. doi: 10.1038/nature11468. PubMed PMID: 22972301; PMCID: PMC5215918.

231.Medkour Y, Svistkova V, Titorenko VI. Cell-Nonautonomous Mechanisms Underlying Cellular and Organismal Aging. Int Rev Cell Mol Biol. 2016;321:259-97. Epub 2016/01/27. doi: 10.1016/bs.ircmb.2015.09.003. PubMed PMID: 26811290.

232.Morimoto RI. Cell-Nonautonomous Regulation of Proteostasis in Aging and Disease. Cold Spring Harb Perspect Biol. 2020;12(4). Epub 2019/04/10. doi: 10.1101/cshperspect.a034074. PubMed PMID: 30962274; PMCID: PMC7111247.

233.Hoffman C, Aballay A. Role of neurons in the control of immune defense. Curr Opin Immunol. 2019;60:30-6. Epub 2019/05/23. doi: 10.1016/j.coi.2019.04.005. PubMed PMID: 31117013; PMCID: PMC6800625.

234.Wani KA, Goswamy D, Irazoqui JE. Nervous system control of intestinal host defense in C. elegans. Curr Opin Neurobiol. 2020;62:1-9. Epub 2019/12/04. doi: 10.1016/j.conb.2019.11.007. PubMed PMID: 31790812; PMCID: PMC7255937.

235.Libina N, Berman JR, Kenyon C. Tissue-specific activities of C. elegans DAF-16 in the regulation of lifespan. Cell. 2003;115(4):489-502. Epub 2003/11/19. doi: 10.1016/s0092-8674(03)00889-4. PubMed PMID: 14622602.

236.Hwangbo DS, Gershman B, Tu MP, Palmer M, Tatar M. Drosophila dFOXO controls lifespan and regulates insulin signalling in brain and fat body. Nature. 2004;429(6991):562-6. Epub 2004/06/04. doi: 10.1038/nature02549. PubMed PMID: 15175753.

237.Ben-David U, Amon A. Context is everything: aneuploidy in cancer. Nat Rev Genet. 2020;21(1):44-62. Epub 2019/09/25. doi: 10.1038/s41576-019-0171-x. PubMed PMID: 31548659.

238.Amelio I, Melino G. Context is everything: extrinsic signalling and gain-of-function p53 mutants. Cell Death Discov. 2020;6:16. Epub 2020/03/29. doi: 10.1038/s41420-020-0251-x. PubMed PMID: 32218993; PMCID: PMC7090043.

239.Uschner F, Klipp E. Signaling pathways in context. Curr Opin Biotechnol. 2019;58:155-60. Epub 2019/04/12. doi: 10.1016/j.copbio.2019.03.011. PubMed PMID: 30974381.

240.Burkewitz K, Morantte I, Weir HJM, Yeo R, Zhang Y, Huynh FK, Ilkayeva OR, Hirschey MD, Grant AR, Mair WB. Neuronal CRTC-1 governs systemic mitochondrial metabolism and lifespan via a catecholamine signal. Cell. 2015;160(5):842-55. Epub 2015/02/28. doi: 10.1016/j.cell.2015.02.004. PubMed PMID: 25723162; PMCID: PMC4392909.

241.Dasgupta M, Shashikanth M, Gupta A, Sandhu A, De A, Javed S, Singh V. NHR-49 Transcription Factor Regulates Immunometabolic Response and Survival of Caenorhabditis elegans during Enterococcus faecalis Infection. Infect Immun. 2020;88(8). Epub 2020/06/03. doi: 10.1128/IAI.00130-20. PubMed PMID: 32482643; PMCID: PMC7375755.

242.Wani KA, Goswamy D, Taubert S, Ratnappan R, Ghazi A, Irazoqui JE. NHR-49/PPAR-α and HLH-30/TFEB promote C. elegans host defense via a flavin-containing monooxygenase. bioRxiv. 2020. doi: 10.1101/2020.09.03.282087.

243.Amrit FR, Ratnappan R, Keith SA, Ghazi A. The C. elegans lifespan assay toolkit. Methods. 2014;68(3):465-75. Epub 2014/04/15. doi: 10.1016/j.ymeth.2014.04.002. PubMed PMID: 24727064.

244.Han SK, Lee D, Lee H, Kim D, Son HG, Yang JS, Lee SV, Kim S. OASIS 2: online application for survival analysis 2 with features for the analysis of maximal lifespan and healthspan in aging research. Oncotarget. 2016;7(35):56147-52. Epub 2016/08/17. doi: 10.18632/oncotarget.11269. PubMed PMID: 27528229; PMCID: PMC5302902.

245.Tan M-W, Ausubel FM. Caenorhabditis elegans: a model genetic host to study Pseudomonas aeruginosa pathogenesis. Current Opinion in Microbiology. 2000;3(1):29-34. doi: https://doi.org/10.1016/S1369-5274(99)00047-8.

246.Holdorf AD, Higgins DP, Hart AC, Boag PR, Pazour GJ, Walhout AJM, Walker AK. WormCat: An Online Tool for Annotation and Visualization of Caenorhabditis elegans Genome-

Scale Data. Genetics. 2020;214(2):279-94. Epub 2019/12/08. doi: 10.1534/genetics.119.302919. PubMed PMID: 31810987; PMCID: PMC7017019.

247.Leiteritz A, Baumanns S, Wenzel U. Amyloid-beta (Aβ1–42)-induced paralysis in Caenorhabditis elegans is reduced through NHR-49/PPARalpha. Neuroscience Letters. 2020;730:135042. doi: https://doi.org/10.1016/j.neulet.2020.135042.

248.Brandstädt S, Schmeisser K, Zarse K, Ristow M. Lipid-lowering fibrates extend C. elegans lifespan in a NHR-49/PPARalpha-dependent manner. Aging (Albany NY). 2013;5(4):270-5. Epub 2013/04/23. doi: 10.18632/aging.100548. PubMed PMID: 23603800; PMCID: PMC3651519.

249.Pujol N, Cypowyj S, Ziegler K, Millet A, Astrain A, Goncharov A, Jin Y, Chisholm AD, Ewbank JJ. Distinct innate immune responses to infection and wounding in the C. elegans epidermis. Curr Biol. 2008;18(7):481-9. Epub 2008/04/09. doi: 10.1016/j.cub.2008.02.079. PubMed PMID: 18394898; PMCID: PMC2394561.

250.Arantes-Oliveira N, Berman JR, Kenyon C. Healthy animals with extreme longevity. Science. 2003;302(5645):611. Epub 2003/10/25. doi: 10.1126/science.1089169. PubMed PMID: 14576426.

251.Van Gilst MR, Hadjivassiliou H, Jolly A, Yamamoto KR. Nuclear hormone receptor NHR-49 controls fat consumption and fatty acid composition in C. elegans. PLoS Biol. 2005;3(2):e53. Epub 2005/02/19. doi: 10.1371/journal.pbio.0030053. PubMed PMID: 15719061; PMCID: PMC547972.

252.Svensk E, Stahlman M, Andersson CH, Johansson M, Boren J, Pilon M. PAQR-2 regulates fatty acid desaturation during cold adaptation in C. elegans. PLoS Genet. 2013;9(9):e1003801. Epub 2013/09/27. doi: 10.1371/journal.pgen.1003801. PubMed PMID: 24068966; PMCID: PMC3772066.

253.Amrit FRG, Ghazi A. Transcriptomic Analysis of C. elegans RNA Sequencing Data Through the Tuxedo Suite on the Galaxy Project. Journal of visualized experiments : JoVE. 2017(122):55473. doi: 10.3791/55473. PubMed PMID: 28448031.

254.Twumasi-Boateng K, Shapira M. Dissociation of immune responses from pathogen colonization supports pattern recognition in C. elegans. PLoS One. 2012;7(4):e35400. Epub 2012/04/20. doi: 10.1371/journal.pone.0035400. PubMed PMID: 22514739; PMCID: PMC3325959.

255.Powell JR, Ausubel FM. Models of Caenorhabditis elegans infection by bacterial and fungal pathogens. Methods Mol Biol. 2008;415:403-27. Epub 2008/03/29. doi: 10.1007/978-1-59745-570-1_24. PubMed PMID: 18370168.

256.Evans EA, Chen WC, Tan MW. The DAF-2 insulin-like signaling pathway independently regulates aging and immunity in C. elegans. Aging Cell. 2008;7(6):879-93. Epub 2008/09/11. doi: 10.1111/j.1474-9726.2008.00435.x. PubMed PMID: 18782349; PMCID: PMC2630471.

257.Lee K, Goh GY, Wong MA, Klassen TL, Taubert S. Gain-of-Function Alleles in Caenorhabditis elegans Nuclear Hormone Receptor nhr-49 Are Functionally Distinct. PLoS One. 2016;11(9):e0162708. Epub 2016/09/13. doi: 10.1371/journal.pone.0162708. PubMed PMID: 27618178; PMCID: PMC5019492.

258.Pulak R. Techniques for analysis, sorting, and dispensing of C. elegans on the COPAS flow-sorting system. Methods Mol Biol. 2006;351:275-86. Epub 2006/09/22. doi: 10.1385/1-59745-151-7:275. PubMed PMID: 16988441.

259.Maduro M, Pilgrim D. Identification and cloning of unc-119, a gene expressed in the Caenorhabditis elegans nervous system. Genetics. 1995;141(3):977-88. Epub 1995/11/01. PubMed PMID: 8582641; PMCID: PMC1206859.

260.Warren CE, Krizus A, Dennis JW. Complementary expression patterns of six nonessential Caenorhabditis elegans core 2/I N-acetylglucosaminyltransferase homologues. Glycobiology. 2001;11(11):979-88. Epub 2001/12/18. doi: 10.1093/glycob/11.11.979. PubMed PMID: 11744632.

261.Fire A, Waterston RH. Proper expression of myosin genes in transgenic nematodes. EMBO J. 1989;8(11):3419-28. Epub 1989/11/01. PubMed PMID: 2583105; PMCID: PMC401492.

262.Folick A, Oakley HD, Yu Y, Armstrong EH, Kumari M, Sanor L, Moore DD, Ortlund EA, Zechner R, Wang MC. Lysosomal signaling molecules regulate longevity in Caenorhabditis elegans. Science. 2015;347(6217):83. doi: 10.1126/science.1258857.

263.Leiser SF, Miller H, Rossner R, Fletcher M, Leonard A, Primitivo M, Rintala N, Ramos FJ, Miller DL, Kaeberlein M. Cell nonautonomous activation of flavin-containing monooxygenase promotes longevity and health span. Science. 2015;350(6266):1375-8. Epub 2015/11/21. doi: 10.1126/science.aac9257. PubMed PMID: 26586189; PMCID: PMC4801033.

264.Menzel R, Yeo HL, Rienau S, Li S, Steinberg CE, Sturzenbaum SR. Cytochrome P450s and short-chain dehydrogenases mediate the toxicogenomic response of PCB52 in the nematode Caenorhabditis elegans. J Mol Biol. 2007;370(1):1-13. Epub 2007/05/15. doi: 10.1016/j.jmb.2007.04.058. PubMed PMID: 17499272.

265.Dillin A, Gottschling DE, Nyström T. The good and the bad of being connected: the integrons of aging. Curr Opin Cell Biol. 2014;26:107-12. Epub 2014/02/18. doi: 10.1016/j.ceb.2013.12.003. PubMed PMID: 24529252; PMCID: PMC3927154.

266.Kodani N, Nakae J. Tissue-Specific Metabolic Regulation of FOXO-Binding Protein: FOXO Does Not Act Alone. Cells. 2020;9(3). Epub 2020/03/19. doi: 10.3390/cells9030702. PubMed PMID: 32182991; PMCID: PMC7140670.

267.Sala AJ, Bott LC, Brielmann RM, Morimoto RI. Embryo integrity regulates maternal proteostasis and stress resilience. Genes Dev. 2020;34(9-10):678-87. Epub 2020/03/29. doi: 10.1101/gad.335422.119. PubMed PMID: 32217667; PMCID: PMC7197353.

268.Taylor RC, Dillin A. XBP-1 is a cell-nonautonomous regulator of stress resistance and longevity. Cell. 2013;153(7):1435-47. Epub 2013/06/26. doi: 10.1016/j.cell.2013.05.042. PubMed PMID: 23791175; PMCID: PMC4771415.

269.Taylor RC, Berendzen KM, Dillin A. Systemic stress signalling: understanding the cell non-autonomous control of proteostasis. Nat Rev Mol Cell Biol. 2014;15(3):211-7. Epub 2014/02/22. doi: 10.1038/nrm3752. PubMed PMID: 24556842; PMCID: PMC5922984.

270.Imanikia S, Ozbey NP, Krueger C, Casanueva MO, Taylor RC. Neuronal XBP-1 Activates Intestinal Lysosomes to Improve Proteostasis in C. elegans. Curr Biol. 2019;29(14):2322-38 e7. Epub 2019/07/16. doi: 10.1016/j.cub.2019.06.031. PubMed PMID: 31303493; PMCID: PMC6658570.

271.Irazoqui JE, Troemel ER, Feinbaum RL, Luhachack LG, Cezairliyan BO, Ausubel FM. Distinct pathogenesis and host responses during infection of C. elegans by P. aeruginosa and S. aureus. PLoS Pathog. 2010;6:e1000982. Epub 2010/07/10. doi: 10.1371/journal.ppat.1000982. PubMed PMID: 20617181; PMCID: PMC2895663.

272.Brock TJ, Browse J, Watts JL. Fatty acid desaturation and the regulation of adiposity in Caenorhabditis elegans. Genetics. 2007;176(2):865-75. Epub 2007/04/17. doi: 10.1534/genetics.107.071860. PubMed PMID: 17435249; PMCID: PMC1894614.

273.Kaletsky R, Lakhina V, Arey R, Williams A, Landis J, Ashraf J, Murphy CT. The C. elegans adult neuronal IIS/FOXO transcriptome reveals adult phenotype regulators. Nature. 2016;529(7584):92-6. Epub 2015/12/18. doi: 10.1038/nature16483. PubMed PMID: 26675724; PMCID: PMC4708089.

274.Tepper RG, Ashraf J, Kaletsky R, Kleemann G, Murphy CT, Bussemaker HJ. PQM-1 complements DAF-16 as a key transcriptional regulator of DAF-2-mediated development and longevity. Cell. 2013;154(3):676-90. Epub 2013/08/06. doi: 10.1016/j.cell.2013.07.006. PubMed PMID: 23911329; PMCID: PMC3763726.

275.Pathare PP, Lin A, Bornfeldt KE, Taubert S, Van Gilst MR. Coordinate regulation of lipid metabolism by novel nuclear receptor partnerships. PLoS Genet. 2012;8(4):e1002645. Epub 2012/04/19. doi: 10.1371/journal.pgen.1002645. PubMed PMID: 22511885; PMCID: PMC3325191.

276.Goudeau J, Bellemin S, Toselli-Mollereau E, Shamalnasab M, Chen Y, Aguilaniu H. Fatty acid desaturation links germ cell loss to longevity through NHR-80/HNF4 in C. elegans. PLoS Biol. 2011;9(3):e1000599. Epub 2011/03/23. doi: 10.1371/journal.pbio.1000599. PubMed PMID: 21423649; PMCID: PMC3057950.

277.Ratnappan R, Ward JD, Yamamoto KR, Ghazi A. Nuclear hormone receptors as mediators of metabolic adaptability following reproductive perturbations. Worm. 2016;5(1):e1151609. doi: 10.1080/21624054.2016.1151609.

278.Munoz MJ, Riddle DL. Positive selection of Caenorhabditis elegans mutants with increased stress resistance and longevity. Genetics. 2003;163(1):171-80. Epub 2003/02/15. PubMed PMID: 12586705; PMCID: PMC1462431.

279.Fabrizio P, Pozza F, Pletcher SD, Gendron CM, Longo VD. Regulation of longevity and stress resistance by Sch9 in yeast. Science. 2001;292(5515):288-90. Epub 2001/04/09. doi: 10.1126/science.1059497. PubMed PMID: 11292860.

280.Hou Y, Meng K, Han Y, Ban Q, Wang B, Suo J, Lv J, Rao J. The Persimmon 9-lipoxygenase Gene DkLOX3 Plays Positive Roles in Both Promoting Senescence and Enhancing Tolerance to Abiotic Stress. Front Plant Sci. 2015;6:1073. Epub 2015/12/24. doi: 10.3389/fpls.2015.01073. PubMed PMID: 26697033; PMCID: PMC4674570.

281.Lee SS, Lee RY, Fraser AG, Kamath RS, Ahringer J, Ruvkun G. A systematic RNAi screen identifies a critical role for mitochondria in C. elegans longevity. Nat Genet. 2003;33(1):40-8. Epub 2002/11/26. doi: 10.1038/ng1056. PubMed PMID: 12447374.

282.Liu K, Case A, Reproductive E, Infertility C. Advanced reproductive age and fertility. J Obstet Gynaecol Can. 2011;33(11):1165-75. Epub 2011/11/16. doi: 10.1016/S1701-2163(16)35087-3. PubMed PMID: 22082792.

283.Rodriguez M, Snoek LB, De Bono M, Kammenga JE. Worms under stress: C. elegans stress response and its relevance to complex human disease and aging. Trends Genet. 2013;29(6):367-74. Epub 2013/02/23. doi: 10.1016/j.tig.2013.01.010. PubMed PMID: 23428113.

284.Miller DL, Horsman J, Heinis FI. Stress Response Pathways. In: Olsen A, Gill MS, editors. Ageing: Lessons from C elegans. Cham: Springer International Publishing; 2017. p. 191-217.

285.Pellegrino MW, Nargund AM, Kirienko NV, Gillis R, Fiorese CJ, Haynes CM. Mitochondrial UPR-regulated innate immunity provides resistance to pathogen infection. Nature. 2014;516(7531):414-7. Epub 2014/10/03. doi: 10.1038/nature13818. PubMed PMID: 25274306; PMCID: PMC4270954.

286.Nargund AM, Pellegrino MW, Fiorese CJ, Baker BM, Haynes CM. Mitochondrial import efficiency of ATFS-1 regulates mitochondrial UPR activation. Science. 2012;337(6094):587-90. Epub 2012/06/16. doi: 10.1126/science.1223560. PubMed PMID: 22700657; PMCID: PMC3518298.

287.Oliveira RP, Porter Abate J, Dilks K, Landis J, Ashraf J, Murphy CT, Blackwell TK. Condition-adapted stress and longevity gene regulation by Caenorhabditis elegans SKN-1/Nrf. Aging Cell. 2009;8(5):524-41. Epub 2009/07/07. doi: 10.1111/j.1474-9726.2009.00501.x. PubMed PMID: 19575768; PMCID: PMC2776707.

288.Singh V, Aballay A. Heat-shock transcription factor (HSF)-1 pathway required for Caenorhabditis elegans immunity. Proc Natl Acad Sci U S A. 2006;103(35):13092-7. Epub 2006/08/19. doi: 10.1073/pnas.0604050103. PubMed PMID: 16916933; PMCID: PMC1559758.

289.Shao Z, Zhang Y, Ye Q, Saldanha JN, Powell-Coffman JA. C. elegans SWAN-1 Binds to EGL-9 and regulates HIF-1-mediated resistance to the bacterial pathogen Pseudomonas aeruginosa PAO1. PLoS Pathog. 2010;6(8):e1001075. Epub 2010/09/25. doi: 10.1371/journal.ppat.1001075. PubMed PMID: 20865124; PMCID: PMC2928816.

290.Tullet JM, Hertweck M, An JH, Baker J, Hwang JY, Liu S, Oliveira RP, Baumeister R, Blackwell TK. Direct inhibition of the longevity-promoting factor SKN-1 by insulin-like signaling in C. elegans. Cell. 2008;132(6):1025-38. Epub 2008/03/25. doi: 10.1016/j.cell.2008.01.030. PubMed PMID: 18358814; PMCID: PMC2367249.

291.Hsu AL, Murphy CT, Kenyon C. Regulation of aging and age-related disease by DAF-16 and heat-shock factor. Science. 2003;300(5622):1142-5. Epub 2003/05/17. doi: 10.1126/science.1083701. PubMed PMID: 12750521.

292.Morrow G, Samson M, Michaud S, Tanguay RM. Overexpression of the small mitochondrial Hsp22 extends Drosophila life span and increases resistance to oxidative stress. FASEB J. 2004;18(3):598-9. Epub 2004/01/22. doi: 10.1096/fj.03-0860fje. PubMed PMID: 14734639.

293.Greer EL, Brunet A. FOXO transcription factors at the interface between longevity and tumor suppression. Oncogene. 2005;24(50):7410-25. Epub 2005/11/17. doi: 10.1038/sj.onc.1209086. PubMed PMID: 16288288.

294.Garigan D, Hsu AL, Fraser AG, Kamath RS, Ahringer J, Kenyon C. Genetic analysis of tissue aging in Caenorhabditis elegans: a role for heat-shock factor and bacterial proliferation. Genetics. 2002;161(3):1101-12. Epub 2002/07/24. doi: 10.1093/genetics/161.3.1101. PubMed PMID: 12136014; PMCID: PMC1462187.

295.Ly DH, Lockhart DJ, Lerner RA, Schultz PG. Mitotic misregulation and human aging. Science. 2000;287(5462):2486-92. Epub 2000/03/31. doi: 10.1126/science.287.5462.2486. PubMed PMID: 10741968.

296.Pushpa K, Kumar GA, Subramaniam K. PUF-8 and TCER-1 are essential for normal levels of multiple mRNAs in the C. elegans germline. Development. 2013;140(6):1312-20. Epub 2013/02/28. doi: 10.1242/dev.087833. PubMed PMID: 23444359; PMCID: PMC3585663.

297.Pagano DJ, Kingston ER, Kim DH. Tissue expression pattern of PMK-2 p38 MAPK is established by the miR-58 family in C. elegans. PLoS Genet. 2015;11(2):e1004997. Epub 2015/02/12. doi: 10.1371/journal.pgen.1004997. PubMed PMID: 25671546; PMCID: PMC4335502.

298.Mertenskotter A, Keshet A, Gerke P, Paul RJ. The p38 MAPK PMK-1 shows heat-induced nuclear translocation, supports chaperone expression, and affects the heat tolerance of Caenorhabditis elegans. Cell Stress Chaperones. 2013;18(3):293-306. Epub 2012/11/03. doi: 10.1007/s12192-012-0382-y. PubMed PMID: 23117578; PMCID: PMC3631094.

299.Mizuno T, Hisamoto N, Terada T, Kondo T, Adachi M, Nishida E, Kim DH, Ausubel FM, Matsumoto K. The Caenorhabditis elegans MAPK phosphatase VHP-1 mediates a novel JNK-

like signaling pathway in stress response. EMBO J. 2004;23(11):2226-34. Epub 2004/04/30. doi: 10.1038/sj.emboj.7600226. PubMed PMID: 15116070; PMCID: PMC419906.

300.Houtkooper RH, Mouchiroud L, Ryu D, Moullan N, Katsyuba E, Knott G, Williams RW, Auwerx J. Mitonuclear protein imbalance as a conserved longevity mechanism. Nature. 2013;497(7450):451-7. Epub 2013/05/24. doi: 10.1038/nature12188. PubMed PMID: 23698443; PMCID: PMC3663447.

301.Ma DK, Vozdek R, Bhatla N, Horvitz HR. CYSL-1 interacts with the O2-sensing hydroxylase EGL-9 to promote H2S-modulated hypoxia-induced behavioral plasticity in C. elegans. Neuron. 2012;73(5):925-40. Epub 2012/03/13. doi: 10.1016/j.neuron.2011.12.037. PubMed PMID: 22405203; PMCID: PMC3305813.

302.Kimura K, Tanaka N, Nakamura N, Takano S, Ohkuma S. Knockdown of mitochondrial heat shock protein 70 promotes progeria-like phenotypes in caenorhabditis elegans. J Biol Chem. 2007;282(8):5910-8. Epub 2006/12/26. doi: 10.1074/jbc.M609025200. PubMed PMID: 17189267.

303.Ragland SA, Criss AK. From bacterial killing to immune modulation: Recent insights into the functions of lysozyme. PLoS Pathog. 2017;13(9):e1006512. Epub 2017/09/22. doi: 10.1371/journal.ppat.1006512. PubMed PMID: 28934357; PMCID: PMC5608400.

304.Boehnisch C, Wong D, Habig M, Isermann K, Michiels NK, Roeder T, May RC, Schulenburg H. Protist-type lysozymes of the nematode Caenorhabditis elegans contribute to resistance against pathogenic Bacillus thuringiensis. PLoS One. 2011;6(9):e24619. Epub 2011/09/21. doi: 10.1371/journal.pone.0024619. PubMed PMID: 21931778; PMCID: PMC3169628.

305.Akira S, Uematsu S, Takeuchi O. Pathogen recognition and innate immunity. Cell. 2006;124(4):783-801. Epub 2006/02/25. doi: 10.1016/j.cell.2006.02.015. PubMed PMID: 16497588.

306.Ghazi A, Henis-Korenblit S, Kenyon C. Regulation of Caenorhabditis elegans lifespan by a proteasomal E3 ligase complex. Proc Natl Acad Sci U S A. 2007;104(14):5947-52. Epub 2007/03/30. doi: 10.1073/pnas.0700638104. PubMed PMID: 17392428; PMCID: PMC1851597.

307.Bakowski MA, Desjardins CA, Smelkinson MG, Dunbar TL, Lopez-Moyado IF, Rifkin SA, Cuomo CA, Troemel ER. Ubiquitin-mediated response to microsporidia and virus infection in C. elegans. PLoS Pathog. 2014;10(6):e1004200. Epub 2014/06/20. doi: 10.1371/journal.ppat.1004200. PubMed PMID: 24945527; PMCID: PMC4063957.

308.Chang HC, Paek J, Kim DH. Natural polymorphisms in C. elegans HECW-1 E3 ligase affect pathogen avoidance behaviour. Nature. 2011;480(7378):525-9. Epub 2011/11/18. doi: 10.1038/nature10643. PubMed PMID: 22089131; PMCID: PMC3245782.

309.van Oosten-Hawle P, Porter RS, Morimoto RI. Regulation of organismal proteostasis by transcellular chaperone signaling. Cell. 2013;153(6):1366-78. Epub 2013/06/12. doi: 10.1016/j.cell.2013.05.015. PubMed PMID: 23746847; PMCID: PMC3955170.

310.Schinzel R, Dillin A. Endocrine aspects of organelle stress-cell non-autonomous signaling of mitochondria and the ER. Curr Opin Cell Biol. 2015;33:102-10. Epub 2015/02/14. doi: 10.1016/j.ceb.2015.01.006. PubMed PMID: 25677685.

311.O'Brien D, van Oosten-Hawle P. Regulation of cell-non-autonomous proteostasis in metazoans. Essays Biochem. 2016;60(2):133-42. Epub 2016/10/17. doi: 10.1042/EBC20160006. PubMed PMID: 27744329; PMCID: PMC5065704.

312.Bai H, Kang P, Hernandez AM, Tatar M. Activin signaling targeted by insulin/dFOXO regulates aging and muscle proteostasis in Drosophila. PLoS Genet. 2013;9(11):e1003941. Epub 2013/11/19. doi: 10.1371/journal.pgen.1003941. PubMed PMID: 24244197; PMCID: PMC3820802.

313.Williams KW, Liu T, Kong X, Fukuda M, Deng Y, Berglund ED, Deng Z, Gao Y, Liu T, Sohn JW, Jia L, Fujikawa T, Kohno D, Scott MM, Lee S, Lee CE, Sun K, Chang Y, Scherer PE, Elmquist JK. Xbp1s in Pomc neurons connects ER stress with energy balance and glucose homeostasis. Cell Metab. 2014;20(3):471-82. Epub 2014/07/16. doi: 10.1016/j.cmet.2014.06.002. PubMed PMID: 25017942; PMCID: PMC4186248.

314.Youngman MJ, Rogers ZN, Kim DH. A decline in p38 MAPK signaling underlies immunosenescence in Caenorhabditis elegans. PLoS Genet. 2011;7(5):e1002082. Epub 2011/06/01. doi: 10.1371/journal.pgen.1002082. PubMed PMID: 21625567; PMCID: PMC3098197.

315.Miyata S, Begun J, Troemel ER, Ausubel FM. DAF-16-dependent suppression of immunity during reproduction in Caenorhabditis elegans. Genetics. 2008;178(2):903-18. Epub 2008/02/05. doi: 10.1534/genetics.107.083923. PubMed PMID: 18245330; PMCID: PMC2248360.

316.Steuerwald NM, Bermudez MG, Wells D, Munne S, Cohen J. Maternal age-related differential global expression profiles observed in human oocytes. Reprod Biomed Online. 2007;14(6):700-8. Epub 2007/06/21. doi: 10.1016/s1472-6483(10)60671-2. PubMed PMID: 17579982.

317.Fischer SE. Small RNA-mediated gene silencing pathways in C. elegans. Int J Biochem Cell Biol. 2010;42(8):1306-15. Epub 2010/03/17. doi: 10.1016/j.biocel.2010.03.006. PubMed PMID: 20227516.

318.Billi AC, Fischer SE, Kim JK. Endogenous RNAi pathways in C. elegans. WormBook. 2014:1-49. Epub 2014/05/13. doi: 10.1895/wormbook.1.170.1. PubMed PMID: 24816713; PMCID: PMC4781133.

319.Ding SW, Lu R. Virus-derived siRNAs and piRNAs in immunity and pathogenesis. Curr Opin Virol. 2011;1(6):533-44. Epub 2011/12/20. doi: 10.1016/j.coviro.2011.10.028. PubMed PMID: 22180767; PMCID: PMC3237678.

320.Coffman SR, Lu J, Guo X, Zhong J, Jiang H, Broitman-Maduro G, Li WX, Lu R, Maduro M, Ding SW. Caenorhabditis elegans RIG-I Homolog Mediates Antiviral RNA Interference Downstream of Dicer-Dependent Biogenesis of Viral Small Interfering RNAs. MBio. 2017;8(2).

Epub 2017/03/23. doi: 10.1128/mBio.00264-17. PubMed PMID: 28325765; PMCID: PMC5362034.

321.Iatsenko I, Sinha A, Rodelsperger C, Sommer RJ. New role for DCR-1/dicer in Caenorhabditis elegans innate immunity against the highly virulent bacterium Bacillus thuringiensis DB27. Infect Immun. 2013;81(10):3942-57. Epub 2013/08/07. doi: 10.1128/IAI.00700-13. PubMed PMID: 23918784; PMCID: PMC3811748.

322.Kudlow BA, Zhang L, Han M. Systematic analysis of tissue-restricted miRISCs reveals a broad role for microRNAs in suppressing basal activity of the C. elegans pathogen response. Mol Cell. 2012;46(4):530-41. Epub 2012/04/17. doi: 10.1016/j.molcel.2012.03.011. PubMed PMID: 22503424; PMCID: PMC3365535.

323.Belicard T, Jareosettasin P, Sarkies P. The piRNA pathway responds to environmental signals to establish intergenerational adaptation to stress. BMC Biol. 2018;16(1):103. Epub 2018/09/20. doi: 10.1186/s12915-018-0571-y. PubMed PMID: 30227863; PMCID: PMC6145337.

324.Moore RS, Kaletsky R, Murphy CT. Piwi/PRG-1 Argonaute and TGF-beta Mediate Transgenerational Learned Pathogenic Avoidance. Cell. 2019;177(7):1827-41 e12. Epub 2019/06/11. doi: 10.1016/j.cell.2019.05.024. PubMed PMID: 31178117; PMCID: PMC7518193.

325.Jin H. Endogenous small RNAs and antibacterial immunity in plants. FEBS Lett. 2008;582(18):2679-84. Epub 2008/07/16. doi: 10.1016/j.febslet.2008.06.053. PubMed PMID: 18619960; PMCID: PMC5912937.

326.Hamatani T, Falco G, Carter MG, Akutsu H, Stagg CA, Sharov AA, Dudekula DB, VanBuren V, Ko MS. Age-associated alteration of gene expression patterns in mouse oocytes. Hum Mol Genet. 2004;13(19):2263-78. Epub 2004/08/20. doi: 10.1093/hmg/ddh241. PubMed PMID: 15317747.

327.Williams AB, Schumacher B. Nematoda: The Caenorhabditis elegans Model for Innate Immunity – Interactions Between Worms and Pathogens, and Their Responses to Immunogenic Damage. In: Cooper EL, editor. Advances in Comparative Immunology. Cham: Springer International Publishing; 2018. p. 117-34.

328.Whitehead KA, Dahlman JE, Langer RS, Anderson DG. Silencing or stimulation? siRNA delivery and the immune system. Annu Rev Chem Biomol Eng. 2011;2:77-96. Epub 2011/01/01. doi: 10.1146/annurev-chembioeng-061010-114133. PubMed PMID: 22432611.

329.Hu B, Zhong L, Weng Y, Peng L, Huang Y, Zhao Y, Liang XJ. Therapeutic siRNA: state of the art. Signal Transduct Target Ther. 2020;5(1):101. Epub 2020/06/21. doi: 10.1038/s41392-020-0207-x. PubMed PMID: 32561705; PMCID: PMC7305320.

330.Takahashi T, Heaton SM, Parrish NF. Mammalian antiviral systems directed by small RNA. PLoS Pathog. 2021;17(12):e1010091. Epub 2021/12/17. doi: 10.1371/journal.ppat.1010091. PubMed PMID: 34914813; PMCID: PMC8675686.

331.Marques JT, Williams BR. Activation of the mammalian immune system by siRNAs. Nat Biotechnol. 2005;23(11):1399-405. Epub 2005/11/08. doi: 10.1038/nbt1161. PubMed PMID: 16273073.

332.Zhi L, Yu Y, Jiang Z, Wang D. mir-355 Functions as An Important Link between p38 MAPK Signaling and Insulin Signaling in the Regulation of Innate Immunity. Sci Rep. 2017;7(1):14560. Epub 2017/11/08. doi: 10.1038/s41598-017-15271-2. PubMed PMID: 29109437; PMCID: PMC5673931.

333.Brenner S. The genetics of Caenorhabditis elegans. Genetics. 1974;77(1):71-94. Epub 1974/05/01. doi: 10.1093/genetics/77.1.71. PubMed PMID: 4366476; PMCID: PMC1213120.

334.Wani KA, Goswamy D, Taubert S, Ratnappan R, Ghazi A, Irazoqui JE. NHR-49/PPAR-alpha and HLH-30/TFEB cooperate for C. elegans host defense via a flavin-containing monooxygenase. Elife. 2021;10. Epub 2021/05/13. doi: 10.7554/eLife.62775. PubMed PMID: 33978570; PMCID: PMC8139828.

335.Chen S, Zhou Y, Chen Y, Gu J. fastp: an ultra-fast all-in-one FASTQ preprocessor. Bioinformatics. 2018;34(17):i884-i90. Epub 2018/11/14. doi: 10.1093/bioinformatics/bty560. PubMed PMID: 30423086; PMCID: PMC6129281.

336.Dobin A, Davis CA, Schlesinger F, Drenkow J, Zaleski C, Jha S, Batut P, Chaisson M, Gingeras TR. STAR: ultrafast universal RNA-seq aligner. Bioinformatics. 2013;29(1):15-21. Epub 2012/10/30. doi: 10.1093/bioinformatics/bts635. PubMed PMID: 23104886; PMCID: PMC3530905.

337.Li B, Dewey CN. RSEM: accurate transcript quantification from RNA-Seq data with or without a reference genome. BMC Bioinformatics. 2011;12:323. Epub 2011/08/06. doi: 10.1186/1471-2105-12-323. PubMed PMID: 21816040; PMCID: PMC3163565.

338.Love MI, Huber W, Anders S. Moderated estimation of fold change and dispersion for RNA-seq data with DESeq2. Genome Biol. 2014;15(12):550. doi: 10.1186/s13059-014-0550-8. PubMed PMID: 25516281; PMCID: PMC4302049.

339.Fahlgren N, Sullivan CM, Kasschau KD, Chapman EJ, Cumbie JS, Montgomery TA, Gilbert SD, Dasenko M, Backman TW, Givan SA, Carrington JC. Computational and analytical framework for small RNA profiling by high-throughput sequencing. RNA. 2009;15(5):992-1002. Epub 2009/03/25. doi: rna.1473809 [pii]

10.1261/rna.1473809. PubMed PMID: 19307293; PMCID: 2673065.

340.Brown KC, Svendsen JM, Tucci RM, Montgomery BE, Montgomery TA. ALG-5 is a miRNA-associated Argonaute required for proper developmental timing in the Caenorhabditis elegans germline. Nucleic Acids Res. 2017;45(15):9093-107. Epub 2017/06/25. doi: 10.1093/nar/gkx536. PubMed PMID: 28645154; PMCID: PMC5587817.

341.Tijsterman M, Okihara KL, Thijssen K, Plasterk RH. PPW-1, a PAZ/PIWI protein required for efficient germline RNAi, is defective in a natural isolate of C. elegans. Curr Biol. 2002;12(17):1535-40. Epub 2002/09/13. PubMed PMID: 12225671.

342.Sijen T, Fleenor J, Simmer F, Thijssen KL, Parrish S, Timmons L, Plasterk RH, Fire A. On the role of RNA amplification in dsRNA-triggered gene silencing. Cell. 2001;107(4):465-76. Epub 2001/11/24. doi: 10.1016/s0092-8674(01)00576-1. PubMed PMID: 11719187.

343.Kato M, Chen X, Inukai S, Zhao H, Slack FJ. Age-associated changes in expression of small, noncoding RNAs, including microRNAs, in C. elegans. RNA. 2011;17(10):1804-20. Epub 2011/08/04. doi: 10.1261/rna.2714411. PubMed PMID: 21810936; PMCID: PMC3185914.

344.Phillips Carolyn M, Montgomery Brooke E, Breen Peter C, Roovers Elke F, Rim Y-S, Ohsumi Toshiro K, Newman Martin A, van Wolfswinkel Josien C, Ketting Rene F, Ruvkun G, Montgomery Taiowa A. MUT-14 and SMUT-1 DEAD Box RNA Helicases Have Overlapping Roles in Germline RNAi and Endogenous siRNA Formation. Current Biology. 2014;24(8):839-44. doi: https://doi.org/10.1016/j.cub.2014.02.060.

345.Claycomb JM, Batista PJ, Pang KM, Gu W, Vasale JJ, van Wolfswinkel JC, Chaves DA, Shirayama M, Mitani S, Ketting RF, Conte D, Jr., Mello CC. The Argonaute CSR-1 and its 22G-RNA cofactors are required for holocentric chromosome segregation. Cell. 2009;139(1):123-34. Epub 2009/10/07. doi: 10.1016/j.cell.2009.09.014. PubMed PMID: 19804758; PMCID: PMC2766185.

346.Charlesworth AG, Seroussi U, Lehrbach NJ, Renaud MS, Sundby AE, Molnar RI, Lao RX, Willis AR, Woock JR, Aber MJ, Diao AJ, Reinke AW, Ruvkun G, Claycomb JM. Two isoforms of the essential C. elegans Argonaute CSR-1 differentially regulate sperm and oocyte fertility. Nucleic Acids Res. 2021;49(15):8836-65. Epub 2021/07/31. doi: 10.1093/nar/gkab619. PubMed PMID: 34329465; PMCID: PMC8421154.

347.Shapira M, Hamlin BJ, Rong J, Chen K, Ronen M, Tan MW. A conserved role for a GATA transcription factor in regulating epithelial innate immune responses. Proc Natl Acad Sci U S A. 2006;103(38):14086-91. Epub 2006/09/14. doi: 10.1073/pnas.0603424103. PubMed PMID: 16968778; PMCID: PMC1599916.

348.Liu J, Dai Q, Chen J, Durrant D, Freeman A, Liu T, Grossman D, Lee RM. Phospholipid scramblase 3 controls mitochondrial structure, function, and apoptotic response. Mol Cancer Res. 2003;1(12):892-902. Epub 2003/10/24. PubMed PMID: 14573790.

349.Loer CM, Calvo AC, Watschinger K, Werner-Felmayer G, O'Rourke D, Stroud D, Tong A, Gotenstein JR, Chisholm AD, Hodgkin J, Werner ER, Martinez A. Cuticle integrity and biogenic amine synthesis in Caenorhabditis elegans require the cofactor tetrahydrobiopterin (BH4). Genetics. 2015;200(1):237-53. Epub 2015/03/27. doi: 10.1534/genetics.114.174110. PubMed PMID: 25808955; PMCID: PMC4423366.

350.Romstad A, Kalkanoğlu HS, Coşkun T, Demirkol M, Tokatli A, Dursun A, Baykal T, Özalp I, Guldberg P, Güttler F. Molecular analysis of 16 Turkish families with DHPR deficiency using

denaturing gradient gel electrophoresis (DGGE). Human Genetics. 2000;107(6):546-53. doi: 10.1007/s004390000407.

351.Sasabe J, Suzuki M. Emerging Role of D-Amino Acid Metabolism in the Innate Defense. Front Microbiol. 2018;9:933. Epub 2018/06/06. doi: 10.3389/fmicb.2018.00933. PubMed PMID: 29867842; PMCID: PMC5954117.

352.Anderson SM, Pukkila-Worley R. Immunometabolism in Caenorhabditis elegans. PLoS Pathog. 2020;16(10):e1008897. Epub 2020/10/09. doi: 10.1371/journal.ppat.1008897. PubMed PMID: 33031414; PMCID: PMC7544110.

353.Rogers AK, Phillips CM. Disruption of the mutator complex triggers a low penetrance larval arrest phenotype. MicroPubl Biol. 2020;2020. Epub 2020/06/17. PubMed PMID: 32542232; PMCID: PMC7295153.

354.Kumar Kingsley SM, Vishnu Bhat B. Role of MicroRNAs in the development and function of innate immune cells. Int Rev Immunol. 2017;36(3):154-75. Epub 2017/05/05. doi: 10.1080/08830185.2017.1284212. PubMed PMID: 28471289.

355.Tabach Y, Billi AC, Hayes GD, Newman MA, Zuk O, Gabel H, Kamath R, Yacoby K, Chapman B, Garcia SM, Borowsky M, Kim JK, Ruvkun G. Identification of small RNA pathway genes using patterns of phylogenetic conservation and divergence. Nature. 2013;493(7434):694-8. Epub 2013/02/01. doi: 10.1038/nature11779. PubMed PMID: 23364702; PMCID: PMC3762460.

356.Phillips CM, Brown KC, Montgomery BE, Ruvkun G, Montgomery TA. piRNAs and piRNA-Dependent siRNAs Protect Conserved and Essential C. elegans Genes from Misrouting into the RNAi Pathway. Dev Cell. 2015;34(4):457-65. Epub 2015/08/19. doi: 10.1016/j.devcel.2015.07.009. PubMed PMID: 26279487; PMCID: PMC4550515.

357.Bukhari SI, Vasquez-Rifo A, Gagne D, Paquet ER, Zetka M, Robert C, Masson JY, Simard MJ. The microRNA pathway controls germ cell proliferation and differentiation in C. elegans. Cell Res. 2012;22(6):1034-45. Epub 2012/03/01. doi: 10.1038/cr.2012.31. PubMed PMID: 22370633; PMCID: PMC3367518.

358.Zhu Q, Kirby JA, Chu C, Gou LT. Small Noncoding RNAs in Reproduction and Infertility. Biomedicines. 2021;9(12). Epub 2021/12/25. doi: 10.3390/biomedicines9121884. PubMed PMID: 34944700; PMCID: PMC8698561.

359.Grover M, Barkoulas M. C. elegans as a new tractable host to study infections by animal pathogenic oomycetes. PLoS Pathog. 2021;17(3):e1009316. Epub 2021/03/05. doi: 10.1371/journal.ppat.1009316. PubMed PMID: 33662043; PMCID: PMC7932123.

360.Kawli T, Tan MW. Neuroendocrine signals modulate the innate immunity of Caenorhabditis elegans through insulin signaling. Nat Immunol. 2008;9(12):1415-24. Epub 2008/10/16. doi: 10.1038/ni.1672. PubMed PMID: 18854822.

361.Zugasti O, Ewbank JJ. Neuroimmune regulation of antimicrobial peptide expression by a noncanonical TGF-beta signaling pathway in Caenorhabditis elegans epidermis. Nat Immunol. 2009;10(3):249-56. Epub 2009/02/10. doi: 10.1038/ni.1700. PubMed PMID: 19198592.

362.Sun J, Singh V, Kajino-Sakamoto R, Aballay A. Neuronal GPCR controls innate immunity by regulating noncanonical unfolded protein response genes. Science. 2011;332(6030):729-32. Epub 2011/04/09. doi: 10.1126/science.1203411. PubMed PMID: 21474712; PMCID: PMC3125668.

363.Cao X, Aballay A. Neural Inhibition of Dopaminergic Signaling Enhances Immunity in a Cell-Non-autonomous Manner. Curr Biol. 2016;26(17):2329-34. Epub 2016/08/16. doi: 10.1016/j.cub.2016.06.036. PubMed PMID: 27524480; PMCID: PMC5021569.

364.Styer KL, Singh V, Macosko E, Steele SE, Bargmann CI, Aballay A. Innate immunity in Caenorhabditis elegans is regulated by neurons expressing NPR-1/GPCR. Science. 2008;322(5900):460-4. Epub 2008/09/20. doi: 10.1126/science.1163673. PubMed PMID: 18801967; PMCID: PMC2831475.

365.Schiffer JA, Servello FA, Heath WR, Amrit FRG, Stumbur SV, Eder M, Martin OM, Johnsen SB, Stanley JA, Tam H, Brennan SJ, McGowan NG, Vogelaar AL, Xu Y, Serkin WT, Ghazi A, Stroustrup N, Apfeld J. Caenorhabditis elegans processes sensory information to choose between freeloading and self-defense strategies. Elife. 2020;9. Epub 2020/05/06. doi: 10.7554/eLife.56186. PubMed PMID: 32367802; PMCID: PMC7213980.

366.Chalfie M, Sulston JE, White JG, Southgate E, Thomson JN, Brenner S. The neural circuit for touch sensitivity in Caenorhabditis elegans. J Neurosci. 1985;5(4):956-64. Epub 1985/04/01. PubMed PMID: 3981252; PMCID: PMC6565008.

367.Chase DL, Koelle MR. Biogenic amine neurotransmitters in C. elegans. WormBook. 2007:1-15. Epub 2007/12/01. doi: 10.1895/wormbook.1.132.1. PubMed PMID: 18050501; PMCID: PMC4781333.

368.Gupta A, Varma M, Singh V. Caenorhabditis elegans sensory neurons modulate pathogen specific responses via HLH-30/TFEB transcription factor and FSHR-1 GPCR axes of immunity. bioRxiv. 2019:609610. doi: 10.1101/609610.

369.Taffoni C, Pujol N. Mechanisms of innate immunity in C. elegans epidermis. Tissue Barriers. 2015;3(4):e1078432. Epub 2015/12/31. doi: 10.1080/21688370.2015.1078432. PubMed PMID: 26716073; PMCID: PMC4681281.

370.Kaletsky R, Yao V, Williams A, Runnels AM, Tadych A, Zhou S, Troyanskaya OG, Murphy CT. Transcriptome analysis of adult Caenorhabditis elegans cells reveals tissue-specific gene and isoform expression. PLoS Genet. 2018;14(8):e1007559. Epub 2018/08/11. doi: 10.1371/journal.pgen.1007559. PubMed PMID: 30096138; PMCID: PMC6105014.

371.Zeng L, Li X, Preusch CB, He GJ, Xu N, Cheung TH, Qu J, Mak HY. Nuclear receptors NHR-49 and NHR-79 promote peroxisome proliferation to compensate for aldehyde

dehydrogenase deficiency in C. elegans. PLoS Genet. 2021;17(7):e1009635. Epub 2021/07/09. doi: 10.1371/journal.pgen.1009635. PubMed PMID: 34237064; PMCID: PMC8291716.

372.Zhao Z, Ukidve A, Kim J, Mitragotri S. Targeting Strategies for Tissue-Specific Drug Delivery. Cell. 2020;181(1):151-67. Epub 2020/04/04. doi: 10.1016/j.cell.2020.02.001. PubMed PMID: 32243788.

373.Dickinson ME, Flenniken AM, Ji X, Teboul L, Wong MD, White JK, Meehan TF, Weninger WJ, Westerberg H, Adissu H, Baker CN, Bower L, Brown JM, Caddle LB, Chiani F, Clary D, Cleak J, Daly MJ, Denegre JM, Doe B, Dolan ME, Edie SM, Fuchs H, Gailus-Durner V, Galli A, Gambadoro A, Gallegos J, Guo S, Horner NR, Hsu C-W, Johnson SJ, Kalaga S, Keith LC, Lanoue L, Lawson TN, Lek M, Mark M, Marschall S, Mason J, McElwee ML, Newbigging S, Nutter LMJ, Peterson KA, Ramirez-Solis R, Rowland DJ, Ryder E, Samocha KE, Seavitt JR, Selloum M, Szoke-Kovacs Z, Tamura M, Trainor AG, Tudose I, Wakana S, Warren J, Wendling O, West DB, Wong L, Yoshiki A, McKay M, Urban B, Lund C, Froeter E, LaCasse T, Mehalow A, Gordon E, Donahue LR, Taft R, Kutney P, Dion S, Goodwin L, Kales S, Urban R, Palmer K, Pertuy F, Bitz D, Weber B, Goetz-Reiner P, Jacobs H, Le Marchand E, El Amri A, El Fertak L, Ennah H, Ali-Hadji D, Ayadi A, Wattenhofer-Donze M, Jacquot S, André P, Birling M-C, Pavlovic G, Sorg T, Morse I, Benso F, Stewart ME, Copley C, Harrison J, Joynson S, Guo R, Qu D, Spring S, Yu L, Ellegood J, Morikawa L, Shang X, Feugas P, Creighton A, Castellanos Penton P, Danisment O, Griggs N, Tudor CL, Green AL, Icoresi Mazzeo C, Siragher E, Lillistone C, Tuck E, Gleeson D, Sethi D, Bayzetinova T, Burvill J, Habib B, Weavers L, Maswood R, Miklejewska E, Woods M, Grau E, Newman S, Sinclair C, Brown E, Ayabe S, Iwama M, Murakami A, Wurst W, MacArthur DG, Tocchini-Valentini GP, Gao X, Flicek P, Bradley A, Skarnes WC, Justice MJ, Parkinson HE, Moore M, Wells S, Braun RE, Svenson KL, de Angelis MH, Herault Y, Mohun T, Mallon A-M, Henkelman RM, Brown SDM, Adams DJ, Lloyd KCK, McKerlie C, Beaudet AL, Bućan M, Murray SA, The International Mouse Phenotyping C, The Jackson L, Infrastructure Nationale Phenomin ICdlS, Charles River L, Harwell MRC, The Toronto Centre for P, The Wellcome Trust Sanger I, Center RB. High-throughput discovery of novel developmental phenotypes. Nature. 2016;537(7621):508-14. doi: 10.1038/nature19356.

374.Blazie SM, Geissel HC, Wilky H, Joshi R, Newbern J, Mangone M. Alternative Polyadenylation Directs Tissue-Specific miRNA Targeting in Caenorhabditis elegans Somatic Tissues. Genetics. 2017;206(2):757-74. Epub 2017/03/30. doi: 10.1534/genetics.116.196774. PubMed PMID: 28348061; PMCID: PMC5499184.

375.Lund J, Tedesco P, Duke K, Wang J, Kim SK, Johnson TE. Transcriptional profile of aging in C. elegans. Curr Biol. 2002;12(18):1566-73. Epub 2002/10/10. doi: 10.1016/s0960-9822(02)01146-6. PubMed PMID: 12372248.

376.Hill AA, Hunter CP, Tsung BT, Tucker-Kellogg G, Brown EL. Genomic analysis of gene expression in C. elegans. Science. 2000;290(5492):809-12. Epub 2000/10/29. doi: 10.1126/science.290.5492.809. PubMed PMID: 11052945.

377.Minogue AL, Tackett MR, Atabakhsh E, Tejada G, Arur S. Functional genomic analysis identifies miRNA repertoire regulating C. elegans oocyte development. Nat Commun.

2018;9(1):5318. Epub 2018/12/16. doi: 10.1038/s41467-018-07791-w. PubMed PMID: 30552320; PMCID: PMC6294007.

378.Salilew-Wondim D, Gebremedhn S, Hoelker M, Tholen E, Hailay T, Tesfaye D. The Role of MicroRNAs in Mammalian Fertility: From Gametogenesis to Embryo Implantation. Int J Mol Sci. 2020;21(2). Epub 2020/01/23. doi: 10.3390/ijms21020585. PubMed PMID: 31963271; PMCID: PMC7014195.

379.Lorenzo R, Onizuka M, Defrance M, Laurent P. Combining single-cell RNA-sequencing with a molecular atlas unveils new markers for Caenorhabditis elegans neuron classes. Nucleic Acids Res. 2020;48(13):7119-34. Epub 2020/06/17. doi: 10.1093/nar/gkaa486. PubMed PMID: 32542321; PMCID: PMC7367206.

380.Sun Y, Yu Q, Li L, Mei Z, Zhou B, Liu S, Pan T, Wu L, Lei Y, Liu L, Drmanac R, Ma K, Liu S. Single-cell RNA profiling links ncRNAs to spatiotemporal gene expression during C. elegans embryogenesis. Sci Rep. 2020;10(1):18863. Epub 2020/11/04. doi: 10.1038/s41598-020-75801-3. PubMed PMID: 33139759; PMCID: PMC7606524.